BEHAVIOR OF COMPOSITE SEMI-RIGID
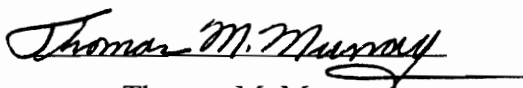# BEAM-TO-GIRDER CONNECTIONS

by

Clinton Owen Rex

Thesis submitted to the faculty of the

Virginia Polytechnic Institute and State University

in partial fulfillment of the requirements for the degree of

MASTER OF SCIENCE

in

Civil Engineering

APPROVED:

W. Samuel Easterling

W. Samuel Easterling, Chairman

Thomas M. Murray

Thomas M. Murray

Don A. Garst

Don A. Garst

January 1994

Blacksburg, Virginia 24061

C.2

S6055
V855
1994
R49
C.2

BEHAVIOR OF COMPOSITE SEMI-RIGID
BEAM-TO-GIRDER CONNECTIONS

by

Clinton Owen Rex

Committee Chairman: W. Samuel Easterling

Civil Engineering

(ABSTRACT)

Advancements in design technology and construction materials have allowed composite floor systems to become longer and shallower. As a result, serviceability considerations rather than strength considerations have started to control designs. Partial continuity in composite floor systems has been suggested as a means by which the serviceability aspects could be improved. A new beam-to-girder connection referred to as a composite semi-rigid beam-to-girder connection is investigated as a possible method to provide partial continuity in floor systems. Four of these connections are evaluated experimentally and analytically to determine their behavior and the feasibility of their use in typical composite floor systems. The results indicate that these connections would improve serviceability aspects of the floor system and would improve the general efficiency of the floor design.

ACKNOWLEGEMENTS

TABLE OF CONTENTS

LIST OF FIGURES

LIST OF TABLES

CHAPTER 1.0

INTRODUCTION

1.1 BACKGROUND

Interesting Quotation

Frame analysis shows that structural deflections and moments "depend more on the connection than on the member behavior. In view of this observation it seems inconsistent to expend much loving care on member behavior, and treat the connections in rather cavalier fashion. No doubt we do this because we can express member behavior in terms of elegant and attractive theory, but connections are messy and uneducated and do not lend themselves readily to analysis."(Acroyd and Gerstle 1990)

1.1.1 General

Advancements in design technology and construction materials have allowed floor systems to become longer and shallower. As a result, serviceability considerations rather than strength considerations have started to control designs. Providing a partially continuous floor system may be one method by which floor serviceability characteristics could be improved.

In recent years several research programs have investigated the strength and rotational stiffness of simple beam-to-column connections in buildings with continuous composite floors (composite semi-rigid connections). The research has shown that these connections provide significant rotational strength and ductility if reinforcing steel is present in the slab and continuous across the support.

1

This concept of composite semi-rigid connections may be one of the most viable methods by which partial continuity in floor systems may be achieved and subsequently serviceability problems minimized and floor design efficiency improved. The purpose of the current research program is to apply this concept to beam-to-girder connections. This includes determining the characteristics of composite semi-rigid beam-to-girder connections and eventually determining the feasibility of their use and developing design guidelines so they may be incorporated into current design procedures.

The following background is intended to give the reader an understanding of why composite semi-rigid beam-to-girder connections will, in concept, provide partial continuity in a floor system and why partial continuity is believed to be the best way to improve current composite floor designs. To convey these ideas, a rather detailed discussion on semi-rigid and composite semi-rigid connections is included. This is intended to give the reader a basic understanding of what is meant by semi-rigid and composite semi-rigid connections and how they differ from ideally rigid and pinned connections.

1.1.2 The Need for a Change in Floor Design

There is a need for more open space in buildings. In particular, building owners want more open space to allow them the flexibility of accommodating a variety of tenants. The amount of open space in a building is a direct result of the floor system used. Three changes in steel design over the last 30-40 years have allowed engineers to provide more open space in buildings with steel framed floors. First, composite steel-concrete floor system technology has developed which allows designers to use the synergy of tying the two floor components (the beam and the slab) together in order to span longer distances. Second, the plastic section analysis and design procedures found in the Load and Resistance Factor Design methods (*Load and* 1986) has allowed an additional increase in span length over Allowable Stress Design (*Specification for* 1989)

procedures. Thirdly, high strength steel, particularly A572 Grade 50 steel, is becoming more readily available and at a cost comparable with A36 steel. Longer and shallower floor systems, and thus more open space, have been made possible by these changes; but, along with these benefits there have also been problems.

Serviceability problems such as floor deflections and vibrations have become an increasing concern as floor systems become longer and shallower. In many cases these problems may control the floor design (Zandonini 1989). It is the current belief that some of these problems may be minimized or solved by designing floor systems with a certain degree of continuity.

1.1.3 Continuous Floor Systems

Structural engineers are aware of the advantage a continuous beam has over a simply supported beam. These include reduced moments, deflections, and possibly improved vibration characteristics. A floor system with continuous members, or at least members with some continuity, may be achieved through various methods.

1.1.3.1 Parallel Beam Approach

One method that has been used in Europe is known as the parallel beam approach or the dual plane grillage system (Brett, et. al. 1987). In this system the secondary beams sit on top of the primary girders (See Figure 1.1-1). Pairs of girders are used so that the columns can be bypassed. This arrangement provides large openings for services and provides continuity across supports for all floor members. Although shown to be rather efficient, this system has not been used in the United States and would represent a radical departure from current designs procedures.

3
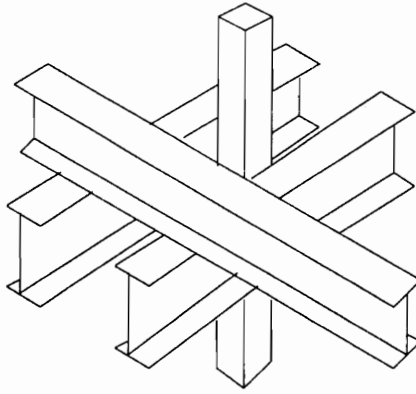
Figure 1.1-1 Parallel Beam Approach

1.1.3.2 Rigid Connections

A second possible method to achieve beam continuity is the use of rigid beam-girder connections. Suggested details for this type of connection are given in Figure 1.1-2. Despite the continuity provided by rigid connections, they do have several disadvantages. First, as can be seen in Figure 1.1-2, rigid connections typically require substantial welding and thus cost more than simple connections in materials and labor. Second, rigid connections attract a large amount of the flexural stress to the connection (See Figure 1.1-3). This is particularly a disadvantage for composite beams because the largest moment capacity of a composite beam is in the positive moment region while the negative moment capacity at the supports is typically reduced as a result of the assumed cracked floor slab. Third, it is recognized that to develop a plastic collapse mechanism in a continuous beam, particularly a continuous composite beam, a large redistribution of moment is necessary between the support and midspan regions. This implies that the connections have adequate ductility as reflected by the plastic plateau in the connection's moment-rotation curve (Jaspart and Maquoi 1990). Because premature failure of rigid connections as a result of local flange and or web buckling is common, it can not be guaranteed that a connection will have sufficient ductility. These conclusions lead to the third option of semi-rigid connections.
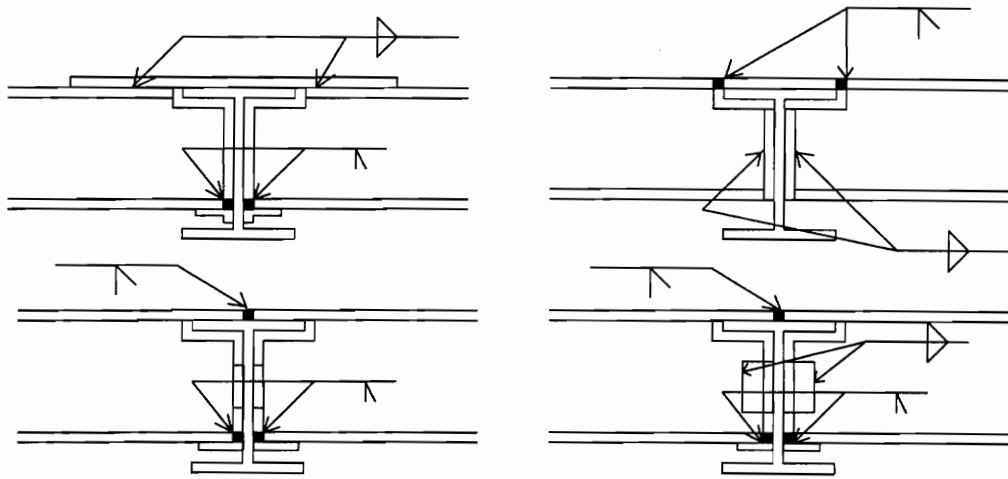
Figure 1.1-2 Rigid Beam-To-Girder Connections

M_e = Moment at End of Beam
M_c = Moment at Beam Midspan
M_{pc} = Plastic Moment Capacity of the Composite Beam

$M_e = 2 \times M_c$

M

M_c

(-)   (+)   (-)

M_{pc}

Moment Capacity in Positive Bending Approximately 1.5 to 2 times
the Moment Capacity in Negative Bending
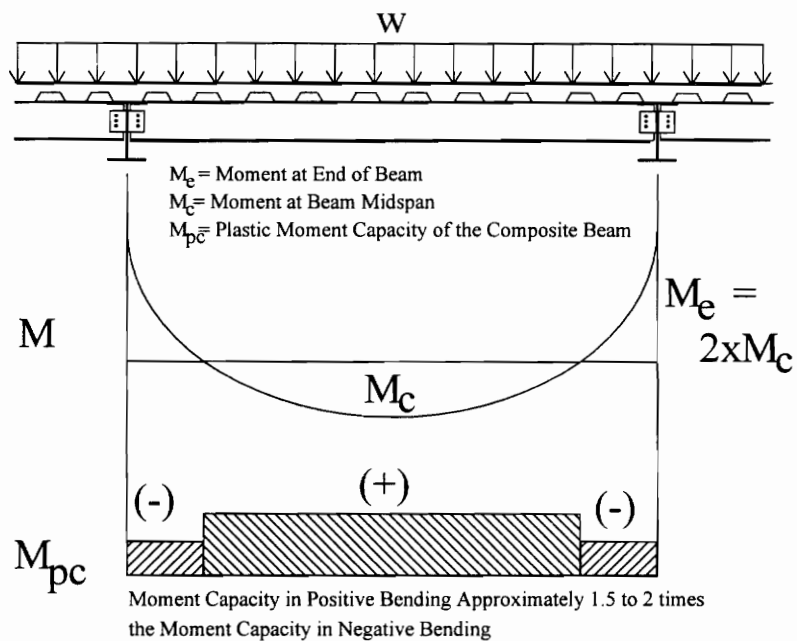
Figure 1.1-3 Moment Distribution For Beam With Rigid Connections Vs. Moment

Capacity of a Typical Composite Beam

5

1.1.3.3 Semi-rigid Connections

It has long been convenient for designers to disregard actual joint behavior in order to simplify analysis for steel frame design. Common design practice is to model all joints as either perfectly fixed/rigid (infinite moment to rotation ratio) or perfectly simple/pinned (infinite rotation to moment ratio) (Zandonini 1989). These assumptions are made despite multiple experiments that have shown the behavior of connections are neither rigid or pinned; rather, they all possess some finite degree of rotational restraint which depends on the type of connection used. The term semi-rigid is used to describe such connections (Anderson and Benterkia 1990).

Connections are classified by their associated moment-rotation behavior. Every connection has a distinct moment-rotation relationship that determines how the connection will behave as load is applied to the beam that it is connecting. The American Institute of Steel Construction (AISC) classifies connections into three groups as indicated in Table 1.

Table 1.1-1 AISC Connection Classification Groups

	ASD	LRFD
Rigid	Type 1	Fully Rigid (FR)
Simple	Type 2	Partially Rigid (PR)
Semi-Rigid	Type 3	Partially Rigid (PR)

The basis for the demarcation between these three general categories of connections is somewhat qualitative. One basis is that proposed by Bijlaard and Zoetemeijer (1986) as shown in Figure 1.1-4. It is based on the ratio of the connection stiffness over the elastic stiffness of the beam, i.e. on the ratio KL/EI, where K= the connection stiffness (the slope of the connection curve in the M_e -Φ region), M_e is the restraining moment provided by the connection, Φ is the beam end rotation, L is the beam length, E is the modulus of elasticity, and I is the beam moment of inertia. If the ratio is greater than or equal to 25 then the connection is classified as rigid, if the ratio is less than or equal to 0.5 then the

connection is classified as simple, and connections that fall between these two extremes are classified as semi-rigid. Connection strength is typically categorized as full strength when its moment capacity equals or exceeds that of the connected beam or as partial strength when it does not (Leon and Zandonini 1992).

Because stiffness is not solely a connection property but is related to the beam stiffness (EI/L), criteria for joint classification should be non-dimensional such as that used by Bijlaard and Zoetemeijer (1986). This is the approach adopted by Eurocode 3 (1993) and Eurocode 4 (1992). These codes for steel (Eurocode 3) and for composite structures (Eurocode 4) have adopted a modified Bijlaard and Zoetemeijer (1986) approach as shown in Figure 1.1-5. The Eurocodes have different performance requirements for a connection in a braced frame versus a connection in an unbraced frame. The separate performance requirements are an attempt to account for the greater influence of joint rotation in unbraced frames due to second-order effects (Leon and Zandonini 1992).
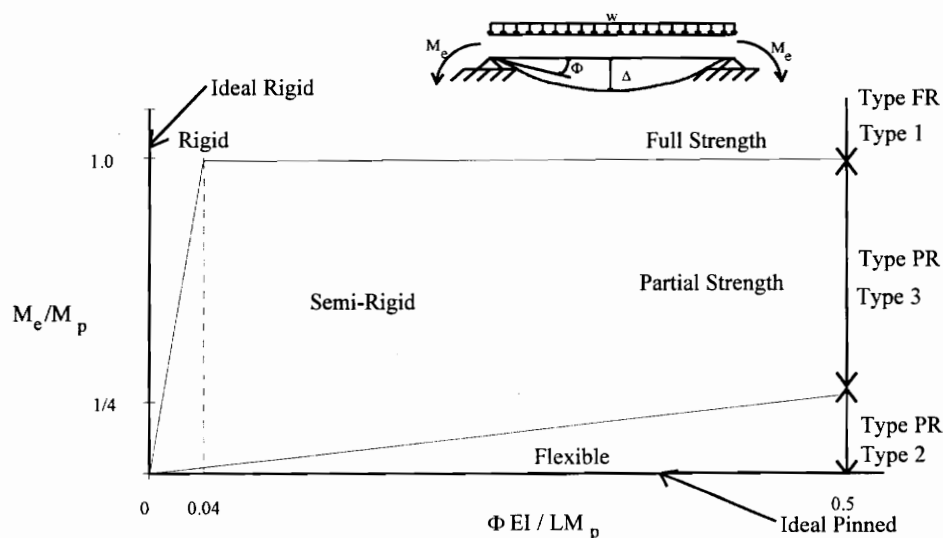
Figure 1.1-4 Joint Classification

7
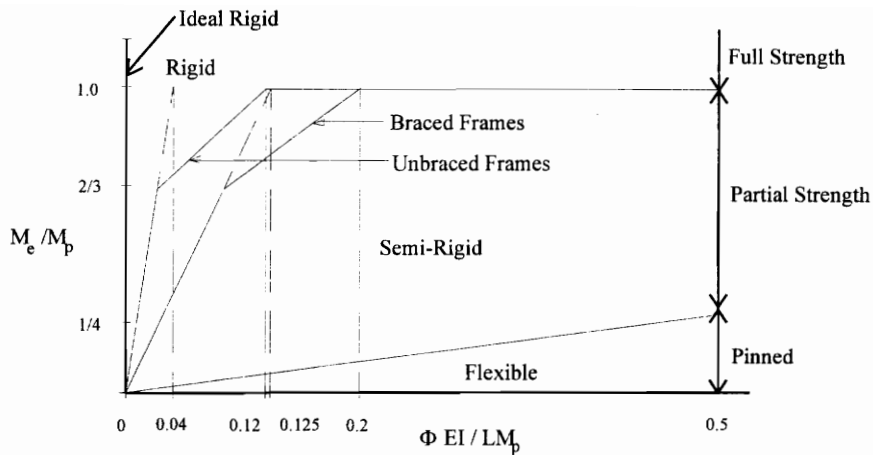
Figure 1.1-5 Joint Classification According to Eurocode 4 (Leon & Zandonini 1992)

Per the above classifications, many of the common connection details that are treated as pinned connections, as well as some that are treated as rigid connections, should be considered semi-rigid (Leon and Ammerman 1987). Qualitative moment-rotation curves for some of the common beam-column connections are shown in Figure 1.1-6.
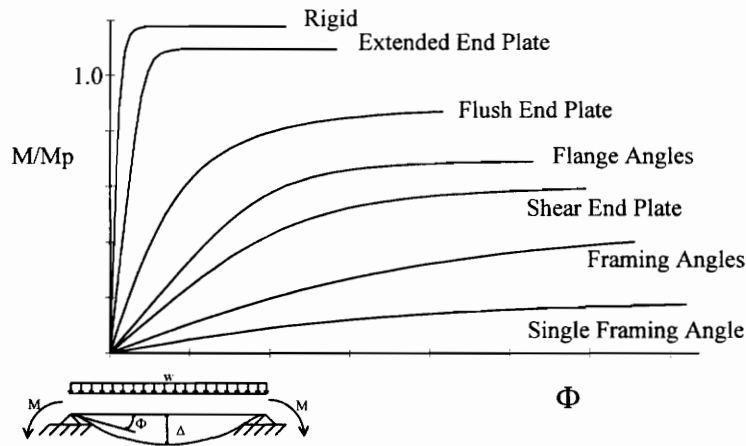
Figure 1.1-6 Common Moment-Rotation Curves

Because semi-rigid connections can range from very flexible to moderately stiff, engineers may regard them as an important and viable design option (Leon and Zandonini 1992). By regarding semi-rigid connections as mechanisms for the control of moment, the designer is able to vary the beam end-fixity to achieve a desirable distribution of

8

positive and negative moments in continuous beams (See Figure 1.1-7). Ideally, the designer would want to design the beam end fixity such that the moments are distributed proportional to the beam strength. This means the designer would want to design the connection such that more moment was distributed to the midspan of the beam than to the end since the midspan moment capacity is typically higher than the moment capacity of the beam end for composite beams.

$$Mc = \frac{wL^2}{24}$$

$$Me = 2 \times Mc$$

M fixed

$$Mc = 1.5 - 2 \times Me$$

Me

M semi-rigid

$$Me = 0$$

M simple

$$Mc = \frac{wL^2}{8}$$

Mc = Centerline Moment
Me = End Moment
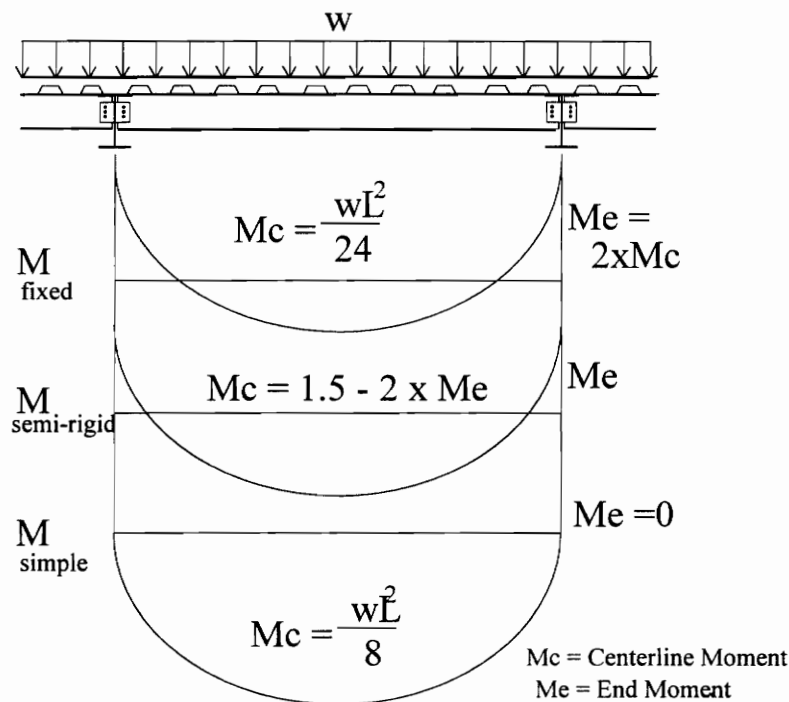
Figure 1.1-7 Beam Moments Associated With Rigid, Semi-Rigid and Simple Connections

Semi-rigid connections are not a new idea. The first research in an attempt to quantify the amount of rigidity in an actual connection was conducted by Batho and Rowan (HMSO 1931) in the 1930s for riveted connections composed of top, seat, and double-web angles (Ammerman and Leon 1987). Few designers have made explicit use of semi-rigid connections despite these early beginnings, the fact that over the past twenty years several hundred articles on semi-rigid steel connection behavior have appeared, and

the fact that several national design codes for steel structures permit semi-rigid joint action to be accounted for in design (Nethercot and Zandonini 1989).

There are probably two main reasons that semi-rigid connections are not commonly used in design. First, the designer must be able to determine the moment-rotation behavior for the connection that is being designed. The moment-rotation curve, or at least the ability to approximate the key parts of the curve adequately, is a prerequisite for performing any sort of analysis that seeks to include semi-rigid connection behavior (Nethercot and Zandonini 1989). The major obstacle to this is the lack of experimental verification and analytical models for the moment-rotation behavior of a variety of connections (Wald 1991). The tremendous amount of literature on the subject has not been of much use because most of it presents the economical, constructional, and technical advantages of semi-rigid over simple and rigid connections while very little addresses actual design issues.

The second reason is the difficulty in accounting for true connection behavior in the analysis. The difficulty in analysis arises from the fact that most semi-rigid connections have highly nonlinear moment-rotation behavior with decreasing stiffness as moment restraint increases. The most common forms of semi-rigid connections have non-linear moment rotation curves for the entire range of rotation (Anderson and Benterkia 1990). As a result of the non-linear connection curve, the analysis of frames and continuous beams with semi-rigid connections can become rather complex even with modern finite element analysis techniques.

The increased use of semi-rigid connections in the future depends mainly on the development of reliable models to determine moment-rotation characteristics for each general type of semi-rigid connection and on the development of readily available and simplified analysis and design procedures (Kulkarni 1990). Inexpensive computing power is allowing analysis and design tools to be more rapidly developed and more readily implemented than ever before. There is no reason why most analysis packages will not soon be incorporating semi-rigid connection capabilities thus bringing the

10

required analysis tools to the engineers desk. More reliable connection models are also on the horizon as researchers begin to focus efforts to utilize previous and ongoing research with the goal of developing usable design equations.

1.1.4 Composite Semi-Rigid Connections

1.1.4.1 Composite Floor Systems

Composite steel-concrete construction has developed significantly over the last 30-40 years and has enabled steel framed floor construction to remain competitive with various other floor systems. For the past 30 years nearly all multistory steel buildings have used composite floor systems. Some of the known benefits of composite construction are reductions of steel area needed to support a given load, an increase of overload capacity over non-composite sections, reductions of construction depths, and an increase on the safety of the system by providing redundant load paths (Johnson and Law 1981).

The increased moment resistance in the negative moment regions of composite continuous beams has been well established particularly in the design of bridge girders (Van Dalen and Godoy 1982). The continuous composite floor slab provides a natural element for composite beams in buildings to achieve a similar continuity in negative moment regions. Currently, this possible continuity is typically not taken advantage of.

1.1.4.2 Composite Semi-rigid Connections

Banard (1970) first introduced the idea of composite semi-rigid connections. He suggested that steel semi-rigid connections could be combined with composite construction to provide continuity over supports. He also proposed details for both beam-to-column composite semi-rigid connections and beam-to-girder composite semi-rigid

11

connections. Since that time various research has been conducted on beam-column semi-rigid composite connections. Results obtained from early investigations proved encouraging and confirmed basic expectations, but until the last few years relatively few studies were conducted (Zandonini 1989).

Semi-rigid composite connections have been the subject of several research projects in recent years. The most comprehensive research programs have been conducted by Leon and colleagues at the University of Minnesota and by Zandonini and colleagues at the University of Trento in Italy. Both of these research teams have studied numerous connections as well as developed design guidelines which can be adapted into current design procedures. A typical connection that was tested during Leon's research is shown in Figure 1.1-8.
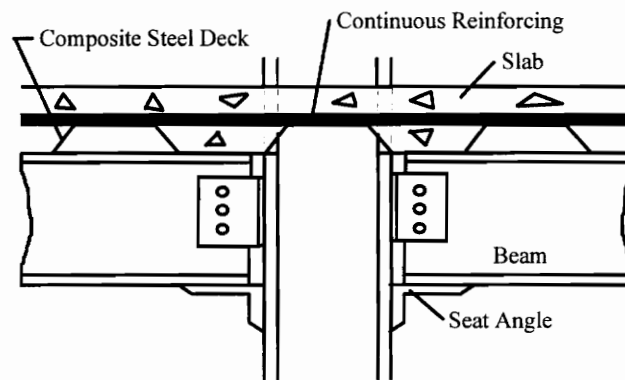
Figure 1.1-8 Typical Semi-Rigid Beam-to-Column Connection

This research has shown that with slight modifications to typical beam-column connections (such as adding a few reinforcing bars over the connection, using slightly larger framing and seat angles, and increasing the number of shear connectors) that these simple connections can be turned into rather stiff semi-rigid composite connections with predictable moment-rotation characteristics and ultimate strength. The tests thus far have shown that by changing minor details, the connection is capable of rotational restraint ranging from very flexible to very rigid. In fact, one particular test showed that with as little as 0.46% of the concrete slab area as slab reinforcement continuing across the support, a beam-column connection was able to develop a moment of resistance at least

equal to the ultimate moment capacity of the associated composite beam. This was despite the fact that the connection between the steel elements themselves had no significant moment carrying capacity (Van Dalen and Godoy 1982).

Desirable characteristics of the composite semi-rigid connections include:

1. The moment-rotation relation in the service load range has a high degree of linearity. This linear behavior can be readily incorporated into linear analysis and design which most designers are already very familiar with.

2. In many cases, composite semi-rigid connections have the same capacity and rigidity as bare steel rigid connections; but, the composite semi-rigid connection achieves this without the high cost of fabrication and erection associated with rigid connections. Local buckling problems associated with rigid connections are also reduced as the composite connections have so far shown tremendous rotation capacity prior to failure.

3. The continuous steel reinforcing will reduce cracking problems across the support. In fact, in many cases today, continuous steel reinforcing is already being placed across the supports for crack control. In these situations composite semi-rigid action would be obtained by simply accounting for this steel in the analysis.

4. The ultimate capacity of the connection is typically easy to determine.

5. The connection detailing and fabrication is basically the same as typical simple connections being used every day. This means that continuity can be developed at the support without significantly increasing the complexity of the connection details. This is particularly important as the cost of workmanship has increased much more rapidly than the cost of materials in recent years (Benussi, et. al. 1987).

1.1.4.3 Composite Semi-rigid Connection Behavior

Composite semi-rigid connections work basically the same as typical steel semi-rigid connections. They develop their rotational restraint through a tension and

compression force that acts through a moment arm. A typical steel semi-rigid beam-column connection and a typical composite semi-rigid connection are illustrated in Figure 1.1-9. The steel connection develops the moment resistance by developing a tension force in the top angle and a compression force in the bottom angle, which act through the moment arm d, where d is the depth of the steel beam. The composite semi-rigid connection develops moment resistance by developing tension in the continuous reinforcing bars and compression in the bottom angle. These forces act through a slightly larger moment arm d + Y2, where Y2 is the distance from the top of the beam to the center of the reinforcing bars.

Semi-Rigid

Semi-Rigid Composite
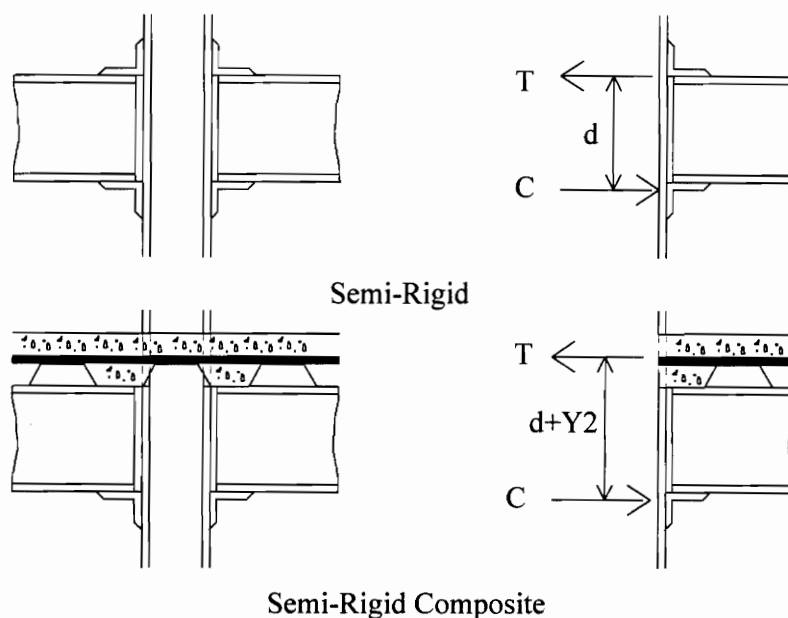
Figure 1.1-9 How Semi-Rigid Connections Develop Moment Capacity

The composite connection has two basic advantages over the steel connection. First, reinforcing bars are specifically designed for tension while framing angles positioned in this manner are less than ideal tension members. The reinforcing bars will deform and yield in a very well understood force-deformation relationship with a well defined yield plateau. However, the framing angle, which bends and yields in a much less predictable manner, may be prone to fail prior to ever developing a yield plateau.

14

Second, the increased moment arm means that the composite connection can develop the same or higher moment capacities than the steel connection while developing smaller tension and compression forces. This helps reduce the likelihood of local instabilities.

1.1.4.4 Extending Composite Semi-rigid Concepts to Beam-Girder Connections

All known work with semi-rigid composite connections has been in refining or developing beam-to-column connections while beam-girder connections have not been investigated. Semi-rigid composite beam-girder connections appear to be a natural extension of the work done with composite beam-to-column connections. The beam-to-girder connections should provide the continuity needed to reduce or eliminate many of the composite floor serviceability issues such as excessive deflections and thus allow the floor design to take full advantage of higher strength steels and plastic section analysis. It is presumed that semi-rigid beam-to-girder connections will exhibit many of the same principles and benefits associated with the beam-to-column semi-rigid connections and that much of the research in beam-to-column connections will be directly applicable to the beam-girder connections. The research described in this thesis deals with determining the characteristics of composite beam-to-girder connections as well as briefly looking at the feasibility of using and capabilities of modeling the connections.

1.2 LITERATURE REVIEW

A literature review typically contains a review of all literature that covers previous work done on the subject being investigated. No information dealing with the behavior of semi-rigid composite beam-to-girder connections was found (with one possible exception, (Davison, et. al. 1990)) nor was any information found for semi-rigid steel beam-to-girder connections. As a result, the information presented in this literature review deals with research on semi-rigid composite beam-to-column connections, which serve as the basis for the beam-to-girder connections of this test program. This literature review is limited to composite connections because the vast amount of information on semi-rigid steel connections is beyond what could be encompassed in this thesis. However, many documents on semi-rigid steel connections subject were reviewed for some insight into semi-rigid behavior.

1.2.1 Connection Element Stiffness Relationships

To develop the connection models presented in Chapter 4 the force to deformation relationships for various connection elements were investigated. The relationships are presented in Chapter 4 along with the description of the models. The relationship used for each connection element was determined from a brief review of readily available literature which is presented in Chapter 4.

1.2.2 Research on Composite Semi-Rigid Beam-Column Connections

Johnson and Hope-Gill (1972) conducted the first series of tests on what could truly be considered semi-rigid composite connections. The steel portion of these connections consisted only of angles attached to the beam bottom flange. When the results of these tests were compared to the results of similar rigid steel connections the

capabilities of the semi-rigid composite connections appeared to be impressive. In general the results showed that the semi-rigid composite connections were able to obtain nearly the same moment capacity of the fully rigid steel connection and at the same time provide a post-ultimate strength region that was characterized by remarkable rotation capacity (a region where abrupt failure of most rigid connections is seen). Despite these apparently excellent results, other studies on semi-rigid composite connections were not performed until the beginning of 1980s (Zandonini 1989).

New studies were undertaken in the 1980s. These studies were mainly in Great Britain and North America where composite construction is more common. A summary of all the composite connection tests known to the writer and which had literature readily available is presented in Table 1.2-1. This summary excludes the research associated with either Leon's or Zandonini's work because these are discussed in the next two sections respectively. In general seven investigations are presented: these include tests conducted by Fisher, Kroll, Daniels; Johnson and Hope-Gill; Echeta and Owens; Dalen and Godoy; Law; Nethercot, Lam, and Davison; and Altman, Maquoi, and Jaspart. All connections tested with one possible exception (see discussion on Nethercot, Lam and Davison 1990) were beam or girder-to-column connections. Although some of the studies included testing of plain steel connections, the majority of the information presented here will deal strictly with the composite connections tested. One page summaries have been prepared for all but a few of the various connections tested. The summaries are found in Appendix A and include information about the connection details, the test setup, test notes, and test results. Sufficient information could not be located for tests which do not have one page summaries. The information about these tests presented in Table 1.2-1 and in the written summaries below was taken from a summary of composite connection research compiled by Zandonini (1989).

The following sections are brief summaries of the seven testing programs and are presented in chronological order. The reader is referred to the summary prepared by

Zandonini (1989) for a more detailed description of the research on semi-rigid composite connections conducted prior to 1987.

1.2.2.1 Daniels, J.H., Kroll, G.D. and Fisher, J.W. (1970)

A series of two test specimens were studied at Lehigh University. The specimen setup was two beams attached to a column in a cruciform type arrangement. The steel connections used for each specimen were rigid beam direct welded. One specimen had a reinforced composite slab that was continuous over the joint while the other had a slab that was not continuous over the joint. These arrangements were meant to represent an interior column connection and an exterior column connection respectively.

The main problem being investigated was the effect of wind loading in the lower stories of multistory frames and the associated response of rigid joints in a sway frame if a continuous composite slab was present. The authors wanted to determine the ultimate strength behavior of these connections to evaluate them in composite frames and determine appropriate plastic design criteria.

The specimens were loaded at the top and bottom of the column which induced positive bending moment on one side of the specimen and negative bending moment on the other. In a frame these two sides of the specimens would represent the windward and the leeward sides of either an interior or exterior column.

All the joints appeared to attain moment capacities equal to the plastic moment capacity of the beam and have some rotation capacity. Test J1 results were limited by the test setup. Test J2 results were as expected by the investigators and J2L showed tremendous ductility for a rigid connection rotating nearly seven mrad. This rotation capacity should be kept in mind as semi-rigid composite connections are examined in the next sections.

Table 1.2-1 Summary of Experimental Work On Semi-Rigid Composite Beam-to-Column Connections

Investigators	Date	Specimen	Loading	Beam	Column	Top Connection	Steel Connection
Fisher, Kroll, Daniels	1970	J1	Monotonic Unsymetric	16 WF 40	14 WF 68	22 #3 bars in two layers	Beam-to-column direct weld moment connection
		J2	Monotonic Unsymetric	16 WF 40	14 WF 68	20 #3 bars in two layers	Beam-to-column direct weld moment connection
Johnson, Hope-Gill	1972	HB50	Monotonic	203x133 UB25	? WF ?	Ar = 1.39 (sq in)	Framing angles attached to top and bottom of beam bottom flange
		HB51	Monotonic	305x165 UB40	? WF ?	Ar = .876 (sq in)	Same as HB50
		HB52	Monotonic	305x165 UB40	? WF ?	Ar = 1.871 (sq in)	Same as HB50
		HB53	Monotonic	305x165 UB40	? WF ?	Ar = 2.063 (sq in)	Same as HB50
		HB54	Monotonic	406x140 UB39	? WF ?	Ar = 2.102 (sq in)	Same as HB50
Echeta, Owens	1981	1B	Monotonic	254x102 UB28	150x100x5 mm RHS Filled	8-8mm bars	Unstiffened Seat Angle With Framing Angles @ Web
Echeta	1982	2BS	Monotonic Unsymmetric	254x102 UB28	150x100x5 mm RHS Filled	6-8mm bars	Unstiffened Seat Angle With Plates Attached to top side of bottom flange and welded to column and framing angles attached to web
		3BS	Monotonic Unsymmetric	254x102 UB28	150x100x5 mm RHS Filled	6-8mm bars	Two Plate end plate connection centered on bottom flange of beam
		4BS	Monotonic Unsymmetric	254x102 UB28	150x100x5 mm RHS Filled	6-8mm bars	Same as 3BS
		5BS	Monotonic Unsymmetric	152x152 UC 37	150x100x5 mm RHS Filled	6-8mm bars	Same as 3BS

Ar = Area of Reinforcing Steel

19

Table 1.2-1 (Cont.) Summary of Experimental Work On Semi-Rigid Composite Beam-to-Column Connections

Investigators	Date	Specimen	Loading	Beam	Column	Top Connection	Steel Connection
Dalen, Godoy	1982	CB1	Monotonic	W8x20	W8x20	8 #3 bars	Unstiffened Seat Angle With Framing Angles Attached to Top Flange
		CB2	Monotonic	W8x20	W8x20	15 #3 bars	Same as CB1
		CB3	Monotonic	W8x20	W8x20	15 #3 bars	Unstiffened Seat Angle With Top & Btm. Flanges Welded to Column
		CB4	Monotonic	W8x20	W8x20	8 #3 bars	Unstiffened Seat Angle With Bottom Flange Welded to Column and a Tension Plate Welded to the Top Flange
		CB5	Monotonic	W8x20	W8x20	15 #3 bars	Same as CB4
Johnson &Law	1983	JX1	Monotonic	457x191 UB 67	203 x 203 UC46	Ar= 1.95 (sq in)	Flush End Plates
		JX2	Monotonic	457x191 UB 67	203 x 203 UC46 Concrete Encased	Ar= 1.95 (sq in)	Flush End Plates
		JY1	Monotonic	457x191 UB 67	WF or EWF	Ar= 1.95 (sq in)	Flush End Plates ? to minor axis of column
		JY2	Monotonic	457x191 UB 67	WF or EWF Concrete Encased	Ar= 1.95 (sq in)	Flush End Plates ? to minor axis of column
		JC1	Monotonic Unsymmetric	457x191 UB 67	EWF Concrete Encased	Ar= 1.95 (sq in)	Flush End Plates ?
		JC2	Monotonic Unsymmetric	457x191 UB 67	EWF Concrete Encased	Ar= 1.95 (sq in)	Flush End Plates ?

Ar = Area of Reinforcing Steel

Table 1.2-1 (Cont.) Summary of Experimental Work On Semi-Rigid Composite Beam-to-Column Connections

Investigators	Date	Specimen	Loading	Beam	Column	Top Connection	Steel Connection
Nethercot, Lam, Davison	1990	C1	Monotonic Unsymmetric	305x165x46 UB	203x203x46 UC	A-142 Mesh	Unstiffened Seat Angle With Single Framing Angle
		C2	Monotonic	305x165x46 UB	203x203x46 UC	6-10mm bars & A-142 Mesh	Same as C1
		C3	Monotonic	356x171x67 UB	203x203x46 UC	A-142 Mesh	Same as C1
		C4	Monotonic	356x171x67 UB	203x203x46 UC	A-142 Mesh	Same as C1
		C5	Monotonic	356x171x67 UB	203x203x46 UC	6-10mm bars & A-142 Mesh	Same as C1
		C6	Monotonic	305x165x46 UB	203x203x46 UC	A-142 Mesh	Same as C1
		C7	Monotonic	305x165x46 UB	203x203x46 UC	6-10mm bars & A-142 Mesh	Same as C1
		C8	Monotonic	305x165x46 UB	203x203x46 UC	8-12mm bars & A-142 Mesh	Same as C1
		C9	Monotonic	305x165x46 UB	203x203x46 UC	6-12mm bars & A-142 Mesh	Same as C1
		C10	Monotonic	356x171x67 UB	203x203x46 UC	A-142 Mesh	Same as C1
		C11	Monotonic	356x171x67 UB	203x203x46 UC	6-12mm bars & A-142 Mesh	Same as C1
		C12	Monotonic	305x165x46 UB	? Girder ?	A-142 Mesh	Same as C1

21

Table 1.2-1 (Cont.) Summary of Experimental Work On Semi-Rigid Composite Beam-to-Column Connections

Investigators	Date	Specimen	Loading	Beam	Column	Top Connection	Steel Connection
Altman, Maquoi, Jaspart	1991	30x3c.2 & .6	Monotonic	IPE 300	HEB 200	12-10 mm bars in two layers	Top & Btm. Framing Angles and Single Web Framing Angle
		30x3c.3 & .8	Monotonic	IPE 300	HEB 200	12-14 mm bars in two layers	Same as 30x3c.2
		30x3c.1 & .7	Monotonic	IPE 300	HEB 200	12-18 mm bars in two layers	Same as 30x3c.2
		30x2c.2 & .5	Monotonic	IPE 300	HEB 200	12-10 mm bars in two layers	Btm. Framing Angle and Single Web Framing Angle
		30x2c.1 & .6	Monotonic	IPE 300	HEB 200	12-14 mm bars in two layers	Same as 30x2c.2
		30x2c.3 & .7	Monotonic	IPE 300	HEB 200	12-18 mm bars in two layers	Same as 30x2c.2
		36x3c.1 & .5	Monotonic	IPE 360	HEB 200	12-10 mm bars in two layers	Top & Btm. Framing Angles and Single Web Framing Angle
		36x3c.2 & .6	Monotonic	IPE 360	HEB 200	12-14 mm bars in two layers	Same as 36x3c.1
		36x3c.3 & .7	Monotonic	IPE 360	HEB 200	12-18 mm bars in two layers	Same as 36x3c.1
		36x2c.2 & .7	Monotonic	IPE 360	HEB 200	12-10 mm bars in two layers	Btm. Framing Angle and Single Web Framing Angle
		36x2c.1 & .6	Monotonic	IPE 360	HEB 200	12-14 mm bars in two layers	Same as 36x2c.2
		36x2c.3 & .5	Monotonic	IPE 360	HEB 200	12-18 mm bars in two layers	Same as 36x2c.2

22

1.2.2.2 Johnson, R.P. and Hope-Gill, M. (1972)

A series of five test specimens were studied at Cambridge University. The specimen setup was two beams attached to a column in a cruciform type arrangement. The steel connection used in all the specimens was a set of three framing angles attached to the bottom flange of the beam; one attached to the bottom face of the flange and two (one each side of the web) to the top face of the flange. All specimens had a reinforced composite slab continuous over the joint.

The basic problem being investigated was the concern of underestimating moments in columns which may be introduced from a continuous composite floor system. If a continuous slab with reinforcing is supplied across the joint the moment induced into the column may not be negligible particularly for the case of unequal adjacent span lengths or unequal loading of adjacent spans. The main parameters investigated were:

1. The reinforcing steel force (A_r x F_{yr}) over the steel beam force (A_{gb} x F_{yb})
    Where:
    A_r = Area of reinforcing steel
    F_{yr} = Yield stress of the reinforcing steel
    A_{gb} = The gross area of the steel beam
    F_{yb} = The yield stress of the steel beam
2. The beam web slenderness with d_w/t_w ratios which ranged from 32.4 to 56.4
    Where:
    d_w = Depth of the beam web
    t_w = Thickness of the beam web

The first of the five specimens (HB50) was tested in 1969 with very successful results. Tests on HB51 through HB54 were conducted based on the results of HB50.

One aspect of interest to the investigators was the comparison of the failures associated with the semi-rigid composite connections compared to the failures associated with rigid connections. These tests showed that semi-rigid composite connections could have the same or larger moment capacities than comparable rigid connections and at the same time provide much greater rotation capacity than their rigid counterpart. Only the connection with the most slender web (HB54) failed from buckling and this would have probably been prevented if a web angle had been provided, as probably necessary for construction stability. The investigators believed that the restraint provided by the seat angle prevented flange buckling for the semi-rigid connections as compared to flange buckling that had occurred in similar rigid connections tested elsewhere.

1.2.2.3 Echeta, C.B. and Owens, G.W. (1981)

A series of five test specimens were studied at Imperial College. The first specimen of the series was an arrangement of two beams attached to a column in a cruciform type arrangement while the arrangement of the remaining four test specimens was one beam attached to a column in a cantilever type arrangement. The two different setups were intended to represent interior and exterior column connections. Information about the first specimen (1B) was located in Echeta and Owens (1981) while information of the remaining connections was apparently only disseminated in Echeta's Ph.D. thesis which the writer was unable to obtain. Thus the information presented about the latter specimens is based solely on the summary by Zandonini (1989).

The steel connection portion of specimen 1B was an unstiffened seat angle connection with a single framing angle attached to the web for stability during construction. On one side of the specimen the beam was set flush against the column face while on the other side the beam was set with a two-millimeter gap between the beam end and the column face (apparently representing possible mill tolerance). Connection 2BS was similar to 1B with the exception that the top side of the bottom

beam flange was also attached to the column by means of two plates located on either side of the web. The steel connections for specimens 3BS through 5BS were modified end plate connections which consisted of two plates that were centered about the bottom flange of the beam.

The primary intent of the test series was the validation of a design approach for semi-rigid composite connections that was developed by Echeta and had been based on the testing program conducted by Johnson and Hope-Gill (1972). They were also seeking to pursue further development of these connections to concrete filled hollow sections.

The loading scheme used for specimen 1B was of particular interest. To control the shear to moment ratio (V/M) applied to the connection, two loads were applied to each beam; one load was applied at the end of the beam while the other was applied directly adjacent to the connection. The second load was attached to the underside of the beam flange (which is not ideal because of the tendency to inhibit local instability of the beam web and bottom flange). By controlling the values of these two loads the V/M ratio could be simulated more realistically compared to the case where one load is applied and thus the V/M ratio is fixed. This allowed the use of a more accurate V/M ratio because it could be changed as the connection softened. The V/M ratio used was based on a hypothetical design situation.

Dead load was simulated on the connection by applying load immediately adjacent to the joint just prior to casting. This subjected the connection to shear but, since the beams were propped at their ends, minimal rotational deformations would have been induced. This is the only test setup for semi-rigid composite connections that attempted to simulate the actual loading sequences of a connection in composite floor construction. The column was also loaded to 55% of the ultimate column capacity to determine if column loading had any effect on the connection deformation behavior.

All the specimen tests were ended as a result of excessive deformation with no beam flange or web buckling. This attests to the concept of semi-rigid composite connections being very ductile and having sufficient rotation capacity to allow plastic

design. The axial load in the column and the interaction between the shear and moment forces resisted by the connection did not appear to cause any adverse affects. The investigators concluded that the connection moment capacity could be conservatively estimated by the reinforcement force (A_r x F_{yr}) acting through its lever arm to the seat angle.

1.2.2.4 Dalen, K.V. and Godoy, H. (1982)

A series of five test specimens were studied at Queen's University. The specimen setup was two beams attached to a column in a cruciform type arrangement. The specimens included connections found in all three connection classification groups; simple, semi-rigid, and rigid. The simple connections were unstiffened seat angles with framing angles attached to the top flange of the beam. The rigid connections were unstiffened seat angles with the beam flanges directly welded to the column with full grove welds. The semi-rigid connection was an unstiffened seat angle with the bottom flange directly welded to the column with grove welds and the top flange attached to the column with a plate welded to the top beam flange at one end and the welded to the column flange at the other. For the simple and semi-rigid connections the steel only connection was tested along with two composite connections with varying degrees of reinforcement. The rigid connection was tested as a steel connection and as a heavily reinforced composite connection. The main items of interest in this study included determining:

1. The yield moment (the point at which linear moment-rotation behavior ceased) and the ultimate moment capacity (the point at which the moment-rotation behavior became horizontal or started to decline)

2. The rotation that the connection could undergo without a significant reduction of moment capacity (i.e., the ductility of the connection)

3. The influence of different amounts of top longitudinal reinforcement on the strength and rotational behavior of the connection

The ultimate moment capacity of the composite connections ranged from 1.5 to 6 times the ultimate moment capacity of the steel only connections. The greatest increases were seen for the weakest steel connections and only moderate increases were seen for the rigid steel connection. The investigators concluded that even the lightly reinforced simple and semi-rigid connections could posses moment capacity equal to or above the negative moment capacity of the composite beam and posses rotation capacity far exceeding conventional rigid connections. An increase in the amount of longitudinal reinforcement resulted in a significant increase in both yield and ultimate moment capacities of the connections. Because of the rotation capacity observed, it appears conventional design procedures used for the analysis of frames with rigid steel connections may be used for frames with composite connections without concern about the adequacy of the rotational capacity of the connections.

It should be noted that although CB1 (the simple steel connection with composite slab) developed a large connection moment, it was only after large rotations and thus these moments may not be obtainable in a practical situation.

1.2.2.5 Johnson, R.P. and Law, C.L.C. (1981)

A series of six test specimens were studied at The University of Warwick. The specimen setup was two beams attached to a column in a cruciform type arrangement. The steel connection for all the specimens was a flush end-plate connection. The beams were attached to the strong column axis for specimens JX1, JX2, JC1, and JC2 and were attached to the weak column axis for specimens JY1 and JY2. The columns were encased in concrete for specimens JX2, JY2, JC1 and JC2 while the other two specimens were attached to the plain steel columns. JX1 had originally been tested without

stiffeners in the column and the column web yielded and then buckled at a moment of only 55% of the connection moment achieved after stiffeners were put in place.

In general this series of tests studied the following parameters (Zandonini 1989):

1. Distribution of shear connectors
2. Encasement of the column
3. Framing into column minor or major axis
4. Slab to beam depth ratio
5. Presence of axial load in the column
6. Effect of unsymmetric loading

One of the main goals of Johnson and Law's testing program was the verification of an analytical model developed for the prediction of upper and lower bounds of the moment rotation curves of flush end-plate composite connections. The moment-rotation stiffness for the flush end-plate connection was developed by combining load deformation relationships for the bolts, the column flanges, and the end-plate. The moment-rotation stiffness for the composite connection was derived through elastic analysis of the portions of the connection associated with composite action only as shown in Figure 1.2-1.
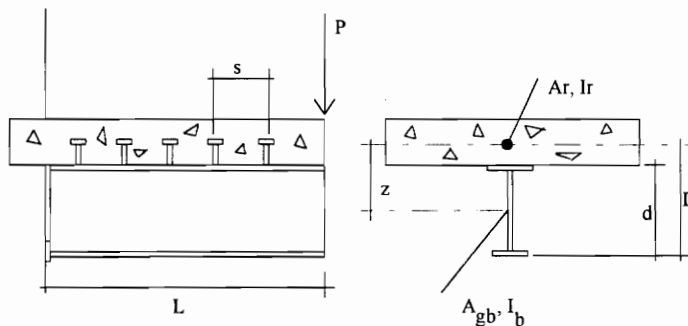
Figure 1.2-1 Main Details of Composite Connection Mechanism

28

The resulting relationship for the composite portion of the connection is given by (Johnson & Law 1981):

$$\theta = \frac{PL^2}{2\sum EI} + \left(\frac{1}{EdA_r} - \frac{z}{\sum EI}\right)\left\{\frac{K_o}{\sqrt{F}}\left(\cosh\sqrt{F}L - 1\right) + \frac{QPL^2}{2F}\right\}$$

Where

A_{gb} = gross area of the steel beam

A_r = area of longitudinal reinforcing in the slab

d = depth of the steel section

D = distance from the bottom flange of the beam to the c.g. of the reinforcing steel

P = applied force as shown in Figure 1.2-1

I_r = the moment of inertia of the reinforcing steel

I_s = the moment of inertia of the steel beam

k = modulus of shear stud connectors

L = distance from the connection to the point where load F is applied (simulating distance to the inflection point of the beam)

s = shear stud connector spacing

z = distance from the c.g. of the steel beam to the c.g. of the reinforcing steel

$$\sum EI = EI_r + EI_s$$

$$F = \frac{k\overline{EI}}{s\overline{EA}\sum EI}$$

$$Q = \frac{kz}{s\sum EI}$$

$$K_o = \frac{PL\left(\frac{1}{D} - \frac{Q}{F}\right)}{\sinh\sqrt{FL}}$$

$$\overline{EA} = \cfrac{1}{\left(\cfrac{1}{EA_r} + \cfrac{1}{EA_s} \right)}$$

$$\overline{EI} = \sum EI + \overline{EA}z^2$$

To develop an analytical model for the composite connection with the flush end-plate, the two models (flush end-plate and composite connection) were combined. Although the analytical relationship derived to describe the end-plate moment-rotation behavior was not believed to be very accurate, Johnson and Law believed that the composite connection was not very sensitive to the steel connection behavior and consequently believed the use of the flush end-plate model combined with the composite connection model was justified.

To examine an upper and lower bound for the moment-rotation behavior of the flush end-plate composite connection, two shear stud distributions were chosen. P-type analysis modeled a connection with shear studs grouped near the point of inflection while F-type analysis modeled a connection with shear studs evenly distributed between the beam end and the inflection point. In both cases the number of shear studs was equal and sufficient to provide full shear connection between the slab and beam.

Specimens JX and JY had one side of each specimen with shear studs grouped near the end of the cantilever (P-type analysis) while the other side had the shear studs evenly distributed (F-type analysis). The moment-rotation behavior observed for these specimens did indicate that these two stud arrangements resulted in upper and lower response curves which the investigators believed were upper and lower bounds for the connection moment-rotation behavior. Comparison of the moment-rotation behavior to the analytical model indicated that the model was reasonably accurate. The distribution of the studs also seemed to affect the crack patterns observed in the specimens. The specimens with shear studs grouped near the end had almost straight cracks running

transversely across the slab. The specimens with uniformly distributed studs had inclined crack patterns indicating increased shear lag.

Concrete encasement was shown to have a significant effect for beams framing into the minor axis of a column while having a minor effect for beams framing into the major axis of the column. JY2 (with column encasement) had an ultimate moment capacity 55% higher than JY1 (without column encasement). The investigators believed that column encasement was sufficient to allow the joint to be assumed to act as rigid up to one-half of the ultimate moment strength of the connection when shear connectors were distributed uniformly.

The effect of unsymmetric loading was studied with specimens JC1 and JC2. One side of the specimen was loaded until the joint was at its plastic moment of resistance then the other side was loaded up to its moment of resistance then both were loaded together to failure. It was observed that the joint which was more heavily loaded (i.e., the first joint loaded) tended to increase the bending stiffness of the opposite joint. The difference between specimens JC1 and JC2 was the depth of the composite slab; JC1 125-mm and JC2 200-mm. The increase in slab depth appeared to have a stiffening effect on the moment-rotation response for the connection.

1.2.2.6 Davison, J.B., Lam, D., and Nethercot, D.A. (1990)

A series of 12 composite specimens ("C" connections) and seven plain steel specimens ("S" connections) were studied at the University of Sheffield. The test setup varied between two beams being attached to a column in a cruciform arrangement and one beam attached to a column in a cantilever arrangement. The steel connection used for all specimens consisted of unstiffened seat angles and single web angles. The composite specimens had light weight concrete composite slabs continuous over the joint with varying degrees of reinforcement.

31

The general goal of the study was to determine what effect the presence of a composite floor slab had on the performance of simple steel connections. To this end, a series of connections were chosen as being a typical array of connections that would be found in a composite floor bay as shown in Figure 1.2-2.

This array of specimens allowed the following effects to be studied:

1. Profiled steel deck orientation
2. Column orientation
3. Internal or external column position
4. Amount of slab reinforcement
5. Varying effective slab widths
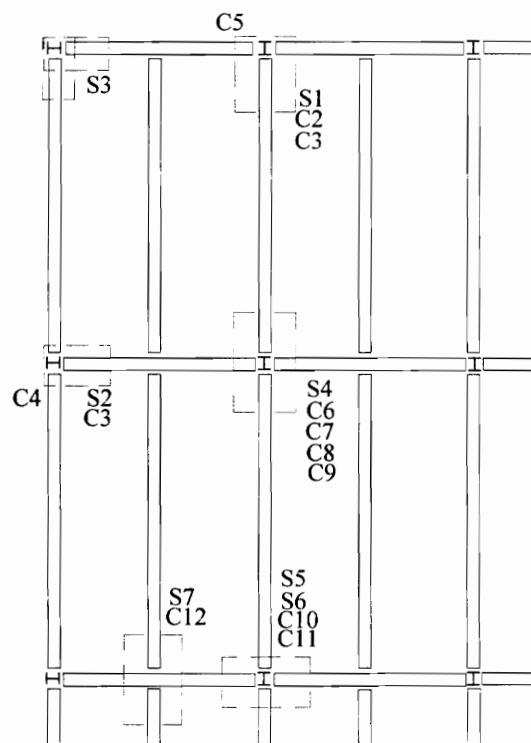
Figure 1.2-2 Theoretical Locations For Test Connections

Connections S7 and C12 appear to have been beam-to-girder connections. Unfortunately the description of the connection details, their setup and results were very minimal and no pertinent conclusions could be drawn nor insight drawn into the testing program.

The seven bare steel connections were tested to provide a basis of comparison for the composite connection and to determine the bare steel connection contribution to the composite connection behavior.

Composite specimens, reinforced with only wire mesh, had moment capacities ranging from 4.2% to 52.6% of the plastic moment capacity of the beam. These specimens lost most of their stiffness once the slab cracked; in addition, the mesh was shown to have very limited ductility. The orientation of the steel decking appeared to have its largest effect on these specimens. The specimens with decking orientated parallel to the beam did much better than the specimens with decking orientated perpendicular. This was primarily because the decking represented a relatively large percentage of the steel in the specimen compared to the specimens with reinforcing steel bars and thus its contribution to the behavior was increased. In general the following conclusion were drawn:

1. Composite joints have enhanced strength and stiffness compared to the plain steel connections.
2. Small increases in the amount of reinforcement over the minimum steel mesh resulted in connection moments close to the plastic moment capacity of the beam.
3. The full width of each specimen was effective in resisting tensile forces (as indicated by strain gages on the concrete and the reinforcing steel).
4. Problems with proper anchorage of the longitudinal reinforcement at external column joints limited the moment capacity that could be developed in these connections.

The reinforcing steel in two specimens fractured at relatively small rotations (approximately 10 mrad). One connection was reinforced with wire mesh only while the second was reinforced with high strength bars and wire mesh. The premature fracture of the mesh was not unexpected because mesh is generally not very ductile. The fracture of the high strength bars was believed to be primarily because of the fact that the base of the connection that failed was prevented from slipping and thus all the connection deformation was forced to occur in the slab. The investigators took the fracture of these two specimens as a warning that semi-rigid composite connections may not provide adequate ductility in all cases.

1.2.2.7 Altmann, Maquoi, and Jaspart (1991)

A series of 38 interior composite joints and 18 exterior and interior bare steel joints were studied at The University of Liege. The specimen setup was two beams attached to a column in a cruciform type arrangement. The steel connections were unstiffened seat angles with single web angles. An additional framing angle attached to the top beam flange for some of the specimens. Composite slabs with varying degrees of reinforcement were continuous over the specimen joints. The variables studied in this series of tests included:

1. The height of the beam (varied by using different beam sections; IPE 240s, IPE 300s, and IPE 360s)
2. The thickness of the framing angles (varied using 0.39-in. and 0.51-in. thickness)
3. Whether or not the top beam flange was attached with a framing angle
4. The percentage of reinforcement (varied between 0.67%, 1.3%, and 2.1% of slab area)

All the IPE 240 beams collapsed from buckling of the lower beam flange and not from connection failure so the results of these were not presented by the investigators.

Test specimens with IPE 300 beams and with 3 framing angles had connection moments varying from 94% to 114% of the plastic moment of the composite beam while those with two framing angles had connection moments varying between 81% and 99% of the beam plastic moment capacity. The IPE 360 specimens with 3 framing angles had connection moments varying from 77% to 85% of the beam plastic moment capacity while those with 2 framing angles had connection moments varying between 67% and 83% of the beam plastic moment capacity. Most failures resulted from column web buckling or excessive yielding of the reinforcing steel. Only one test, 30x2c.1, had a brittle failure resulting from shear failure of the bolts attaching the bottom flange of the beam to the seat angle. General conclusions were:

1. Increase in reinforcement percentage increased rigidity and ultimate strength of connections; in addition, the increase in reinforcing may change the failure mode from excessive yielding of the reinforcing to buckling of the column web
2. Framing angle thickness had little or no effect on the connection behavior
3. Addition of an upper cleat did not have much effect until large deformations were incurred at which time it supplied some additional moment capacity to the connection

1.2.3 Leon's Research and Design Guidelines

Dr. Roberto T. Leon is an associate professor in the department of Civil and Mineral Engineering at the University of Minnesota, USA, and was the recipient of the 1993 AISC T.R. Higgins Award for his work on semi-rigid composite connections. Over the past ten years Leon has been involved in developing the concept of semi-rigid composite connections and semi-rigid composite frames. He has conducted comprehensive experimental and analytical studies, investigating the behavior of semi-rigid composite connections (SRCC) and semi-rigid composite frames (SRCF) under gravity, wind, and seismic forces. Based on these investigations Leon has developed design recommendations and design procedures which incorporate SRCC and SRCF into standard composite girder and frame design (Leon 1993).

Based on the research performed, Leon believes the real advantage of semi-rigid composite connections is their use in unbraced composite frames up to ten stories to resist a combination of gravity and lateral loads. By using semi-rigid composite frames rather than fully rigid frames a significant reduction in connection cost could be achieved.

He feels the use of semi-rigid composite connections will not create a significant cost savings in the girder design because the decrease in the girder steel area will most likely be offset by an increase in the cost resulting from 100% composite action (currently suggested for SRCC design) and the additional reinforcing steel required at the supports. The major difference in the girder design would be a substantial decrease of service load deflections for girders with semi-rigid composite connections versus a girder without semi-rigid composite connections (Leon and Ammerman 1990). A cost savings may be realized for cases where the live load exceeds the dead load by a factor of approximately two or above (i.e. a case where the steel beam section is not chosen based on construction loads)(Leon 1990).

Aside from the cost advantage that semi-rigid composite frames would have over rigid frames the semi-rigid composite frames have another very desirable aspect. Modern

seismic design codes utilize capacity design, the frame deforms at pre-determined and carefully detailed locations, while the remaining structure remains elastic. To prevent yielding and buckling of columns it is necessary to use a strong column weak beam design approach. The semi-rigid composite connections provide the link between the these two elements and because the capacity of the connection is limited by its details it is possible to limit the amount of force transferred from the beam to the column and accommodate the needed deformation in the connection (Leon 1993).

1.2.3.1 Experimental Investigation

A summary of Leon's experimental program is presented in Table 1.2-2. Tests SRCC1MR through SRCC6CR have been conducted and results have been reported in Leon et. al. (1987), Ammerman and Leon (1987), and Leon (1990). Tests SRCC7C through SRCC10M were originally intended as part of the experimental investigation but no information has been located on this series of tests. One page summaries of each specimen are located in Appendix B. These summaries give details of the connection, test setup and moment rotation curves. For additional details the reader is referred to the previously mentioned references.

Table 1.2-2 Summary of Experimental Work Associated With Leon

Specimen Label	Type	Column Size	Beam Size	Top Connection	Bottom Connection	Web Connection
SRCC1MR	1MA	W14x99	W14x38	Solid 4-in slab with eight No. 4, and L6x4x3/8, 8 in wide	L6x4x3/8, 8 in wide, four 3/4-in A325 bolts to beam and two to column flange	Two L4x3-1/2x1/4, 8-1/2 in wide, three 3/4-in A325 bolts
SRCC1ML	1MA	W14x99	W14x38	Solid 4 in slab with 8 No.	Same as SRCC1MR	Same as SRCC1MR
SRCC1C	1CB	W14x99	W14x38	Same as SRCC1ML	Same as SRCC1MR	Same as SRCC1MR
SRCF2C	1CC	W14x120	W14x38	5-in slab on 2-in metal deck with eight No. 4 bars (?4-in Slab?)	L7x4x3/8, 8 in wide, four 1-in A325 bolts to beam and two to column flange	Two L4x4x1/4, 11 in wide, three 1-in A325 bolts
SRCC3C	1CB	W14x120	W14x38	Sames as SRCF2C (?Without Metal Deck?)	L7x4x1/2, 9-1/2in wide, four 3/4-in A325 bolts to beam and two to column flange	Same as SRCF2C
SRCC4CM	2MA	W14x145	W14x57	Sames as SRCF2C	Plate 8 in wide, 10 in long, 1/2 in thick, 1/2 fillet weld to beam, full pen grove to column	Two L5x5x5/16, 14 in wide, with five 7/8-in A325 bolts
SRCC5M	3MA	W14x145	W14x57	Sames as SRCF2C	L8x8x3/4, 11-1/4 in wide, six 7/8 in A325 bolts on each leg	None
SRCC6CL	4CA	W14x145	W14x57	Sames as SRCF2C	None	Two L5x5x1/2, 17.5 in wide, with six 7/8-in A325
SRCC6CR	4CA	W14x145	W14x57	Sames as SRCF2C	None	Same as SRCC6CL
SRCC7C	2CA	W14x145	W14x57	Sames as SRCF2C	Same as SRCC4M	Same as SRCC4M
SRCC8C	3CA	W14x145	W14x57	Sames as SRCF2C	Same as SRCC5M	Same as SRCC5M
SRCC9M	4MA	W14x145	W14x57	Sames as SRCF2C	Same as SRCC6CL	Same as SRCC6CL
SRCC10M	4MA	W14x145	W14x57	Sames as SRCF2C	Same as SRCC6CR	Same as SRCC6CR

1.2.3.2 Analytical Investigation

The analytical investigation conducted by Leon and colleges consists of two parts; finite element modeling of semi-rigid composite connections and a series of frame designs. The finite element models were used to develop parametric equations that could be utilized to model semi-rigid composite connections. The frame designs were conducted to develop a simplified method to design semi-rigid composite frames.

A three dimension finite element model was developed by Kulkarni (1990) using the finite element program ADINA. Figure 1.2-3 shows the general configuration of the connection modeled. In developing the model the following considerations were addressed (Leon, et. al. 1987):

38

1. The distribution of stresses in both the slab and the beam. The distribution of stresses in the experimental composite slabs was found to be non-uniform across the slab width and the distribution of stresses in the beam was not linear near the connecting elements.

2. Effect of bolt tension on the slip of the connections. The bolt tension in the seat angles was determined experimentally to have a significant impact on the slip of the connection.

3. Effect of the type and amount of slip between the angles and beams. The friction force, consequently the coefficient of friction between the steel parts, determines the initial type of slip (sudden or gradual) and the milling tolerances of the bolt holes determines the amount of slip.

4. Effectiveness of shear connections. The performance of the shear connectors used to connect the slab to the beam is a function of shear connector size, shape, arrangement, location and concrete strength.

5. Effect of yielding reinforcing bars, growth of cracks in the concrete slab, and the possibility of local bond failures between the bars and concrete.

6. Effect of the web angles which are ideally included only to carry the shear force from the beam to the column.

7. Tension stiffening of the slab was neglected.
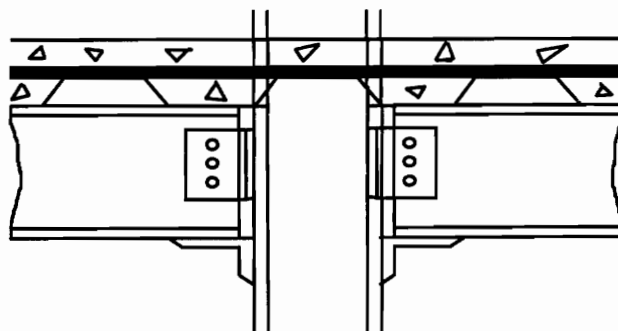
Figure 1.2-3 General Connection Configuration For Finite Element Model

39

The first part of the finite element modeling involved modeling the framing angles used in the connections. These models were developed to determine the load deformation behavior of the angles. Once the load deformation behavior for the framing angles was determined, the full connection was modeled with the framing angles replaced by equivalent truss elements that included the non-linear load deformation response determined in the first part. This model was then modified and calibrated to the experimental investigation results. A number of general observations were noted from the results of the finite element analysis.

1. The initial portion of the moment-rotation curve was always very linear.
2. The negative moment-rotation behavior was predominantly governed by yielding of the slab reinforcing steel.
3. The web angles did not impact the connection response significantly until large rotations were reached (i.e., greater than 20 mrad). In this region the web angles provided a stiffening effect that allowed the connection to continue to increase moment capacity with rotation (Kulkarni 1990)(Leon 1993).
4. Yielding of the column flanges was limited.
5. The connections initial stiffness varies linearly with the depth of the section and is not affected by the amount of reinforcing steel in the slab.
6. The percentage of the total element strength used at two critical stages of connection behavior were:

Yield Moment	Reinforcing Steel	68%	Seat Angle	17%
Ultimate Moment	Reinforcing Steel	98%	Seat Angle	25%

Based on parametric studies utilizing this finite element model, equations for the connection moment-rotation behavior were developed for both negative and positive moment regions. The following exponential equation was proposed for the negative moment-rotation behavior:

$$M(\theta) = C1(1 - e^{-C2\theta}) + C3\theta$$

Where:

$$C1 = 0.180[4(A_r)(F_{yr}) + 0.857(A_{sl})(F_{ysl})](d + Y2)$$
Controls the initial stiffness of the curve

$$C2 = 0.775$$
Determines the exact location for yielding of the connection

$$C3 = 0.007(A_{sl} + A_{wl})(F_{ysl})(d + Y2)$$
Controls the strain hardening portion of the curve

For positive moment-rotation behavior:

$$M(\theta) = C1(1 - e^{-C2\theta}) + (C3 - C4)\theta$$

Where:

$$C1 = 0.2400[0.48(A_{wl}) + A_{sl}](d + Y2)F_{ysl}$$
$$C2 = 0.0210(d + Y2/2)$$
$$C3 = 0.0100(A_{sl} + A_{wl})(F_{ysl})(d + Y2)$$
$$C4 = 0.0065(A_{wl})(F_{ysl})(d + Y2)$$

Where for both positive and negative moment-rotation behaviors:

θ = Rotation in mrad

Y2 = Distance from top of steel beam to center of reinforcing

d = Depth of beam

F_{ysl} = Seat angle yield stress

F_{ywl} = Web angle yield stress

F_{yr} = Reinforcing steel yield stress

A_r = Area of reinforcing steel continuous across support

A_{sl} = Cross-sectional area of seat angle

A_{wl} = Cross-sectional area of web angles

It should be noted that the exponential portion of the connection equations is very similar to the exponential equation developed by Fisher (1965) to model the load deformation behavior of bolts in double shear, and given by:

$$R = R_{ult}[1-e^{-\mu\Delta}]^{\lambda}$$

Where:

R = Bolt force

R_{ult} = Ultimate bolt force

e = Base of natural logarithm

μ = regression coefficient for bolt

λ = regression coefficient for bolt

Δ = Total bolt deformation and bearing deformation of the connected material

The second part of the connection equations is simply a strain hardening term and resembles that proposed by Richard, et. al. (1980) as an elastic plastic stress strain equation, and given by:

$$R = \frac{K_1\Delta}{\left[1+\left(\frac{K_1\Delta}{R_o}\right)^n\right]^{1/n}} + K_p\Delta$$

Where:

R = Parameter being modeled (typically a moment or a force)

R_o = A reference constant

n = A shape parameter

K_p = Slope of response in the extreme yielding stage

Δ = Some deformation (typically strain, rotation, or linear displacement)

In order to perform preliminary design checks, equations were developed to approximate the connection moment at service and ultimate loads for both positive and negative moment. The following equations were developed for the negative moment regions:

Service Load $\quad M_{\theta s} = 0.17[(4)(A_r)(F_{yr}) + (A_{sl})(F_{ysl})](d + Y2)$

Ultimate Load $M_{\theta u} = 0.245[(4)(A_r)(F_{yr}) + (A_{sl})(F_{ysl})](d + Y2)$

For positive moment regions:

Service Load $\quad M_{\theta s} = 0.25[0.5(A_{wl})(F_{ywl}) + (A_{sl})(F_{ysl})](d + Y2/2)$

Ultimate Load $M_{\theta u} = 0.25[1.25(A_{wl})(F_{ywl}) + 1.35(A_{sl})(F_{ysl})](d + Y2/2)$

Where variables are as defined previously.

In addition to the finite element modeling, Leon and colleagues designed a series of 27 three-bay, fixed-base frames utilizing semi-rigid composite connections (Leon and Forcier 1991)(Leon and Forcier 1991)(Leon 1993). Two important conclusions were derived from this study. The first conclusion is that accounting for the non-prismatic nature of composite girders did not make a significant difference in the frame response for combinations of gravity and lateral loads. Consequently, it seems reasonable to use a prismatic approximation of the beam for frame analysis. The second conclusion is that semi-rigid composite frames had increased collapse loads compared to rigid frames

(although small, approximately 2% for most of the cases covered). However, the corresponding drift at collapse was significantly increased because connections had reached the horizontal portions of their connection curves at frame collapse. (Kulkarni 1990) Additional details of this frame design study can be found in the previously mentioned references.

1.2.3.3 Design

Based on the experimental and analytical investigations discussed above, Leon and colleagues developed various recommendations for the design of frames and girders utilizing semi-rigid composite connections.

1.2.3.3.1 Frame Design

Possibly the most significant application for composite semi-rigid beam-to-column connections is in the design of unbraced frames less than 10 stories subjected to moderate wind and seismic loads. By replacing costly full moment connections with semi-rigid composite connections the overall cost of construction should be reduced. The following design guidelines have been suggested for semi-rigid composite frames (Leon and Forcier 1991)(Leon 1988):

Step 1) Design the columns of the frame as if the frame was a rigid non-composite frame. Size the steel beams as simply supported beams subjected to factored construction loads or factored dead loads.

Step 2) Provide sufficient shear connection to ensure 100% composite action.

Step 3) Replace rigid connections with semi-rigid composite connections and represent the connection behavior with a bi-linear model.

Step 4) Analyze the frame using a program that incorporates linear spring elements for the connections and find the resulting end moments.

Step 5) Design the connection slab steel based on the following relationship

$$M_{ue} = 0.66 \, A_r \, F_{yr} \, (d + Y2)$$

Where:

M_{ue} = Connection Moment Capacity

A_r = Area of reinforcing steel

F_{yr} = The yield stress of the reinforcing steel

d = The nominal depth of the steel beam section

$Y2$ = The distance from the top of the beam to the c.g. of the reinforcing steel

As a general rule the connection should be detailed for a connection moment being the lesser of $M_{fe}/2$ or $M_p/2$; where, M_{fe} is the fixed end moment for the loads and M_p is the plastic moment capacity of the beam (Ammerman and Leon 1990).

Step 6) Design the seat angle providing enough bolts to prevent slip under service loads and using minimum gage distances.

Step 7) Provide double web angle shear connections to carry entire shear force and increase the angle area by 50% above what would be required for shear alone. The area of the web angles should be increased by 50% since they will be

45

subjected to additional tension and fatigue from cyclic loading of wind and earthquake (Ammerman and Leon 1990).

It is recommended that a second order analysis be used for all unbraced frames which rely on semi-rigid composite connections for sway resistance. Although it is typical that P-Δ moments for frames less than 10 stories are small when rigid connections are used, the drifts associated with even low-rise structures can be substantial and the P-Δ moments can become significant when semi-rigid composite connections are used (Ammerman and Leon 1990).

1.2.3.3.2 Girder Design

Designers may want to take advantage of semi-rigid composite connections in braced frames to reduce live load deflections and possibly to reduce cost in cases where the ratio of live load over dead load is greater than two (Leon and Ammerman 1990). As mentioned before, the major reason the use of semi-rigid composite connections will not generally result in a cost savings, in this type of application, is because the increase in cost from the reinforcing steel and the use of 100% composite action will generally offset any resulting savings in steel beam weight. If nominal reinforcing steel is being provided in order to help control cracking over supports (as is done in many designs currently) the possibility for cost savings increases. Partially composite girders with semi-rigid connections should also work and would allow a significant savings over partially composite girders without semi-rigid connections. Partial composite action is not currently suggested because no experimental data has been gathered to determine the effect partial composite action would have on the connection moment-rotation behavior (Leon and Ammerman 1990).

The following are general considerations incorporated into semi-rigid composite girder design in braced frames. Many of the considerations also apply to unbraced frames (Leon and Ammerman 1990).

1. Unshored construction is assumed.
2. The beam is treated as a simply supported fully braced steel beam for all loading that occurs prior to concrete hardening.
3. The composite connection is subject only to loads applied after the concrete hardens.
4. The practical range for connection moment is between 50% to 85% of the fixed end moment from live load.
5. Connections are designed with slip critical bolts for which a one-in. diameter is a practical upper limit for bolt size. A325 or A490 bolts can be used. The connection should be checked as slip critical under service loads and as bearing for ultimate loads. Six bolts in the seat connection (three each side of the web) is believed to be the upper limit for the number of bolts.
6. Effective slab width of 4-7 column flange widths has been recommended based on the testing program (It should be noted that an effective slab width of 5 column flange widths was used in the finite element model development (Kulkarni 1990) and eight times the slab thickness was used in the design of the test specimen frame SRCF2C (Leon, et. al. 1987)).
7. Connections to exterior columns should be designed as simple connections to limit the unbalanced moment transfer into the column.
8. Currently it is suggested that semi-rigid composite connections should not be used on spans greater than 48-ft., section depths greater than a W27, and flange thickness (t_f) greater than 0.8-in.
9. Both light weight and normal weight concrete can be used.
10. The girder is not required to have the same connection at both ends.

11. A double angle shear connection is designed for the factored shear force as a bearing type connection. A minimum of 3 bolts is suggested since all double angles in the testing program had 3 or more bolts.

12. The recommendations for fully welded steel moment connections can be used as a conservative design approach when considering column side limit states. (It should be noted that this may be an unconservative approach as seen in Test SRCF2C because shear yielding of the interior column panel zone occurred despite the fact that the column met all recommendations for fully rigid connections (Leon 1987)).

The following steps have been recommended as the design procedure for girders with semi-rigid composite connections in braced frames (Leon and Ammerman 1990). Many steps also apply to girder design in unbraced frames.

Step 1)   Determine all loads and resulting moments.

Step 2)   Choose the desired end moment (M_{ue})based on the ranges indicated earlier.

Step 3)   Choose a steel beam that has an design moment capacity exceeding the factored construction moment and a design yield moment capacity exceeding the factored dead load moment. Check to ensure that the resulting composite beam with the end moments chosen in Step 2 is sufficient for factored loading, (as the construction loading will usually govern the steel beam selection, the designer may choose to revise the design end moment based on the end moment required to satisfy the ultimate moment on the composite beam).

Step 4)   Select a seat angle with sufficient cross-sectional area (A_{sl}) to develop the required horizontal force (H_a) based on the connection moment.

$H_a = M_{ue}/(d + Y2)$

$A_{sl} = 1.33 \, H_a/F_{ysl}$

Where:

F_{ysl} = The nominal yield strength of the seat angle

d = The nominal depth of the steel beam

$Y2$ = The distance from the top of the beam to the c.g. of the reinforcing steel

The factor of 1.33 is used to help ensure that the reinforcing steel will yield prior to the seat angle, a factor of 1.5 is suggested for unbraced frames because of possible reverse cyclic loading.

Select the number of bolts required and the appropriate bolt size in the seat connection, the required slip critical shear force per bolt (V_b) is

$V_b = H_a / L.F. / N$

Where:

L.F. = 1.6 assuming live load is the only load applied after the concrete has hardened and

N = number of bolts (usually assumed to be 6 witch is the maximum practical limit)

Select a seat angle width (l_a) at least as wide as the beam flange and an outstanding leg length as required for proper bolt spacing (minimum bolt gages and spaces are recommended)

Determine the minimum thickness for the seat angle (t_a)

$$t_a = A_{sl}/l_a$$

Step 5) Calculate the amount of slab reinforcing (A_r).

$$A_r = H_a/F_{yr}$$

Where:

F_{yr} = The nominal yield stress of the reinforcing steel

Care should be taken not to provide excess steel so that the reinforcing steel will yield prior to any local failures of the connection occurring.

Place the steel within the effective slab width as described previously

Step 6) Determine the moment capacity for the connection using equations developed and proposed by Kulkarni (for negative moment capacity).

Service Load:
$$M_{\theta s} = 0.17[(4)(A_r)(F_{yr}) + (A_{sl})(F_{ysl})](d+Y2) \geq M_{ue} / L.F.$$

Ultimate Load:
$$M_{\theta u} = 0.245[(4)(A_r)(F_{yr}) + (A_{sl})(F_{ysl})](d+Y2) \geq M_{ue}$$

Where variables are as defined previously.

Redesign the connection as required if above criteria not satisfied.

Step 7) Check compatibility; (Two Methods)

Method 1 (Simplified)

Assume that the connection rotation (θ) has a value of 2.5 mrad at service load and 10 mrad at ultimate load. Determine the connection moments at service and ultimate load by using the following equation for these values of rotation.

$$M(\theta) = C1(1 - e^{-C2\theta}) + C3\theta \geq M_{ue} \text{ or } M_{ue} / L.F.$$

Where:

$$C1 = A_r F_{yr}(d + Y2)$$

$$C2 = 32.9(A_{sl} / A_r)^{0.15}(d + Y2)$$

$$C3 = 24 A_{sl} F_{yl}(d + Y2)$$

$$\theta = \text{Rotation in radians}$$

Check to ensure that these moments exceed the required moments at service and ultimate loads.

Note: There appears to be discrepancies between the above connection coefficients and those reported in Kulkarni's thesis (1990).

When designing unbraced frames, the connection moment-rotation behavior must be modeled so that it can be included in the analysis. A tri-linear approximation has been suggested (Leon, et. al. 1990) in place of the exponential curve above. The following describes how to develop the tri-linear approximation:

Region 1

Region 1 starts at zero moment and rotation and assumes the initial stiffness (K_1) is 80% of the initial slope of the exponential curve.

$$K_1 = 0.8(C1 \times C2 + C3)$$

Region 2

Region 2 starts at the intersection of K_1 and the exponential portion of the connection curve, as related by:

$$K_1 \times \theta_1 = C1[1-e^{-C2\theta_1}] + C3 \times \theta_1$$

Where:

θ_1 = rotation at intersection

Then:

$M_1 = K_1 \times \theta_1$ = moment at intersection

$K_2 = (M_2\text{-}M_1)/(\theta_2\text{-}\theta_1)$ = stiffness in the second region

Note: Designer will likely need to solve for θ_1 using numerical or graphical solution since the equation is non-linear.

Region 3

Region 3 starts at the intersection of Region 2 with the connection curve at the point where the exponential term has reached 10% of its final value, as related by:

$$e^{-C2\theta_2} = 0.1 \quad \text{or} \quad \theta_2 = \ln(0.1)/\text{-}C2$$

Where:

θ_2 = rotation at intersection

Then:

$M_2 = 0.9C1 + C3\theta_2$ = moment at intersection

$K_3 = (M_3\text{-}M_2)/(\theta_3\text{-}\theta_2)$ = stiffness in the third region

Region 4

Starts at a rotation believed to be the maximum which would be seen by this type of connection in an unbraced frame.

$\theta_3 = 0.02$ radians = maximum expected rotation

$M_3 = C1 + 0.02\ C3$ = connection moment capacity

$K_4 = 0$ = stiffness in fourth region

Method 2 (Beam Line)

Develop beam lines for the service and factored loads. When developing these beam lines it has been suggested that the composite beam moment of inertia, I_{cb}, be taken as a weighted average of the positive flexure moment of inertia (I_{cbp}) and negative flexure moment of inertia (I_{cbn}) (lower bound moments of inertia found in the LRFD Manual (*Manual of* 1986) can be used to approximate these values) based on the portions of the beam in positive and negative bending.

$I_{cb} = 0.6\ I_{cbp} + 0.4\ I_{cbn}$

This relation is based on the idea that under uniform gravity loading, a fixed-fixed beam has about 60% of its length in positive bending and the remaining 40% in negative bending (Leon and Forcier 1991). It should be noted that in studying lateral load response of semi-rigid composite frames, Leon determined that the difference between treating the beam as prismatic, with the above assumption for I_{cb}, and analyzing the beam as non-prismatic did not yield a significant difference in the frame response, except for a slight increase in the frame collapse load for the prismatic case over the non-prismatic case (Leon and Forcier 1991). This, of course, only proves that for lateral loading there is

53

not a significant difference in the frame response. This may not be true for a girder subjected mainly to gravity loading.

Plot the exponential connection curve as defined in Method 1

Determine the connection moment and rotation at the intersections of the two beam lines and the connection curve. Check to ensure the connection moments exceed the required moments at service and factored loads.

Step 8) Check stresses in the steel section that result from unfactored loads

$\sigma_t = \sigma_D + \sigma_L$ = total stress in steel beam

Where:

$\sigma_D = M_D / S_s$ = dead load stress in steel beam

$\sigma_L = M_{LL} / S_{tr}$ = live load stress in steel beam

S_s = elastic section modulus of the steel beam

$S_{tr} = I_{LB} / (3d/4 + Y2/2)$ = transformed section modulus of the composite beam

I_{LB} = lower bound moment of inertia for the composite beam and can be obtained from the LRFD Manual (*Manual of* 1986)

The total stress from live and dead load should be less than F_{yb}; or, the total stress based on the arbitrary point in time concept:

$\sigma_t = 1.2\sigma_D + 0.5\sigma_L \leq 0.9\,F_{yb}$

Step 9) Design web angles for the maximum factored shear. These should be designed as a bearing connection using the same size of bolts selected for the seat connection.

Step 10) Determine the dead load deflection for required cambering based on the simply supported steel beam. Determine the service live load deflection based on a simply supported composite beam minus the contribution from the connection moment.

$$\delta_{SL} = \delta_{\text{Simple Support}} - (L/4)\theta_{SR}$$

Where θ_{SR} is the rotation at service load found in Step 7.

Step 11) Determine the required number of shear studs for full composite action. In the positive moment region use ΣQ_n to determine the required number of studs and use $A_r \times F_{yr}$ in the negative moment region.

The above design procedure is illustrated in an example located in Ammerman and Leon (1990).

1.2.4 Zandonini's Research and Design Guidelines

Dr. Riccardo Zandonini is an associate professor in the department of Structural Mechanics and Design Automation at the University of Trento, Italy. Over the past several years he has been involved with semi-rigid connections and over the last seven years he has been involved with a research study focusing on the behavior of partially restrained composite frames. The general goals of the research program include (Benussi, et. al. 1989):

1. The experimental description of the behavior of semi-rigid composite joints and determination of the main parameters governing this behavior
2. Study the most common types of joints through numerical analysis
3. Carry out parametric studies on the influence of semi-rigid joints on the behavior of frames
4. Evaluate and assess criteria and rules for the design of semi-rigid composite joints as well as of semi-rigid composite frames

The following is a summary of the experimental investigation, most of the analytical work, and design guidelines developed under Zandonini's guidance.

1.2.4.1 Experimental Investigation

The purpose of the experimental investigation was to determine the behavior of semi-rigid composite joints and to determine the main parameters that controlled this behavior. A summary of all connections tested (and with published information available) is presented in Table 1.2-3. Details of the connections, test setup, and test results are presented in the form of one page summaries located in Appendix C (for all but CT1C through CT4C)(Bernuzzi, et. al. 1991).

Table 1.2-3 Summary of Experimental Work Associated With Zandonini

Specimen Label	Applied Loading	Column Size	Beam Size	Top Connection	Steel Connection Connection
SJA10	Monotonic	HEB 260	IPE 300	8- 10mm bars	End Plate Near Bottom Flange
SJA14	Monotonic	HEB 260	IPE 300	8- 14mm bars	Same as SJA10
SJB10	Monotonic	HEB 260	IPE 300	8- 10mm bars	Flush End Plate
SJB14	Monotonic	HEB 260	IPE 300	8- 14mm bars	Same as SJB10
SJA14/1	Monotonic	HEB 260	IPE 300	8- 14mm bars	Same as SJA10
SJA14/2	Monotonic	HEB 260	IPE 300	8- 14mm bars	Same as SJA10
SJA14/3	Monotonic	HEB 260	IPE 300	8- 14mm bars	Same as SJA10
SJA14/4	Monotonic	HEB 260	IPE 300	8- 14mm bars	Same as SJA10
SJA14/5	Monotonic	HEB 260	IPE 300	8- 14mm bars	Same as SJA10
RJ 14	Monotonic	HEB 260	IPE 300	8- 14mm bars	Direct Weld Moment Connection
CT1	Monotonic	HEB 260	IPE 330	8- 14mm bars	Angles Attached to Both top and bottom of bottom flange
CT2	Monotonic	HEB 260	IPE 330	8- 14mm bars	Bottom Extended, Top Flush End Plate
CT3	Monotonic	Concrete Filled Tube	IPE 330	8- 14mm bars	Same as CT2
CT1C	Cyclic	HEB 260	IPE 330	8- 14mm bars	Same as CT1
CT2C	Cyclic	HEB 260	IPE 330	8- 14mm bars	Same as CT2
CT3C	Cyclic	HEB 260	IPE 330	8- 14mm bars	Same as CT3
CT4C	Cyclic	HEB 260	IPE 330	?	Seat Angle and Double Web Angles

Results from the test program showed that all the connections with solid slabs exhibited similar moment rotation behavior characterized by four basic stages (Bernuzzi, et. al. 1991):

1. Elastic behavior before the slab cracks

2. Elastic behavior after the slab cracks

3. Inelastic behavior as the connection deteriorates and the reinforcing steel yields

4. Plastic behavior with slightly increasing stiffness resulting from strain hardening of the reinforcing steel and the steel connection

Results also showed that the rotational capacity was always very high (typically between 20 to 30 mrad) for all the solid slab connections except RJ14 which failed as a result of the bottom flange buckling; after which, the specimen immediately dropped in load carrying capacity. The fact that bottom flange buckling also occurred for some of the SJ specimens but that they were able to still maintain substantial loading and continue to rotate indicated an important point. Rigid steel connections will tend to create composite connections with very low rotation capacity compared to composite connections using simple steel connections (Bernuzzi, et. al. 1991).

The mechanical fasteners performed very similar to the welded fasteners until the connection was in the vicinity of its ultimate moment capacity. At this point the mechanical fasteners allowed significant uplift of the concrete slab (Bernuzzi, et. al. 1991).

All specimens with metal decking (except CT1C through CT4C) failed as a result of longitudinal shear failure of the slab. This pointed out that the transverse reinforcement design was a rather important detail (simple steel wire mesh was provided as the transverse reinforcing) for these connections. When the transverse reinforcing was increased for connections CT1C through CT4C the longitudinal shear failure did not occur, instead these connections failed from low cycle fatigue of the steel connection while under positive moments (compression in the slab)(Bernuzzi, et. al. 1991).

1.2.4.2 Analytical Investigation

A few of the many analytical investigations that have been performed under Zandonini's guidance are briefly discussed in the following paragraphs. The finite element program ABAQUS was used to do all the analysis described in this section.

A frame modeling scheme was developed for frame analysis under static loading. This was developed to allow parametric studies of semi-rigid composite frames to be

conducted without requiring excessive computational time and effort and without making overly gross simplifications and assumptions(Zandonini and Zanon 1992). The unique aspects of this modeling scheme include how the composite beam and beam column joint is modeled as well as the fact that only common finite elements are utilized.

To model the composite beam certain assumptions had to be made. First, the beam is fully composite and the flexibility of the shear connectors can be ignored. Second, the flexural behavior of the concrete slab is small and can be ignored compared to the flexural behavior of the composite section. Third, the cross-section of the deformed beam remains plane (i.e., plane sections remain plane and no shear lag in the concrete slab). Fourth, the steel beam and concrete slab are in contact throughout the entire load history of the beam (i.e., no slab uplift).

With these assumptions the composite beam is modeled by replacing it with one beam element and two truss elements. The beam element is the steel beam and is located at the centroid of the steel beam. The constitutive properties for the beam are assumed to be linearly elastic. The first truss element is the reinforcing steel and is located at its centroid. The constitutive properties for the reinforcing steel are assumed to be perfectly elastic plastic. The second truss element is the concrete slab and it is located where it would create a statically equivalent beam when compared to the composite beam in the elastic portion of its behavior. The constitutive properties for the concrete are elastic plastic for compression and elastic with a cutoff for tension. The nodal points of the beams are independent while the nodal points of the truss elements are slaves to the beam node (based on the idea of plane sections remaining plane).

The joints are simulated with extensional and/or rotational spring elements and it is assumed that all joint deformation is concentrated at the end of the beam. The reader is referred to Zandonini and Zanon (1992) for additional details or clarification of this modeling scheme.

Analysis of two three-bay semi-rigid composite frames was performed using the above modeling scheme (Benussi, et. al. 1989). The two bays differed from each other in

the bay length and the interior to exterior beam span ratio. The moment-rotation behavior of connections SJA10 and SJA14 were used to define the characteristics of the rotational spring. The results of this analysis indicated the following:

1. For both ultimate and service loading, semi-rigid composite connections improve the load carrying capacity and the stiffness of the beam even when simply detailed steel connections are used.

2. As the slenderness of the composite beam increases, so does the effect the composite joint has on the overall deformability of the beam.

3. The collapse is always related to the development of a plastic mechanism (the order of the hinge development depends of the moment-rotation behavior model used for the joint and is discussed subsequently).

The influence of the model used to approximate the moment-rotation behavior of the joint (either multi-linear or bi-linear) on the response of the composite beam was another aspect studied. The choice of behavior model had little to no effect on the column moments but the multi-linear model did result in larger midspan deflections than when the bi-linear model was used. The most significant difference in the beam response was the order in which beam hinges formed. A midspan beam hinge formed first when the multi-linear model was used and thus the plastic mechanism developed once the joints reached their ultimate moment and rotation capacities. Hinges at the joints formed first when the bi-linear model was used. The joints were then required to continue to rotate after they had reached their ultimate moment in order to allow the midspan mechanism to develop. Overall, it is believed that the use of the bi-linear model provides sufficient accuracy for values of deflection (under service load), beam moments and columns moments, and will significantly simplify the frame analysis (Amadio, et. al. 1989).

An additional series of frame analysis were done in order to determine how semi-rigid composite frames would perform under seismic loading. The frames modeled were

designed according to Ammerman and Leon (1987). The joint behavior of test specimen CT1C was used for the joint response model in the analysis. Results were very satisfactory(Zandonini and Zanon 1992):

1. The interstory drift met Eurocode limits
2. Inelastic behavior was similar to that expected
3. The required joint rotation was far below the rotational capacity for CT1C determined experimentally
4. A low number of inelastic cycles occurred

Because it is convenient to measure joint rotation experimentally at some distance from the actual point at which the rotation is assumed to occur (i.e., the face of the column or the axis of the column) a relationship is needed to transform the measured moment-rotation values to actual moment-rotation values. In Puhali, et. al. (1990) beam curvature integration is used to develop a mathematical model that allows this transformation of values. The mathematical model is then confirmed by a non-linear finite element analysis of the joint.

1.2.4.3 Design

1.2.4.3.1 Accounting for Beam-to-Column Continuity

Two main philosophies may be adopted in designing braced (non-sway) frames. One way is to assume the beam-to-column joint provides continuity between the beam and the column and the other is to assume the joint does not provide continuity to the column but instead only provides continuity with an adjacent beam. The basic idea here is that semi-rigid composite joints develop their bending continuity through two mechanisms; continuity with the column and continuity with an adjacent beam.

If the joint is detailed such that the continuity to the column is negligible (such as by placing spacers around the column to avoid contact between it and the slab and by using a flexible steel connection) then the moment capacity of the joint can only be developed through continuity with an adjacent slab. If this is the case, analysis of the semi-rigid composite beam as an isolated beam may lead to serious inaccuracies (i.e., the beam should be analyzed as part of a continuous system of beams). Also, because the column is not continuous with the beam, the only moment induced into the column would be that found from an imbalance of shears between the two adjacent beams and can thus be analyzed on its own. If the joint is detailed such that bending continuity with the column is fully developed then the composite beam may be analyzed as an isolated beam without significant inaccuracies but the column analysis should include the effects of this continuity.

In reality there is always some degree of continuity with the column and it is suggested that the node at the column be modeled with two rotational springs and a torsional spring as shown in Figure 1.2-4. Where the moment-rotation behavior of the torsional spring is obtained by factoring the moment-rotation behavior of the joint by the ratio $(1-\chi)/\chi$. Where χ is an interaction coefficient which is zero if there is no joint-column interaction and 1 if there if full joint-column interaction. For service loads χ is about 0.85 if the concrete slab is in contact with the column and about 0.4 if not. Near collapse χ is about 0.8 and 0.3 respectively.(Puhali, et. al. 1990)
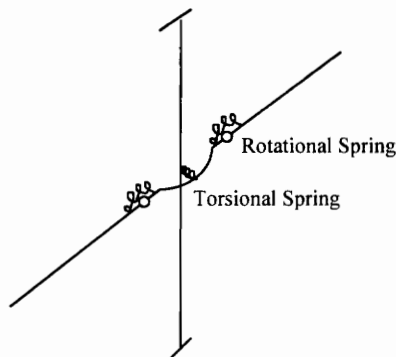
Figure 1.2-4 Suggested Beam-to-Column Joint Model

1.2.4.3.2 Simplified Analysis of Beams With Semi-Rigid Connections

A simplified approach of beam analysis was developed for the beam shown in Figure 1.2-5. This beam represents a typical composite beam in an interior floor bay. The semi-rigid connections used are assumed to provide sufficient continuity between the beam and the column such that the beam may be accurately analyzed separate from the rest of the structure. The method is a modified beam line analysis that accounts for the non-prismatic properties inherent in a composite beam subject to both positive and negative bending. The method for composite beams was derived by Balerini (1992) and some details of its use for composite and plain steel beams are given in Puhali et. al. (1990), Zandonini and Zanon (1991), and Zandonini and Zanon (1992).
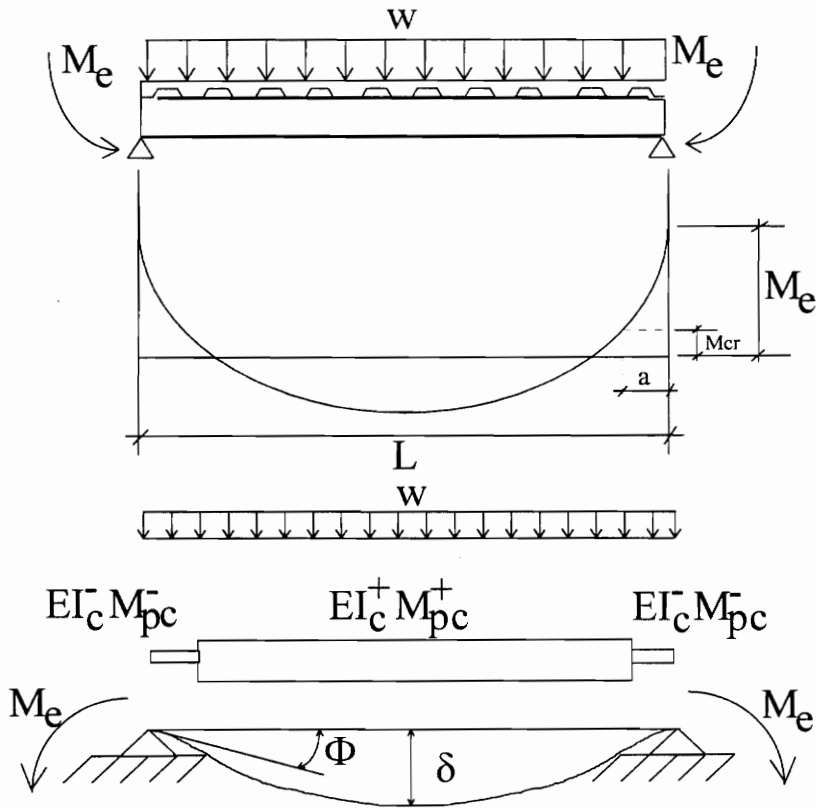
Figure 1.2-5 Main Features of Beam Model

The method assumes that full shear connection between the slab and the steel beam is supplied, tension stiffening in the regions of negative bending can be ignored, the steel section meets the requirements for plastic analysis of composite beams and the plastic hinge model may be used. With these assumptions the beam response can be fully described with four parameters; w, M_e, δ, and Φ as defined in Figure 1.2-5 using equilibrium and compatibility equations.

The four parameters w, M_e, δ, and Φ lead to four "Limit State Multi-Domains" (Zandonini and Zanon 1991) as shown in Figure 1.2-6. Each domain is related to the others through equations of equilibrium and compatibility.
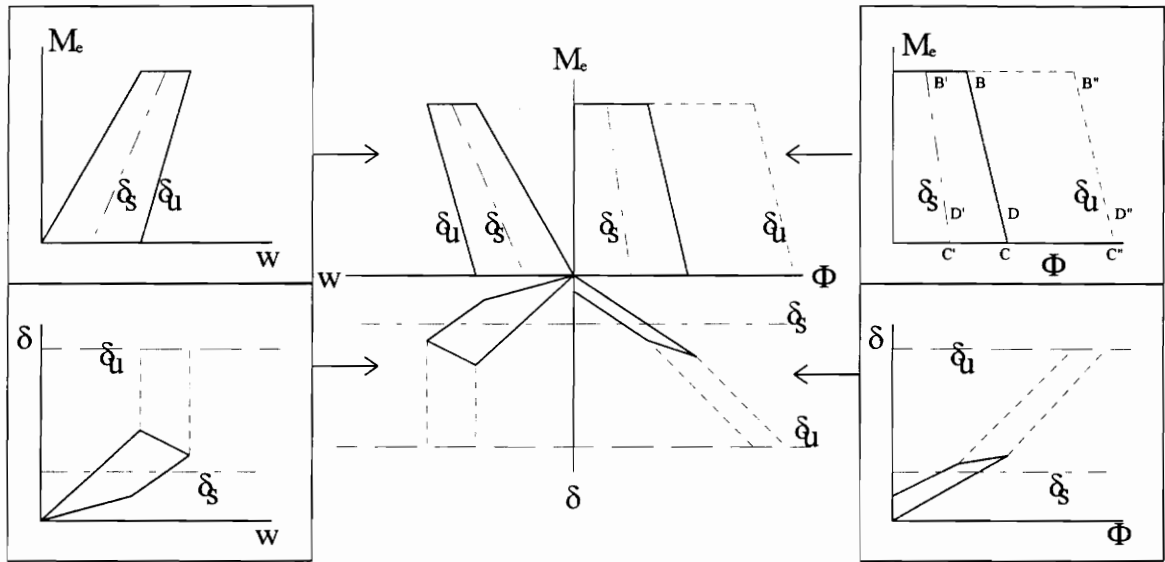
Figure 1.2-6 The Limit State Multi-Domains (Zandonini and Zanon 1991)

A convenient dimensionless form of the limit state domains for composite beams can be adopted. The equations governing the dimensionless $\bar{m}-\bar{\Phi}$ domain (See Figure 1.2-7 for location of the indicated lines) are given by:

Line C D $\qquad \bar{\Phi} = 1 - \dfrac{\bar{m}}{2} = \bar{w} - \dfrac{3}{2}\bar{m}$ $\qquad\qquad For\ \ 0 \leq \bar{m} \leq \bar{m}_{cr}$

Line D B

$$\bar{\Phi} = (1+\gamma)\left(1-\frac{\bar{m}}{2}\right) - \gamma\left(1-\frac{\bar{m}_{cr}}{2}\right)\sqrt{\frac{1+\bar{m}_{cr}}{1+\bar{m}}} = (1+\gamma)\left(\bar{w}-\frac{3}{2}\bar{m}\right) - \frac{\gamma}{2}\left(2\bar{w}-2\bar{m}-\bar{m}_{cr}\right)\sqrt{1-\frac{\bar{m}-\bar{m}_{cr}}{\bar{w}}}$$

$$For \ \bar{m}_{cr} \le \bar{m} \le \bar{m}^-$$

Line C' D' $\bar{\Phi} = \bar{\delta}_s - \dfrac{3}{10}\bar{m}$ $For \ 0 \le \bar{m} \le \bar{m}_{cr}$

Line D' B' $\bar{\Phi} = \bar{\delta}_s - \dfrac{3}{10}\bar{m} + \dfrac{3\gamma}{20\bar{w}}\left(2\bar{m}+3\bar{m}_{cr}\right)\left(\bar{m}-\bar{m}_{cr}\right)$ $For \ \bar{m}_{cr} \le \bar{m} \le \bar{m}^-$

With: $\bar{w} = \left(\bar{\delta}_s + \dfrac{6}{5}\bar{m}\right)\left[\dfrac{1}{2} + \dfrac{1}{2}\sqrt{1 + \dfrac{4\gamma\left(\bar{m}-\bar{m}_{cr}\right)^2}{5\left(\bar{\delta}_s + \dfrac{6}{5}\bar{m}\right)^2}}\right]$

Note: The equations for line D'B' are approximate equations because the use of the true relationship would include the solution of a fourth order polynomial which is generally not very convenient.

Line C" D" $\bar{\Phi} = \dfrac{1}{8}\left(5\bar{\delta}_u + 3 - 3\bar{m}\right)$ $For \ 0 \le \bar{m} \le \bar{m}_{cr}$

Line D" B" $\bar{\Phi} = \dfrac{1}{8}\left(5\bar{\delta}_u + 3 - 3\bar{m} - 3\gamma\dfrac{\bar{m}^2 - \bar{m}_{cr}^2}{1+\bar{m}}\right)$ $For \ \bar{m}_{cr} \le \bar{m} \le \bar{m}^-$

Where:

$$\bar{m} = \frac{Me}{M_{p,c}^+} \qquad \bar{w} = \frac{w}{w_o} \qquad \bar{\Phi} = \frac{\Phi}{\Phi_o} \qquad \bar{\delta} = \frac{\delta}{\delta_o} \qquad \bar{\delta}_u = \frac{\delta_u}{\delta_o} \qquad \bar{\delta}_s = \frac{\delta_s}{\delta_o}$$

δ_u typically L/50

δ_s typically L/360 or L/240

$$w_o = \frac{8 M_{p,c}^+}{l^2} \qquad \Phi_o = \frac{M_{p,c}^+ l}{3 E I_c^+} \qquad \delta_o = \frac{5 M_{p,c}^+ l^2}{48 E I_c^+} \qquad \bar{m}^- = \frac{M_{p,c}^-}{M_{p,c}^+} \qquad \bar{m}_{cr} = \frac{M_{cr}}{M_{p,c}^+}$$

$$\gamma = \frac{E I_c^+ - E I_c^-}{E I_c^-} \quad = \text{non-dimensional parameter related to the ratio between uncracked and}$$

cracked composite beam stiffness

$M_{p,c}^+$ positive plastic moment of composite beam

$M_{p,c}^-$ negative plastic moment of composite beam

M_{cr} cracking moment of composite beam

$E I_c^+$ uncracked stiffness of composite beam

$E I_c^-$ cracked stiffness of composite beam

The resulting limit state domain is presented in Figure 1.2-7. The limit state boundaries are straight lines until M_e exceeds the cracking moment of the composite beam in negative flexure; after which, the limit state boundaries are curved because of the non-prismatic properties of the composite beam. Boundary line C' B' represents the service load deflection limit state while the line C" B" represents the excessive deformation limit state or the ultimate factored plastic design load limit state. Boundary line C B represents the ultimate factored elastic design load limit state.
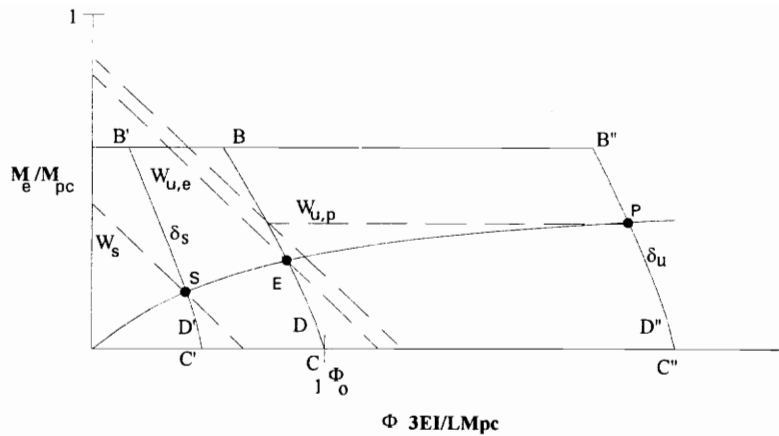
Figure 1.2-7 $\bar{m}$– $\bar{\Phi}$ **Limit State Domain**

Many design procedures may be envisioned with this type of method. The following is one possible method (Zandonini and Zanon 1991).

Given: Beam span, Steel grade, Loads, Load factors, Deflection Limits

Find: Composite beam section and required connection properties

Step 1) Determine whether elastic or plastic ultimate limit states will be used.

Step 2) Select a composite beam on the basis of a predetermined level of connection moment.

Step 3) Define the beam limit state domains for the composite beam selected using the previously defined equations.

Step 4) Determine point S which is the intersection of the beam line for W_s and the service load deflection boundary line.

Step 5) Determine point E or P (depending on whether elastic or plastic design was chosen), which is the point at which the beam line for W_{ue} or W_{up} intersect their respective boundary lines.

Step 6) Determine the required connection properties that will provide a connection with sufficient stiffness and rotational capacity to pass above points S and E or

points S and P depending on whether elastic or plastic design is chosen (the sample connection curve shown just meets these requirements).

Where:

W_s = Serviceability Uniform Load

W_{ue} = Elastic Ultimate Uniform Load

W_{up} = Plastic Ultimate Uniform Load or the load causing excessive deformation

This method of design for beams with semi-rigid connections has two outstanding features. First, the method can be easily implemented within a CAD environment allowing the immediate generation of the design domains particularly the curved domain boundaries associated with composite beams. Second, this method allows the problem to be visualized which should allow required design changes to be determined easily. The reader is referred to Balerini (1992) for further details of this method and the additional relationships and for the remaining three design domains.

1.3 OBJECTIVE AND SCOPE OF RESEARCH

With the apparent success and many advantages of composite semi-rigid beam-to-column connections, it seems natural to extend this concept to beam-to-girder connections to improve composite floor serviceability characteristics. From a theoretical point of view there are a number of factors which could affect the response of a semi-rigid composite joint (Benussi, et. al. 1989).

- The action in the composite slab and therefore on:
  1. the type of slab (i.e., solid concrete or with metal decking)
  2. the type of shear connection and degree of interaction
  3. the characteristics of the steel reinforcement (i.e. distribution, amount, grade)
  4. the relative stiffness of the slab with respect to the steel section
  5. the tensile strength of the concrete
- The characteristics of the beam-to-girder interaction and therefore on:
  1. the type of beam to-girder steel connection
- The type of the elements being joined and therefore on:
  1. the class of the steel beam section (compact, non-compact, slender)
- The loading conditions, and therefore on
  1. The load distribution on the beam connected and possibly on adjacent beams
  2. The loading process (monotonic, reverse-cyclic, cyclic, static, dynamic)

As is apparent from this list a comprehensive experimental study, in which all parameters are investigated, would be costly and time consuming. A more realistic approach would be to concentrate the experimental investigation around the main features of the connection behavior, thus hopefully eliminating many of the factors that could affect the overall joint behavior.

With this aim in mind, an initial series of four connection tests were designed, details of which are shown in Figure 1.3-1. Connection #1 is a typical single plate shear connection. Connection #2 is the same as Connection #1 except a seat angle has been added and the amount of reinforcing steel has been reduced. The single plate connection (the second most widely used shear connection) was chosen over a double framing angle shear connection (the most widely used shear connection) based on the fact that the single plate connections have typically exhibited higher rotational stiffness compared to the double framing angle connections. Single plate framing connections are also simpler to fabricate and allow faster erection in the field.

Connections #3 and #4 are two innovative connections which were designed with the goal of creating a connection that would exhibit significant rotational stiffness before and after concrete is in place. A connection that exhibits significant stiffness before concrete is placed is particularly useful in composite beam design. This is because the beam size is typically determined by the construction loading which must be resisted by the plain steel section.
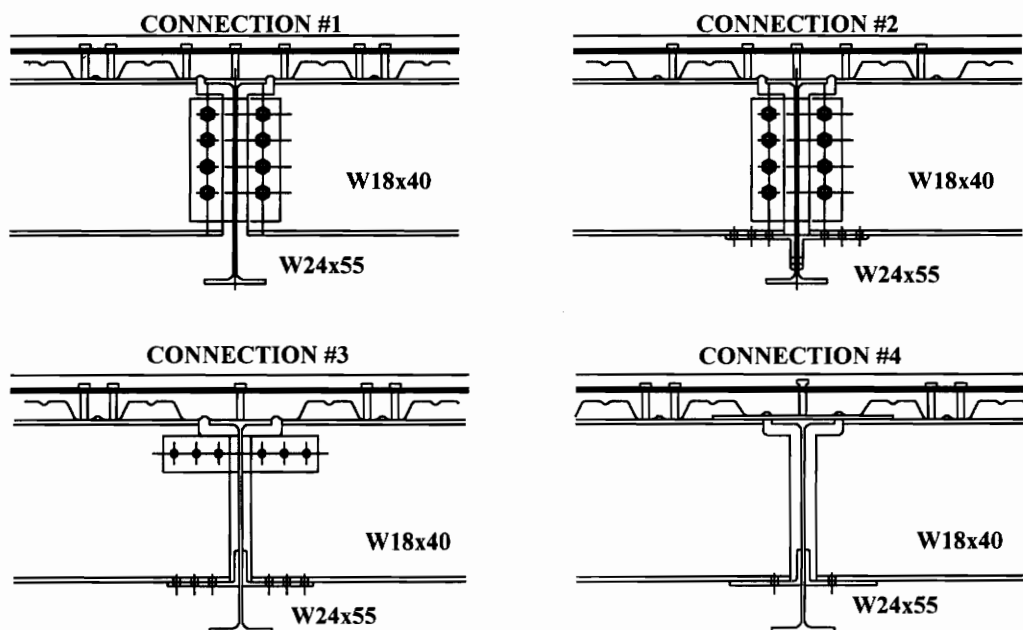
Figure 1.3-1 Composite Semi-Rigid Beam-to-Girder Connections

70

The steel portion of the connection specimens was subjected to a simulated dead load while the composite connection was tested to failure. It was the intent of this testing scheme to subject the connection to the actual loading history that it would normally be subjected to during unshored construction, as this is by far the most common form of composite floor construction used today.

The goal of this portion of the research was to determine the strength and behavior of the four beam-to-girder composite semi-rigid connections. The rotational behavior of the four specimens was of primary interest along with the ultimate strength and the feasibility of using these connections in a typical floor design.

The results of the testing program are reported in Chapter 3. Conclusions and recommendations for further research are presented in Chapter 5. To determine the effect composite semi-rigid beam-to-girder connections would have on the behavior of a composite beam, a brief analytical study was conducted and results are presented in Chapter 4. Analytical models of the connections are presented in Chapter 4. Eventually, the concepts used in these analytical models will be incorporated into finite element models of the connections as part of the continuing research. Also, as part of the continuing research, design guidelines following an LRFD (*Load and* 1986) format will be developed.

CHAPTER 2.0
EXPERIMENTAL INVESTIGATION

2.1 TEST SPECIMENS

Four semi-rigid composite beam-to-girder connections were tested under this portion of the test program. The four connections are shown in Figure 2.1-1 and Figure 2.1-4 through Figure 2.1-6 and are simply labeled Connection #1 through Connection #4. Connection #1 is a typical single plate connection. Connection #2 is the same as Connection #1 except a seat angle has been added and the amount of reinforcing steel has been reduced. The single plate connection (the second most widely used shear connection) was chosen over a double framing angle shear connection (the most widely used shear connection) based on the fact that the single plate connections have typically exhibited higher rotational stiffness compared to the double framing angle connections. Single plate framing connections are also simpler to fabricate and allow faster erection in the field.

Connections #3 and #4 are two innovative connections which were designed with the goal of creating a connection which would exhibit significant rotational stiffness before and after concrete is in place and which could be constructed using simple connection details. A connection that exhibits significant stiffness before concrete is placed is particularly useful in composite beam design because the beam size is typically determined by the construction loading which must be resisted by the plain steel section.

To determine the general details of the test connections a hypothetical design situation was developed. The hypothetical design is a 40-ft. long composite beam with 15-ft. beam spacing. Uniform live and dead loads of 100 psf and 60 psf respectively were used. The loads were not reduced according to ANSI/ASCE 7-88 for purposes of this design although the live load would normally be reduced in this design situation. It was

recognized that this design situation was rather extreme for a building design but it was believed that with upcoming improvements in composite steel deck floors that this design scenario could be very feasible in the future. It was also believed that semi-rigid composite beam-to-girder connections will be particularly useful in these extreme design situations.

Connection angles and plates were fabricated out of A36 steel because this is the most common practice today. All welds were shop welded using a shielded metal arc welding (SMAW) process with a continuous feed.

The beams were W18x40s and the girder was a W24x55. Both were fabricated from A572 Grade 50 steel. Details of the beams and the girder are presented in Figure 2.1-7 and Figure 2.1-8 respectively. The choice of beam and girder section size was based on the above hypothetical design. New beams were used for each connection while the girder was reused because it only sustained local nominal stresses as a result of the symmetrical loading arrangement used. The beams, girder and all connection parts were white-washed to identify yield patterns during testing.

The test specimen beam lengths varied between 54-in. and 66-in., depending on the connection. Originally, the length of the beam and the position where load was applied was chosen based on projected inflection points for the beam in the hypothetical design. However, the design of Connections #3 and #4 were modified during the test program. The beams for these specimens had been originally fabricated for different connection details which conceptually would not have had the same moment-rotation characteristics of the final connections. As a result the beams used in Connections #3 and #4 were shorter than needed based on estimates of the inflection point and connection behavior.

One-in. diameter and 3/4-in. diameter A325 bolts were used in all the connections. All bolts except for bolts used to attach the seat angle to the girder and the bolts in Connection #4 were pre-tensioned by turn-of-the-nut method. All 3/4-in. diameter bolts were tightened to snug with a 16-in. long spud wrench, while all one-in.

diameter bolts were tightened to snug with a 18-in. long ratchet and socket. Bolts were tightened to snug by the writer who weighs 200 pounds and is six-ft. one-in. tall with an average build. No excessive force was used while tightening any of the bolts to snug.

For bolt lengths up to and including four diameters, the turn-of-the-nut method requires 1/3 turn of the nut relative to the bolt after the nut is snug tight (Salmon & Johnson 1990). The one-in. diameter bolts were pre-tensioned using a ratchet with a seven-ft. length of pipe attached to the end while the 3/4-in. diameter bolts were pre-tensioned using a ratchet with a four-ft. length of pipe attached. Despite the seven-ft. length of pipe, the one-in. diameter bolts took considerable effort to achieve the 1/3 turn from snug. This confirms the belief that one-in. diameter bolts are the practical limit for bolt size when bolts have to be fully pre-tensioned. The 3/4-in. diameter bolts did not require near the effort required for the one-in. diameter bolts. All bolts were A-325-X (threads excluded from the shearing plane) with round washers. The bolts in the single plate connections have the bolt head flush against the plate and the bolts in the seat angles had bolt heads flush against the top side of the beam bottom flange.

A 60-in. wide composite slab was placed on top of the beam-to-girder connection. The 60-in. width was chosen because it was a common width used in the composite semi-rigid beam-to-column connection tests discussed in the literature review. The composite deck consisted of a five-in. slab for Connections #1 and #2 and a five and one-half in. slab for Connections #3 and #4. The slabs were cast on a two-in. deep composite steel deck and reinforced with WWF 6x6 - W1.4x W1.4 mesh and #4 grade 60 reinforcing bars (the particular number of reinforcing bars depends on the connection tested). The bars were placed on one-in. reinforcing steel stands.

Four-in. x 3/4-in. welded headed shear studs were used to attach the slab to the beam and girder. In general, the number of studs depends on the amount of reinforcing steel in the slab. The stud layouts are presented in Figure 2.1-9. It should be noted that when there are not two studs per steel deck trough, the single stud was placed in the strong stud position (i.e., the position in which the most concrete is present between the

stud and the side of the deck trough in the direction of relative movement.) Connections #1 and #2 have studs adjacent to the edge of the beam flange closest to the girder. During a meeting of the Advisory Committee for this research project, it was pointed out that a stud would not normally be placed in such a position as a result of special steel flashing that is typically used at the girder to insure a proper haunch of concrete. As a result, Connections #3 and #4 did not have studs welded in this location.
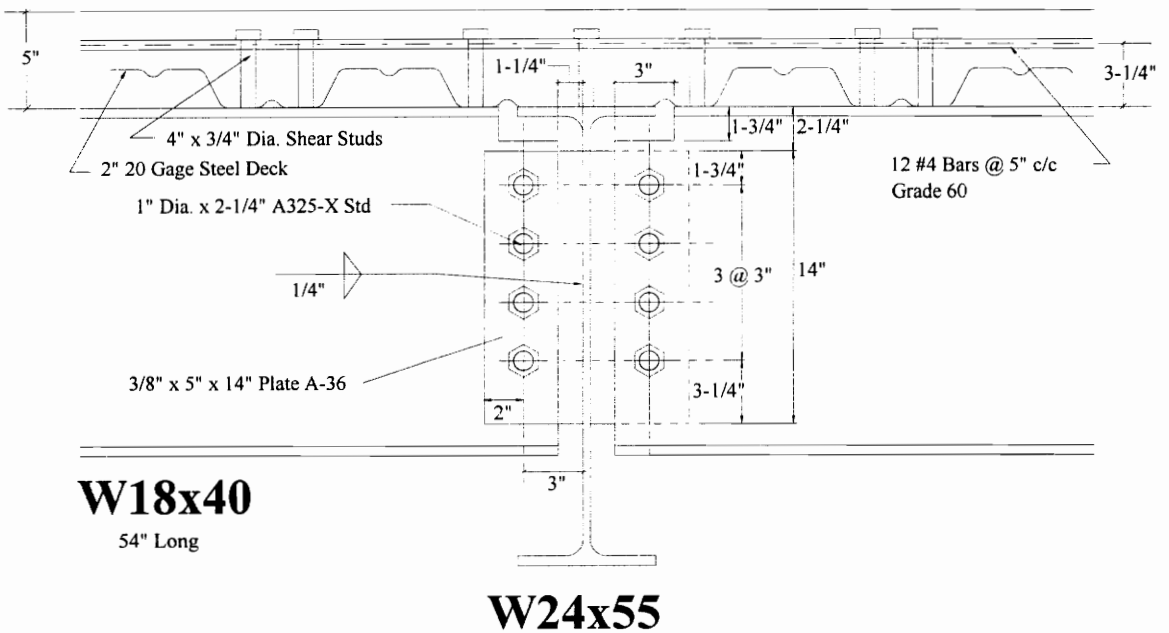
Figure 2.1-1 Connection #1 Details

2.1.1 Connection #1 Design

Connection #1 is a typical single plate connection with one-in. diameter bolts at a three-in. pitch. The steel portion of the connection was designed following the design guidelines presented in *The Manual Of Steel Construction Volume II Connections* (*The Manual* 1992) with the exception that the plate length was chosen to allow as many bolts

as would fit in the connection. As a result of the typical three-in. pitch associated with single plate framing connections, one-in. diameter bolts were chosen to allow the largest bolt capacity while using the current practice of the three-in. pitch. Larger bolts were not used based on steel erector preference not to use bolts larger than one-in. diameter as a result of the difficulty encountered in tightening the bolts (as also encountered by the writer and mentioned previously). The plate thickness was checked to ensure that it would not be weaker than the beam web in bolt bearing / tearout. Based on estimates of the connection behavior 12 #4 bars were chosen. This amount of slab steel was chosen in an attempt to fail the steel portion of the connection after the reinforcing bars had significantly yielded. Number 4 bars were chosen because they represent a bar size that would likely be chosen by designers who were placing reinforcing steel across supports to control cracking of the composite slab.

The amount of reinforcing steel for the connection, the location of the applied ram loads, and the estimate of the connection's ultimate moment strength were based on the following design procedure which was developed by the writer in the preliminary stages of the research project. The actual numbers used in the design of Connection #1 have been included for illustrative purposes.
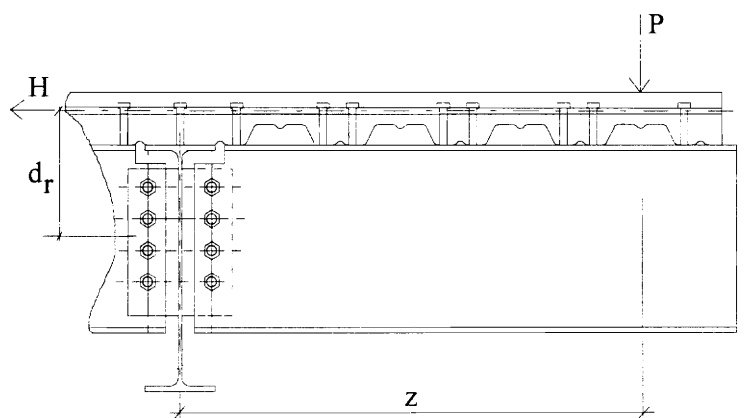
Figure 2.1-2 Main Features of Connection #1 Design Problem

Step 1) Determine the Controlling Bolt Limit State

Bolt Single Shear

R_n = nominal bolt strength = A_b x F_v

F_v = bolt shear stress, 84 ksi as suggested by Salmon & Johnson (1990)

A_b = effective area of the bolt, 0.7854 for 1-in. dia. bolt with threads eXcluded from shear plane

R_n = 0.7854 x 84 = 66 Kips

Bearing / Tearout Failure

R_n = 2.4 x F_u x t x d_b

Beam Web F_u = 65 ksi (A572 Gr 50) t_w = 0.315" (W18x40)

R_n = 2.4 x 65 x 0.315 x 1" = 49.1 Kips

Shear Tab F_u = 58 ksi (A36) t_p = 3/8"

R_n = 2.4 x 58 x 3/8 x 1" = 52.2 Kips

Thus: Controlling Bolt Limit State = Beam Web Bearing / Tearout

R_n = 49.1 Kips

Step 2) Determine Connection Moment Desired

Try M_{ue} = M_p/2 as recommended by Leon and Ammerman (1990)

ϕM_p = 0.9 x F_{yb} x Z_x = 0.9 x 50 ksi x 78.4 = 3528 K-in

ϕM_p/2 = 3528/2 = 1764 K-in

Try M_{ue} = 1700 K-in = 142 K-ft

Step 3) Determine Inflection Point for Hypothetical Design

Factored Live Load = 100 psf x 15' x 1.6 / 1000 = 2.4 K/ft

Factored Dead Load = 60 psf x 15' x 1.2 / 1000 = 1.08 K/ft

W_u = factored uniform load = 2.4 + 1.08 = 3.48 K/ft

V_u = factored end shear force = 3.48 K/ft x 40'/2 = 69.6 Kips

$$\text{Inf. Pt.} = \frac{V_u - \sqrt{V_u^2 - 2W_u M_{ue}}}{W_u} = \frac{69.6 - \sqrt{69.6^2 - 2(3.48)\ 142}}{3.48} = 2.16\text{-ft.}$$

Step 4) Choose Value of z

The writer wanted the load to be applied at some distance beyond the inflection point so:

Try z = 3.5-ft. = 42-in. > 2.16-ft.

Step 5) Determine the required ram load P

$P = M_{ue} / z = 1700 / 42 = 40.5$ Kips

Step 6) Determine allowable horizontal force H_{all}

$$H_{all} = \sqrt{R_n^2 - P^2} = \sqrt{(4 \times 49.1)^2 - 40.5^2} = 193.4 \text{ Kips}$$

Step 7) Determine required horizontal force H_r

$H_r = M_{ue} / d_r$

Where: d_r comes from the geometry that was determined in the preliminary design

$H_r = 1700/11.75" = 144.7$ Kips <= 193.4

Step 8) Choose reinforcing steel required to develop H_r

$A_r = H_r / F_{yr} = 144.7/60$ ksi = 2.41 sq in.

For #4 bars the number of bars required = A_r/A_b = 2.41/0.2 = 12.05 bars

Try 12 #4 bars New H = 12 bars x 0.2 sq in x 60 ksi = 144 Kips

Step 9) Ultimate strength analysis of connection

Use ultimate strength design procedures (as found in the LRFD Specification (*Load and* 1986) for eccentricity loaded bolt groups to determine the instantaneous center (I.C.) of rotation and the resulting moment for the connection.
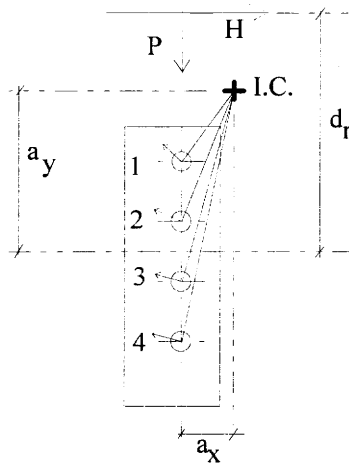
Figure 2.1-3 Ultimate Strength Analysis of Connection

Referring to Figure , choose trial a_y and a_x values and solve for $\sum F_x$ and $\sum F_y$. Try new values of a_y and a_x until $\sum F_x$ and $\sum F_y$ have values of zero. It is suggested that this process be done on a spread sheet or with a basic program to more easily deal with the iterative process involved in solving for the instantaneous center. For example, try $a_y = 4.88$-in. and $a_x = 0.79$-in. The solution for these values is shown in Table 2.1-1.

Table 2.1-1 Ultimate Strength Analysis

Bolt	dx	dy	di	D	Ri	Mi	Ry	Rx
1	0.79	0.38	0.88	0.03	23.98	21.02	21.61	10.39
2	0.79	3.38	3.47	0.13	40.83	141.71	9.29	39.76
3	0.79	6.38	6.43	0.23	46.4	298.28	5.7	46.05
4	0.79	9.38	9.41	0.34	48.2	453.67	4.04	48.03
	di max =	9.41			Sum:	914.68	40.65	144.22
						P & H	40.5	144
						Sum:	0.15	0.22

Where:

$$d_i = \sqrt{d_x^2 + d_y^2} \qquad \Delta_i = 0.34 \frac{d_i}{d_{i\,max}} \qquad R_i = R_{i,\,ult}\left(1-e^{-10\,\Delta}\right)^{0.55}$$

$R_{i,\,ult} = 49.1$ Kips $M_i = R_i\,d_i$ $R_y = R_i\,(d_x/d_i)$ $R_x = R_i\,(d_y/d_i)$

Since $\sum F_x$ and $\sum F_y$ are approximately zero, this solution appears to have located the I.C. of the connection and thus the connection moment can be determined from:

M_r = moment due to reinforcing steel = H (d_r-a_y) = 144 (11.75 - 4.88) = 989 K-in.

M_v = moment due to vertical shear = - P a_x = -(40.5) (0.79) = -32 K-in.

M_c* = moment from the steel connection (from Table 2.1-1) = 915 K-in.

Thus M_{ue} = M_r + M_v + M_c* = 989 - 32 + 915 = 1872 K-in.

Step 10) Iterate until convergence

Because M_{ue} is not what was assumed the ram load P is not correct, thus modify the shear load until it matches the connection moment capacity. For this particular case, P = 44.5 Kips and M_{ue} = 1872 K-in. are the values at convergence. The designer could opt to reduce the reinforcing steel at this stage to develop a moment closer to that originally chosen in Step 2 (1700 K-in.). The writer decided to leave the connection as designed and used the 12 #4 bars. Note that the new inflection point for the increased M_{ue} is 2.4-ft. which is still less than the 3.5-ft. distance to the applied live load chosen.

2.1.2 Connection #2 Design

Connection #2 was the same connection as Connection #1 with the exception that a seat angle was added to the bottom flange and the amount of reinforcing steel was reduced. The seat angle was shown to be an important part of many of the composite semi-rigid beam-to-column connections previously tested. The seat angle serves two main purposes. First, it forces the connection to rotate near the bottom of the connected beam. Second, it stabilizes the bottom flange thus preventing early local buckling in the

flange. This will enhance the beam-to-girder connection behavior by increasing the rotational stiffness and stability of the connection both before and after concrete hardens.
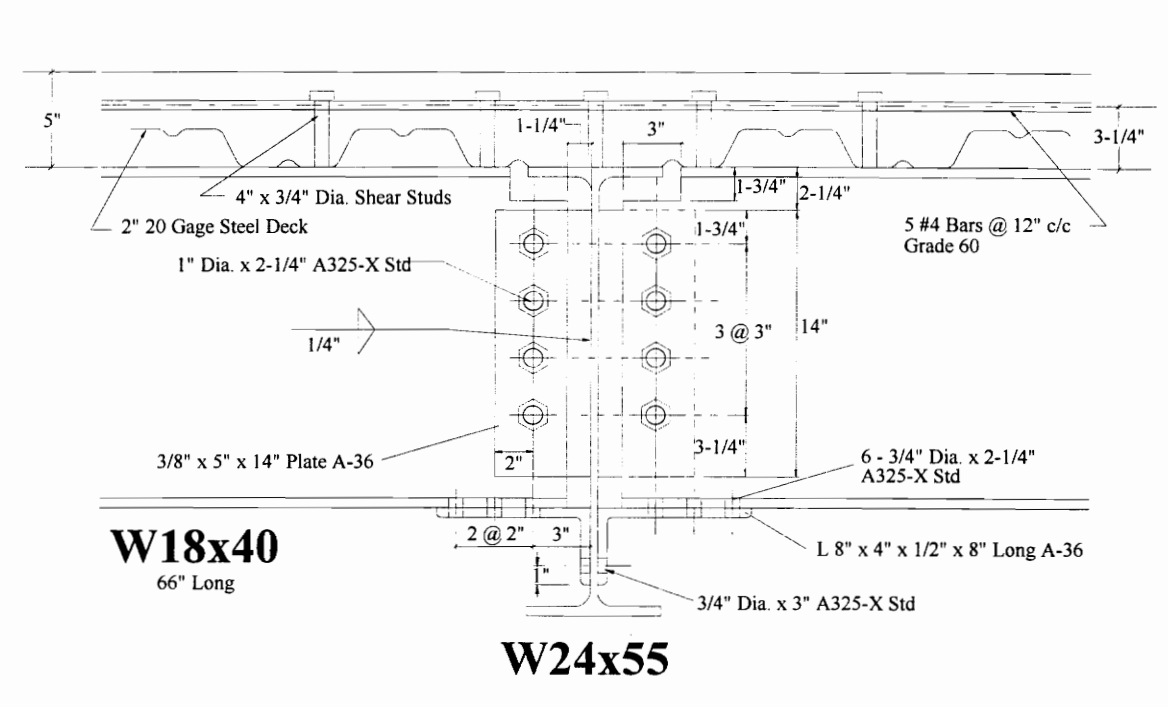
Figure 2.1-4 Connection #2 Details

Originally a L9 x 4 x 5/8 seat angle was chosen for this connection as the largest angle that would fit in the area between the bottom beam flange and the bottom girder flange, but as a result of limited availability of this angle size the L8 x 4 x 1/2 seat angle was used instead. The eight-in. angle length was chosen based on the width of the beam flange. The 3/4-in. diameter bolts and bolt pattern were chosen to develop a maximum horizontal shear capacity between the bottom flange of the beam and the seat angle. The two-in. bolt pitch is 2-2/3 the diameter of the bolt which is the minimum pitch as recommended by AISC (*Load and* 1986). The one-in. edge distance is the minimum edge distance for a rolled edge as recommended by AISC (*Load and* 1986). Ideally the bolts in the single plate on this connection would also be 3/4-in. diameter based on steel erector and fabricator preference not to deal with multiple bolt sizes. It was decided to

81

leave the one-in. diameter bolts in the connection so that there would be a better comparison between the results of this connection and Connection #1.

The amount of reinforcing steel was reduced because of an increase in the moment arm it acts through. Instead of rotation occurring somewhere around the top of the connection, as in Connection #1, it is believed that rotation will now occur about the seat angle, thus increasing the moment arm for the reinforcing steel significantly.

The load position for the simulated dead load was chosen based on available locations where the dead load frame could be located, while the location for the applied live load was chosen based on a design procedure similar to that described for Connection #1 except that the connection was assumed to rotate about the toe of the bottom beam flange. This assumption eliminated all the iterative work associated with the design of Connection #1 and the seat angle was chosen based on the horizontal force developed by the reinforcing steel and bolts as determined in the ultimate strength analysis step.

2.1.3 Connection #3 Design

The same basic connection elements used in Connection #2 were used in Connection #3 but the single plate orientation was changed. To increase the moment-rotation capacity of the bare steel connection, the plate was placed as close to top of the connection as seemed feasible (i.e., the top of the plate was flush with the top of the beam cope) and extended out from the girder far enough to allow the number of bolts required to fully develop the yield strength of the plate. Short vertical slots were used in the plate to allow simpler field erection, which was a trade off for the possible shear resistance that would have been provided by the plate if standard holes had been used. The plate was designed so that it would not yield under construction loading but would yield under ultimate loading to allow the reinforcing steel in the composite slab to properly develop. The reinforcing steel was chosen to be the same as Connection #2 to have a better comparison between the two connections as well as the fact that #4 bars at 12-in. spacing

would be a reasonable amount of reinforcing steel for a designer to specify to control cracking over supports.
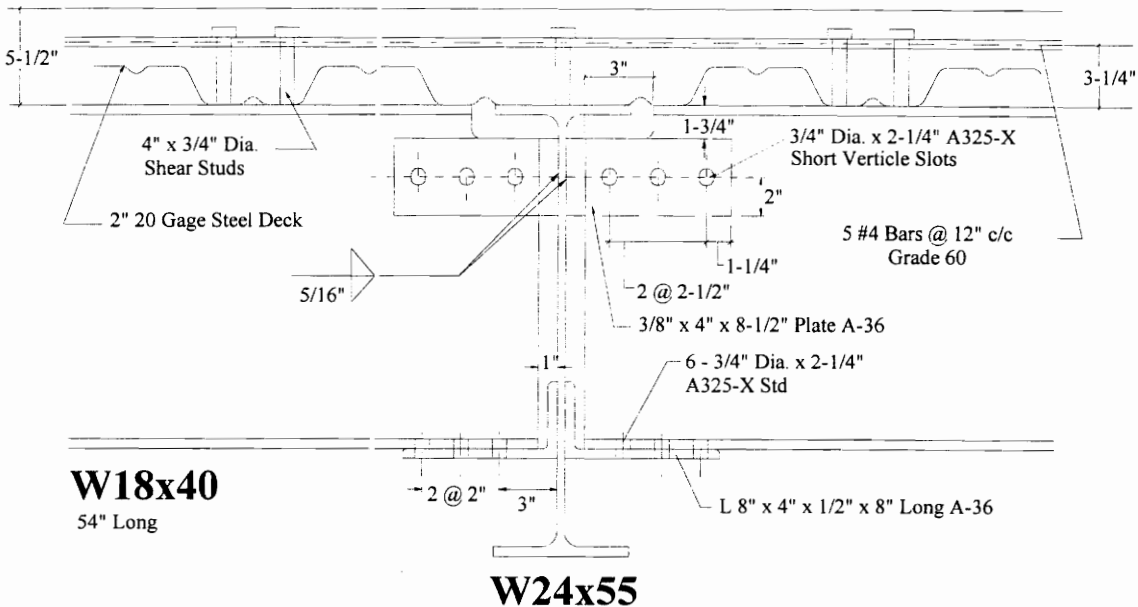
Figure 2.1-5 Connection #3 Details

The key to both Connection #3 and #4 (details of Connection #4 are discussed in the following section) was the behavior of the seat angle and its ability to properly transmit both shear and axial load. Unlike Connection #2, which had a shear plate that could carry most of the shear force, Connection #3 and #4 did not have any element except the seat angle which would theoretically carry shear force. At the same time, the seat angle must also resist the horizontal load developed by the top portion of the bare steel connection and the reinforcing steel.

The current methodology used to design unstiffened seated beam connections was reviewed (Garrett & Brockenbrough 1986) and was deemed inappropriate for the design of either connection. The method currently used makes two assumptions that did not seem to be valid when considering the details of Connection #3 and #4. Firstly, the method assumes that the shear force is transferred to the seat angle at the center of a

bearing length which is based on the lesser of the beam web yielding limit state or the available length of seat angle. In general, this idea seems reasonable; but, a constraint placed on the web yielding criteria was that the bearing length must be a minimum of 2.5 times the k distance of the beam. The basis of this constraint was not understood by the writer and was believed to be inappropriate. Secondly, the method assumes that the seat angle is free to rotate separate from the beam flange. This was clearly not the case for any of the connections tested because they all had sufficient connection between the bottom flange and the seat angle to ensure that the two must behave in a similar manner.

Without any particular guidance or design procedure available to help provide insight into the behavior of the seat angle, it was decided to use the same seat angle that had been used in Connection #2. The seat angle was inverted from its orientation in Connection #2 to eliminate the restrictions on the angle size that occur because of the limited space between the bottom of the beam and the top of the bottom girder flange. Ideally a much larger seat angle could now be used if orientated in this manner. The seat angle was welded rather than bolted to the girder because the single plate of Connection #3 was also welded to the girder and typical fabricator practice dictates that only one operation (i.e., either bolting or welding) be done on any particular steel member whenever possible.

The loading position for both Connections #3 and #4 under live and dead load test stages was 48-in. This loading position was not chosen based on approximate inflection points for the hypothetical design and estimates of the connection behavior for reasons discussed previously. For a 54-in. beam 48-in. to the load point was determined as the closest point to the beam end for which the beam could still be safely loaded.

2.1.4 Connection #4 Design

Connection #4 was designed in an attempt to further simplify connection details and provide an increase in the bare steel connection's moment-rotation capacity. The

details for this connection are very similar to details given in *The Manual Of Steel Construction Volume II Connections* (*The Manual* 1992) for one of the beam-to-girder moment connections. The construction sequence for this type of connection could be envisioned as: 1) the beam would be placed on the seat angle and bolted with erection bolts, 2) a plate would be placed across the top of the beams and girder, 3) the plate and seat angle would be welded to the beam. It is believed that welding the seat angle and the top plate to the beam would be comparable in time and cost to bolting the elements to the beam with fully pre-tensioned bolts, particularly because the welds are all down hand fillet welds. It is also believed that the connection moment-rotation characteristics will be enhanced by welding the elements rather than bolting the elements to the beam.
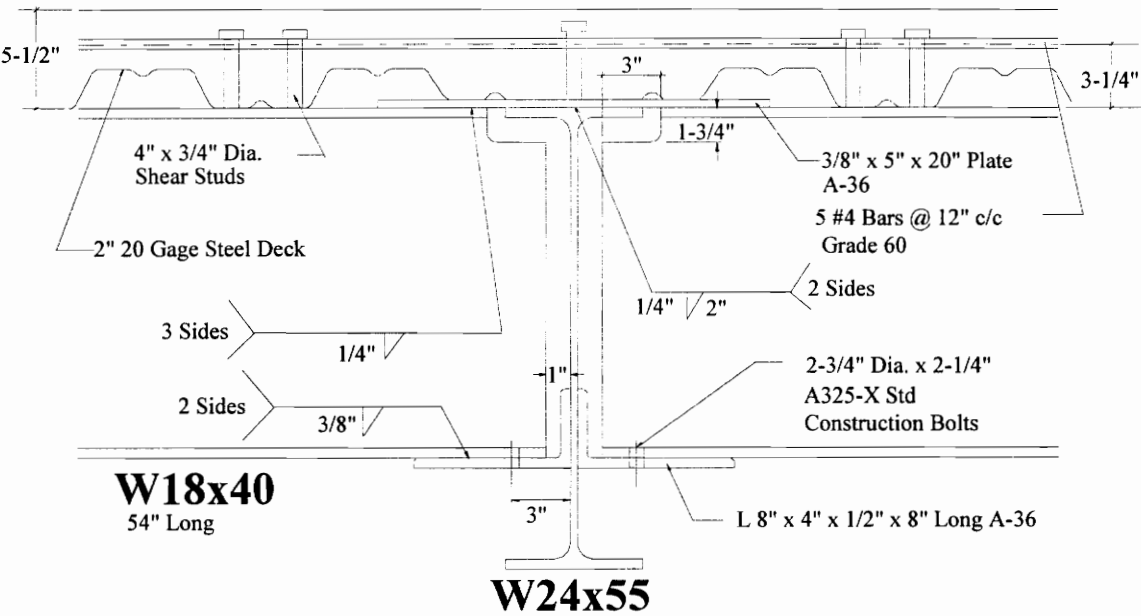
Figure 2.1-6 Connection #4 Details

The top plate for this connection was designed so that it would not yield under construction loading but would yield under ultimate loading to allow the reinforcing steel in the composite slab to properly develop. The top plate was originally designed to be a four-in. wide 3/8-in. thick plate; but, as a result of an error in fabrication the plate used was a five-in. wide 3/8-in. thick plate instead. The erection bolts for the seat angle were

only snug tight (i.e., not fully tensioned). Welds were designed to fully develop the connection element being attached; although, the weld attaching the bottom beam flange to the seat angle was limited by the flange thickness and would have been designed larger if possible. The design of the seat angle and position of loading is described under Section 2.1.3 and will not be repeated here.
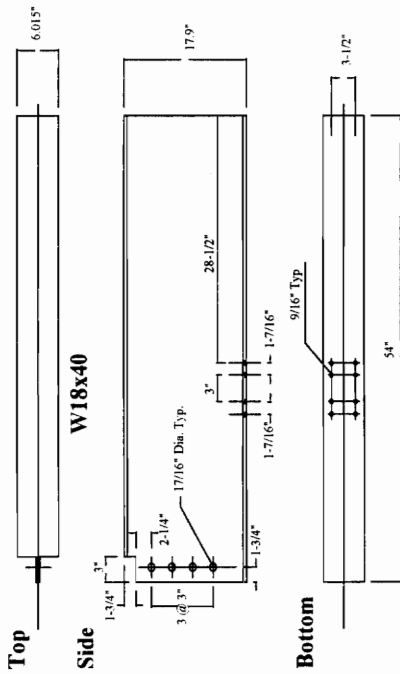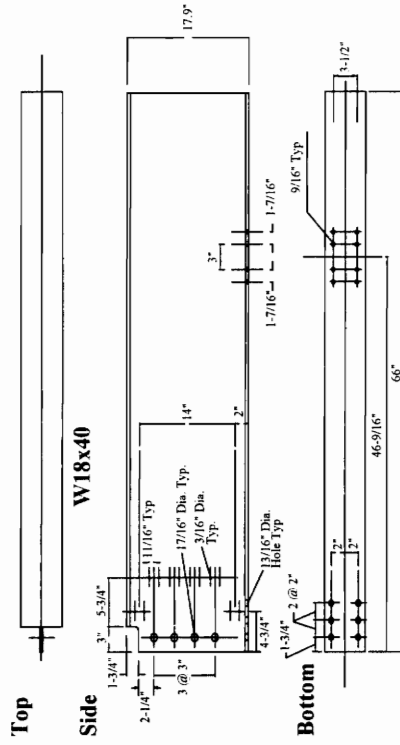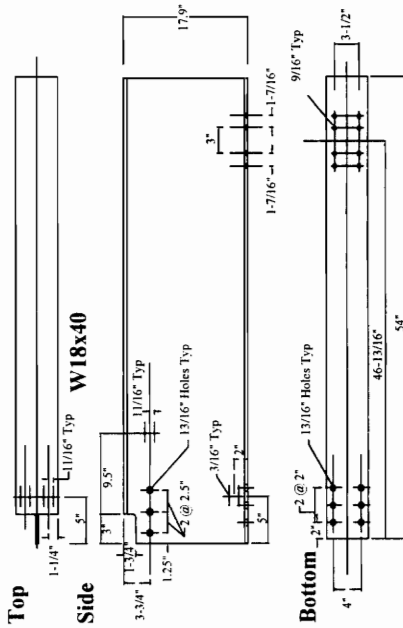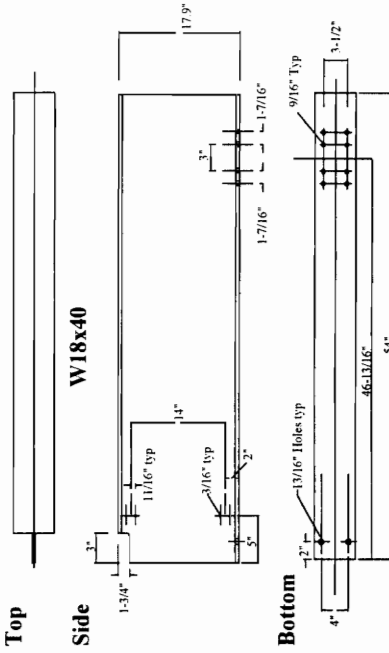
Figure 2.1-7 Beam Fabrication Details

87
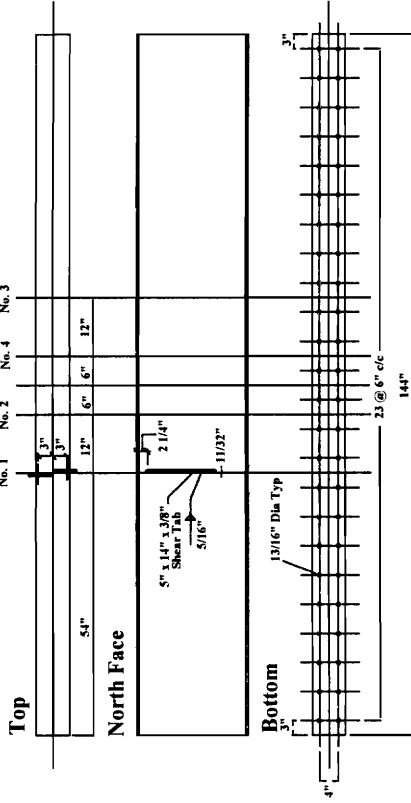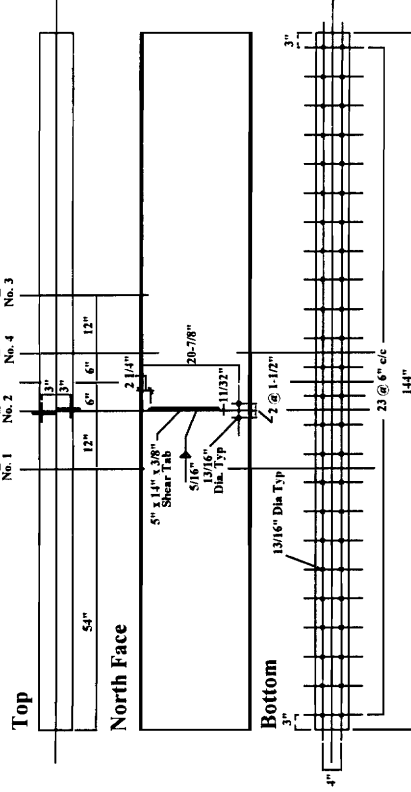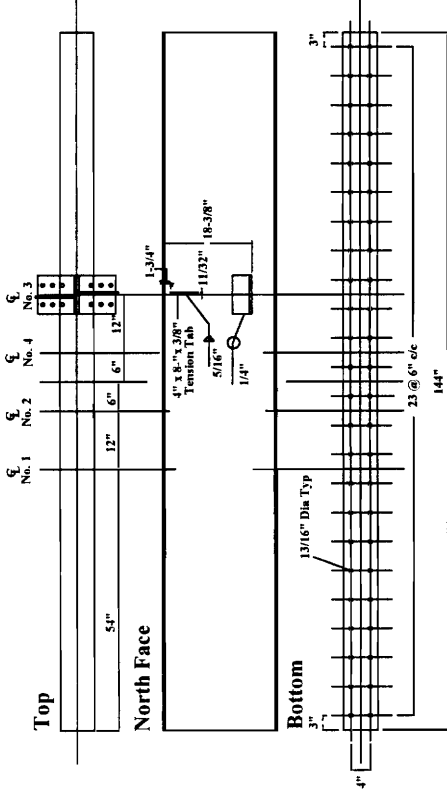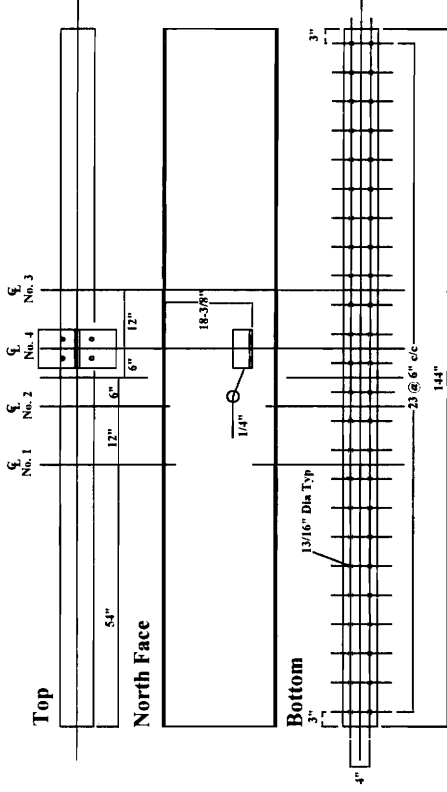
Figure 2.1-8 Girder Fabrication Details
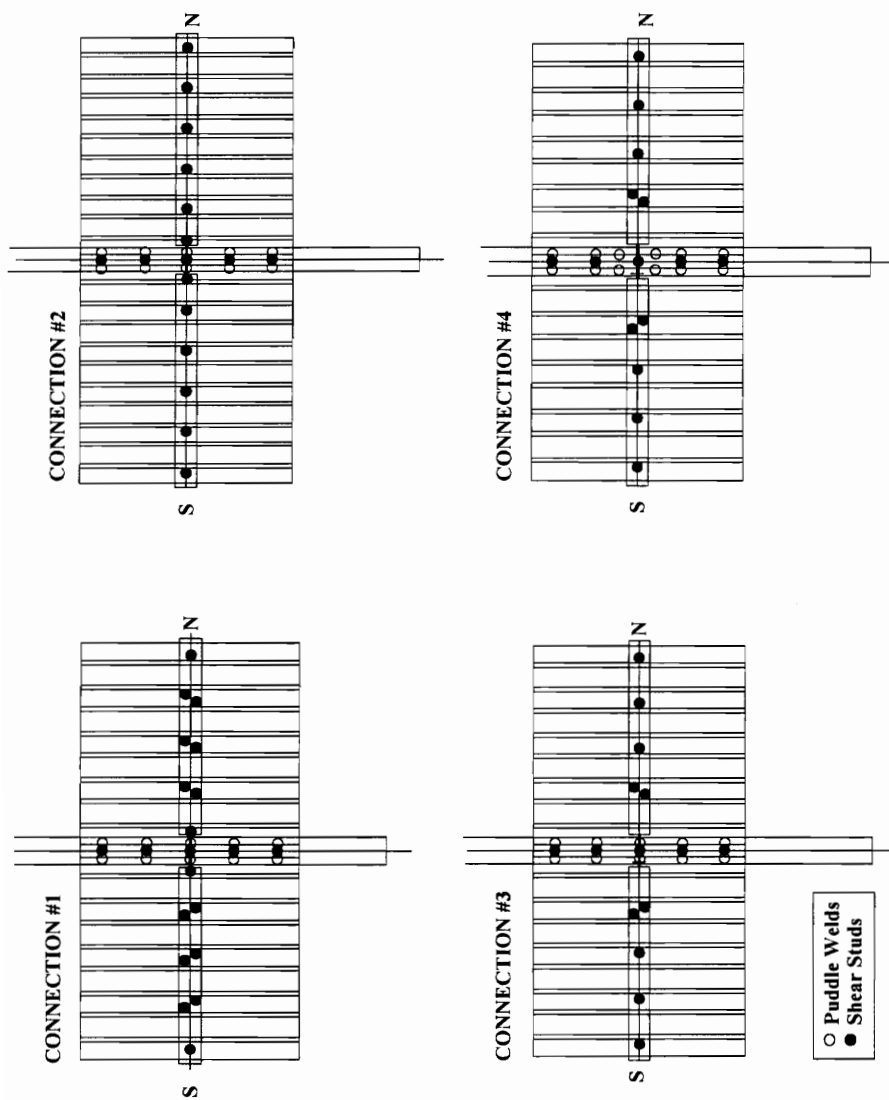
Figure 2.1-9 Steel Deck and Stud Layout

89

2.2 INSTRUMENTATION

The main goal of the testing program was to determine the moment-rotation behavior for four beam-to-girder composite semi-rigid connections. This could have been done with relatively few pieces of instrumentation. A second goal of the overall research program (although not the primary goal of this thesis) is to develop an analytical model capable of predicting the basic moment-rotation response of these connections based on their mechanical and geometrical properties. The majority of the instrumentation was aimed at allowing some insight into the second goal. To verify any model developed, it is not sufficient to only compare the moment-rotation behavior measured with the values produced by the model. The model must also predict the various deformations and stress distributions associated with all elements of the connection. Each of the instrumentation schemes developed was chosen to allow specific verification of model response versus measured response for various elements of the connection.

2.2.1 General Instrumentation

2.2.1.1 Beam Instrumentation

To determine beam flange and web strains, and subsequently the stresses, uniaxial strain gages were placed on the top and bottom flanges and web of the test specimen beams. Gages were placed on the top and bottom flanges at four separate cross-sections for the first two connections and at three cross-sections for the second two connections. The information gathered from the gages in the fourth cross-section for the first two connections was not very informative and it was felt that these gages would give better information if they were placed in the web. Consequently connections #3 and #4 had two cross-sections of gages on the web while connections #1 and #2 had only one cross-

section of gages through the web. The additional web gages were deemed necessary to evaluate variation in the web stress distribution.

Linear motion transducers were attached to the web of the beams to measure relative motion of the beam web and the various elements of the connection. The transducers were spring loaded such that they were able to measure both directions of motion without being tied to the connection.

Transducers (similar to those described above) located at the top and bottom of the beams were used to determine the relative rotation of the beam with respect to the face of the girder. These transducers were attached to either the web or the flange of the beam approximately six-in. from the face of the girder and rested against the face of the girder. The rotation was obtained by dividing the difference between the horizontal displacements of the transducers by the distance between them. It was assumed that the flexural rotation of the beam between the beam end and the location where the transducers were attached was small. Subsequently, the rotation measured by the transducers was taken as the rotation associated with the connection.

Wire transducers were attached to the beam ends and locations near the connections to determine relative vertical displacement of the girder, connection elements, and beam end. In order to measure slip between the composite slab and the top beam flange, two LVDTs (one for each beam) were attached to the underside of the composite slab and rested against a plate attached to the top flange of the beam.

2.2.1.2 Reinforcing Bar Instrumentation

To determine factors such as shear lag, the effective width of slab that can be included in the connection design, and the reinforcing steel force contribution to the connection moment capacity it was necessary to determine reinforcing bar forces in the slab. Uniaxial strain gages were attached to the reinforcing bars along three lines; one above the centerline of the girder and two at 12-in. from the girder centerline (one line

each side). Figure 2.2-1 shows the reinforcing steel layout and strain gage locations for all four test specimens. The reinforcing bars were prepared for the gages by removing the lugs in a three-in. area around the intended gage location. The gages were then installed in a normal fashion. To protect the gages from the concrete they were encased in multiple protective coatings; 1) polyurethane, 2) Teflon, 3) FB butyl rubber, 4) FN neoprene rubber, 5) aluminum tape, 6) nitrile rubber. The wires for the gages were then either routed through a small hole in the deck near the gage or were encased in shrink-wrap tubing and routed out over the edge of the slab. Just prior to concrete placement, the gages were coated in ball bearing grease to ensure the concrete did not attach itself to the outer gage covering.

Once the gages were installed, the reinforcing bars were placed in an universal testing machine to calibrate each gage. Calibrating each gage is believed to be the best way of determining reasonable values of the forces in the reinforcing bar. Strains could not be directly related to forces in the bar without calibration as a result of varying area of the bar and uncertainty of the actual allignment of the gage with respect to the longitudinal axis of the bar. Although the gages were calibrated, it should be noted that the measured strains induced into the reinforcing steel when they were in the universal testing machine could be quite different from the strains induced by the concrete slab. In general it was assumed that the reinforcing was primarily in direct tension and that bending could be ignored. The gages were attached to the sides of the reinforcing steel rather than the top and bottom in an attempt to minimize any bending that would occur in the slab, (i.e., ideally if the gage is located at the neutral axis for bending of the reinforcing bar then the gages should only detect axial strain in the bar rather than the combination of axial and bending strains).

A PC-based data acquisition system was used to collect and record data.

2.2.1.3 Instrumentation Nomenclature

The nomenclature used to identify the various gages and other pieces of instrumentation are as follows:

R "#" - "#2" **Reinforcing** bar gage where the first # is the bar number and second # is the gage location on the bar

Example: R01-1 means a gage on reinforcing bar #01 and at the first location on the bar

STF - "#" Gage located on the **South Top** beam **Flange** where # indicates the cross-section

Example: STF-4 means a gage on the south top flange located at cross-section #4

SBF - "#" Same as STF-"#" except located on **Bottom** flange

NTF - "#" Same as STF-"#" except located on **North** beam

NBF - "#" Same as STF-"#" except located on **Bottom** flange and **North** beam

NW - "#" Gage located on the web of the **North** beam at location #

Example: NW-1 means a gage located on the web of the north beam and at location #1

SW - "#" Same as NW - "#" except South beam

STR - "#" **Rosette** located on the **Top** of the **South** plate where # indicates which rosette arm

Example: STR-2 means the #2 arm on the rosette located at the top of the south shear plate

SMR - "#" Same as STR - "#" except **Middle** rosette

SBR - "#" Same as STR - "#" except **Bottom** rosette

NTR - "#" Same as STR - "#" except **North** connection

NMR - "#" Same as STR - "#" except **North** connection and **Middle** rosette

NBR - "#"   Same as STR - "#" except **N**orth connection and **B**ottom rosette

SWR"#"-"#"   **R**osette located on the South beam **W**eb where the first # indicates rosette location and the second # indicates which rosette arm (if the first number is not present then only one rosette was used)

Example: SWR1-1 is arm #1 on the rosette located at location #1 on the south beam web

NWR"#"-"#"   Same as SWR"#"-"#" except **N**orth beam

SPR - "#"   **R**osette located on the South tension **P**late where # indicates which rosette arm

NPR - "#"   Same as SPR - "#" except **N**orth plate

SPT   Strain gage on the **T**op of the South **T**ension plate

NPT   Same as SPT except **N**orth beam

SPB   Same as SPT except **B**ottom of plate

NPB   Same as SPB except **N**orth beam

NRT   Potentiometer used to measure the displacement of the **T**op of the **N**orth beam relative to the girder face, used in combination with NRB to determine the **R**otation of the connection (if a number was included it simply indicates there were more than one potentiometers used and the number indicates which one is being referred to)

NRB   Potentiometer used to measure the displacement of the **B**ottom of the **N**orth beam relative to the girder face, used in combination with NRT to determine the **R**otation of the connection

SRT   Same as NRT except **S**outh beam

SRB   Same as NRB except **S**outh beam

SP - "#"   Potentiometer used to measure the **P**late movement on the **S**outh connection where # indicates the location (For Connection #4 this symbol means the strain gage located on the top side of the tension plate)

	Example: SP-1 is a potentiometer measuring the plate movement at location #1
NP - "#"	Same as SP - "#" except **North** beam
SB - "#"	Same as SP - "#" except measuring **B**olt movement
NB - "#"	Same as SB - "#" except **North** beam
SVD - "#"	DCDT or strain gage transducer measuring **V**ertical **D**isplacement on the **S**outh beam at location #
	Example: SVD-1 is a DCDT at location #1
NVD - "#"	Same as SVD - "#" except **North** beam
GVD - "#"	Same as SVD - "#" except attached to the **G**irder
S-Slip	LVDT measuring **Slip** between the **S**outh beam and the composite slab
N-Slip	Same as S-Slip except **North** beam
NSA - "#"	Strain gage located on the **N**orth **S**eat **A**ngle at location #
	Example: NSA-1 is a strain gage on the north seat angle at location #1
SSA - "#"	Same as NSA - "#" except **S**outh beam
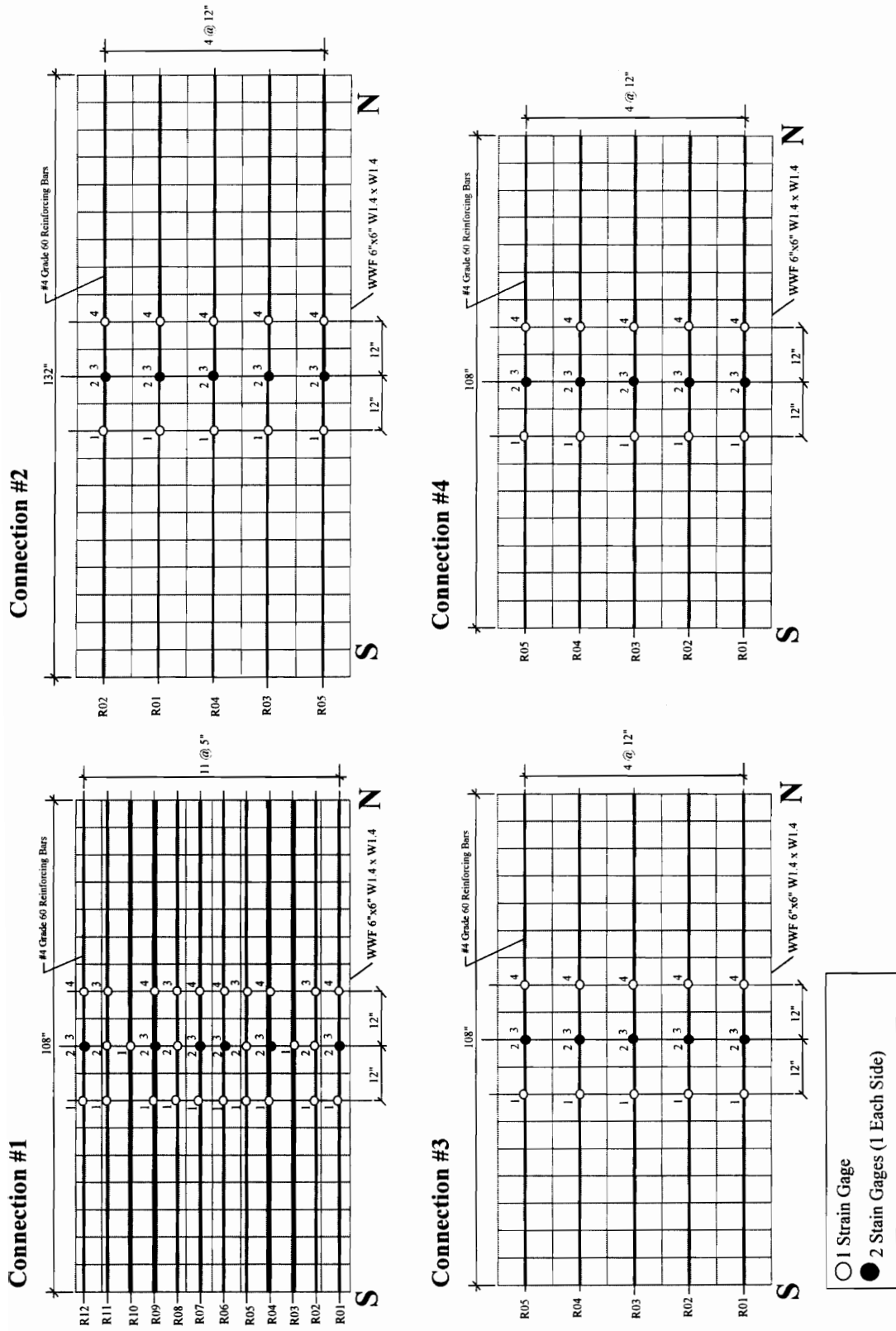
Figure 2.2-1 Reinforcing Bar, Mesh Layout/Instrumentation

2.2.2 Details of Connection #1 Instrumentation

The beam instrumentation for Connection #1 is shown in Figure 2.2-2. Uniaxial gages were located on the beam flanges and web as described previously to determine the bending distribution in the steel section. Three arm, 45-degree, strain rosettes were attached in three locations on each plate of the shear plate connections. The rosettes were used to determine the stress distribution in the plate during the test. This information will be of particular interest when finite element modeling of the connection is done and in general is interesting because the stress distribution in the shear tab connection is still not well understood and could be critical in determining a proper design procedure.

There were eight linear motion transducers attached to the web of each beam. Four of these for each beam rested against small steel tabs that were attached to the shear tab connection plate. The remaining transducers were located on the opposite side of the beam web and rested against a plate attached to the nut for the bolts used to attach the beam to the shear tab plate. The transducers resting against the steel tabs attached to the shear tab were used to measure relative movement between the beam web and the edge of the shear tab plate. The transducers resting against the nuts measured the relative movement between the nut and the beam web. This combination of bolt and plate transducers allowed relative measurement of all parts of the connection in an attempt to identify a pattern of deformation in the connection and a reasonable measurement of the slip between the bolt and the plate. The measurement of the slip between the bolt and the plate is particularly important for the validation of any detailed model developed for the connection.

Wire transducers were attached to the beam ends, the bottom flange of the beam under the connection, and to the connection plate. The transducer at the end of the beam was used to measure vertical displacement while the other two transducers measured relative movement between the beam and connection plate.

97
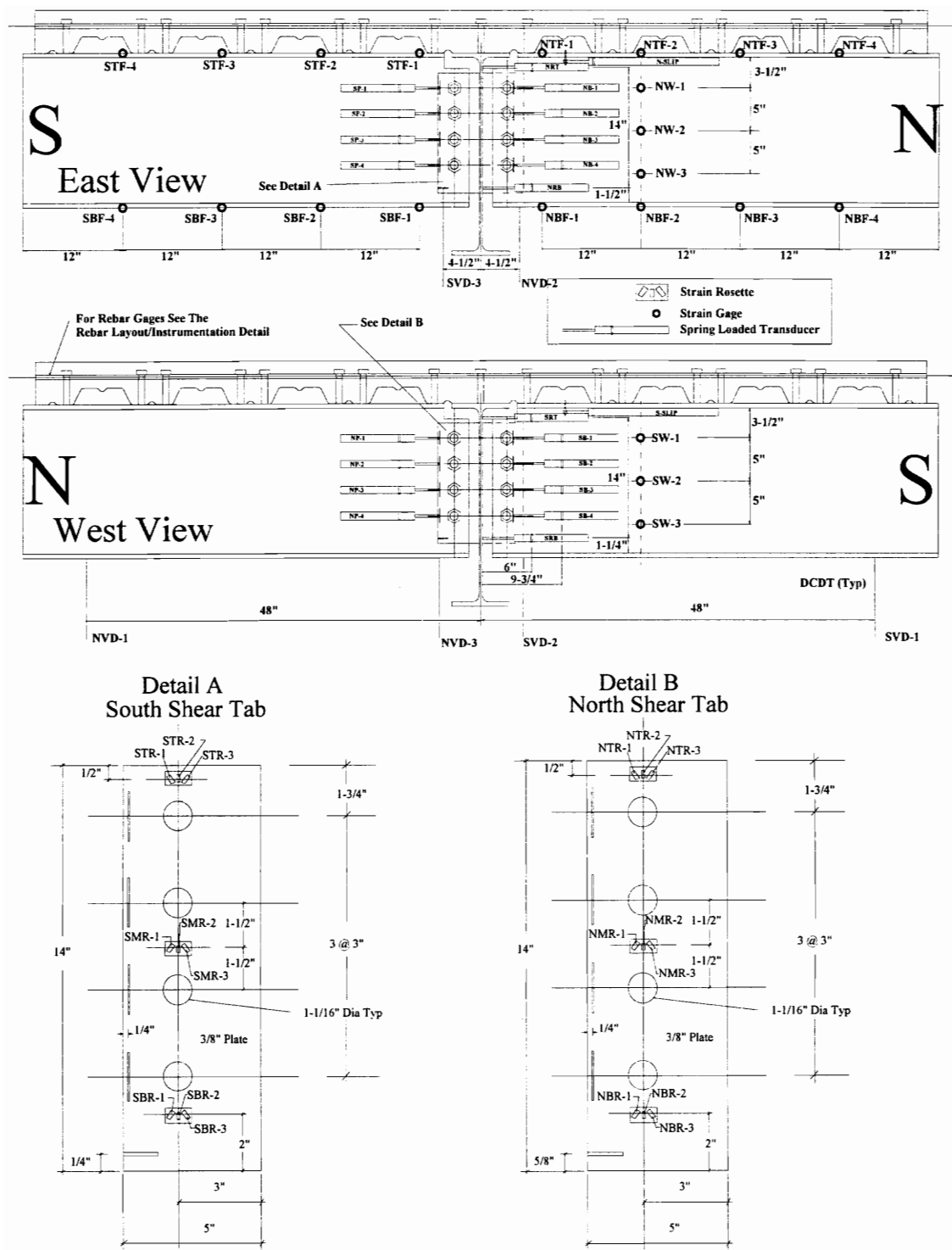
Figure 2.2-2 Details of Connection #1 Instrumentation

98

2.2.3 Details of Connection #2 Instrumentation

The beam instrumentation for Connection #2 is shown in Figure 2.2-3. Uniaxial gages were located on the beam flanges and web as described previously to determine the bending distribution in the steel section. Three arm, 45-degree strain, rosettes were attached in three locations on each plate of the shear plate connections. The rosettes were used to determine the stress distribution in the plate during the test. The location of the rosettes was changed from that in Connection #1. The location chosen for Connection #2 was believed to provide more reliable information about the stress distribution in the shear tab plate because they were located at a critical section for both bending and shear of the plate. Additionally, local stresses from the bolts should have less effect on the gages in this location versus the location chosen for Connection #1.

Two uniaxial strain gages were attached to the bottom face of the seat angle. These were placed along the toe of the angle fillet, which is believed to be the critical location for bending stresses in unstiffened seat angle connections. The purpose of these gages was to evaluate the stress that the seat angle was subjected to during the test. Because these were located at the bottom face of the angle, the strain measured was a combination of axial and bending strain. Consequently, no direct strain component (i.e., either axial or bending) could be determined. This meant that the axial or bending forces could not be directly determined.

There were eight linear motion transducers attached to the web of the south beam and seven attached to the web of the north beam. Four of these for each beam rested against small steel tabs that were attached to the shear tab connection plate. The remaining transducers were located on the opposite side of the beam web and rested against the nut for the bolts used to attach the beam to the shear tab plate. The transducers resting against the steel tabs attached to the shear tab were used to measure relative movement between the beam web and the edge of the shear tab plate.

99
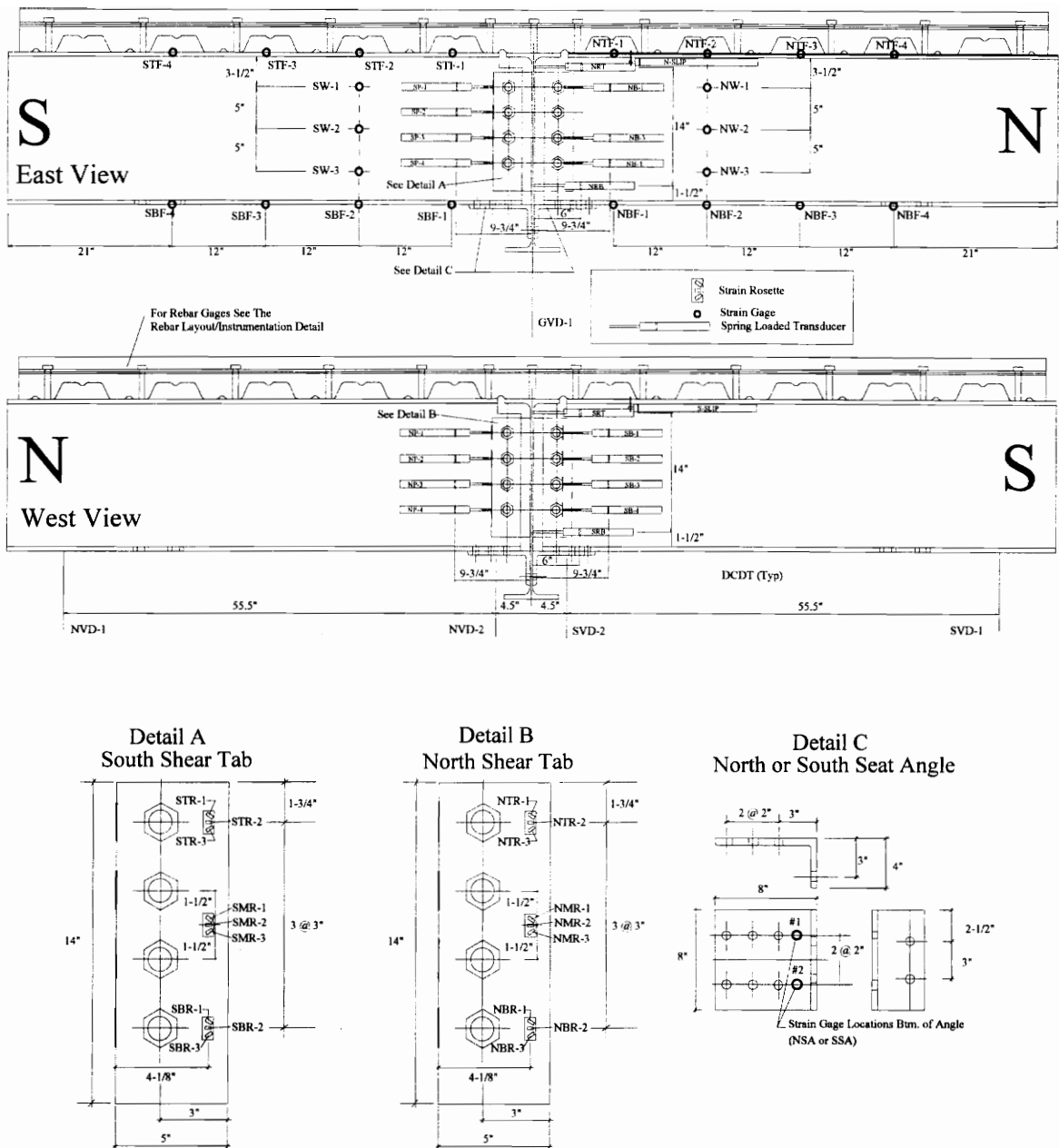
Figure 2.2-3 Details of Connection #2 Instrumentation

The transducers resting against the nuts measured the relative movement between the nut and the beam web. This combination of bolt and plate transducers allowed relative measurement of all parts of the connection in an attempt to identify a pattern of

100

deformation in the connection and a reasonable measurement of the slip between the bolt and the plate. As with Connection #1, the measurement of the slip between the bolt and the plate is particularly important for the validation of any detailed model developed for the connection.

Wire transducers were attached to the beam ends and the bottom flange of the beam under the connection. The transducer attached to the shear tab plate in Connection #1 was not used here because it did not appear to give any useful information based on the results from Connection #1. The two transducers measure vertical displacement at their respective locations.

2.2.4 Details of Connection #3 Instrumentation

The beam instrumentation for Connection #3 is shown in Figure 2.2-4. Uniaxial gages were located on the beam flanges and web as described previously to determine the bending distribution in the steel section. A three arm, 45-degree, strain rosette was attached in one location on each of the tension plates. The rosettes were used to determine the stress distribution in the plate during the test. The location of the rosette was originally believed to be an ideal spot to determine the axial and shear forces that were imparted into the plate in the plane of the connection. Uniaxial strain gages were then located at the top and bottom of each tension plate to determine the bending stresses in the plane of the connection.

Two uniaxial strain gages were attached to the bottom face of the seat angle along with two gages (one each side) attached to the side of the seat angle. These were placed along the toe of the angle fillet which is believed to be the critical location for bending stresses in unstiffened seat angle connections. This combination of gages allowed an estimate of the axial component and bending component of strains induced into the seat angle.

101
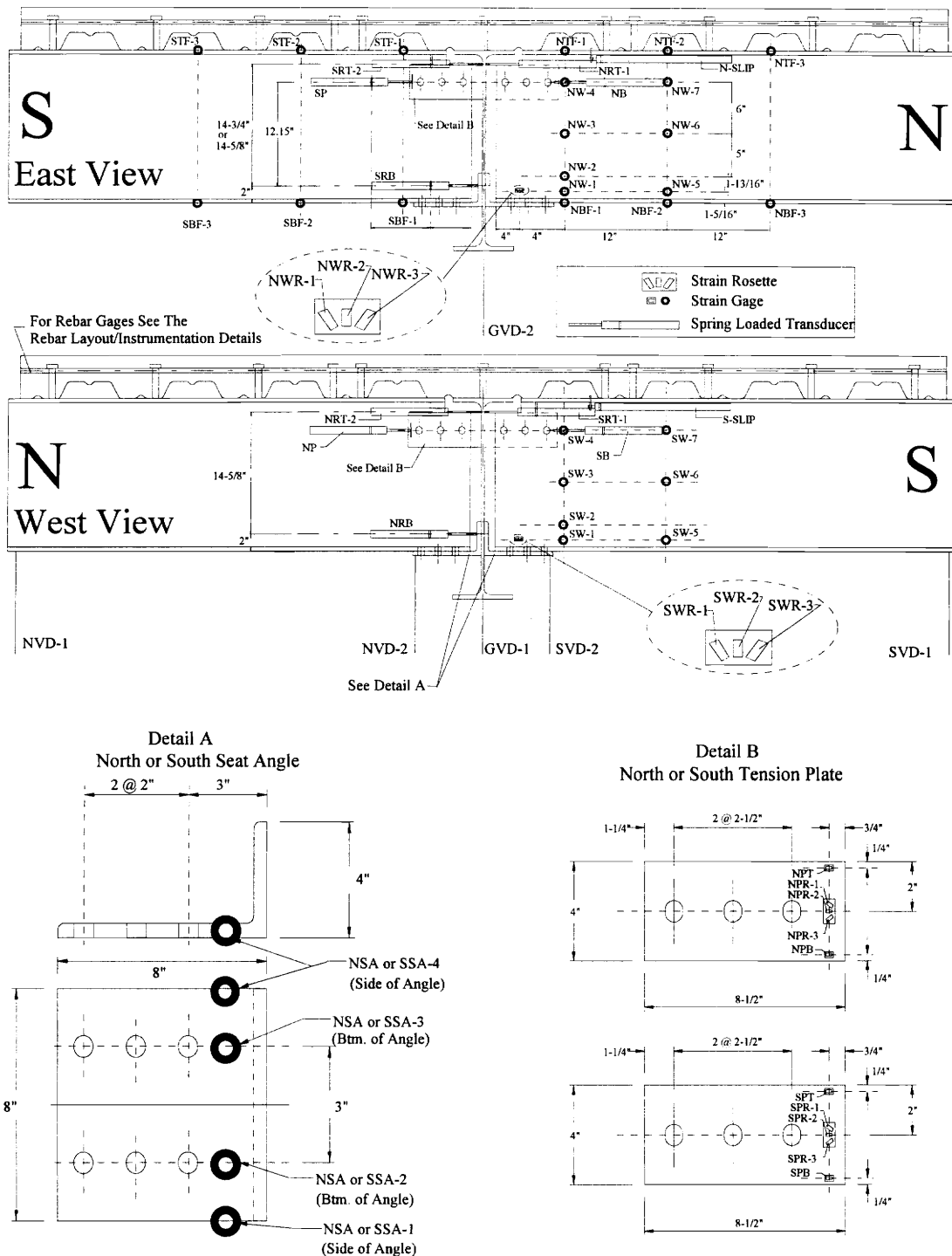
Figure 2.2-4 Details of Connection #3 Instrumentation

102

Based on these strain components, rough estimates of the axial and moment forces resisted by the seat angle could be determined.

A three arm, 45-degree, strain rosette was attached to the beam web near the toe of each beam. Ideally, this region should be one of the highest stressed areas of the beam, because most of the shear for the connection will be taken out in the seat angle. Also, a large compressive force must be developed in this region to develop the moment resistance for the connection.

Two linear motion transducers were attached to the web of each beam. One of these for each beam rested against a small steel tab that was attached to the tension plate. The other transducer was located on the opposite side of the beam web and rested against the nut for one of the bolts used to attach the beam to the tension plate. The transducer resting against the steel tab was used to measure relative movement between the beam web and the edge of the tension plate. The transducer resting against the nut measured the relative movement between the nut and the beam web. This combination of bolt and plate transducers allowed relative measurement of all parts of the tension plate connection in an attempt to identify a moment to slip relationship for the tension plate and relative slip between the bolt and the tension plate.

As shown in Figure 2.2-4, two transducers were attached to the underside of the beam top flange to measure the connection rotation relative to the girder face. These transducers could not be attached to the web of the beam as had been done in Connections #1 and #2 because of the location of the tension plate. Two transducers were used at this location to eliminate any out-of-plane twisting that might occur (i.e., the average displacement of the two transducers was assumed to be the actual displacement of the top beam flange).

Wire transducers were attached to the beam end, end of the seat angle and to the girder on the east and west side of the connection. The transducer attached to the beam end measured relative vertical displacement. The transducers attached to the girders and

103

the edge of the seat angle connection measured the relative displacement of the seat angle.

2.2.5 Details of Connection #4 Instrumentation

The beam instrumentation for Connection #4 is shown in Figure 2.2-5. Uniaxial gages were located on the beam flanges and web as described previously to determine the bending distribution in the steel section. Uniaxial strain gages were located on the top side of the tension plate, two over the south side and two over the north side. Because the plate was welded all around its edges to the top beam flange the ideal location for these gages would have been some location past the edge of the beam cope (i.e., the plate would have to be fully developed in this region). Unfortunately, the steel deck prevented placement of the gages at this location and the locations shown in Figure 2.2-5 were chosen instead. Because the plate is most likely not fully developed at the locations of the gages, the full force resisted by the plate cannot be directly determined from the strains at these gages. These gages do however give a general indication of the amount of stress being induced into the plate.

Two uniaxial strain gages (one each side) were attached to the side of the seat angles. These were placed along the toe of the angle fillet which is believed to be the critical location for bending stresses in an unstiffened seat angle connection. Because gages could not be attached to the seat angle before the beam was welded to it (i.e., the gages would have been destroyed during the welding process) the gages that had been located on the bottom of the seat angle in Connections #2 and #3 could not be properly attached and as such they were not included in the instrumentation. The gages located on the side of the angle allow a reasonable estimate of the axial force that was resisted by the seat angle.

A series of three three-arm, 45-degree, strain rosettes were attached to the beam web near the toe of each beam. This series of rosettes allowed determination of the stress

104

distribution occurring in the web at this particularly critical location. Ideally this region should be one of the highest stressed areas of the beam because most of the shear for the connection will be taken out in the seat angle and a large compressive force must be developed in this region to develop the moment resistance for the connection.

As shown in Figure 2.2-5, two transducers were attached to the bottom of the web and one to the top to determine the connection rotation. Two transducers were attached to the bottom to eliminate any out-of-plane twisting effects (i.e., the average displacement of the two transducers was assumed to be the actual displacement of the web). Only one transducer was attached to the bottom of the web during the dead load simulation stage of the test but because this load was small compared to the ultimate load it is believed that any out-of-plane twisting would also be small.

Wire transducers were attached to the beam end, to the end of the seat angle, and to the girder on the east and west side of the connection. The transducer attached to the beam end measured relative vertical displacement while the transducers attached to the girders and the edge of the seat angle connection measured the relative displacement of the seat angle.
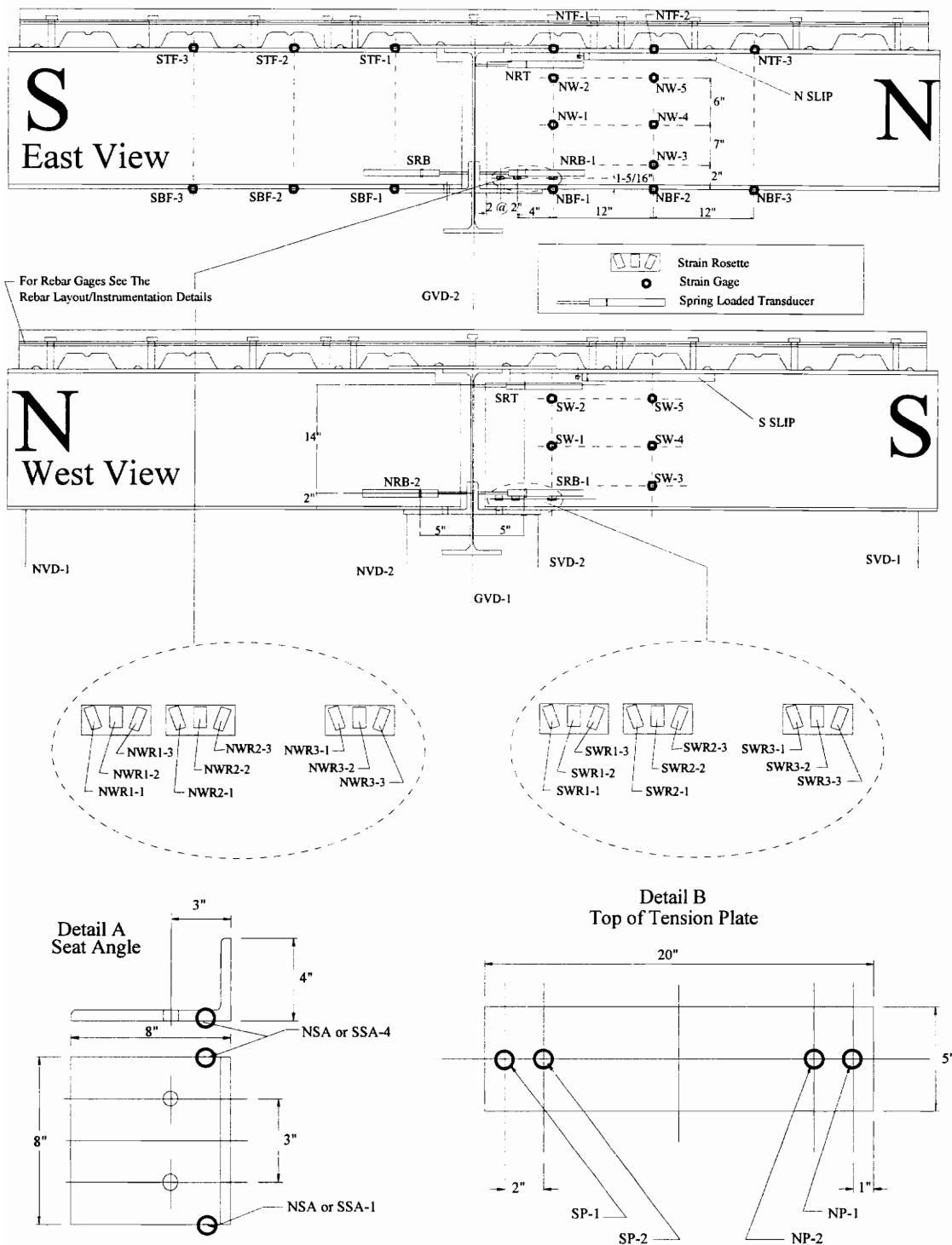
Figure 2.2-5 Details of Connection #4 Instrumentation

2.3 GENERAL TEST SETUP AND LOAD FRAMES

The basic testing arrangement was a cruciform setup in which the specimens were subjected to static loading. As part of the original proposal for this research, it had been suggested that cyclic loading with reverse curvature would be used to test the beam-to-girder connections. This suggestion had been based on investigations by Leon which had shown that composite connections subjected to cyclic loading with reverse curvature tended to have moment-rotation behavior that degraded with each cycle. Because Leon tested beam-to-column connections this type of loading made sense. The question arose as to whether of not beam-to-girder connections could also be subject to cyclic loading with reverse curvature.

To determine if reverse curvature could occur, a simple four beam span model was developed and evaluated. Figure 2.3-1 shows the basic features of the model. The beams were attached to each other with semi-rigid connections and it was assumed that the interior girders would not provide any rotational resistance (i.e., the moment on each side of the girder is the same). The connections at the exterior girders were assumed to be pins (which is how a designer would want to design the exterior connections to limit the amount of unbalanced moment being transferred to the exterior girder). Uniform loads were applied to the beams. To determine if the connection at the center of the four span arrangement could be subject to reverse curvature the two outside spans were loaded with live and dead load while the interior spans were subjected to only dead load. The live load to dead load ratio was varied from two to four and the ratio of exterior to interior span length was varied between one to one and one-half. A summary of the cases studied and the results is presented in Table 2.3-1. The connection stiffness was arbitrarily chosen but is believed to be a reasonably high value for semi-rigid composite connections. As can be seen by comparing Trial #6 and Trial #7, the stiffer the connection the more likely reverse curvature can occur so a high connection stiffness should result in conservative results.
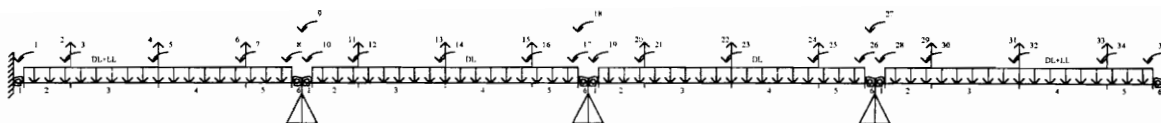
Figure 2.3-1 Four Beam Span Model With Semi-Rigid Connections

Table 2.3-1 Results From Multiple Span Investigation

Trial	DL (plf)	DL+LL (plf)	Stiffness (K/rad)	Lout-Lin (ft)	I(+)	I(-)	Moment(K")
Trial #1	720	3600	811492	30-30	1778	1778	-12.948
Trial #2	720	3600	811492	30-30	2204	1138	-87.635
Trial #3	720	3600	811492	30-20	1778	1778	295.63
Trial #4	720	3600	811492	30-20	2204	1138	201.389
Trial #5	720	2160	811492	30-20	2204	1138	24.534
Trial #6	720	2160	811492	30-20	1778	1778	89.8661
Trial #7	720	2160	600000	30-20	1778	1778	42.046
Trial #8	720	2160	811492	40-30	1778	1778	130.535
Trial #9	720	2160	811492	30-25	1778	1778	-47.121

The last column of Table 2.3-1 presents the resulting moment at the center connections. Negative moment values indicate no reverse curvature while positive moment values indicate reverse curvature. The worst case was Trial #3 and Trial #4 where the live load to dead load ratio was four and the exterior to interior span ratio was one and one-half. The difference between the moment values for these two trials results from the use of different section properties for the composite beam. Trial #3 uses an average moment of inertia for the entire beam as suggested by Leon and Ammerman (1990) while Trial #4 uses a more exact analysis that accounts for the different moment of inertia in the positive and negative moment regions of the beam. This case obviously represents an extreme and unlikely case but even in such an unlikely case the resulting reverse curvature moment was only 200 to 300 kip-in., which is small considering the magnitude of the loads applied. Based on this brief study it was decided that cyclic loading with reverse curvature did not appear to be necessary and the cruciform arrangement with static loading was determined to be the most appropriate for this type of

108

connection arrangement. However, it should be noted that although reverse curvature does not appear to be likely, the connections should eventually be tested under cyclic loading at service load levels to determine what, if any, deterioration may occur to the connection under repeated loading and unloading.

The general test setup used during the dead load simulation and live or failure loading is presented in Figure 2.3-2 and Figure 2.3-3 respectively. These figures present the general setup for all four connections.

The girder was supported by and bolted to three W10x49 columns which were spaced at four-ft. intervals. The two outside columns were bolted to the reaction floor while the middle column, which was directly under the connection, bears against the reaction floor. Each beam was connected to the girder with the connection specified for the particular test.

During the live load portion of the test the free end of the beam for all four connections was braced against lateral movement with a lateral brace system attached to the bottom flange of the beam. The lateral bracing system allows the beam end to have free vertical movement while preventing lateral movement. The brace is believed to merely provide the same lateral stability that would be provided by the rest of the beam in a real floor system. As a result of some anti-symmetric loading during the live load portion of Connection #2 it was decided to also brace the girder top from lateral movement for the last two connections. Again, this bracing merely simulates the stability that would normally be provided by the actual floor system in a real building.

The dead load simulation frame (Figure 2.3-2) consisted of short cruciform columns that were bolted to reaction floor beams and a structural tube that spanned between the two cruciform columns. A short length of horizontal 1-1/2-in. diameter threaded rod was attached to the bottom beam flange with four U-bolts. The horizontal rod was then connected to a vertical 1-1/2-in. diameter rod with an eye nut. The top section of vertical rod was instrumented with strain gages to form a load cell transducer. The load cell was calibrated to determine a sensitivity that could be used to evaluate the

applied axial load in the threaded rod. At the time the trial loading and dead load was applied Connection #1 the rod had only been instrumented with one strain gage. Since the rod appeared to be under bending and axial loads it was apparent that the one gage would not give accurate results. The additional gages to form the load cell transducer were added after the dead load was removed from Connection #1.

The bottom of the rod with the load cell was attached to a turnbuckle which was intern attached to another portion of threaded rod that was anchored to the tube section. The turnbuckles were tightened to apply the simulated dead load. The distance from the centerline of the connection to the applied load is either 24-in. or 48-in. depending on the particular connection tested.
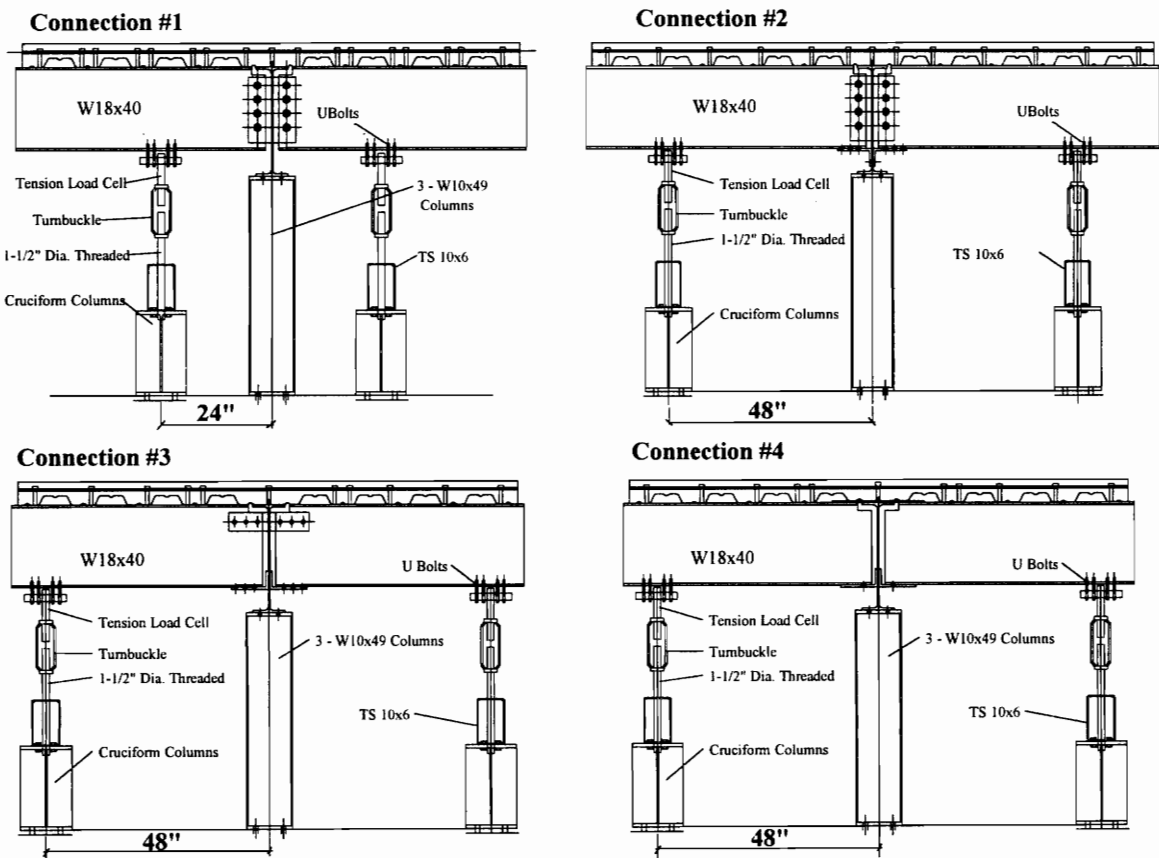
Figure 2.3-2 Dead Load Simulation Setup

110

The live load frame consisted of W21x62 columns, which were attached to the reaction floor (Figure 2.3-3). Two C15x50 sections spanned between the columns and support a short reaction beam at their mid span. Two 100 kip capacity displacement controlled hydraulic rams powered by an electric motor were used to load the test specimen. The rams reacted against the composite slab through a block and roller arrangement with the load distributed through a 38-in. long, 8-in. wide, 1-in. thick plate. The roller allowed rotation of the beam end while maintaining a vertical applied load. The plate allowed the load to be distributed across the end of the slab. A 500 kip capacity load cell was placed above each ram to determine ram load. The distance from the centerline of the specimen to the point of applied load was either 42-in., 48-in., or 54-in. depending on the connection. For Connections #1 and #2, loads were applied at different locations for the different connections as well as the different stages of loading in an attempt to be just beyond the approximate inflection point that would occur in the beam of the hypothetical design. For Connections #3 and #4 the loads were applied at the practical extreme end of the beam as it was believed that the hypothetical inflection point for these beams was beyond the actual beam length.
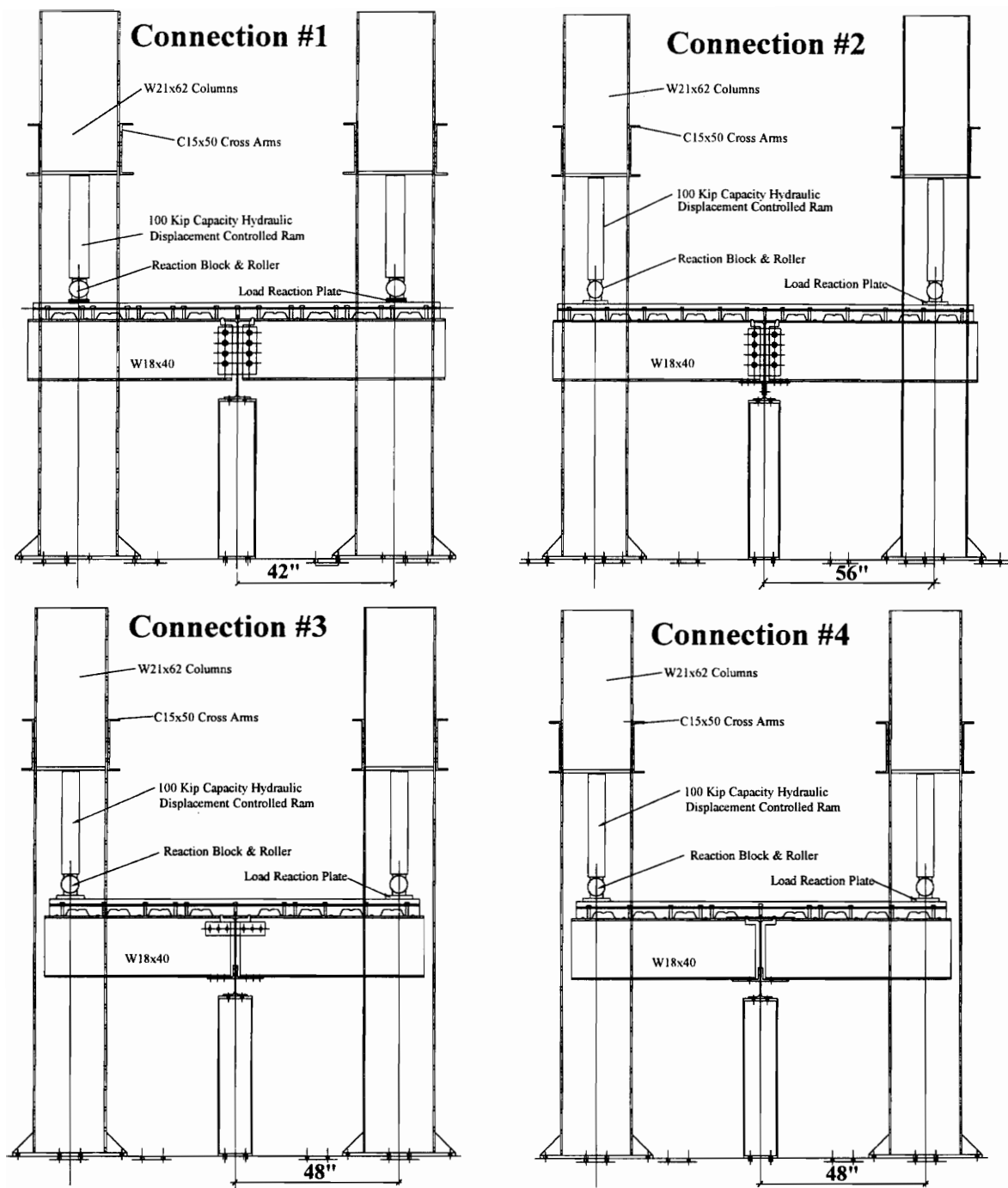
Figure 2.3-3 Live Load Test Setup

112

2.4 TESTING PROCEDURE

Because the majority of composite beams are currently built using unshored construction it is apparent that the connections associated with these beams will have two distinct stages of behavior; before and after concrete hardens. Before the concrete hardens, the only rotational resistance of the beam-to-girder connection will be provided by the simple steel component of the connection (i.e., either the shear plate, shear plate and seat angle or the seat angle and tension plates in this test series). After concrete hardens the composite connection will provide rotational restraint against all additionally applied load.

The loading history for the test specimens was designed to simulate the typical loading history for unshored construction. Immediately after placement of concrete the dead load frame was used to apply a load of 15 kips for Connections #1 and #2 and 17 kips for Connections #3 and #4. This load was based on the fresh concrete load for the beam in the hypothetical design discussed previously. Larger dead loads were applied to Connections #3 and #4 to account for the increased slab thickness (5-1/2-in. versus 5-in.). The load was typically applied in one to two kip increments by tightening the turnbuckle of the dead load frame. All relevant instrumentation was monitored and data collected at each load increment.

Because the test loads were actually being applied to two cantilever beams rather than two full span beams, it was particularly important to monitor the moment-rotation behavior of the connection. During the dead load stage of loading, load was applied until either the specified dead load was reached, the connection reached a horizontal plateau in the in its moment-rotation behavior, or the connection rotation exceeded that which would have occurred in the hypothetical beam design. The rotational limit of the latter is based on the beam-line for the non-composite beam under the specified dead load. The simulated dead load was left on the specimen until it was ready for the ultimate loading test stage.

The simulated dead load was removed within a couple of days of when the ultimate test loading was going to be applied. All instrumentation was monitored and the moment-rotation curve for the connection was plotted through all stages of the dead load removal. Once the dead load was removed the dead load frames and loading rods were dismantled and the live load frames were brought into position.

The simulated live load was applied until the moment-rotation plot showed that the connection had reached the same position (on the moment-rotation curve) that it had been prior to the removal of the dead load. The connection was then unloaded. This preliminary loading and unloading was conducted in order to ensure all instrumentation and the test frames were operating properly. The specimens were then rapidly reloaded to the previous load level; after which, the load was increased in increments believed to be reasonable for the type of connection being loaded (generally one to four kip increments). Load was increased until the moment-rotation behavior of the connection started to become fairly non-linear or until it was necessary to unload for other reasons such as problems with the test setup. The specimen was then unloaded and reloaded to determine the unloading and reloading stiffness characteristics of the joint. After reloading, the load increments were based on both load and deformation. Loading was stopped when the specimen failed; i.e., the specimen was incapable of taking additional load, or the specimen was distressed to the point where violent failure was considered likely.

It should be noted that the test loading for Connection #1 included loading and unloading the connection prior to the composite deck being constructed. This additional loading was for purposes of testing the experimental setup and for determining the type of data that would be collected from later testing. The dead load was removed but the specimen was not returned to its original condition before the composite deck was constructed.

Connection #3 was also loaded and unloaded before the composite deck was constructed. This loading and unloaded was to study the effect of bolt tightening on the moment-rotation behavior of the steel connection. During this loading and unloading all

114

the instrumentation in place at the time was monitored to ensure that the connection did not become overly stressed in any area that might affect the behavior of the composite connection. After Connection #3 was loaded and unloaded, for the two cases studied, the specimen was returned to its original position, the bolts were re-tightened, and the composite slab was constructed.

CHAPTER 3.0

RESULTS

3.1 GENERAL

The tests results indicate that the four beam-to-girder composite semi-rigid connections tested in this test program had significant strength, rotational stiffness, and ductility. The full moment-rotation history for the north side of each connection is presented in Figure 3.1-1.
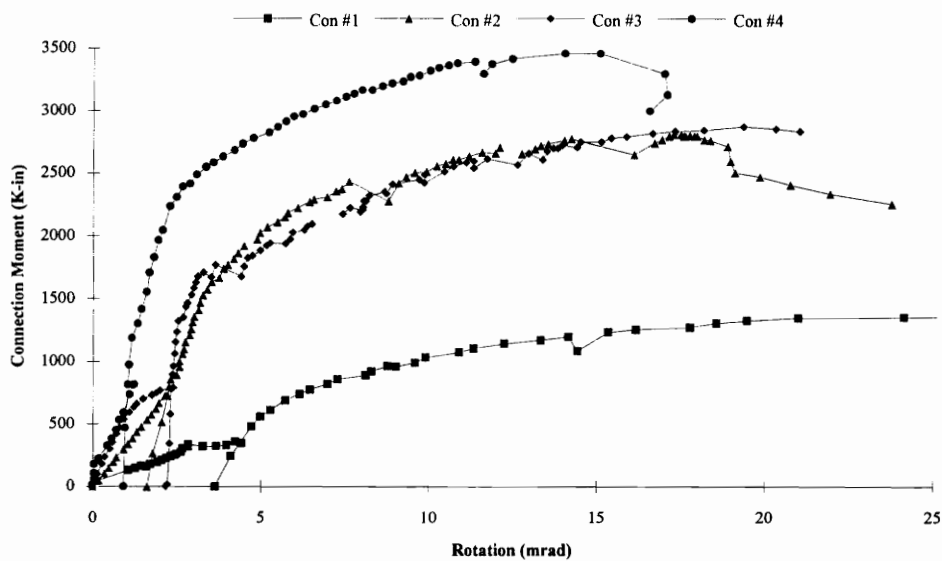
Figure 3.1-1 Moment Rotation Behavior for Test Connections

Steel Connection Behavior

In general the stiffness of the steel connection increased for each connection test (i.e., #1 the most flexible #4 the stiffest). Connection #1 was a single plate shear connection. The moment-rotation stiffness for this connection was the least of all the connections. This behavior was also the most unpredictable because of the significant influence sudden slips at the bolt locations had on the moment-rotation behavior.

116

Connection #2 was the same as Connection #1 except a length of seat angle was used to attach the bottom flange to the girder face. This moment-rotation response was very linear and much stiffer than the behavior of Connection #1. Connection #3 was a seat angle connection like Connection #2 but the shear plate of Connection #2 was replaced with a horizontal tension plate. The moment rotation response was very smooth and predictable and slightly stiffer than that seen for Connection #2. The last connection, Connection #4, was the stiffest of all the connections. This connection consisted of a welded seat angle connection and a steel plate welded to the top of the beam. This connection response was extremely linear and would have most likely continued to be for a much higher load than what was applied during the dead load simulation.

Composite Connection Behavior

The moment-rotation stiffness for the composite connections followed the same general trend as seen for the steel connections (i.e., stiffness increased for each test). The behavior of all the connections can be broken up into three general regions; before severe flexural composite slab cracks, after slab cracks, and plastic. These regions are generally seen as three different slopes to the connection stiffness.

Connection #1 was characterized by the least stiffness of all the connections. However, the lower stiffness did seem to be accompanied by an increase in ductility. Unfortunately the connection failed from local buckling prior to any reinforcing steel yielding and consequently never reached its full moment capacity.

Connection #2 and #3 appear as if they were almost the same composite connections. Connection #3 was slightly stiffer than Connection #2 in the early regions of the moment-rotation behavior, but quickly softened and was soon rotating in a manner similar to that seen in Connection #2. Connection #2 was never loaded to complete failure as a result of test limitations, but it appeared that it would have failed from tearout of the top bolts in the shear plate through the web of the beam. It should be noted that, although the connection itself was not loaded to failure, that a shear stud had failed above

the south beam. This failure appeared to reduce the effectiveness of the slab which eventually would have resulted in failure of the connection. Connection #3 failed as a result of tension rupture of the bolted tension plate.

Connection #4 was the stiffest of all the connections. The moment-rotation behavior was characterized by what appeared to be an almost vertical response until severe cracking had occurred in the composite slab. Subsequently, the moment-rotation behavior leveled off and was soon into its plastic region. The connection failed when the web on the north side crippled just above the seat angle connection and the tension plate welds ruptured along the top of the north beam.

The composite connection behaviors are shown in a non-dimensional form in Figure 3.1-2. Also shown are the connection classification boundaries as defined by Eurocode 3 (1993) and Eurocode 4 (1992) for a braced frame (note that M_{pc} is the nominal moment capacity of the composite beam in positive flexure). As can be seen in Figure 3.1-2, Connections #2 through #4 would be considered rigid partial strength connections while Connection #1 would be considered a semi-rigid partial strength connection.
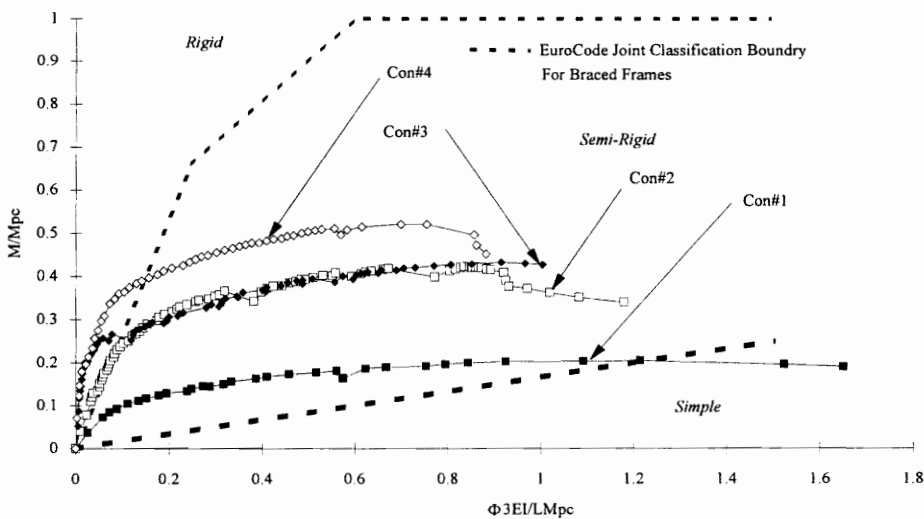
Figure 3.1-2 Normalized Moment-Rotation Behavior of Composite Connections

3.2 BEHAVIOR OF CONNECTION #1

3.2.1 Moment-Rotation Behavior and Test History

Connection #1 was loaded at three different times: immediately after construction, at the time of concrete casting, and at the time when failure loading was applied. The moment-rotation behavior for the entire load history is presented in Figure 3.2-1 and Figure 3.2-2. For comparison purposes, the moment-rotation behavior for the two sides of the specimen have been plotted together for the dead load portion of the test and for the live load portion of the test. These plots are presented in Figure 3.2-3 and Figure 3.2-4 respectively. The specimen was considered to have failed when the bottom flange of the north side beam buckled at a location adjacent to the connection.
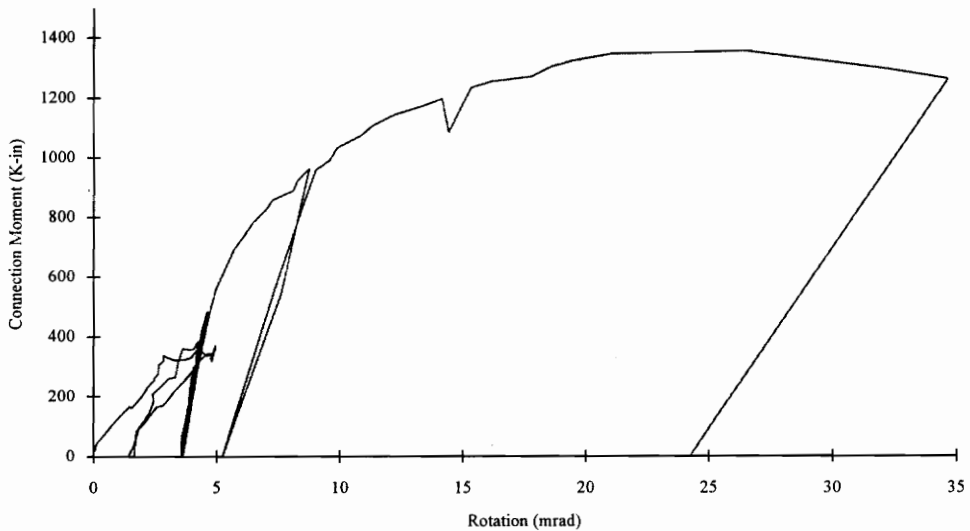
Figure 3.2-1 Moment-Rotation Behavior of North Connection

The connection was first tested immediately after the connection was built but before the composite slab was in place. This allowed changes in the test setup to be made without worrying about damaging the composite slab. This stage of loading also enabled

119

the writer to determine the type of data that would be collected and the best way to interpret this data. The connection moment-rotation behavior in this region was somewhat erratic but overall had a general trend that is typical of steel semi-rigid connections.
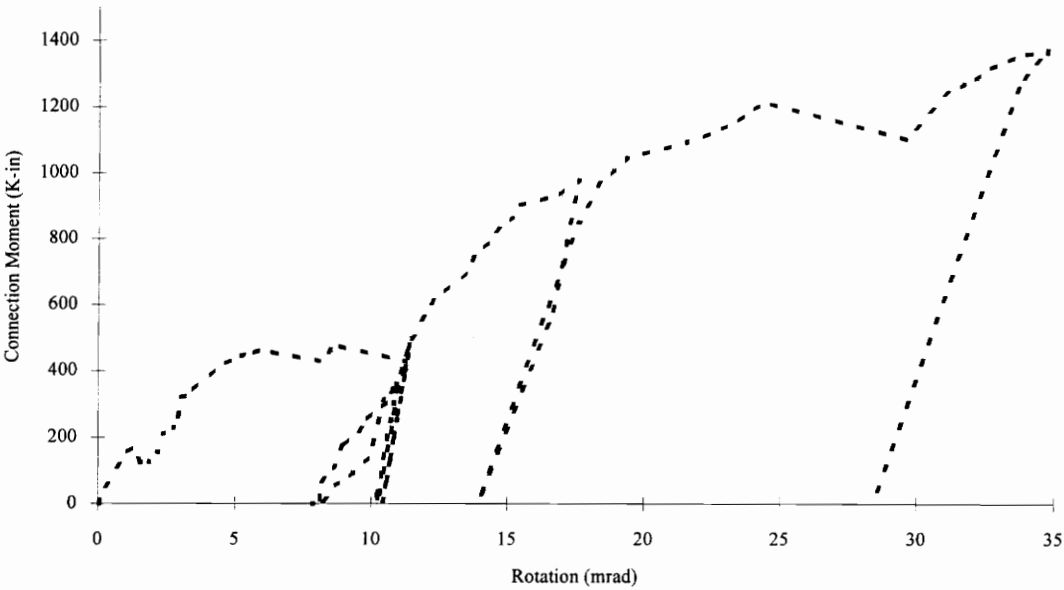
Figure 3.2-2 Moment-Rotation Behavior of South Connection

During the first loading, the connection appeared to be loaded unsymmetrically with the south beam taking more load than the north beam. The stress levels, as determined from strain gage readings, also suggested that the connections were being loaded unevenly. This is most likely why the south side appeared to slip into bearing during application of the dead load and the north did not. Part of the apparent uneven loading is believed to be associated with the instrumentation used on the dead load frame at the time Connection #1 was loaded. The load rod had only one strain gage attached to determine the load in the rod. It is believed that the rod was subject to both bending and axial load and that the single gage was subject to this combination of strains. Consequently the gage readings most likely lead to inaccurate estimates of the applied

120

load. The single gage was replace with four gages in a full bridge arrangement after the dead load frame was removed so that this would not be a problem in subsequent connection tests.

The application of dead load was stopped after the north side appeared to be loaded to the 15 kip design dead load and the south connection had rotated just beyond the dead load beam line. The test specimen was then unloaded and the composite slab was constructed. The test specimen was not returned to its original position prior to the composite slab being constructed. The day the slab was cast the 15 kip design dead load was applied again. As shown in Figure 3.2-3 the connections appeared to follow similar moment-rotation paths (although the south started at a rotation much higher than the north side) and the loading appeared to be much more symmetrical.
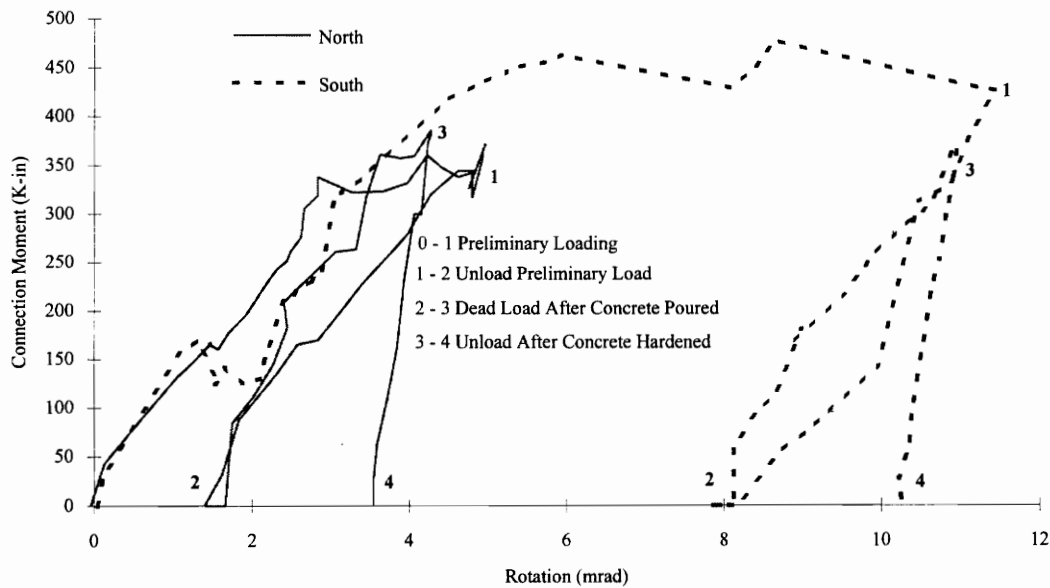
Figure 3.2-3 Moment-Rotation Behavior of Steel Connections

After 28 days the specimen was unloaded and the dead load frames were replaced with the live load frames. As can be seen in the moment-rotation diagrams shown in Figure 3.2-3, the connections followed a very linear unloading path as the dead load was

121

removed. Once the live load frames were in place the hydraulic rams were used to load the specimen back to the same point on the moment-rotation curve that the specimen had been at prior to removal of the dead load. The connection was then unloaded. As shown in Figure 3.2-1 and Figure 3.2-2 this loading and unloading followed the same path as when the dead load was removed. This preliminary loading and unloading was conducted in order to ensure all instrumentation and the test frames were operating properly.

After the specimen was reloaded beyond the dead load moment (approximately 490 K-in. on each connection) loads were increased in one kip increments. First cracks in the slab appeared at approximately 830 K-in. There were three initial cracks, one directly above the girder centerline and two parallel to the girder but offset approximately 12-in. to the left and right of the girder center. These locations appeared to correlate with the locations of the reinforcing bar gages. At around 930 K-in., a loud snap was heard but the source of the sound was never identified.
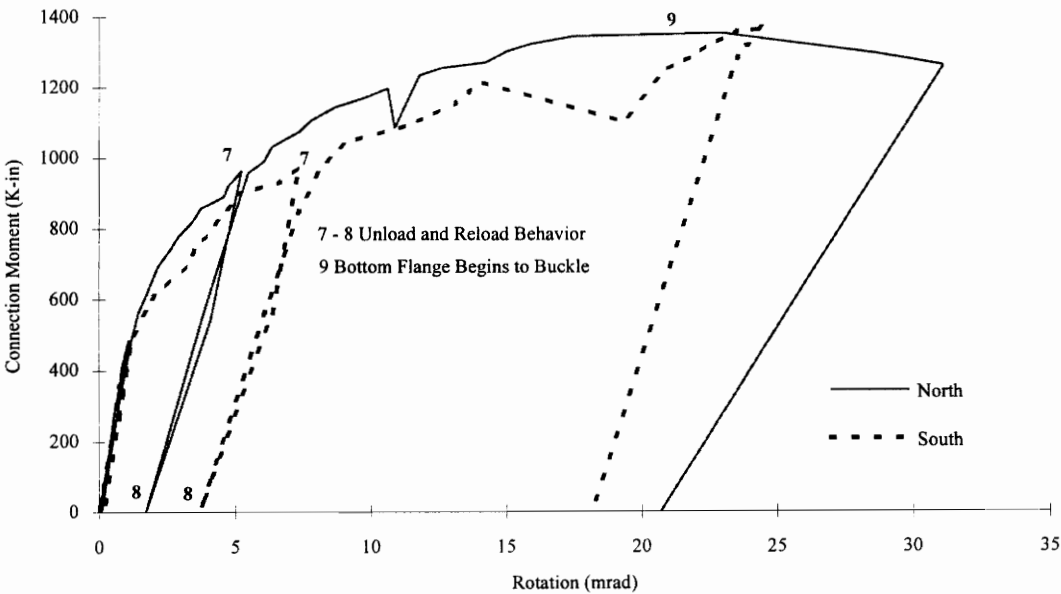
Figure 3.2-4 Moment-Rotation Behavior of Composite Connections

122

At 970 K-in. the connection was unloaded and reloaded, and as seen in Figure 3.2-4 the connections behaved in a very linear fashion. After this point, loads were increased in one kip increments unless large rotations were seen, then the connections were loaded based on the connection rotation. At around 1000 K-in. more cracking was heard and a five-in. long crack just above the end of the south beam was noticed. The crack was just above and parallel to the web of the beam. At 1090 K-in. a similar crack appeared above the end of the north beam. At 1180 K-in. new cracks were seen adjacent and parallel to the original three cracks. These cracks were approximately 24-in. on each side of the girder center line. As load was being increased from 1200 K-in., an extremely loud pop was heard and load was lost as the south steel connection appeared to slip further into bearing. Yield lines also appeared at the base of the south connection plate. At 1300 K-in. a new crack was noticed above the north beam adjacent to the load plate. This crack was more curved than the previous cracks which possibly indicated some shear lag in this region. A similar crack soon followed above the south beam.

At approximately 1360 K-in. yielding was noticed around the bottom bolt of the north connection. After this point the beams would not take any additional load as they quickly rotated to accommodate any displacement induced by the hydraulic rams. As rotation increased it became apparent that the bottom flange of the north beam had started to buckle adjacent to the connection. After it was seen that the north beam would not take any additional load the specimen was unloaded and the test was ended.

The center of connection rotation versus the moment at the connection is plotted in Figure 3.2-5 and Figure 3.2-6. The center of rotation was determined by evaluating the displacement at the top and bottom of the connection as determined from the displacement transducers located at these locations. The center of rotation for the bare steel connections on both the north and south sides steadily declined from the top to the center of the connection. This was most likely a result of some initial stiffening provided by the steel deck and the reinforcing steel in the wet concrete.
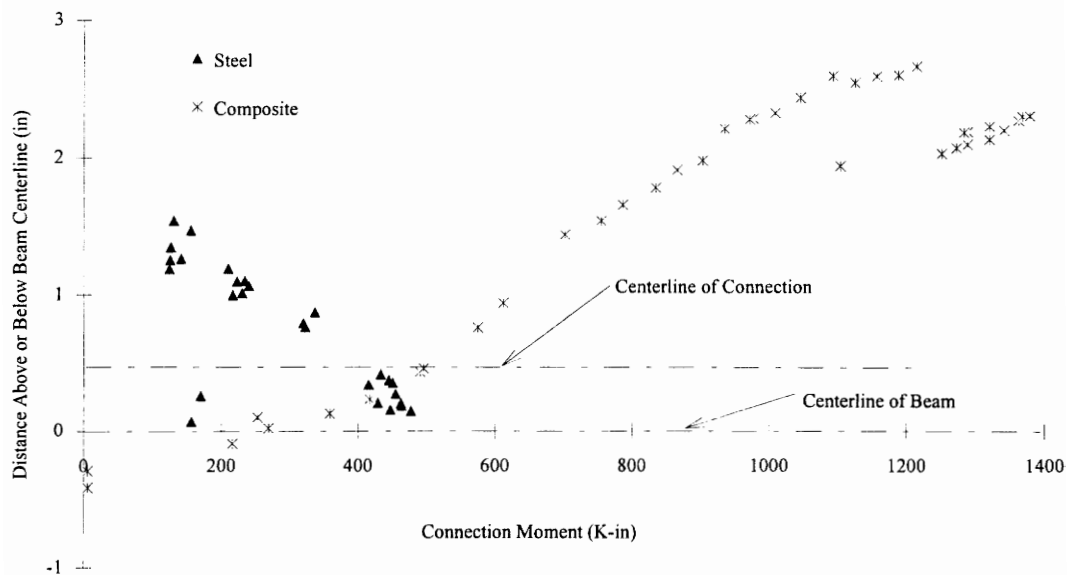
Figure 3.2-5 Center of Connection Rotation South Connection
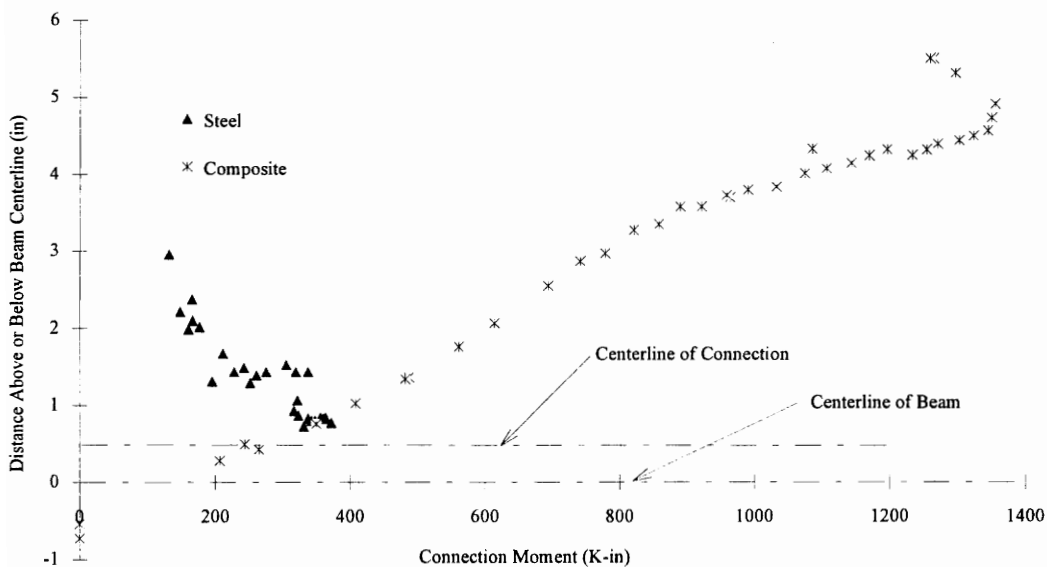
Figure 3.2-6 Center of Connection Rotation North Connection

124

This stiffness quickly diminished as moment increased. Once the composite slab was effective the center of rotation steadily rose from the center of the steel connection to near the top of the steel connection. This occurred because the composite slab was much stiffer than the steel connection and the steel connection started to soften as load was increased. More steel connection force was required to resist the composite slab force in order to develop the connection moment. In both sides of the specimen, the change in rotation center followed a fairly linear behavior up to failure of the connection. It is apparent that because the connection rotation on the north side moved much higher than that on the south side, that the steel connection was stiffer on the south side than on the north.

3.2.2 Steel Connection Behavior

Linear displacement transducers measured the relative movement between the web of the beam and the connection plate. The data from these transducers is presented in Figure 3.2-7 through Figure 3.2-10. The slip of the south side (approximately 1200 K-in.) is very apparent in these figures. It is also apparent that the general shape of the behavior plots looks similar to the moment-rotation behavior for moments below the deal load moment. This leads to the conclusion that understanding the load slip relationship for the high strength bolts is key to predicting the moment-rotation behavior for the bare steel connection.

The slip of the top part of the connection indicated that the web and the plate were separating (in the plane of the connection) until the composite slab became effective. After this point, the movement at all the bolt locations showed the web and the plate moving toward each other. This indicated that the entire steel connection was developing force in the opposite direction of the composite slab. These figures also show that the sharp increase in the south connection rotation that occurred during the trial loading was mainly associated with slip of the top and bottom bolts.
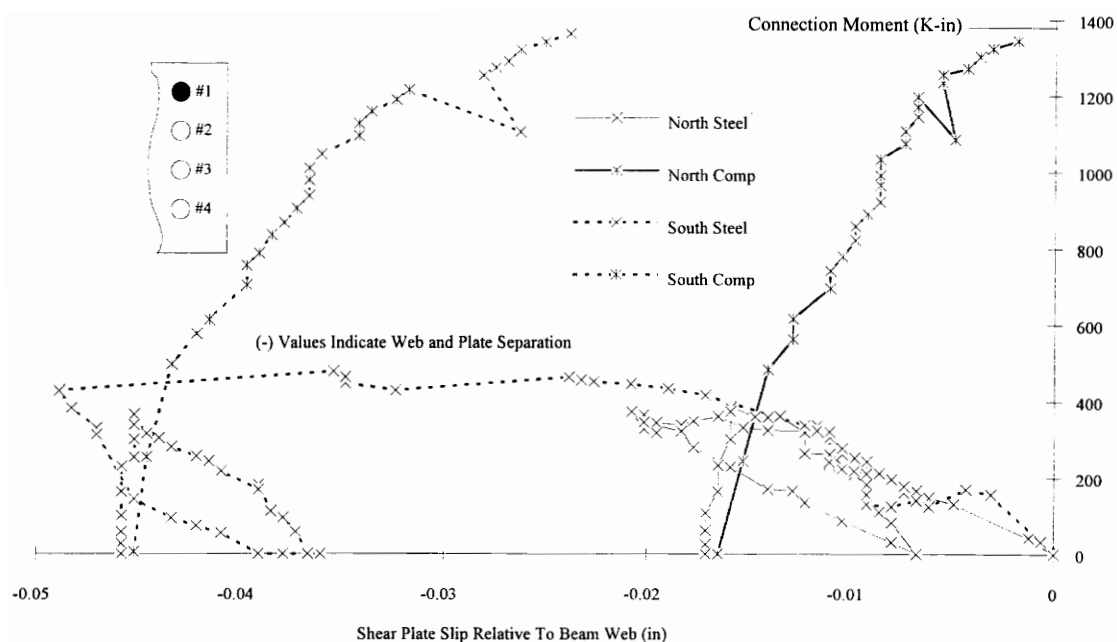
Figure 3.2-7 Moment Vs. Plate Slip For Bolt Location #1
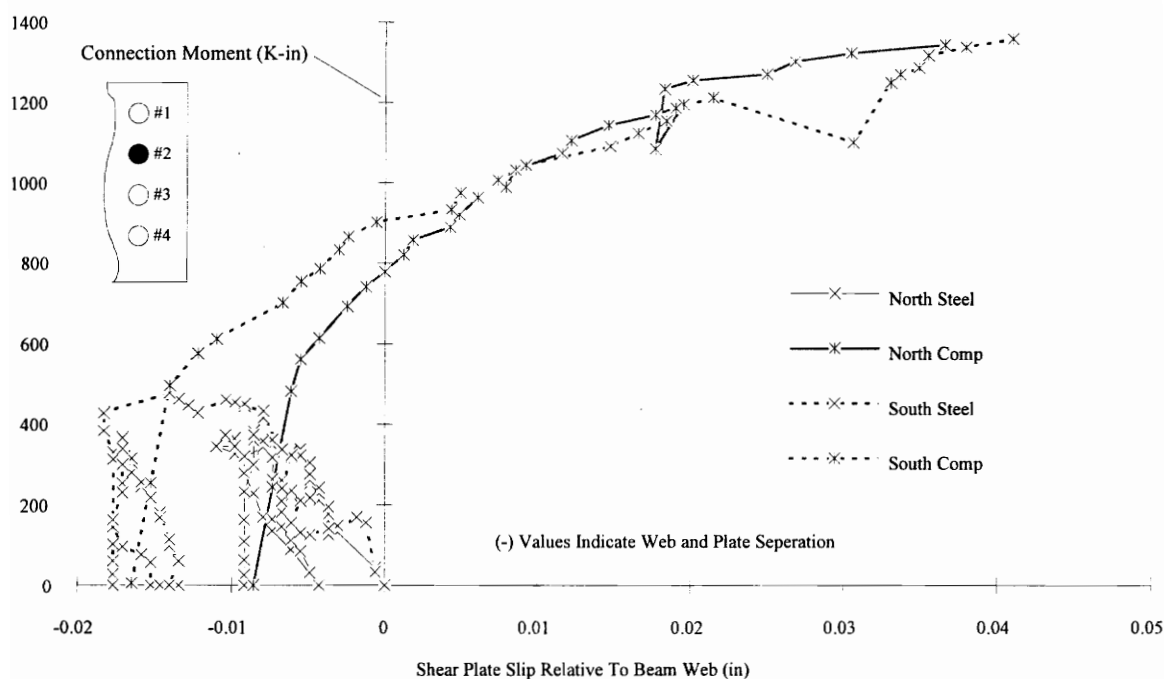
Figure 3.2-8 Moment Vs. Plate Slip For Bolt Location #2
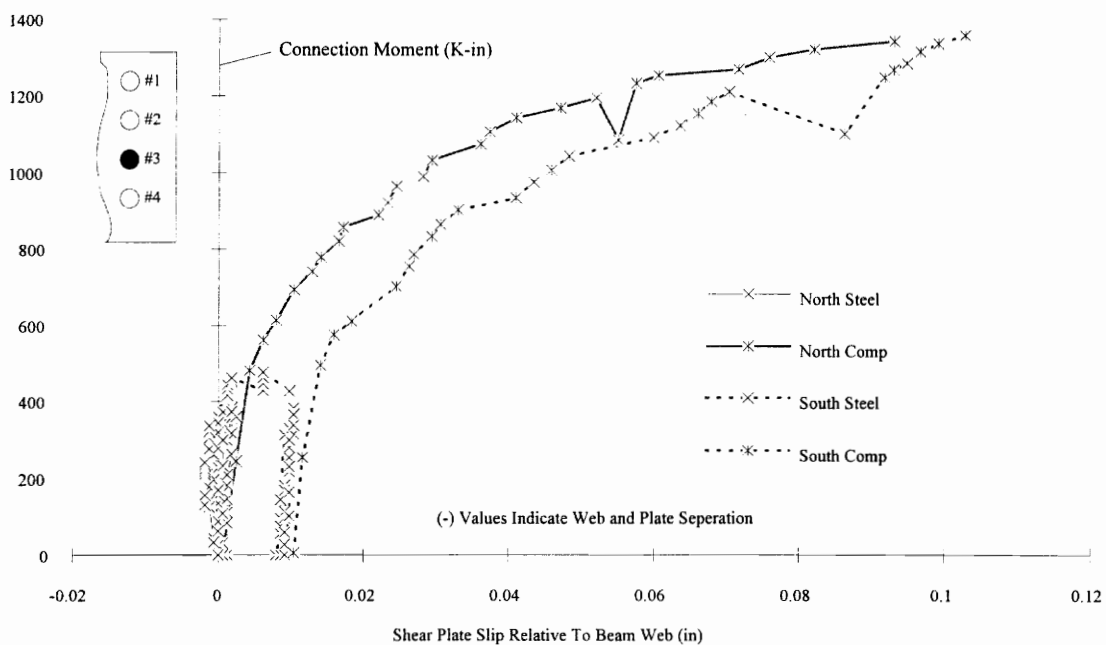
Figure 3.2-9 Moment Vs. Plate Slip For Bolt Location #3
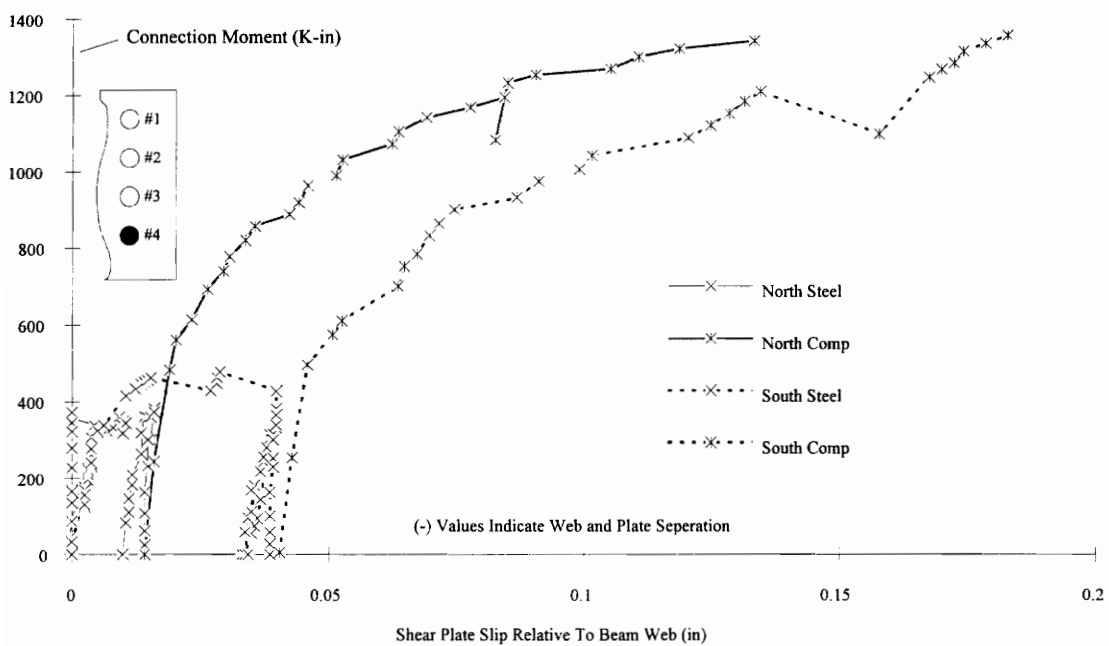
Figure 3.2-10 Moment Vs. Plate Slip For Bolt Location #4

127

When the composite connection on the south side slipped at 1200 K-in. all four bolts appeared to have slipped. This indicates that the top and bottom bolts were critical for the steel connection and that all the bolts were critical for the composite connection. This would be expected based on the results of the ultimate strength analysis (discussed in Chapter 2) that was used to predict the connection behavior.

The data obtained from the strain rosettes that were attached to the top, middle, and bottom of the connection plate is presented in Figure 3.2-11 through Figure 3.2-14. Each line in the figures represents a stress contour for a given value of connection moment. The line was generated by connecting the values of the stress at the three rosette locations. The writer is unsure of the accuracy of the information obtained from the strain rosettes because the connection plate was not subject to in-plane stresses alone. The plate was also believed to be subject to some out-of-plane bending which would severely affect the values of strain measured by the rosettes. The rosettes were also most likely subject to local stresses because of their proximity to the bolts. The information has been included here because it appears that the values are correct in sign and relative magnitude.

There were two basic trends noticed in how the shear stresses were distributed in the connection plate. First, when the bare steel connection was resisting the dead load, shear stress in the top and bottom of the plate increased slowly compared to the shear stress at the center of the plate. Second, when the composite connection started to resist live load, shear stress increased rapidly in the top of the plate and dropped near zero at the bottom of the plate. The high shear stresses at the center of the plate is no surprise since this is the natural location for the maximum shear stress. The manner in which the shear stress was distributed in the top and bottom of the plate seems to indicate that the amount of shear stress resisted may be related to the normal stress being resisted. For the bare steel connection, the moment in the connection was developed by normal stresses in the top and bottom of the plate and consequently little shear stress was developed.

128
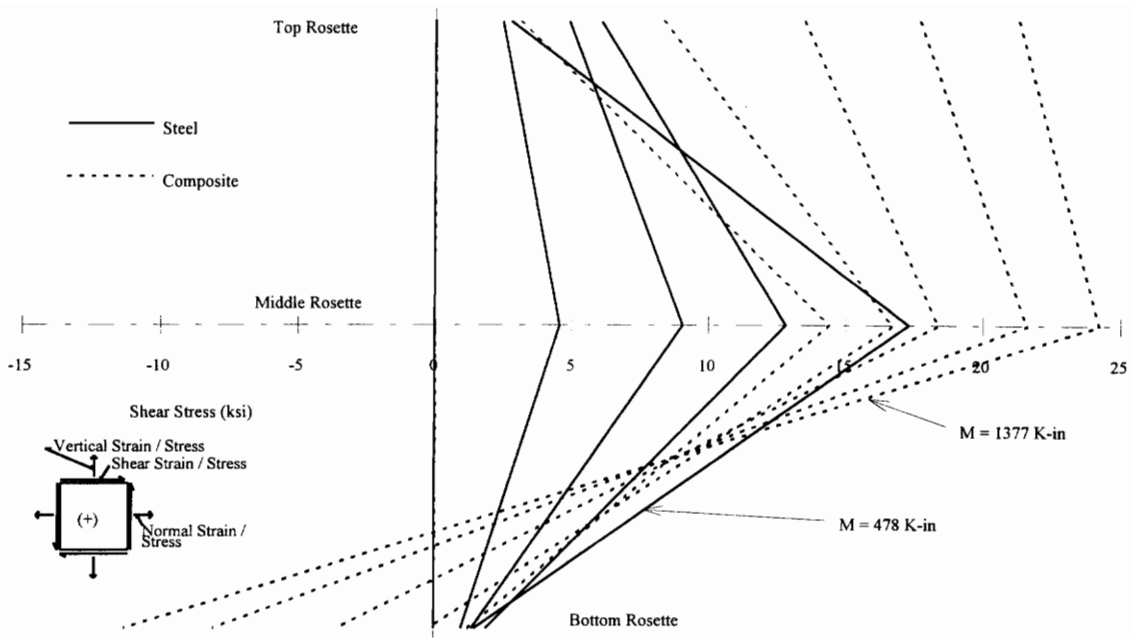
Figure 3.2-11 Shear Stress Distribution South Shear Tab Plate
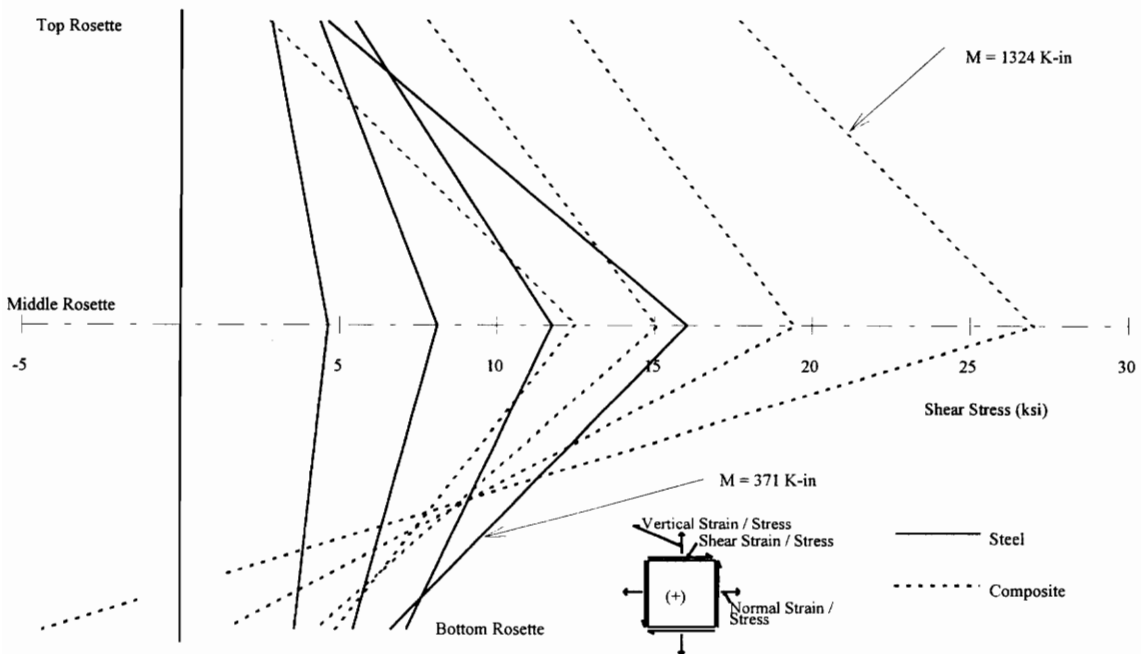
Figure 3.2-12 Shear Stress Distribution North Shear Tab Plate

129

For the composite connection the moment in the connection is developed primarily by forces in the composite slab and in the lower portion of the connection. Consequently the shear stress near the bottom of the plate was small and the shear stress in the top of the plate increased rapidly since it was no longer needed to develop significant normal stresses.

The normal stress contours shown in Figure 3.2-13 and Figure 3.2-14 indicate that the top and bottom of the shear plates were not subject to high normal stresses for the bare steel connection. This is contrary to what would be expected based on the discussion of the shear stress distribution. The normal stresses, most likely, appear to be small at the top and bottom of the plates because of the locations of the rosettes. The normal forces in the plate were probably developed in the plate between the location of the bolt and the location where the plate is welded to the girder.
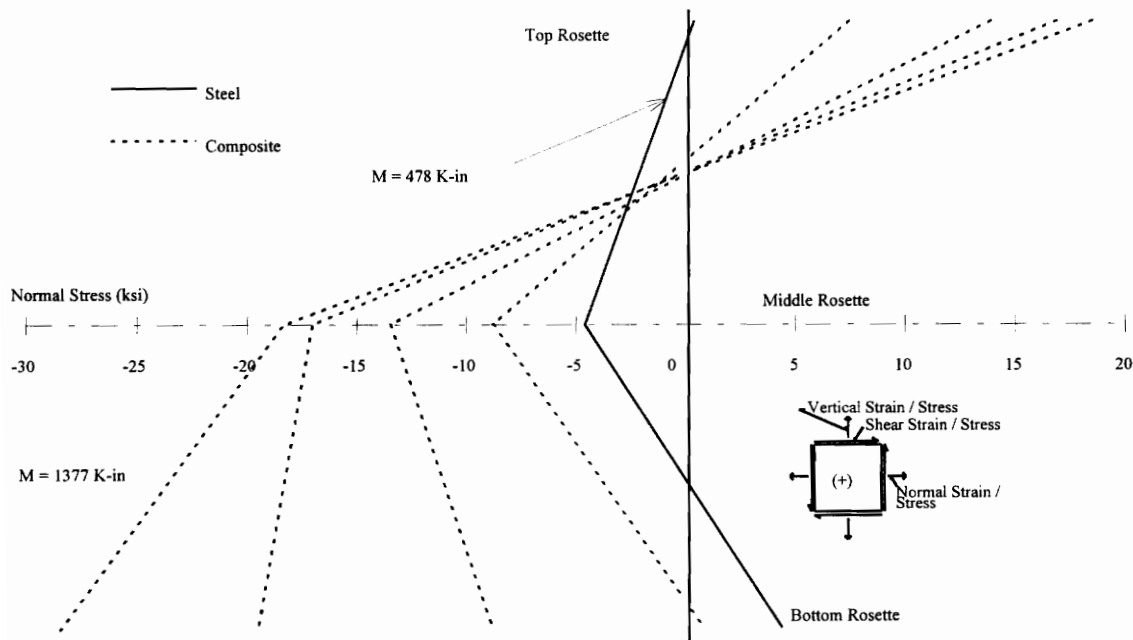
Figure 3.2-13 Normal Stress Distribution South Shear Tab Plate
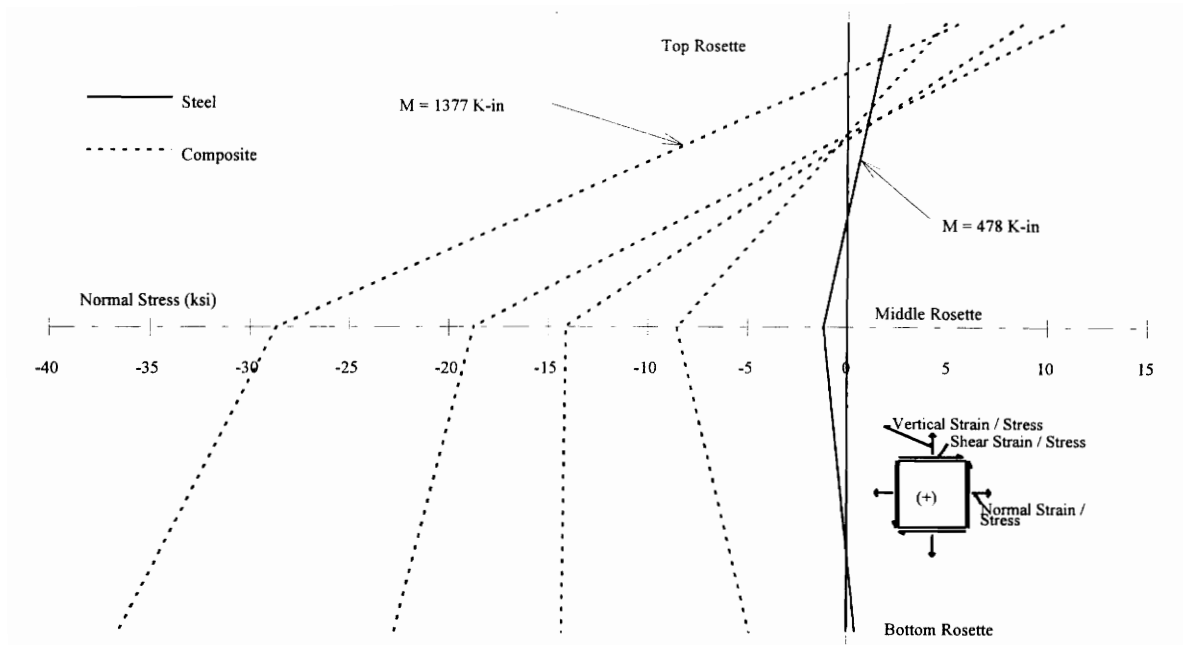
Figure 3.2-14 Normal Stress Distribution North Shear Tab Plate

Because the rosettes were directly above and below the top and bottom bolts respectively, they were not in a good position to measure these normal stresses. The normal forces indicated during loading of the composite connection are most likely the result of local bolt stresses and out of plane bending of the plate; although, they do seem to present a general trend that would be expected, i.e., the top of the plate under little to no tension while the bottom of the plate would be under large compression.

3.2.3 Composite Slab Behavior

The reinforcing bar forces along the three gage lines are presented in Figure 3.2-15 through Figure 3.2-17. Each line in the figure represents a contour of reinforcing steel forces at a given value of connection moment. The line is generated by connecting the values of reinforcing steel force determined at each gage location across the width of the composite slab. The center gage line was directly over the centerline of the girder and some of the values indicated represent the average value of two gages at that location.

131

The south and north gage lines were located 12-in. on each side of the girder centerline. It should be noted that 37 out of 38 of the reinforcing bar gages functioned properly throughout the test.

Based on tensile coupons of the reinforcing steel, the yield stress for the reinforcing steel was 70 ksi which leads to a yield force for a #4 bar of approximately 14 kips. None of the reinforcing steel reached force values of this magnitude and the strain values did not indicate that any of the steel had yielded. The connection had originally been designed to have the reinforcing steel yield prior to connection failure. This most likely did not occur because the bottom flange of the north side buckled prior to the specimen developing its full capacity. This indicates that the amount, or strength, of the reinforcing steel is bounded by the ability of the beam to resist local buckling. Shear lag did not appear to be significant along the south and north gage lines. The center gage line indicated an apparent shear lag of between two to four kips between center reinforcing bars and reinforcing bars lying greater than 10-in. away from the centerline.
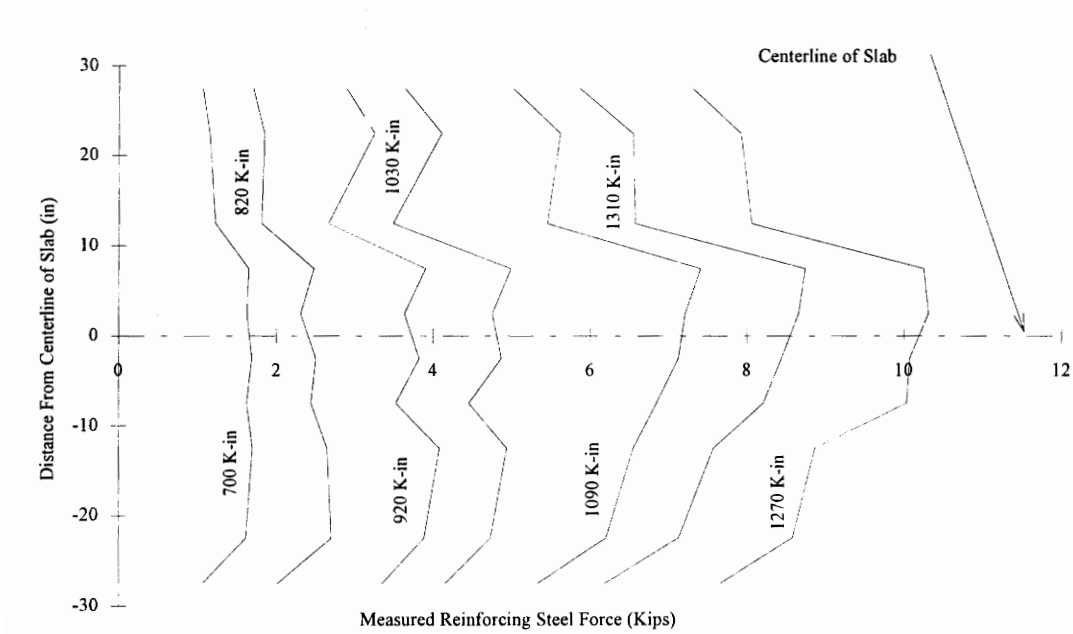
Figure 3.2-15 Reinforcing Steel Force Distribution Pattern Along South Gage Line
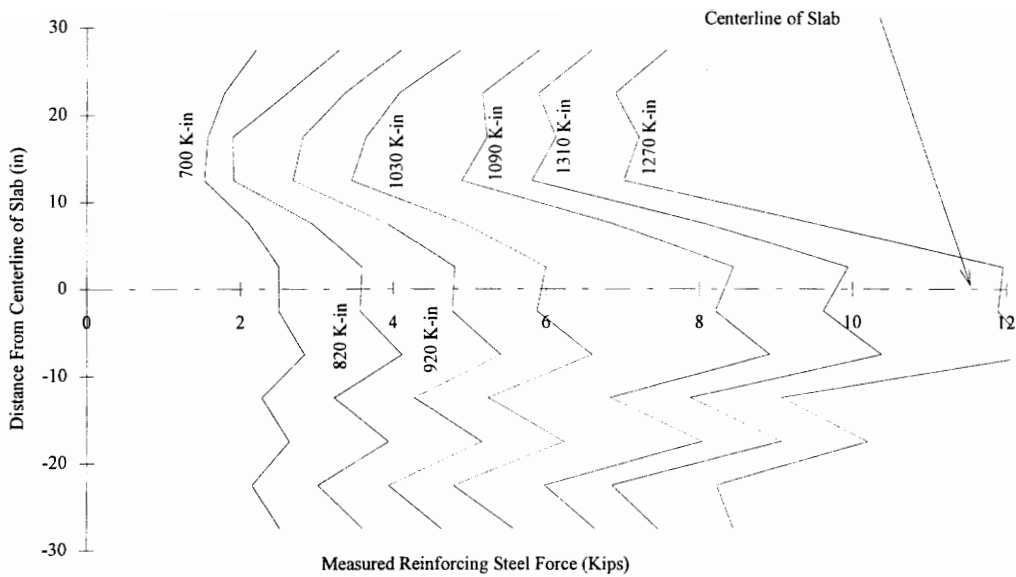
Figure 3.2-16 Reinforcing Steel Force Distribution Pattern Along Center Gage Line
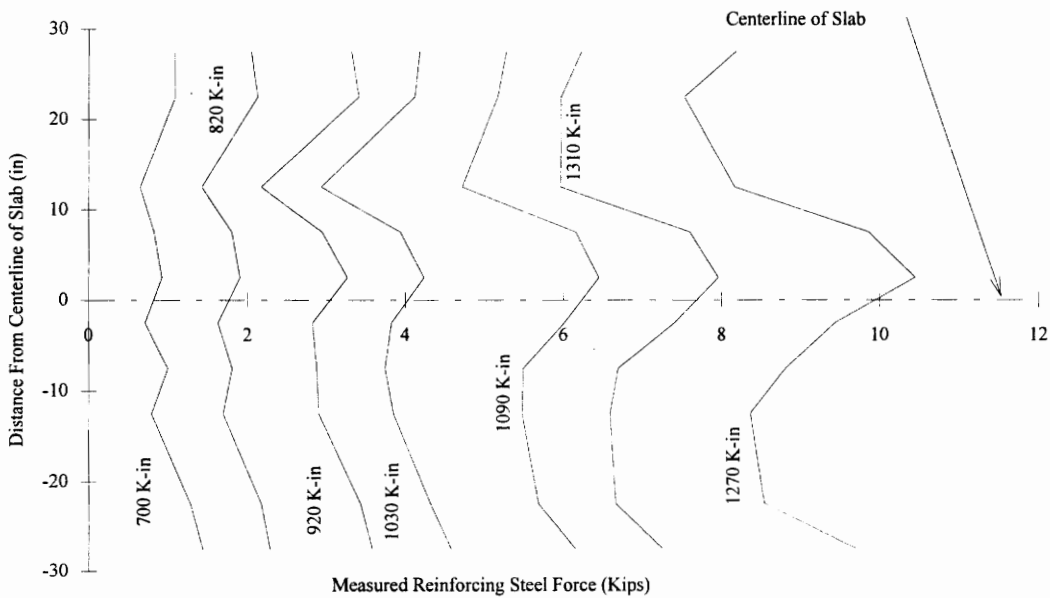
Figure 3.2-17 Reinforcing Steel Force Distribution Pattern Along North Gage Line

133

The force developed by the reinforcing steel is plotted against the connection moment in Figure 3.2-18. The steel did not develop significant force until the concrete hardened. Consequently the force in the steel is shown as zero until the connection moment increases past the dead load moment. The moment then increased with little increase in reinforcing steel force until the composite slab cracked.
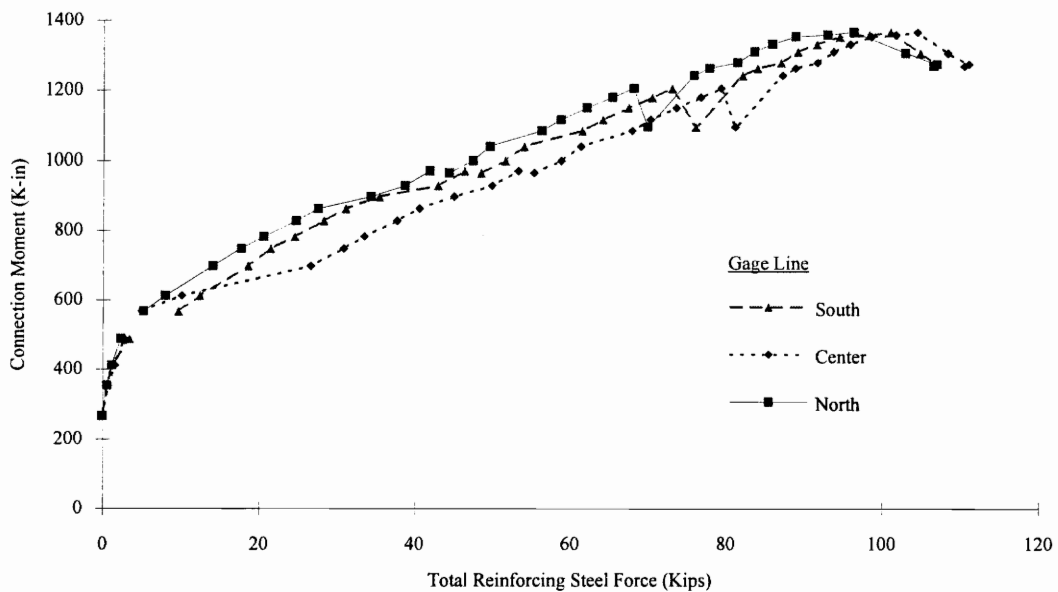
Figure 3.2-18 Reinforcing Steel Force Across Width of Slab

At this point there was a slight jump in the reinforcing steel force and then the force increased almost linearly with increase in moment up to failure of the connection. The slight jump in force around 80 kips was a result of a drop in moment when the south connection slipped.

The history of the composite slip is shown in Figure 3.2-19 and Figure 3.2-20. It is apparent that when the south connection slipped (approximately 1200 K-in.) the deformation in the slab also increased. This indicates that the sharp increase in rotation of the south connection was a result of sudden deformation in both the slab and the bolts.

134

The north slab was starting to slip severely as the connection approached failure. Although the slips are small in magnitude, the trend seemed to indicated that if the beam had not buckled then the shear connection between the beam and slab may have been inadequate to properly develop the reinforcing steel.
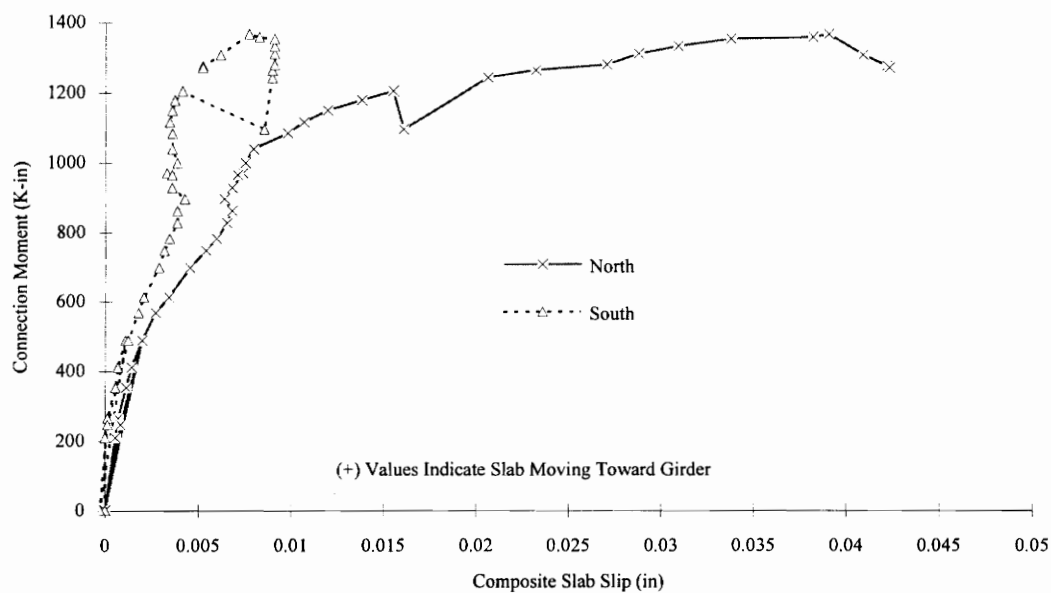
Figure 3.2-19 Composite Slab Slip Vs. Connection Moment

The reader should notice the beginning region of Figure 3.2-20. At first, the load in the reinforcing steel is increasing very slowly compared to the rate of slip. After the concrete cracks, the rate at which the reinforcing steel load increases versus rate of slip increases dramatically. This behavior is characteristic of a reinforced slab in tension. In the first region the load is being carried almost exclusively by the concrete since it is much stiffer than the reinforcing steel. After cracking, most of the load in the slab is carried by the reinforcing steel.
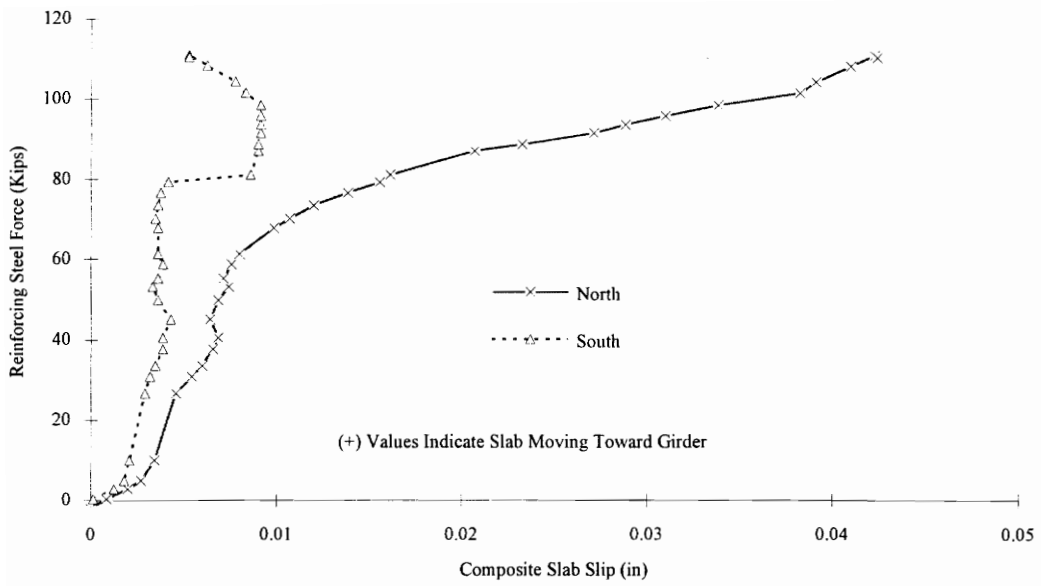
Figure 3.2-20 Composite Slab Slip Vs. Reinforcing Steel Force

3.3 BEHAVIOR OF CONNECTION #2

3.3.1 Moment-Rotation Behavior and Test History

Connection #2 was loaded at two different times: at the time of concrete casting and at the time when failure loading was applied. The moment-rotation behavior for the entire load history is presented in Figure 3.3-1 and Figure 3.3-2. For comparison purposes, the moment-rotation behavior for the two sides of the specimen have been plotted together for the dead load portion of the test and for the live load portion of the test. These plots are presented in Figure 3.3-3 and Figure 3.3-4 respectively. The specimen was not loaded to failure as a result of severely uneven deflections of the north side relative to the south side; although, the south side of the specimen was under severe distress and would have most likely failed with very little increase in load. As seen in Figure 3.3-2 the south side of the specimen had rotated far beyond what would most likely be required in design situations.
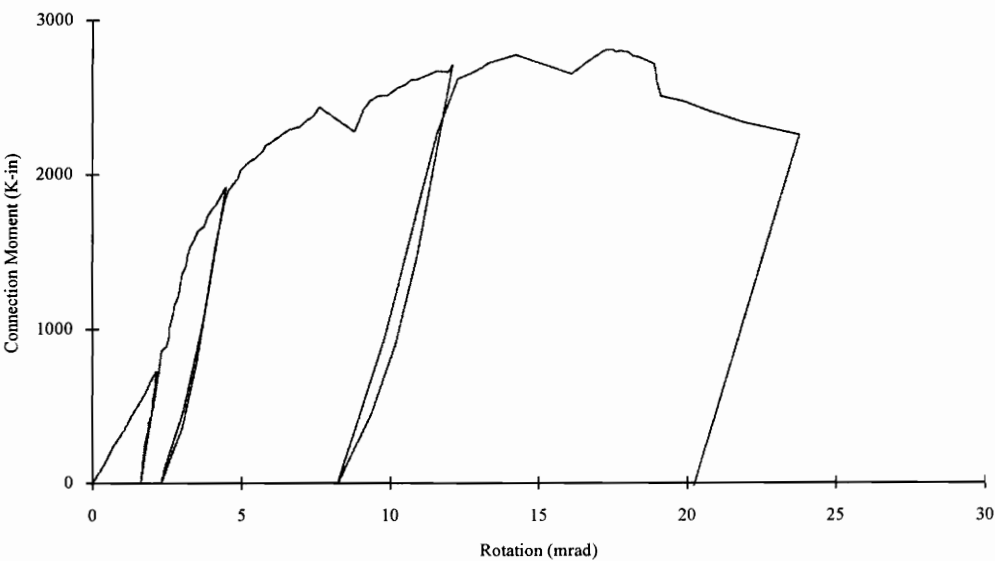
Figure 3.3-1 Moment-Rotation Behavior North Connection

137

The day the slab was cast the simulated dead load was applied. The full load of 15 kips was applied because the connection had not rotated to the dead load beam line or reached a horizontal plateau in its behavior. As shown in Figure 3.3-3 the connections appeared to follow similar and linear moment-rotation paths. The linearity of the connection curve indicates that the bolts in the steel plate had not reached a load level that would cause them to slip or become non-linear in their load-deformation response. This linearity is also believed to be caused by some partial contribution of the composite slab. This resulted from the concrete starting to set before the dead load was fully applied and is discussed in more detail in Section 3.3.3.
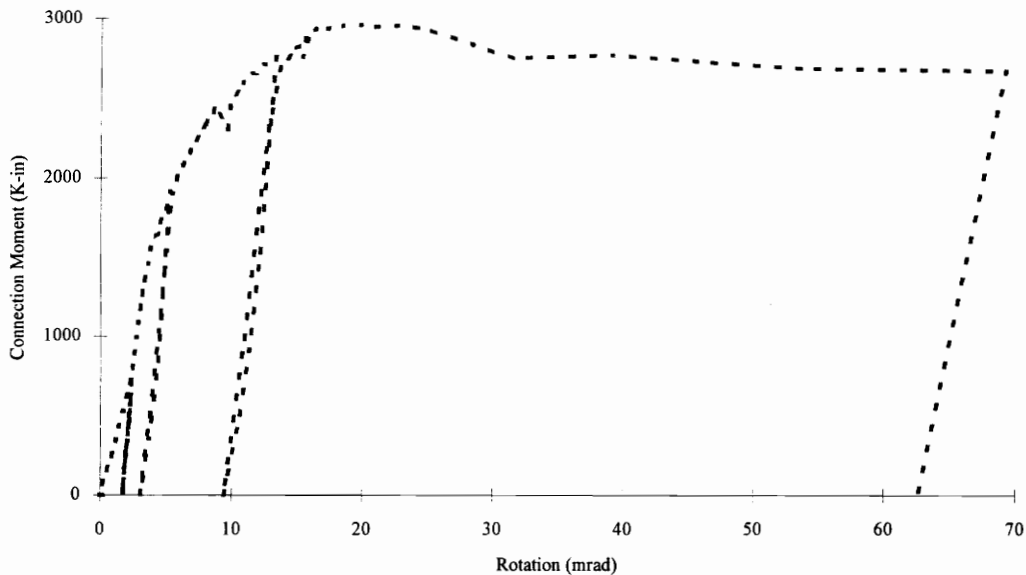
Figure 3.3-2 Moment-Rotation Behavior South Connection

After approximately 28 days the specimen was unloaded and the dead load frames were replaced with the live load frames. As can be seen in the moment-rotation diagrams presented in Figure 3.3-3, the connections followed very linear unloading paths as the dead load was removed. Hairline cracks were noticed above the centerline of the girder prior to the live load frames being put in place. The origin of these small cracks is unknown, but they did not appear to impair the slab structurally.

138
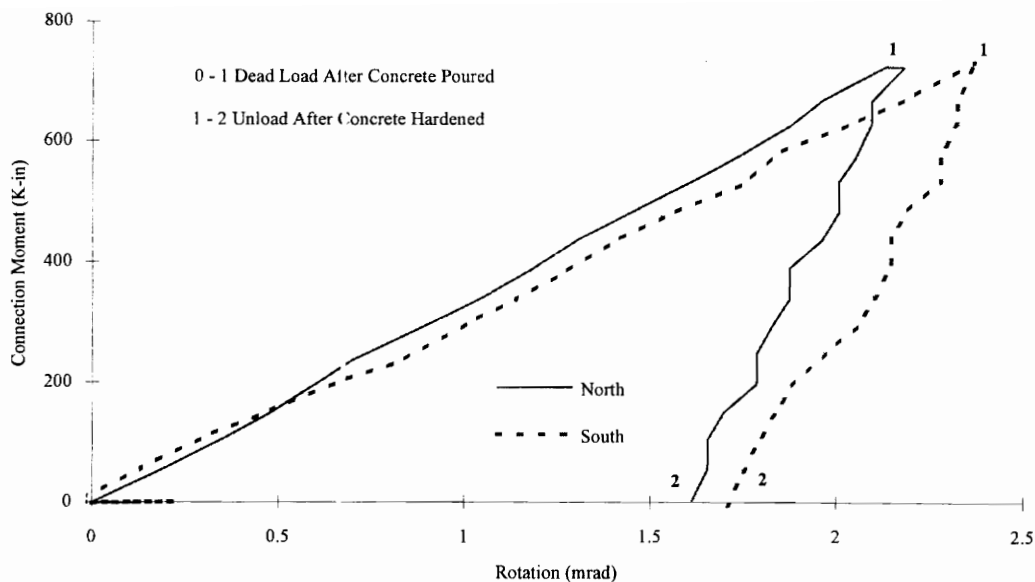
Figure 3.3-3 Moment-Rotation Behavior Steel Connections

Once the live load frames were in place the hydraulic rams were used to load the specimen back to the same point on the moment-rotation curve that it had been at prior to removal of the dead load. It was noticed that hydraulic fluid was leaking from the south hydraulic ram during the application of load. The connection was then unloaded and the connections between the hydraulic line and the ram were tightened. As shown in Figure 3.3-1 and Figure 3.3-2 this loading and unloading followed the same path as when the dead load was removed. This preliminary loading and unloading was conducted to ensure all instrumentation and the test frames were operating properly.

The connection was loaded back to the level of the dead load moment. After this moment was attained, load was increased in approximate one kip increments. The first new cracks (i.e., aside from those present before loading) were noticed above the north and south reinforcing steel strain gage locations at around 890 K-in. Despite the slab cracking the connection behavior remained very linear although it did appear to exhibit a slightly reduced stiffness.
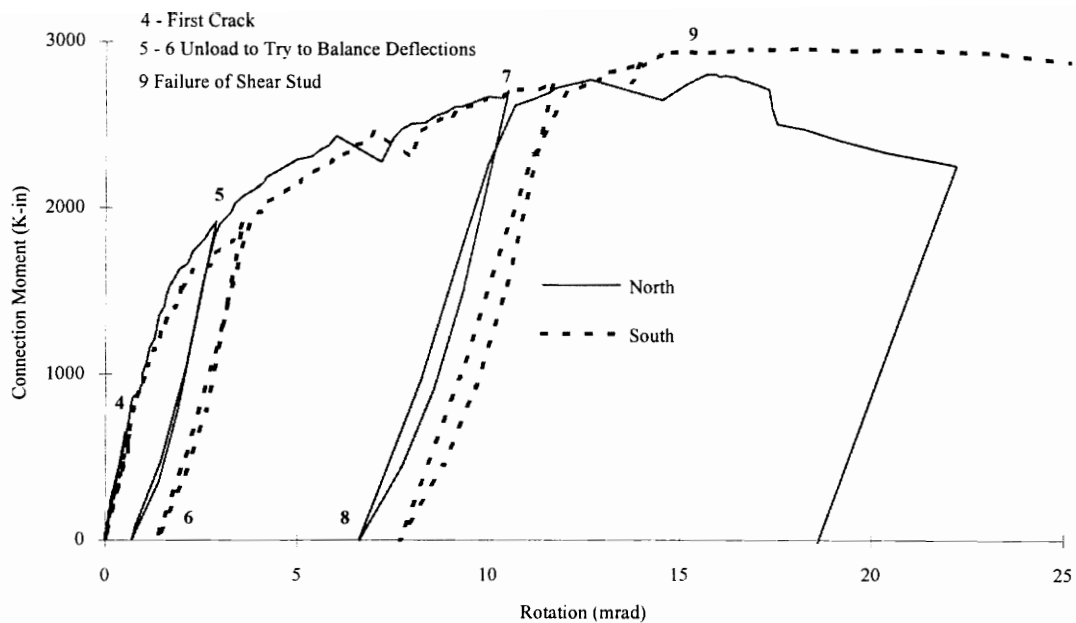
Figure 3.3-4 Moment-Rotation Behavior Composite Connections

A crack over the south beam end just past the point of load application and parallel to the beam web was noticed at 950 K-in. Some yielding of the south side connection shear plate was noticed in the vicinity of the bottom bolt at 1150 K-in. A crack over the south beam which was parallel to the beam was noticed at 1300 K-in. and was soon followed by a crack over the end of the north beam just past the point of load application and parallel to the beam web. Some yielding of the shear plate around the top bolt location on the south side was noticed at 1560 K-in. At approximately 1700 K-in. loud cracking sounds were heard and what were believed to be the first flexural cracks over the girder centerline appeared. A slight yielding pattern in the top side of the bottom beam flange was noticed around the bolts that were farthest from the girder at 1850 K-in. A crack parallel to the beam web and similar to that on the south side was noticed over the north beam at 1900 K-in.

Up to this point in the loading sequence the north side of the specimen appeared to be deflecting while the south side was not deflecting at all. In an attempt to correct this

140

situation the specimen was unloaded and the hydraulic fluid return lines were switched between the north and south hydraulic rams. The return line on the south side had been leaking and it was believed that possibly switching the lines might relieve the uneven deflections. The connection was then reloaded to the point it had been prior to unloading. This seemed to help the deflection problem a little but the two sides of the specimen were still rather unbalanced.

At approximately 2300 K-in. both seat angle connections appeared to slip and yielding patterns on the top side of the bottom beam flange were noticed around all the bolt locations. First yielding of reinforcing steel was noticed at 2500 K-in. as well as additional slab cracking and widening of existing cracks. Yielding was noticed in the shear plate around the top bolt on the north side of the specimen at 2700 K-in.

The unbalanced deflections were again very severe and the connection was unloaded in an attempt to balance the deflections as well as to study the unloading and reloading stiffness of the connection. As the specimen was reloaded, yielding around the bolts in the shear plates was noticed on both the north and south sides.

Diagonal cracks appeared above the north and south sides in the area around the load rams at about 2800 K-in. The connections were at or near their plastic plateau at this point and any additional load was soon reduced as the connections rotated to accommodate the hydraulic ram displacement. At approximately 2900 K-in. a loud snap was heard and the south connection started to rotate much quicker than the north. This was most likely when one of the shear studs on the south side failed by pulling out of the top beam flange (the failure of the stud was not discovered until after the test was over). Because the slab load was now being carried by the remaining studs the slab stiffness was severely reduced and it started to shed some load to the shear plate. The slab continued to slip as load was applied and the bolts in the top portion of the south side shear plate started to cause bearing failure in the beam web. The south connection continued to rotate without taking additional load and the deformations around the shear plate bolts in both the beam web and shear plate continued to increase. At this point the specimen was

141

severely out of balance with the north side having almost five-in. more deflection than the south. Because of this unbalance the girder was being stressed and yield lines were starting to appear along the toe of the girder. The test was stopped at this point to prevent any sudden failure and to keep from permanently damaging the girder.

The center of connection rotation versus the moment at the connection is plotted in Figure 3.3-6 and Figure 3.3-12. The center of rotation appears to drop from between three to four-in. below the beam centerline to five to six-in. below the beam centerline as the dead load was being applied. This simply indicates a softening of the shear plate portion of the connection compared to the seat angle portion. Once the composite slab became effective the center of rotation rose back to around three to four-in. below the centerline and stayed there for most of the test until the bottom angles slipped. The slip of the angles is indicated by the sudden reduction in moment and the jump of the center of rotation toward the centerline of the beam.
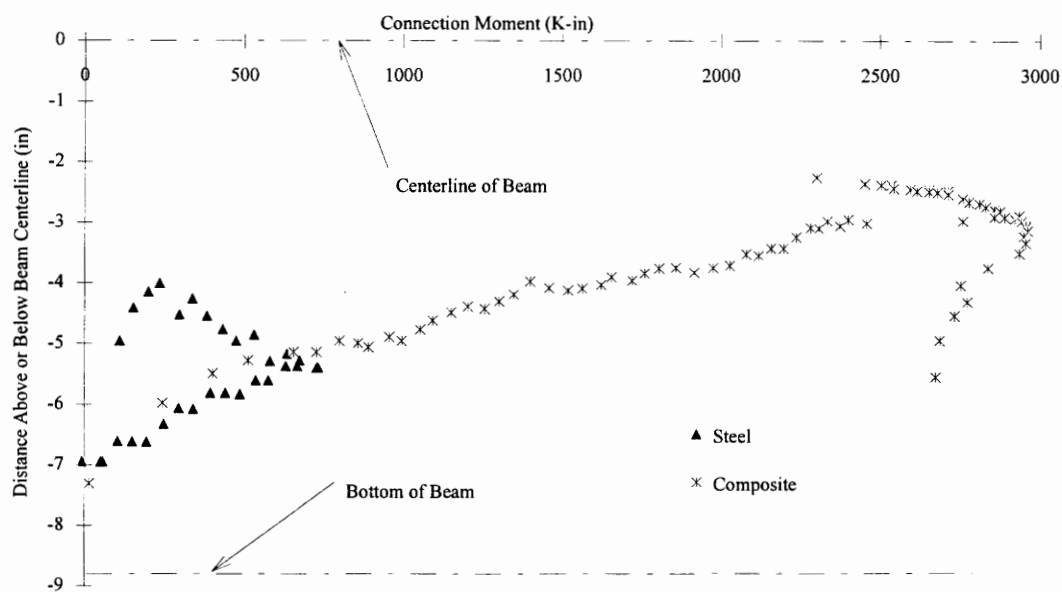
Figure 3.3-5 Center of Connection Rotation South Connection

142
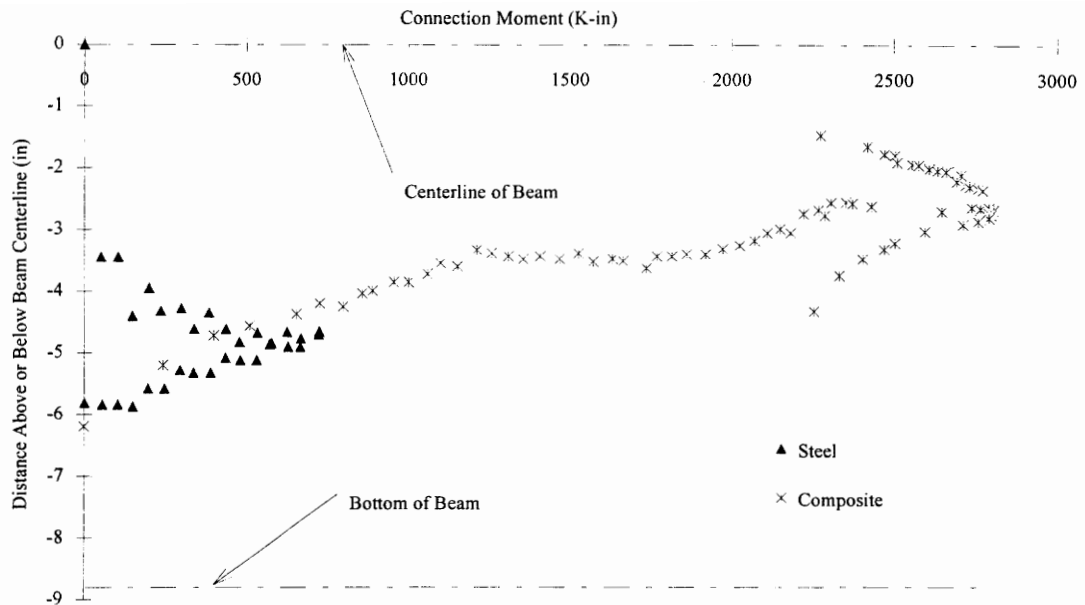
Figure 3.3-6 Center of Connection Rotation North Connection

As load was reapplied, the center of rotation came back to where it had been before and then moved toward the bottom of the beam when the slab started to yield and the stud on the south beam fractured. The reader will notice that the center of rotation is always located below the centerline of the beam. This indicates that the seat angle was a more rigid element in compression than the composite slab was in tension.

3.3.2 Steel Connection Behavior

The strain readings from the locations along the bottom side of the seat angle along the line of the seat angle toe are presented in Figure 3.3-7. The strain values shown represent the average for the two gages. Up to the yield strain (approximately 1400 micro-strains) the response of the north and south angles appeared to be very similar. After the yield strain was reached the north and south responses diverged. The south continues on a somewhat linear path with a slowly decreasing stiffness while the north

shows a sharp increase in stiffness and then a sharp decrease near connection failure. Because the gages are located on the bottom side of the angle, the strains measured include bending and axial strain. The difference in the response measured by these two gages may be a result of a difference in the amount of bending induced into the angle. Because the measured values are a combination of axial and bending strains, the behavior does not exhibit a horizontal plateau when the theoretical yield strain is attained. This is because most of the remaining cross-section of the seat angle has not yielded; although, the stiffness should be reduced as seen in the response of the south seat angle. Despite what appears to be significant yielding of the angle along the bottom side of the toe, the angles did not appear to be severely deformed based on visual inspection after the specimen was dismantled. The only noticeable distress was a slight inclination of the angle from horizontal.
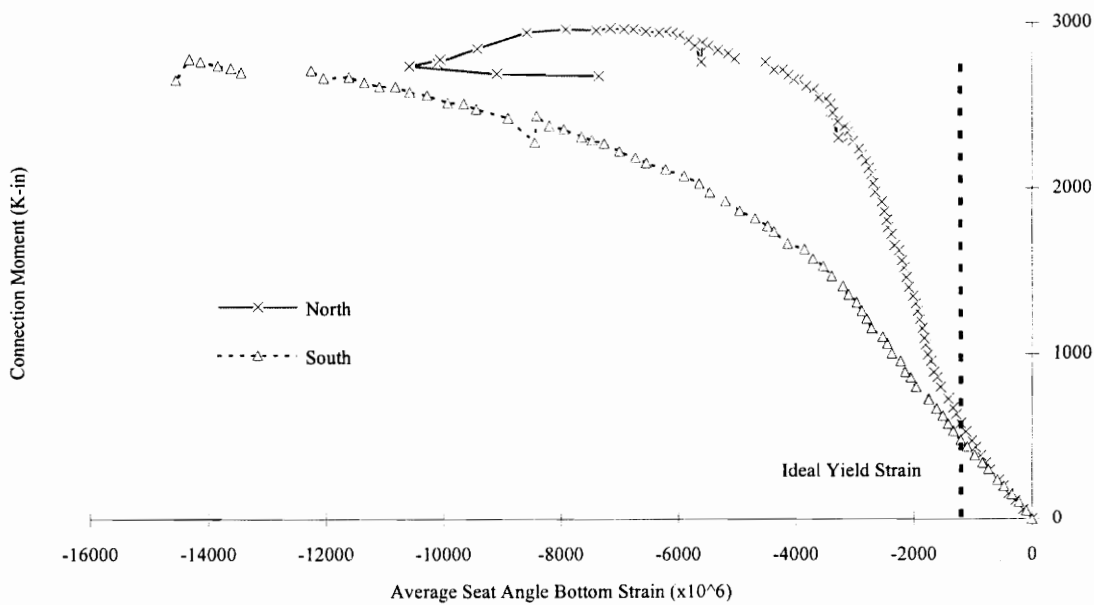
Figure 3.3-7 Seat Angle Bottom Strain Vs. Connection Moment

Linear displacement transducers measured the relative movement between the web of the beam and the connection plate. The data from these transducers is presented

144

in Figure 3.3-8 through Figure 3.3-11. These figures indicate that the top two bolts were working with the composite slab to resist tensile forces while the bolt in location #3 (third from the top) was not contributing significantly to either the composite slab or the seat angle. The bottom bolt appears to have been contributing force to resisting the compression until the connection started to fail. At the time when the shear stud failed over the south beam the plate slip moved significantly to the left which indicates that all the bolts were now acting to resist tensile forces. This is particularly evident in Figure 3.3-11 as the movement abruptly changed direction from the general trend it had been following up to the stud failure. Figure 3.3-8 also indicates the severity of the bearing failure that was occurring in the beam web with almost a 0.7-in. deformation, most of which was seen in the beam web (0.3-in. is generally considered the limit for bearing failure).
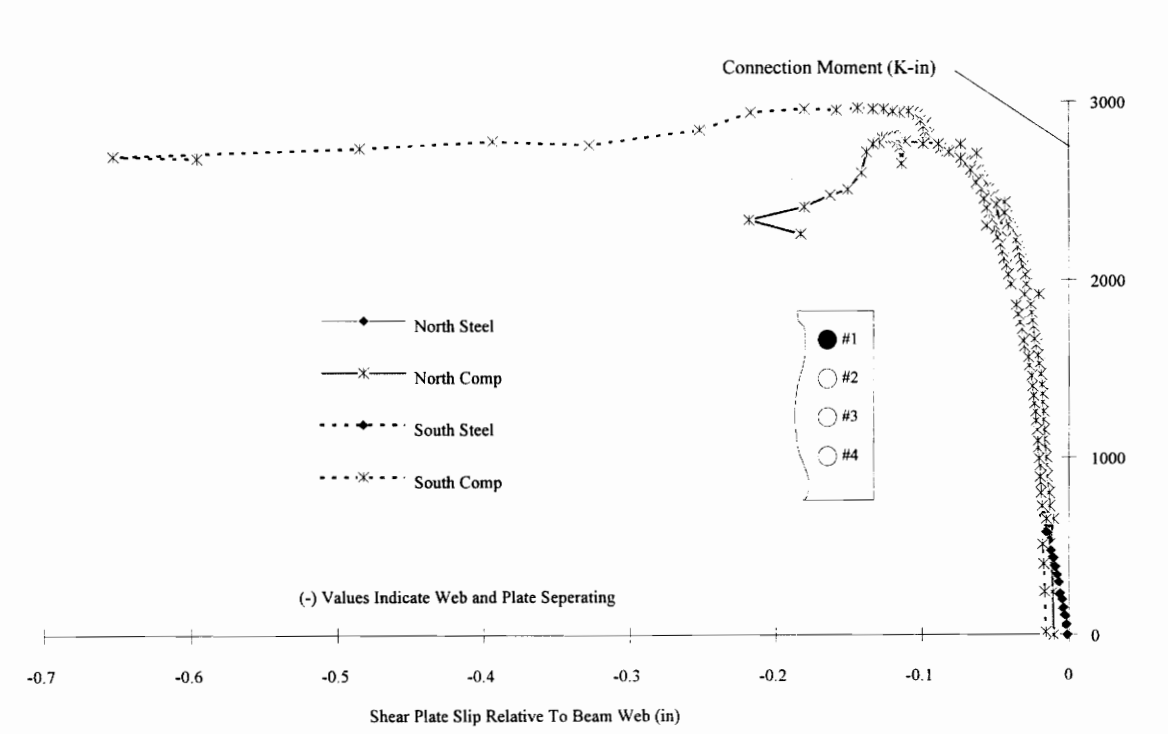
Figure 3.3-8 Moment Vs. Plate Slip For Bolt Location #1
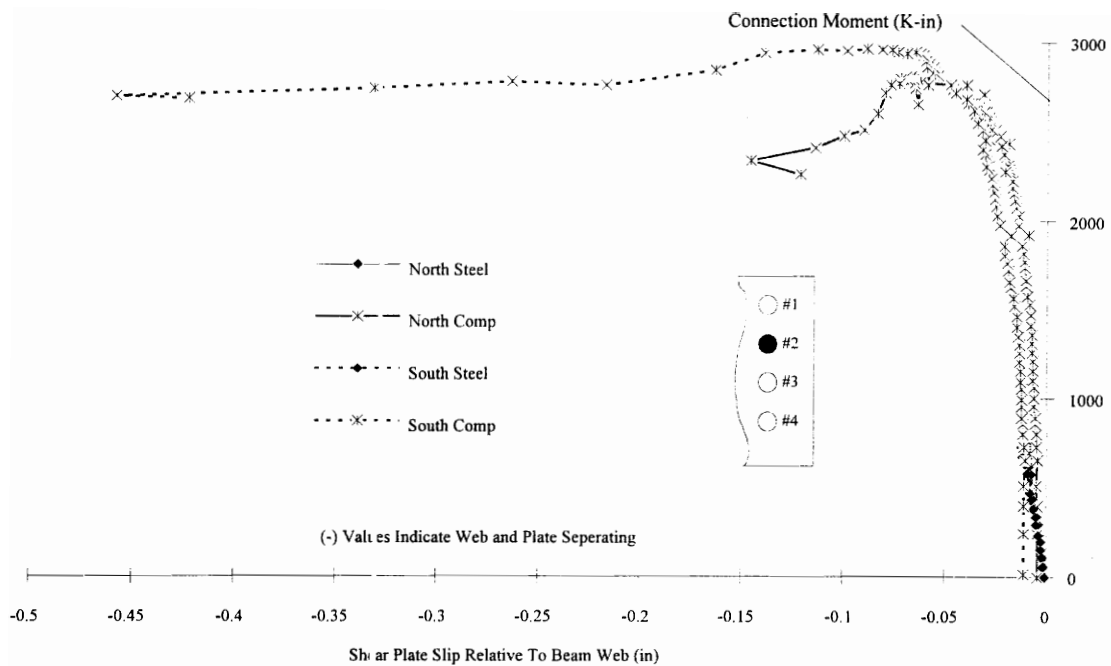
Figure 3.3-9 Moment Vs. Plate Slip For Bolt Location #2
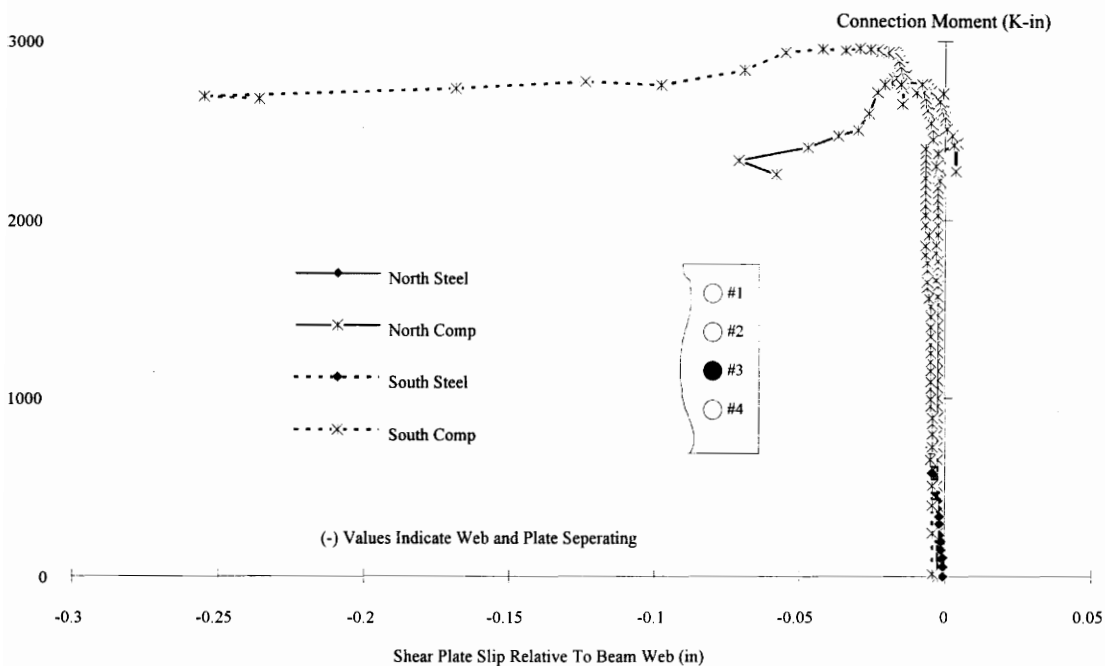
Figure 3.3-10 Moment Vs. Plate Slip For Bolt Location #3

146
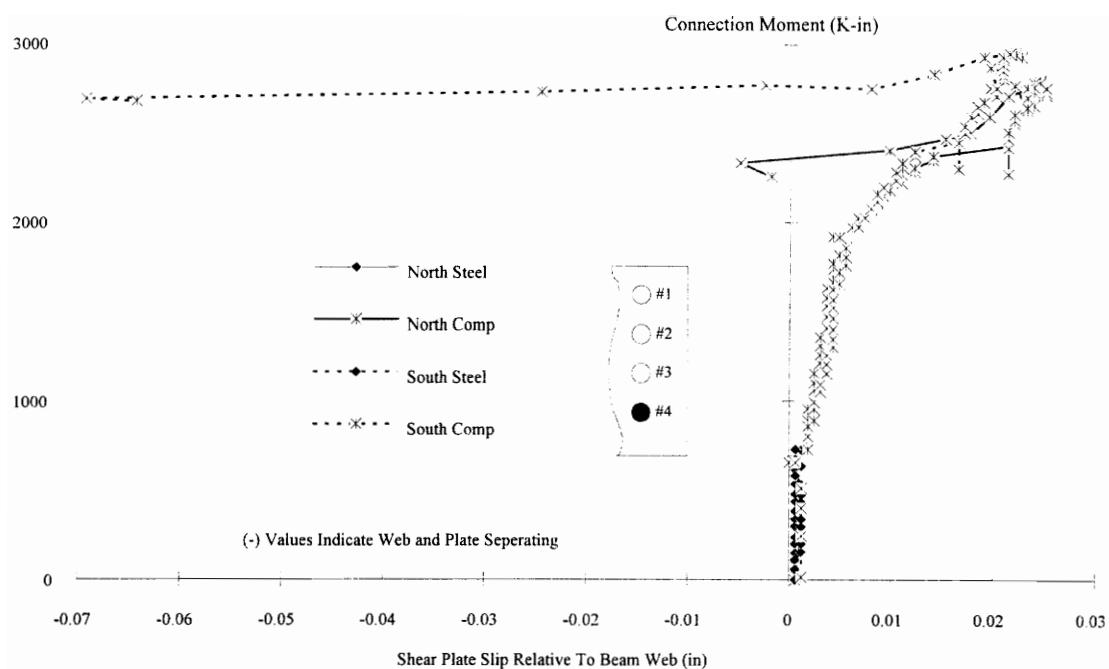
Figure 3.3-11 Moment Vs Plate Slip for Bolt Location #4

Strain rosettes had been attached to the shear plate. Evaluation of the data obtained from these gages indicated that the measurements were not indicative of the behavior that should have been occurring (i.e., shear in the wrong direction and other strange behavior). This was probably a result of out-of-plane bending in the shear plate. As such, the data from these gages has not been included in this summary.

3.3.3 Composite Slab Behavior

The reinforcing bar forces along the three gage lines are presented in Figure 3.3-12 through Figure 3.3-14. This force distribution is based on the strain gage readings prior to yield. Yield was determined by examining the strain data and determining where a severe or abnormal jump in strain occurred. The center gage line was directly over the centerline of the girder and the values represent the average value of two gages at that location. The south and north gage lines were located 12-in. on each side of the girder

147

centerline. It should be noted that 20 out of 20 of the reinforcing bar gages functioned properly throughout the test.

All the reinforcing bars yielded at locations over the centerline of the girder and some at locations along the north and south gage lines. When the bars yielded above the girder centerline they all yielded within 100 to 200 K-in. of each other. This indicates little shear lag was occurring which can be seen by examining Figure 3.3-13. The shear lag at the north and south gage locations is even less noticeable which is to be expected because these regions should not be as highly stressed as the region just above the girder centerline. As described in the discussion of Connection #1, the yield force for the reinforcing steel is theoretically 14 Kips.
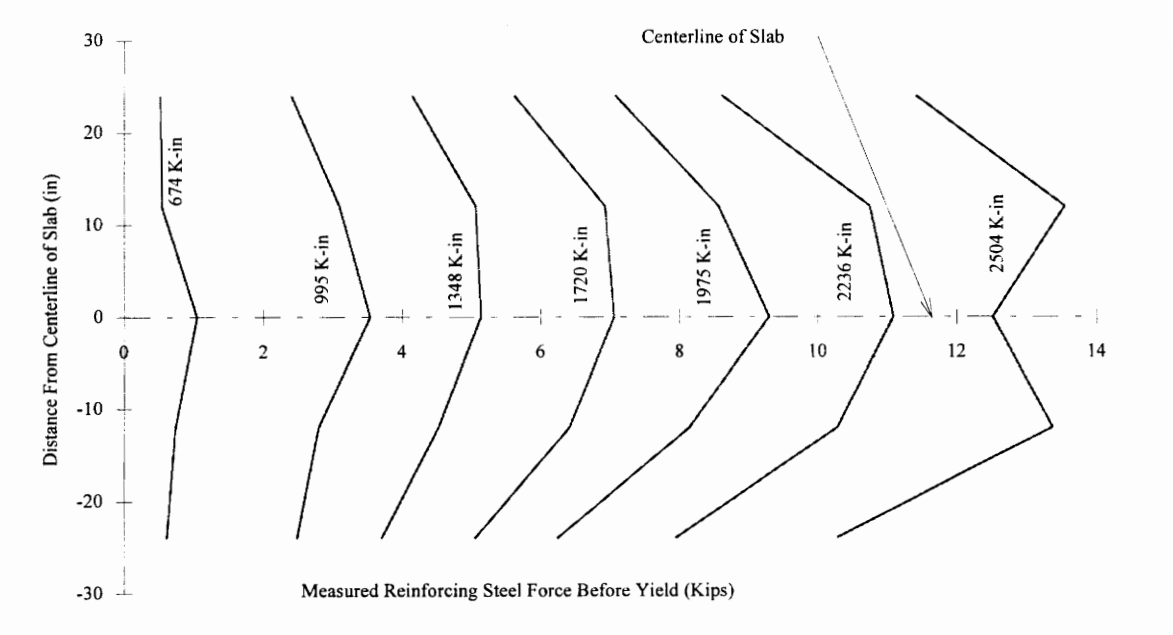
Figure 3.3-12 Reinforcing Steel Force Distribution Pattern Along South Gage Line

148
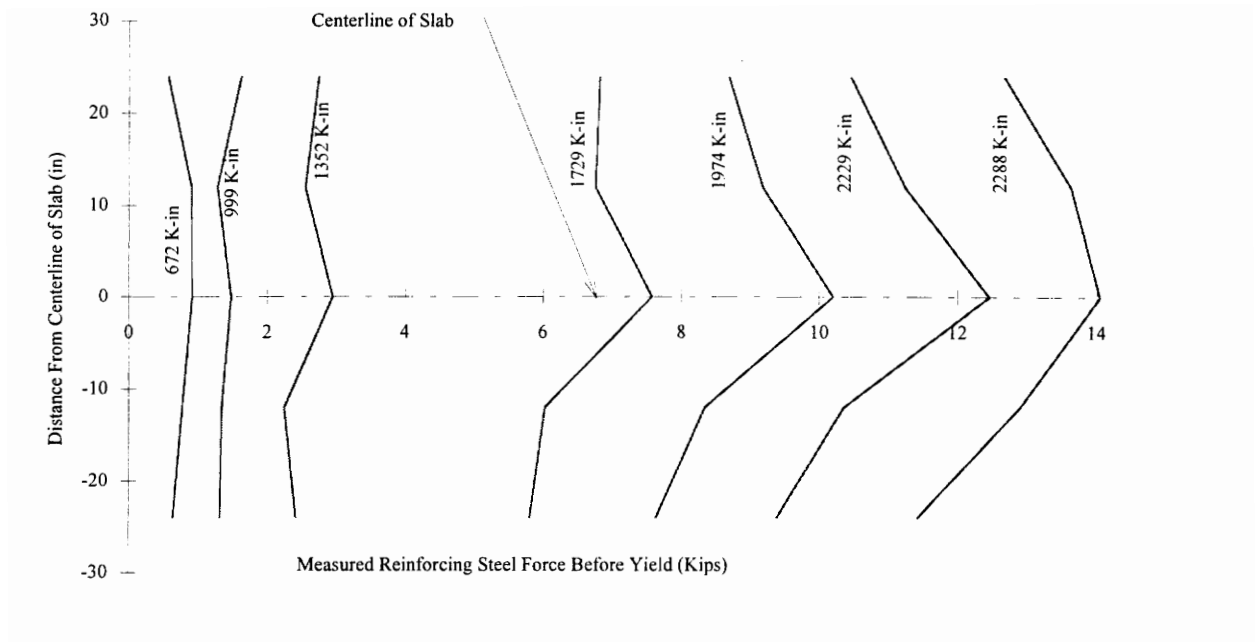
Figure 3.3-13 Reinforcing Steel Force Distribution Pattern Along Center Gage Line
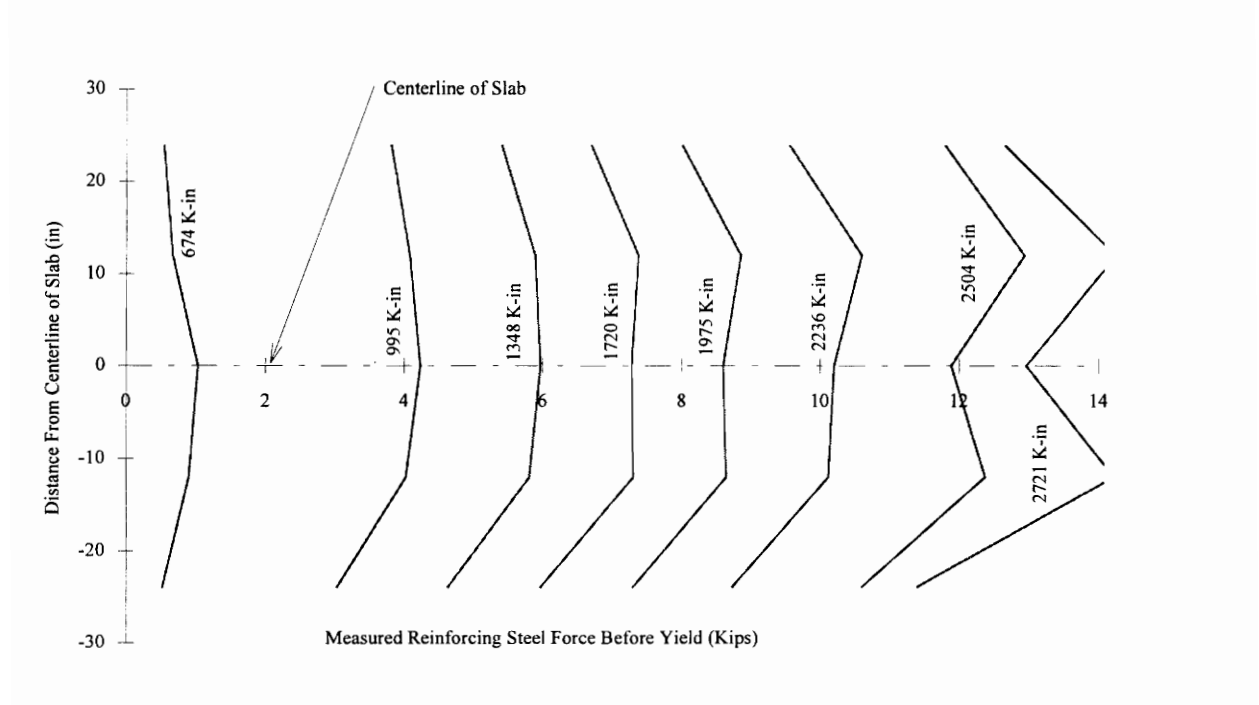
Figure 3.3-14 Reinforcing Steel Force Distribution Pattern Along North Gage Line

149

The force developed by the reinforcing steel versus the connection moment is plotted in Figure 3.3-15. The reinforcing steel should not develop any significant force until the concrete hardens. Consequently the force in the steel should be zero until the connection moment increases past the dead load moment. Because the dead load moment was approximately 700 K-in. and the force, as shown in Figure 3.3-15, is well above zero at this point, the writer believes that the dead load was not applied to the specimen before the concrete was able to begin to set. As a result the reinforcing steel appears to have contributed some to the overall response of the steel connection.
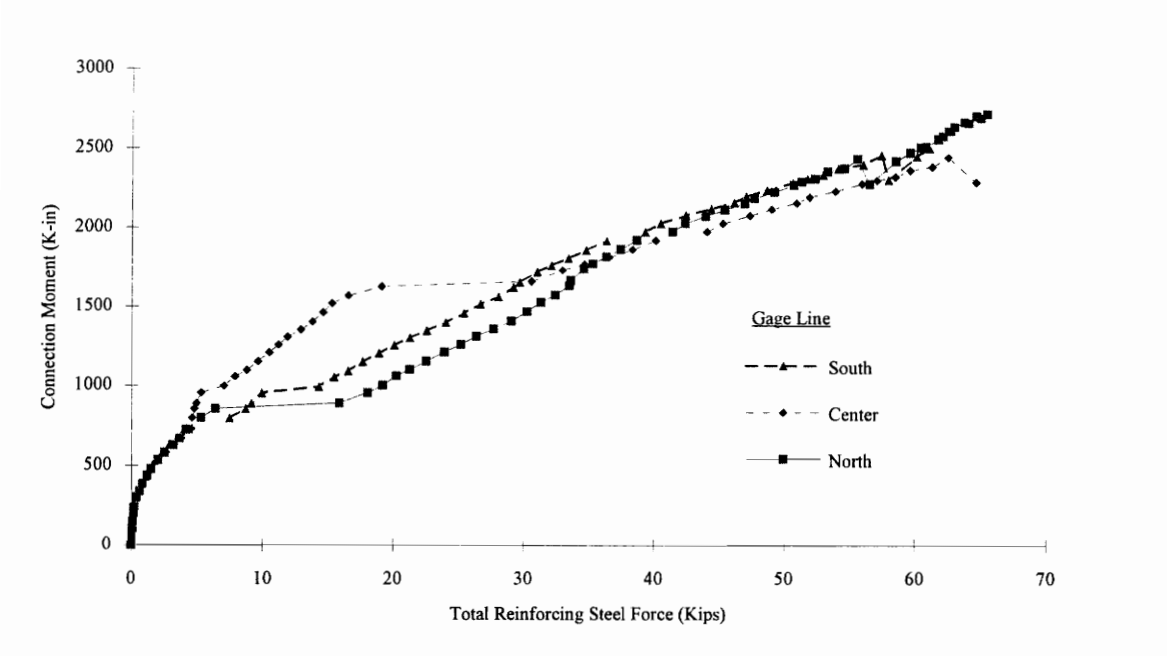
Figure 3.3-15 Reinforcing Steel Force Across Width of Slab

Before the concrete cracked the forces in the reinforcing steel appeared to be identical. The point at which concrete cracked around each gage location is very apparent in Figure 3.3-15 as indicated by the sharp increases in reinforcing steel force. This is also very evident in Figure 3.3-12 through Figure 3.3-14 as seen by a sharp increase in reinforcing steel force and a small increase in the moment associated with the force contour. Figure 3.3-15 also indicates that when the cracks opened over the south and north gage lines that the crack over the north gage line was more severe and thus resulted

150

in more load being resisted by the reinforcing steel at this location compared to the south gage line. Once the flexural cracks over the centerline of the girder appeared (at around 1600 to 1700 K-in.) the force in the reinforcing steel appeared to be very similar at all the gage locations again and seemed to increase linearly until the reinforcing started to yield.

The history of the composite slab slip is presented in Figure 3.3-16 and Figure 3.3-17. Neither slab appeared to have any significant jumps in slip until the shear stud failed on the south side. At this point the south slab slipped considerably as the full slab load was placed on the remaining studs. Buckling of the steel deck around the remaining studs was noticed as the slab continued to slip. The sharp increase in the slip of the south slab is not seen in Figure 3.3-17 because it occurred after the reinforcing steel yielded. As discussed in Section 3.2.3, the behavior exhibited in the initial region of the plots in Figure 3.3-17 are indicative of a reinforced slab in tension.
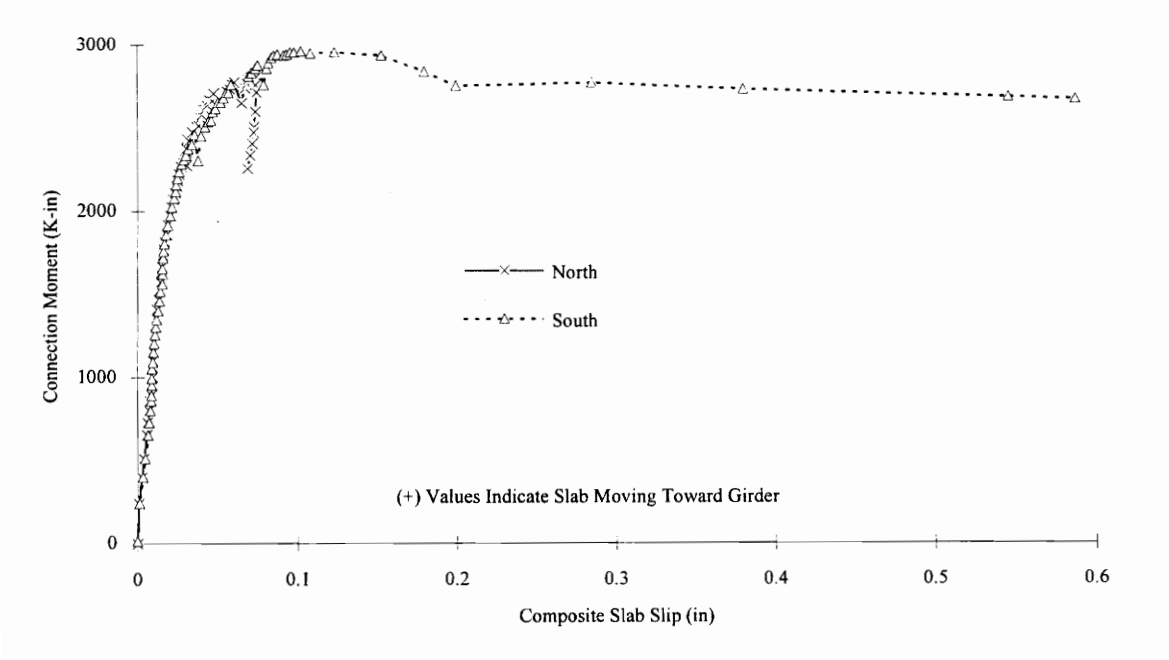
Figure 3.3-16 Composite Slab Slip Vs. Connection Moment
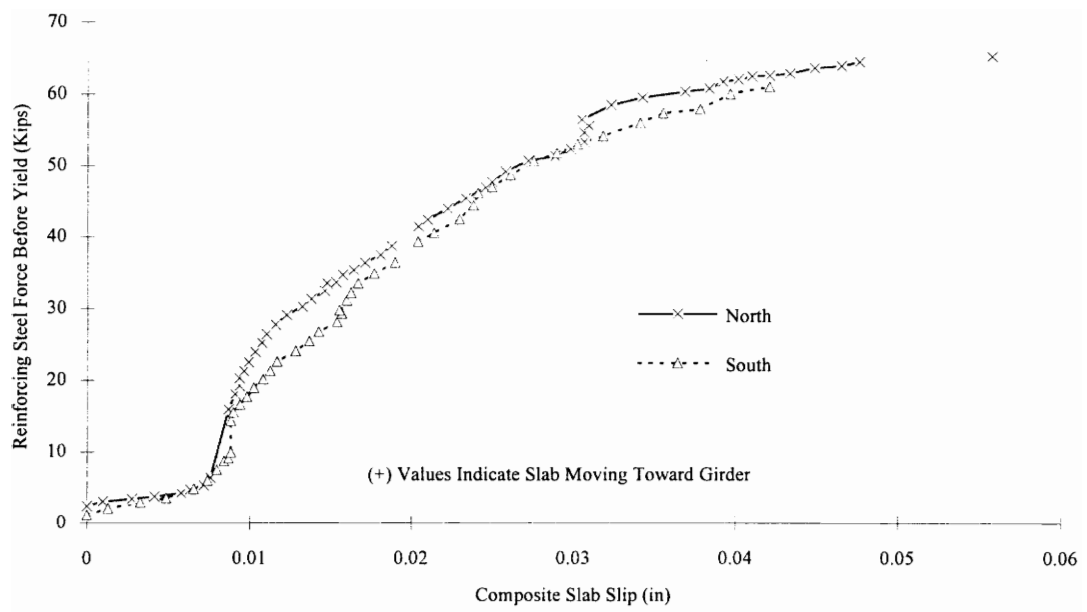
Figure 3.3-17 Composite Slab Slip Vs. Reinforcing Steel Force

3.4 BEHAVIOR OF CONNECTION #3

3.4.1 Moment-Rotation Behavior and Test History

Connection #3 was loaded at three different times: immediately after the connection was constructed, at the time of concrete casting, and at the time when failure loading was applied. The moment-rotation behavior for the entire load history is presented in Figure 3.4-1 and Figure 3.4-2. For comparison purposes, the moment-rotation behavior for the two sides of the specimen have been plotted together for the dead load portion of the test and for the live load portion of the test. These plots are presented in Figure 3.4-4 and Figure 3.4-5 respectively. The specimen was considered to have failed when the bolted tension plate on the south side of the specimen failed in tension rupture.
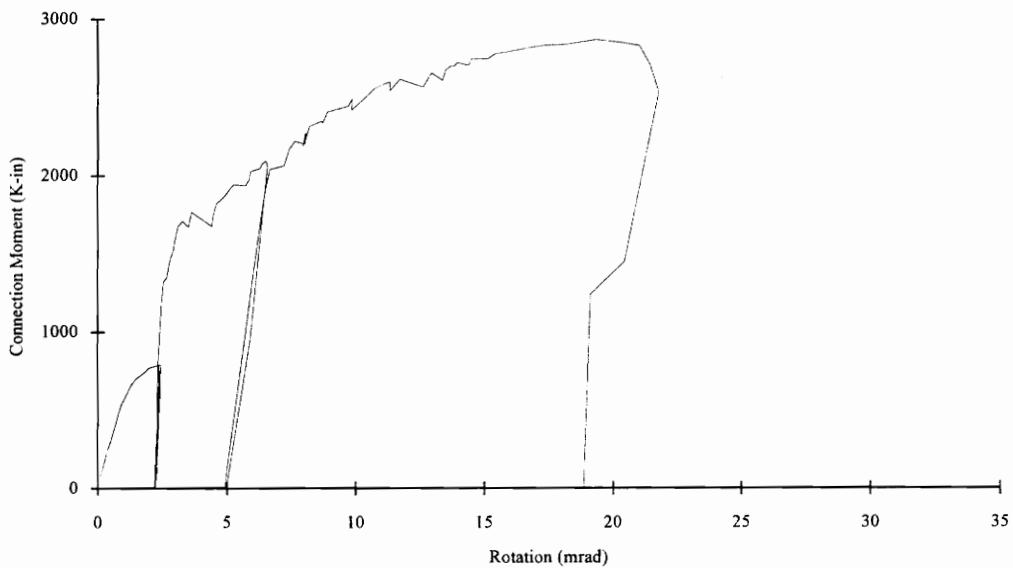
Figure 3.4-1 Moment-Rotation Behavior North Connection

To determine what effect fully tensioned bolts versus snug tight bolts had on the steel connection behavior, the connections were loaded and unloaded twice prior to the

153

composite slab being constructed. During the first loading all the bolts in the connection were left snug tight. These bolts were tightened with a spud wrench and were considered snug once a relatively low amount of effort was required to tighten them any further.
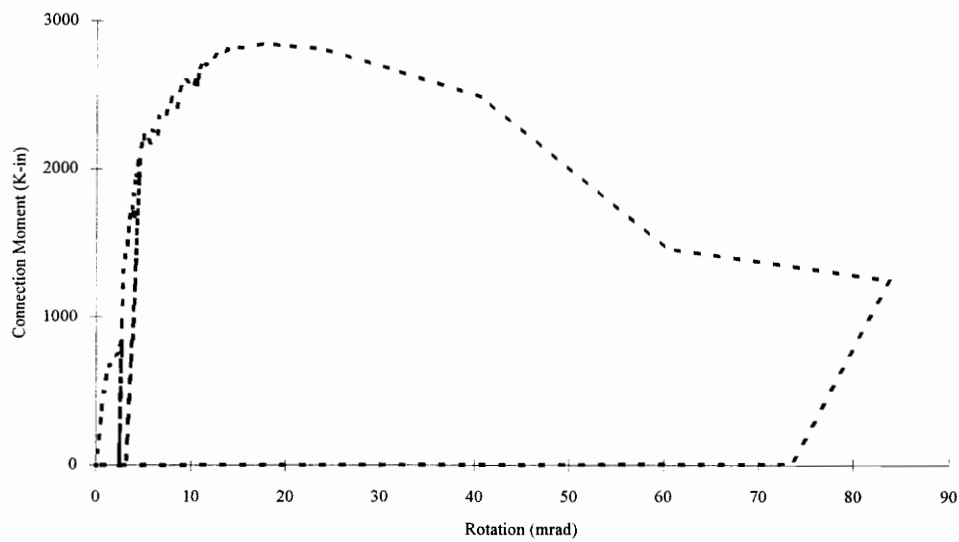
Figure 3.4-2 Moment-Rotation Behavior South Connection

The specimen was loaded using the dead load frames and load was applied by tightening the turnbuckles. Load was applied until the connection rotation appeared to be passed the beam line for a 40 psf dead load. This dead load was lower than that used in the hypothetical design because determining the behavior of the connection in this configuration was not the primary goal of the test specimen. Using the 40 psf insured that the steel connection would not be over stressed in these preliminary load trials. The loads were then removed, the bolts were loosened and the specimen was brought back into its original configuration. The bolts were then fully tightened using the turn-of-the-nut method.

After the bolts had been tightened the load was increased until the connection approximately intersected the dead load beam line. Again, additional load was not

154

applied to insure the connection was not over stressed. The resulting moment-rotation behavior of the two load trials is presented in Figure 3.4-3.

Both sides of the specimen appeared to behave in very similar manners for both tests. The response of the fully tightened connection was much stiffer than the response of the snug tight connection initially, although the fully tensioned connection started to lose most of its stiffness at approximately 600 K-in., while the snug tight connections seemed to be increasing in stiffness.

Although the behavior of the two types of connections is very different, the difference that the connection behavior would have on the beam behavior would depend on the load applied. This difference depends on the connection moment which is determined by the intersection of the beam line and the connection curve. Thus for low loads the difference in moments at the intersection of the beam line with the two curves is relatively high. And for high loads this difference is reduced. Consequently for a reasonably high dead load (say 50 to 60 psf) the difference in the beam response may not be very significant for these two connection cases. There would most likely always be some improved behavior associated with the fully tightened bolts versus the snug tight bolts.

Although the fully tightened bolts may not provide significant changes in the beam response in all cases, there is one important benefit they do provide. Connections with fully tightened bolts should have a more predictable connection behavior. The ability to model connections depends on the ability to accurately predict the behavior of the elements that make up the connection. Studies have been conducted to predict the load slip behavior of fully tensioned bolts, but little has been done to try to predict the behavior of snug tight bolts. As a result it would currently be much more difficult to predict the connection behavior of connections with snug tight bolts compared to connections with fully tightened bolts.

155
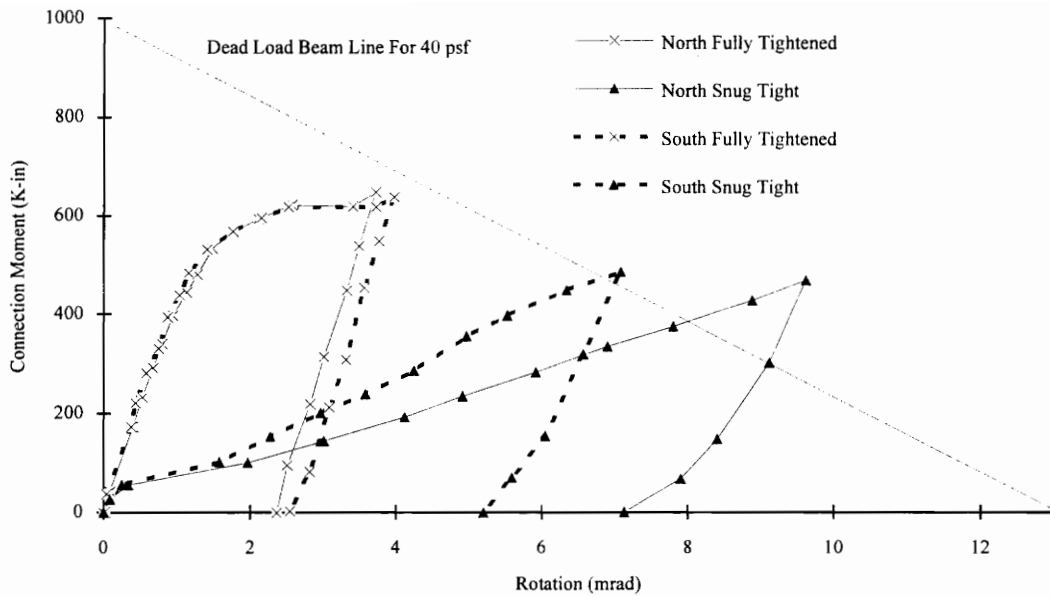
Figure 3.4-3 Moment-Rotation Behavior of Steel Connection Under Trial Loads

After the preliminary loading was complete, the bolts of the connection were loosened, the specimen was returned to its original position, the bolts were re-tightened, and the composite slab was constructed. The day the slab was cast the simulated dead load was applied. The full load of 17 kips was applied because the connection had not rotated to the dead load beam line or reached a horizontal plateau. As shown in Figure 3.4-4, the connections appeared to follow similar and stiff moment-rotation paths. The first portion of this behavior is linear up to about 600 K-in. After this the connection starts to soften and the stiffness is steadily reduced. This seems to indicate that the bolted tension plate started to slip.

After approximately 28 days the specimen was unloaded and the dead load frames were replaced with the live load frames. As can be seen in the moment-rotation diagrams presented in Figure 3.4-4, the connections followed a relatively linear unloading path as the dead load was removed. Hairline cracks were noticed above the centerline of the

156

girder prior to the live load frames being put in place. The reason for these small cracks is unknown.
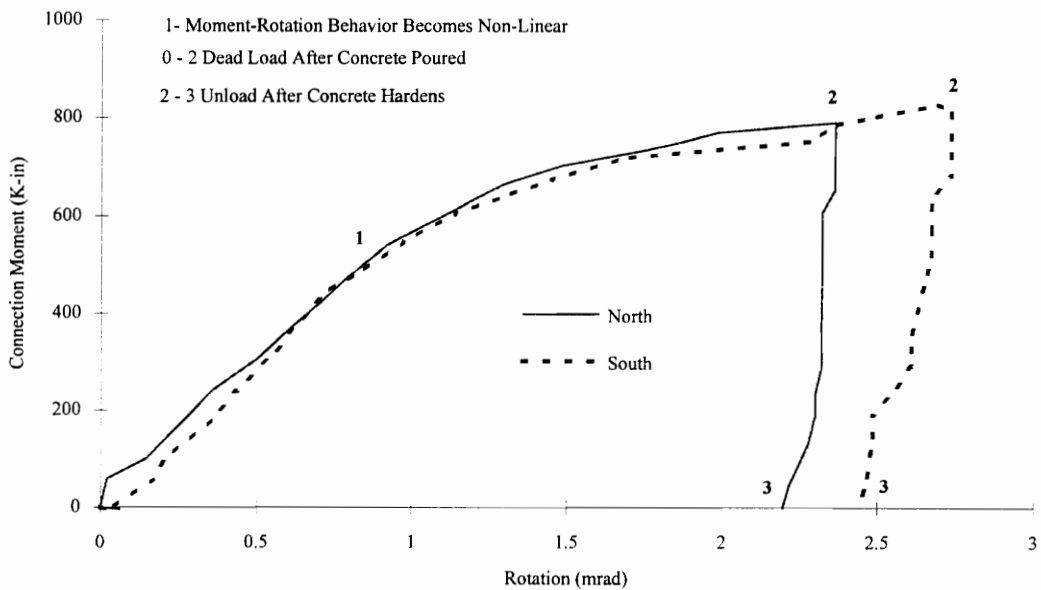
Figure 3.4-4 Moment-Rotation Behavior Steel Connections

Once the live load frames were in place the hydraulic rams were used to load the specimen back to the same point on the moment-rotation curve that it had been at prior to removal of the dead load. The connection was then unloaded. As shown in Figure 3.4-1 and Figure 3.4-2 this loading and unloading followed the same path as when the dead load was removed. This preliminary loading and unloading was conducted to ensure all instrumentation and the test frames were operating properly.

The connection was loaded back to the dead load moment location. After this moment was attained, load was increased in approximate one to two kip increments. The first cracking over the centerline of the girder, sufficient to shed load to the reinforcing steel, was noticed at 1340 K-in. This crack continued to widen and spread without any additional cracks appearing at other locations until 1700 K-in., at which time cracks over the south and north reinforcing steel gage lines appeared.

157
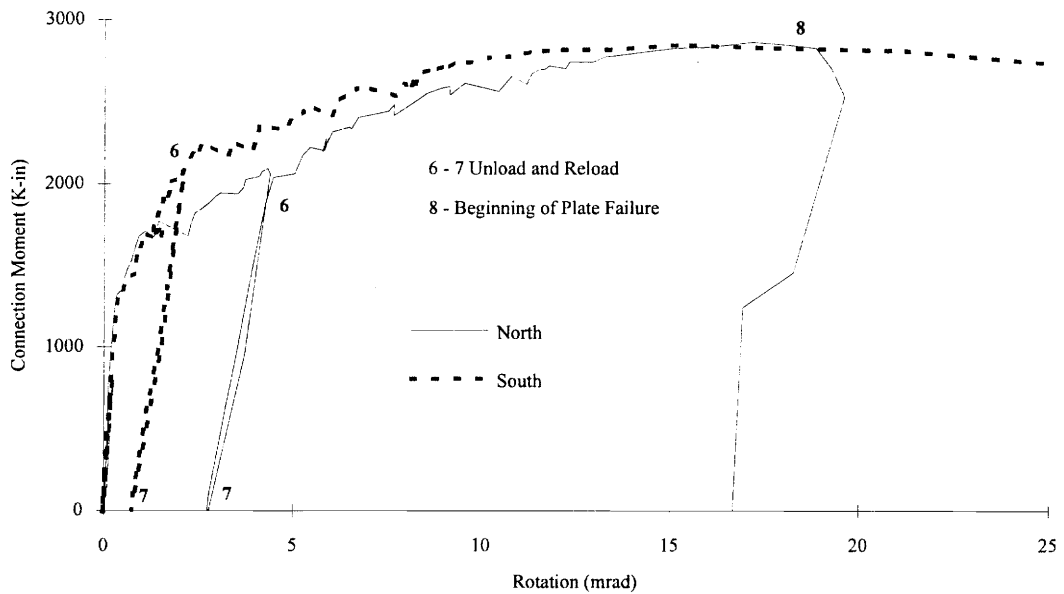
Figure 3.4-5 Moment-Rotation Behavior Composite Connections

At approximately the same point, some yielding was noticed around the toe of the south beam adjacent to the connection. In addition, a significant slip occurred in the north tension plate bolts, which most likely slipped into bearing. Some tension plate yielding was noticed at 1750 K-in. This was first noticed around the bolt closest to the girder face. At 1830 K-in. a parabolic shaped crack opened up around the north load ram and later, at 2100 K-in., longitudinal (parallel to the beams) cracks appeared around the north and south load rams.

The top potentiometers used to measure rotation on the south side appeared to be very close to riding up on the fillet of the girder. The connection was unloaded at this point in order to place additional spacers between the potentiometer and the top beam flange so that the possibility of it riding up on the girder fillet would be eliminated. The reason this was a concern was that if the potentiometer rode up onto the girder fillet it would not indicate the true displacement of the connection with respect to the girder face and would make the connection appear stiffer than it actually was.

158

As the connection was reloaded a loud pop was heard around 2000 K-in. This appeared to be the south tension plate bolts slipping into bearing. At 2200 K-in. cracks appeared behind both load rams and yielding was noticed around the bolts in the seat angle of the south side. Additional yielding of the tension plate on the south side was noticed at 2300 K-in. New cracks in the composite slab continued to develop.

The first reinforcing steel yielded at 2440 k-in. This yielding occurred in the bar directly over the beam centerline and the bar 12-in. to one side. The reinforcing bar on the other side of the center bar yielded at 2500 K-in. The north side rotation increased sharply at the same point. This increase appeared to be caused by a slip of the bolted tension plate. The two exterior reinforcing bars yielded at 2600 K-in. along with noticeable yielding around the middle bolt in the bolted tension plate on the south side.

Yield lines were noticed around the bolts in the seat angle connection on the north side at approximately 2800 K-in. In addition, severe yielding of the tension plate on the south side was occurring. As the plate yielded, load was redistributed to the slab as indicated by a sharp increase in the rate of slab slip. At the same time, the steel deck on the south side was deforming around the shear stud locations. The tension plate soon failed in tension rupture at the net section around the bolt hole nearest the girder face. After connection failure, the test was continued in an attempt to fail the north side of the specimen. But, as a result of the reduced moment capacity of the south connection, the moment on the north side could not be increased because the girder could not resist the unbalanced moment.

The center of connection rotation versus the moment at the connection is plotted in Figure 3.4-6 and Figure 3.4-7. The center of rotation was initially at the center of the beam but dropped toward the bottom of the beam as moment was increased and the tension plate softened. Once the composite slab was effective, the center of rotation rose from near the bottom of the beam to five to six-in. below the center of the beam.

159
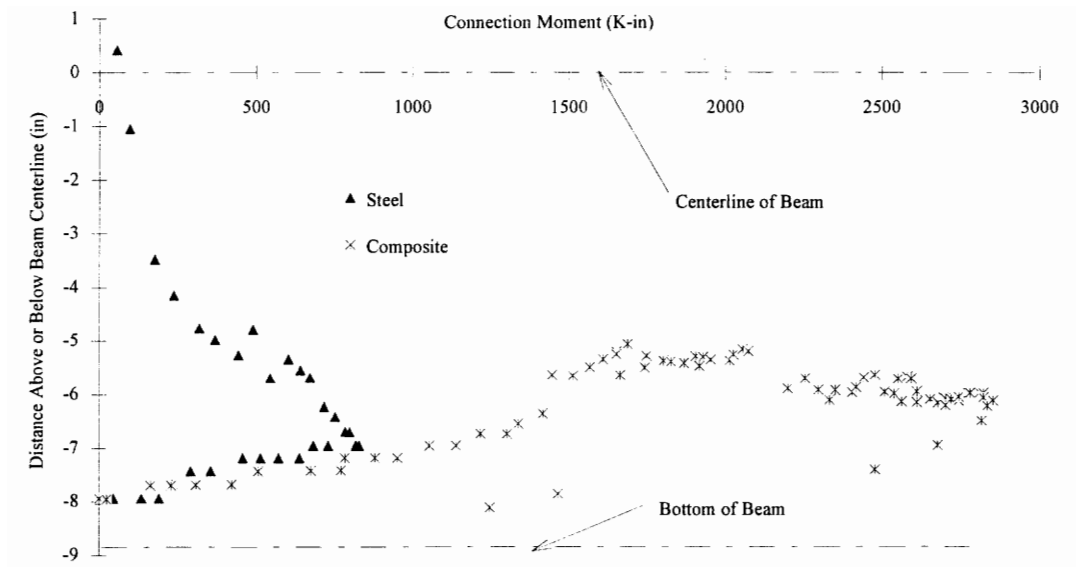
Figure 3.4-6 Center of Connection Rotation South Connection
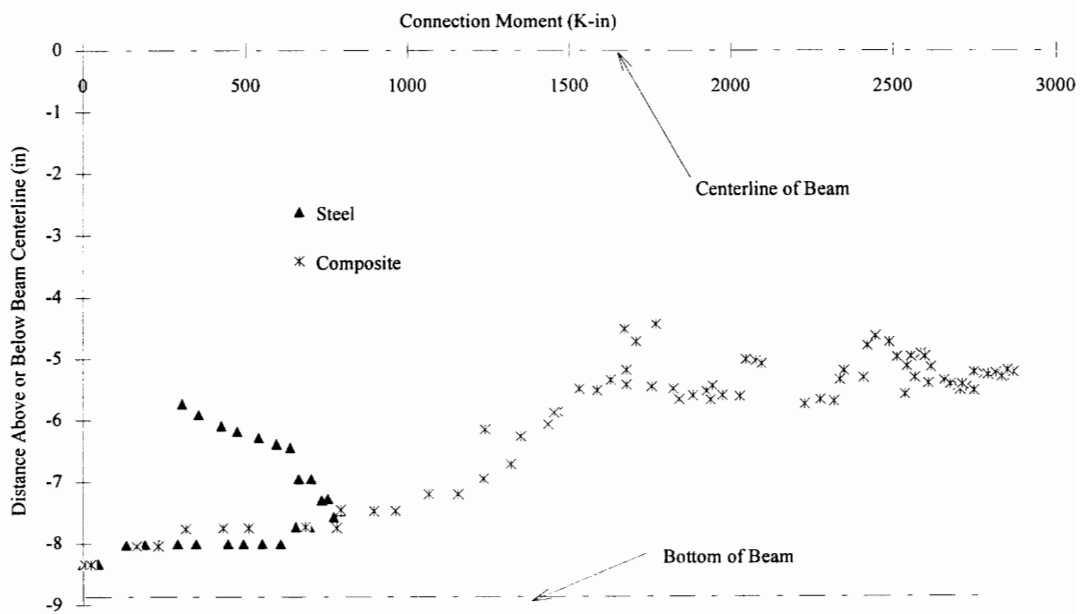
Figure 3.4-7 Center of Connection Rotation North Connection

160

It stayed in this region until near connection failure, at which time it abruptly returned to near the bottom of the beam for the side that failed, but remained in the five to six-in. range for connection that did not fail. The reader will notice that the center of rotation is always located below the centerline of the beam. This indicates that the seat angle was a more rigid element in compression than the composite slab and the tension plate were in tension. The fact that the connection rotated about five to six-in. below the beam centerline for most of the composite connection test indicates that the stiffness of the seat angle was degrading at about the same rate as the stiffness of the combination of the slab and tension plate.

3.4.2 Steel Connection Behavior

Linear displacement transducers measured the relative movement between the web of the beam and the tension plate. The data from these transducers is presented in Figure 3.4-8. Throughout the entire load history, the connection plate was slipping away from the beam web leading to the conclusion that the plate was always in tension. The initial portion of the figure closely resembles the moment-rotation behavior pattern for the bare steel connection. This indicates that understanding the behavior of the bolted tension plate is particularly important in order to predict the behavior of this type of steel connection. The response for both the north and south sides is almost vertical after the composite slab became effective. This most likely indicates that the plate took little additional load in this region because the slab was so much stiffer than the plate. As the composite slab started to degrade additional load was placed on the tension plates. This is when they appeared to slip into bearing and then deform in bearing as additional load was applied. The total slip is not as large as what was seen in Connection #2. This occurred because the plate itself failed instead of causing bearing failure in the web of the beam.

161
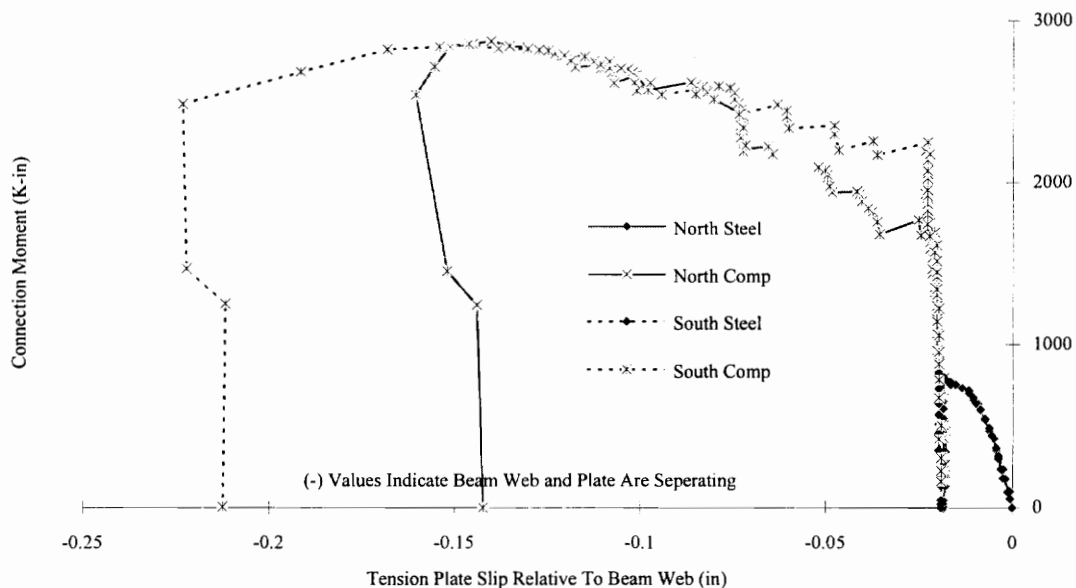
Figure 3.4-8 Moment Vs. Tension Plate Slip

Strain readings from the locations on the seat angle connection are presented in Figure 3.4-9 and Figure 3.4-10. The strain value shown in the figures represents the average of the two gages along the side of the seat angle and the average of the two gages on the bottom face of the angle respectively. The axial strain shown in Figure 3.4-9 shows a very linear behavior up to where the approximate yield strain was reached. After this point, the moment versus strain behavior became almost horizontal indicating that the seat had essentially yielded fully and would not increase in load until the steel started to strain harden. As mentioned before, the response indicated by the gages on the bottom of the seat angle remained linear even after the yield strain was reached because the whole section was still far from being fully yielded. In fact the behavior shown in Figure 3.4-10 only becomes non linear after the axial strain shown in Figure 3.4-9 went beyond the ideal yield strain.
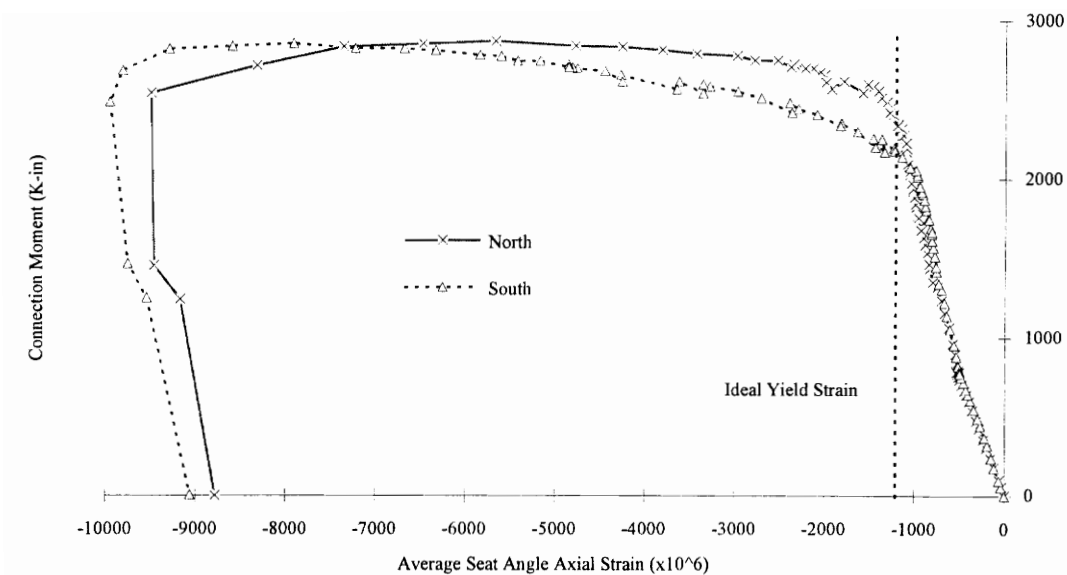
Figure 3.4-9 Seat Angle Axial Strain Vs. Connection Moment
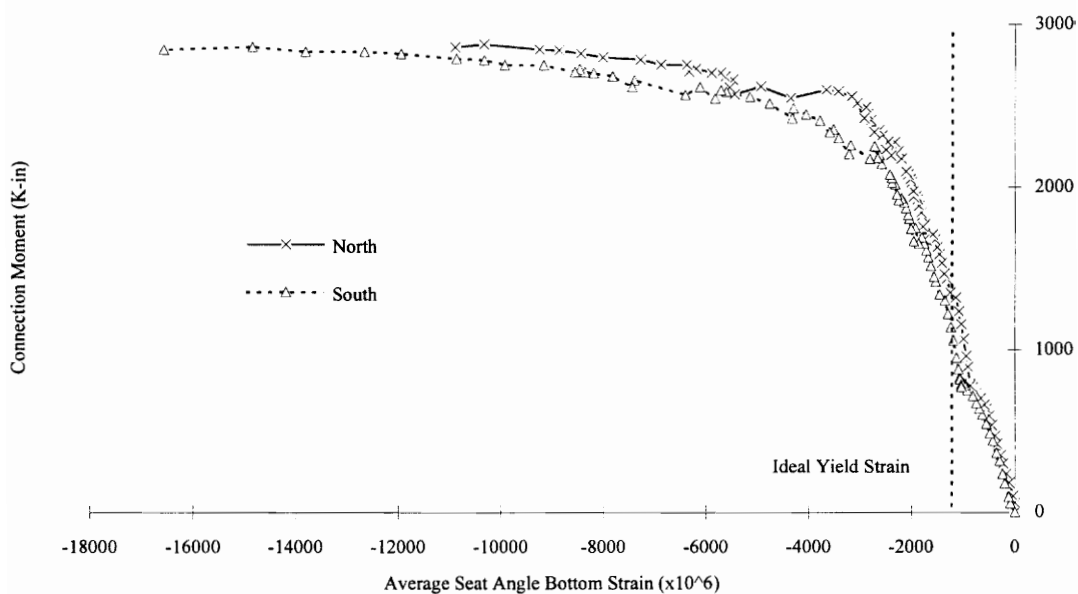
Figure 3.4-10 Seat Angle Bottom Strain Vs. Connection Moment

163

Despite what appears to be a significantly yielded seat angle, visual inspection of the steel angle after the connection was dismantled did not indicate severe distress. The angle had been slightly bent from horizontal about the seat angle toe and there were shallow indentations on the top side of the angle where the beam had set.

A strain rosette was attached to the bolted tension plate near the face of the girder. The original intent in placing this gage had been to allow the determination of the tensile and shear forces developed in the plate. The maximum principal strains from the rosette measurements are presented in Figure 3.4-11. As can be seen in the figure, the maximum principal strains were compression strains during application of the dead load. Since the plate was known to be in high tension during this time these measurements do not make any practical sense. The data is most likely not subject to rational interpretation as a result of out-of-plane bending of the plate which could not be accounted for. As a result, no definite conclusions about what happened to the plate could be drawn from this data due.

A strain rosette was placed at the toe of the beam near the connection. This region was of particular interest because it should ideally be one the highest stressed areas in the beam. The value of the maximum principal strain versus the connection moment is plotted in Figure 3.4-12. As expected, this response is very linear until the approximate yield strain of the beam material was reached. This occurred at 2400 K-in. as indicated on the figure. After this point the connection loss stiffness as the web started to yield in this region.

The shear stress and the normal stress are presented in Figure 3.4-13 and Figure 3.4-14 respectively. The shear stress is plotted negative because of the orientation of the rosette. The response of the shear and normal strains became nonlinear at the same point as the principal strain (i.e., at 2400 K-in.). The shear strains were extremely high in this region while the normal strains were fairly low. This was expected as most of the horizontal forces should have been resisted by the bottom flange and because the web typically carries the shear forces for the beam.

164
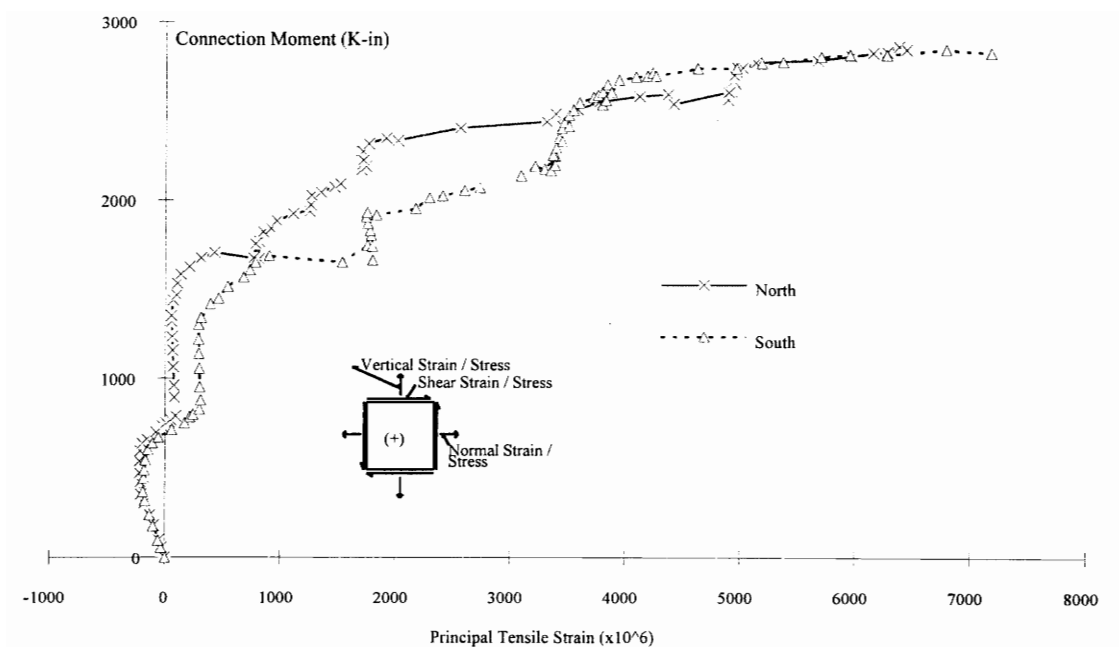
Figure 3.4-11 Tension Plate Maximum Principal Strain As Measured by Rosette
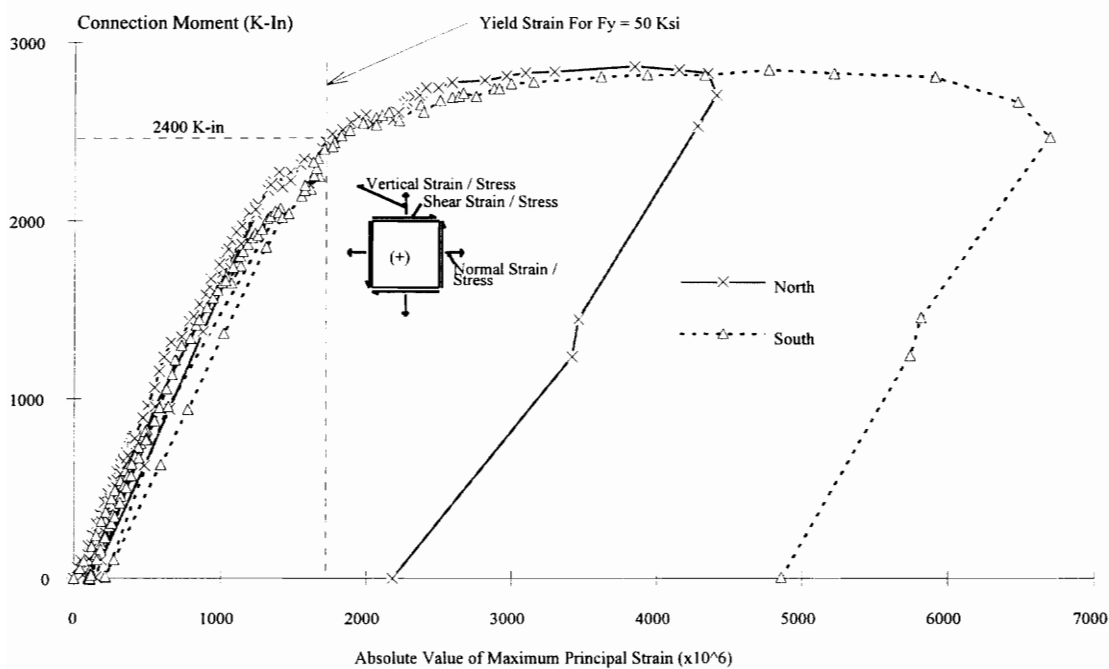
Figure 3.4-12 Maximum Principal Strains in Beam Web Toe

165
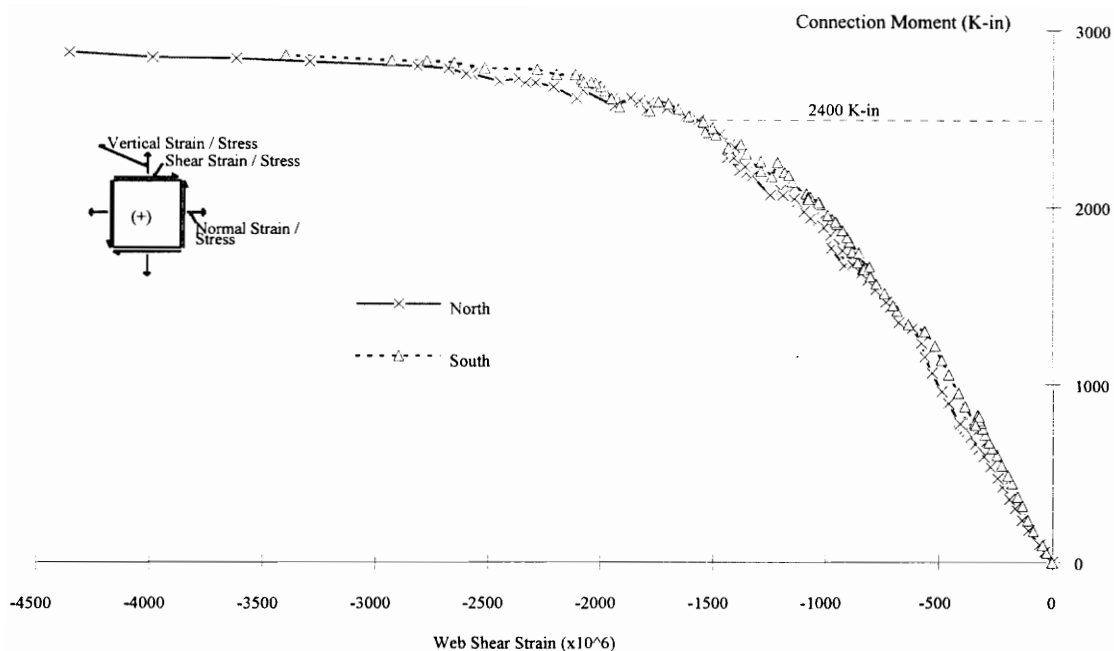
Figure 3.4-13 Shear Strain in Beam Web Toe at Rosette Location
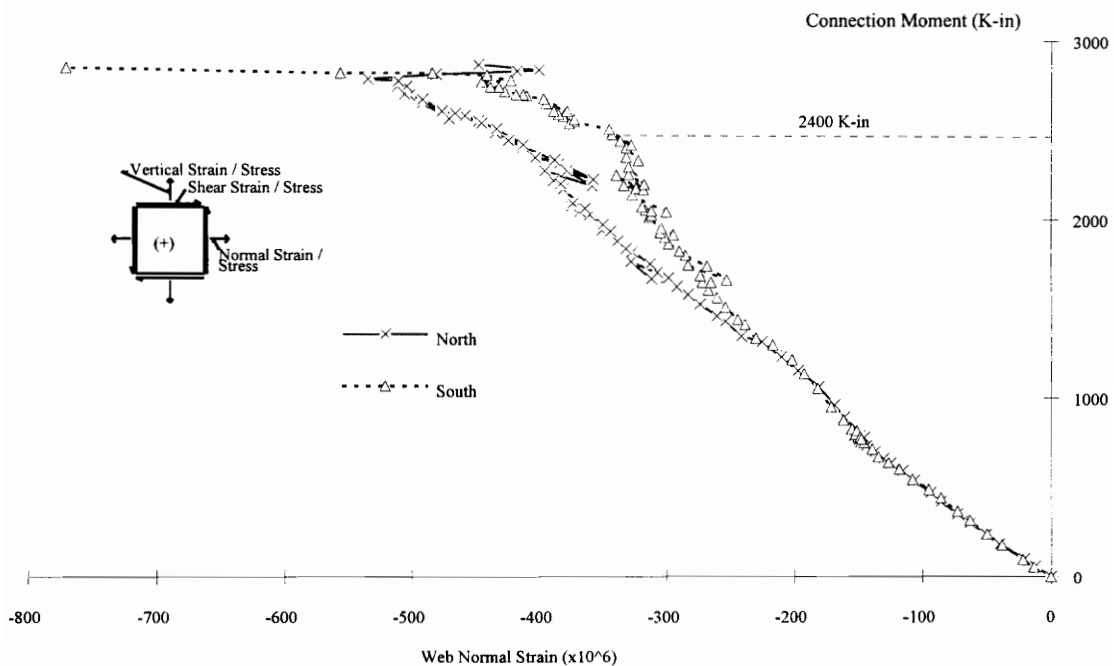
Figure 3.4-14 Normal Strain in Beam Web Toe at Rosette Location

166

3.4.3 Composite Slab Behavior

The reinforcing bar forces along the three gage lines are presented in Figure 3.4-15 through Figure 3.4-17. This force distribution is based on the strain gage readings prior to yield. Yield was determined by examining the strain data and determining where a sharp or abnormal jump in strain occurred. The center gage line was directly over the centerline of the girder and the values represent the average value of two gages at that location. The south and north gage lines were located 12-in. on each side of the girder centerline. It should be noted that 20 out of 20 of the reinforcing bar gages functioned properly throughout the test. As described in the discussion of Connection #1, the yield force for the reinforcing steel was 14 Kips.

All the reinforcing bars yielded at locations over the centerline of the girder and some at locations along the north and south gage lines. When the bars yielded above the girder centerline they all yielded within 100 to 200 K-in. of each other. This indicates little shear lag which can be seen by examining Figure 3.4-16.
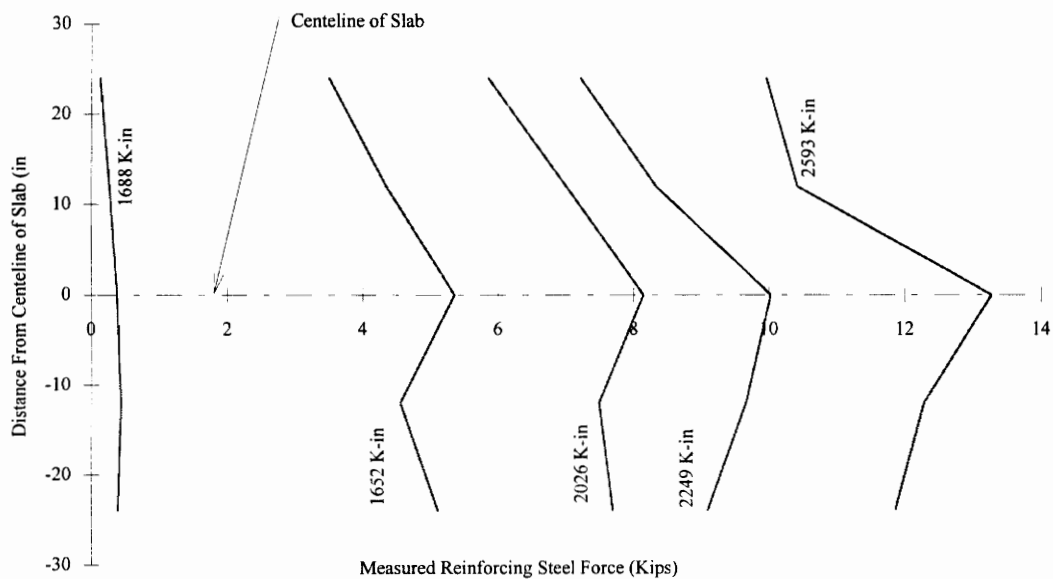
Figure 3.4-15 Reinforcing Steel Force Distribution Pattern Along South Gage Line
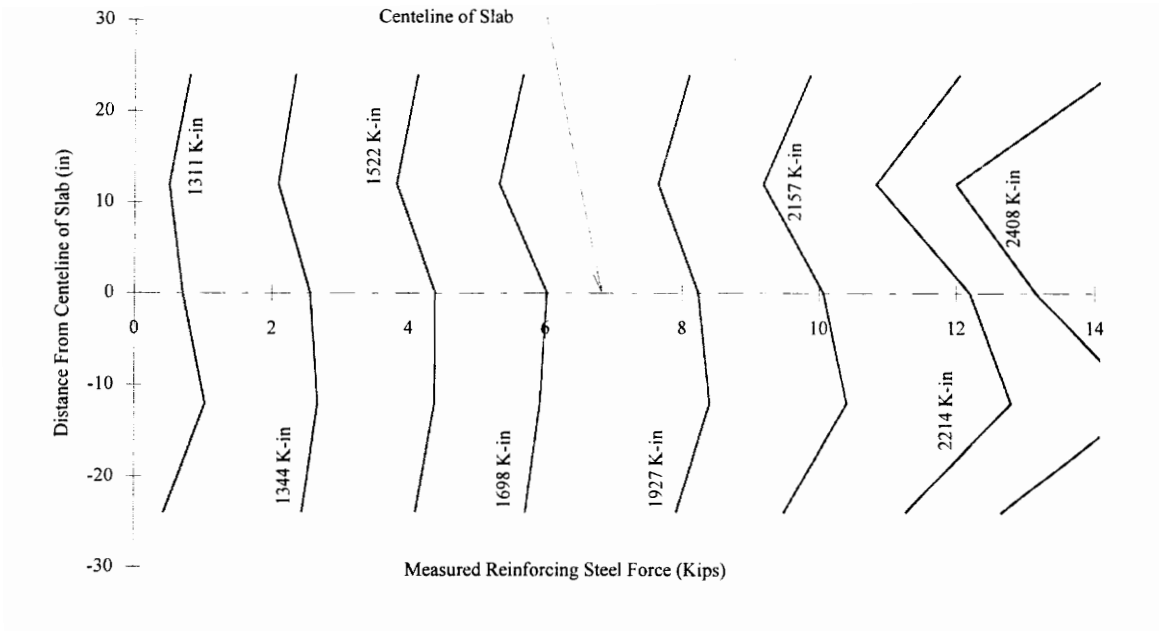
Figure 3.4-16 Reinforcing Steel Force Distribution Pattern Along Center Gage Line
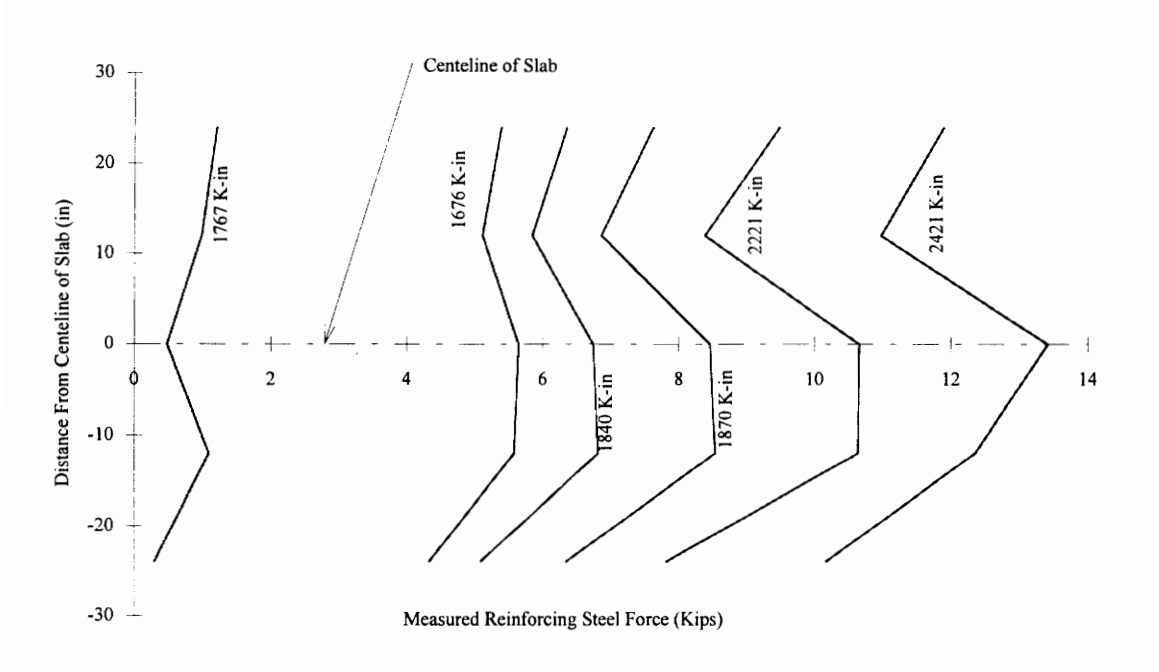
Figure 3.4-17 Reinforcing Steel Force Distribution Pattern Along North Gage Line

168

The shear lag along the north and south gage locations appeared to be more pronounced than above the girder centerline. There also appears to be some strange distribution of forces which may indicate that the slab was not loaded symmetrically, that some bending was occurring within the plane of the slab, or the slab had not cracked evenly across these gage lines.

The reinforcing steel force versus the connection moment is plotted in Figure 3.4-18. The reinforcing steel did not develop significant force until moments were above the dead load moment. Before the concrete cracked, the forces in the reinforcing steel appeared to be identical. The first significant cracking occurred along the center gage line. It appears that because the behavior of the reinforcing steel above the centerline started to diverge from the behavior along the north and south gage lines prior to a large jump in force, that small cracking was occurring along the centerline which had some minor effects on the response prior to any major cracks.
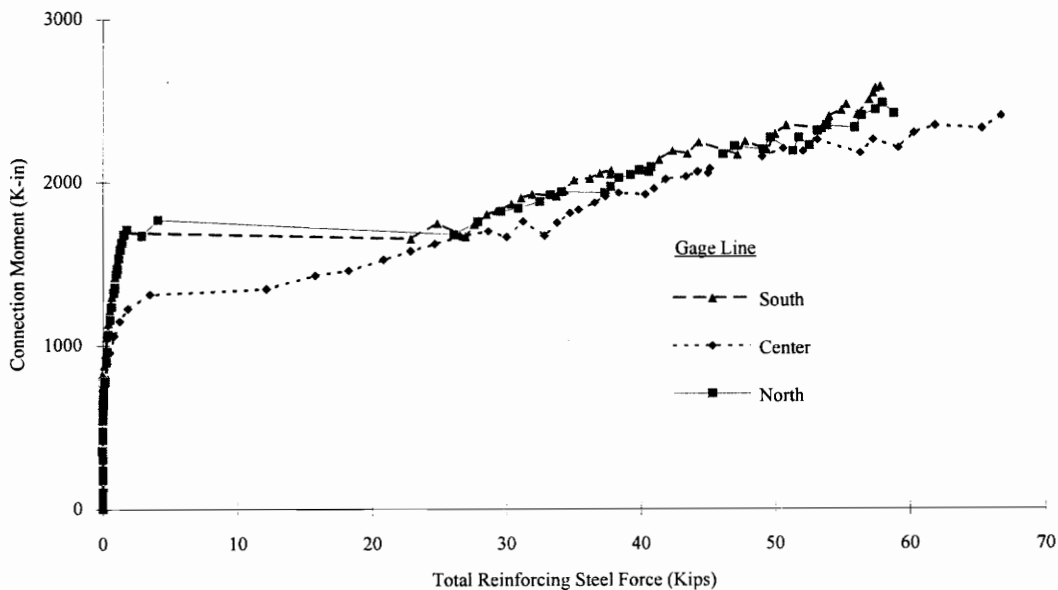
Figure 3.4-18 Reinforcing Steel Force Across Width of Slab

169

Significant cracks did not appear around the north and south gage lines until a much higher connection moment was attained. The first crack being over the center may have been a result of the many hairline cracks that were noticed above the girder centerline prior to applying the live load. Because the centerline crack was at a location that would allow rotation of both the north and south sides of the connection the slab did not need to crack above the north and south sides until much higher moments were developed. Once the flexural cracks over the north and south gage lines appeared (at approximately 1600 to 1700 K-in.) the force in the reinforcing steel appeared to be very similar at all the gage locations again and seemed to increase linearly until the reinforcing started to yield.

The history of the composite slab slip is presented in Figure 3.4-19 and Figure 3.4-20. As seen in Figure 3.4-20, the north side of the slab appeared to slip away from the girder at around the moment that the slab cracked. This was because the slab crack allowed the portion of the slab, which the LVDT was attached to, to move along with the beam for a short period of time before being pulled back in its original direction of motion. Except for this jump in the slip behavior, the overall response appeared very linear until the reinforcing steel started to yield. At this point, as a result of increased cracking in the composite slab and the high load on the shear studs, the slip behavior started to degrade. Finally, when the tension plate failed, the slab slip on the south side showed a sharp increase as load was redistributed from the tension plate to the slab on this side. Again, as discussed in Section 3.2.3, the behavior of the composite slab as shown in the initial regions of Figure 3.4-20 is typical of reinforced slabs in tension.
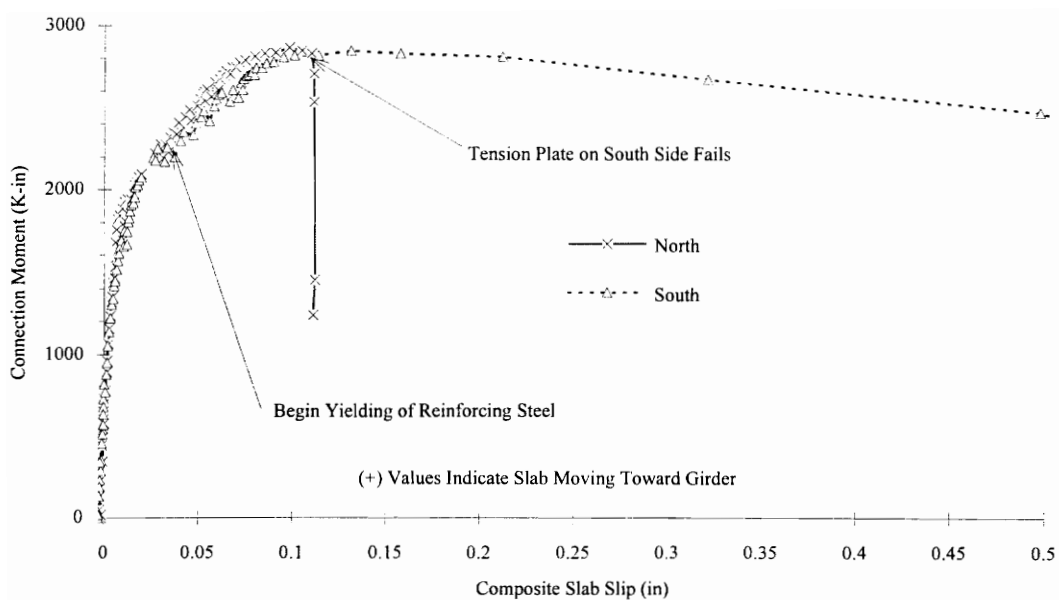
Figure 3.4-19 Composite Slab Slip Vs. Connection Moment
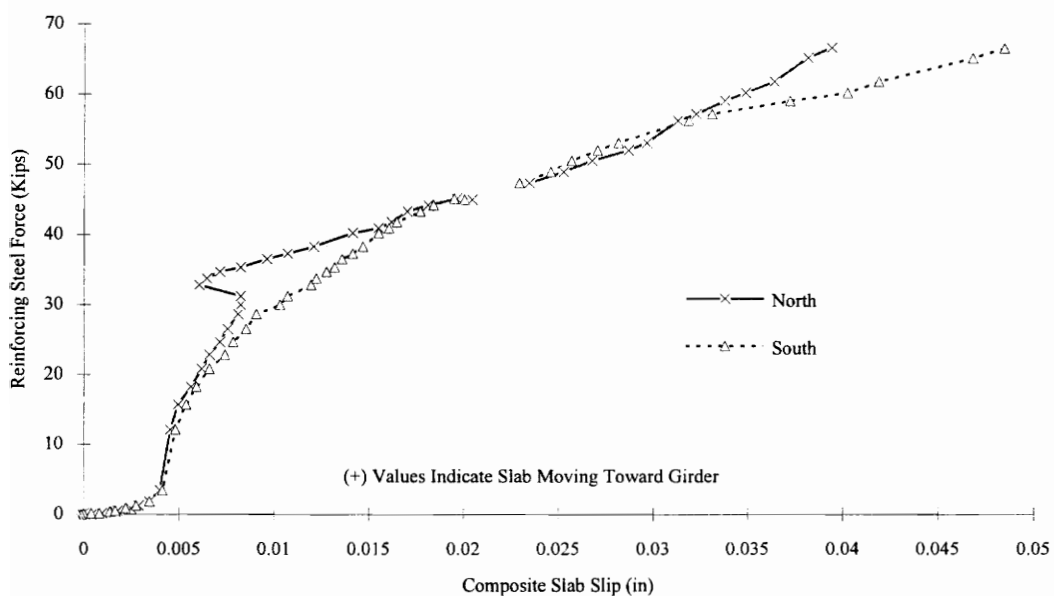
Figure 3.4-20 Composite Slab Slip Vs. Reinforcing Steel Force

171

3.5 BEHAVIOR OF CONNECTION #4

3.5.1 Moment-Rotation Behavior and Test History

Connection #4 was loaded at two different times: at the time of concrete casting and at the time when failure loading was applied. The moment-rotation behavior for the entire load history is presented in Figure 3.5-1 and Figure 3.5-2. For comparison purposes, the moment-rotation behavior for the two sides of the specimen have been plotted together for the dead load portion of the test and for the live load portion of the test. These plots are presented in Figure 3.5-3 and Figure 3.5-4 respectively. The specimen was considered to have failed when the web of the north side crippled and the welds connecting the tension plate to the top beam flange ruptured.
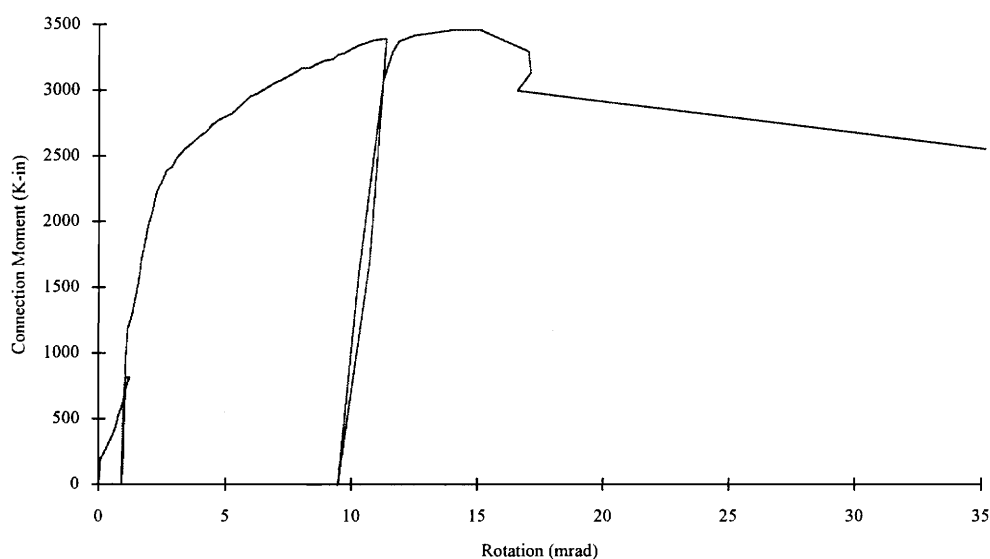
Figure 3.5-1 Moment-Rotation Behavior North Connection

The day the slab was cast the simulated dead load was applied. The full load of 17 kips was applied because the connection had not rotated to the dead load beam line or reached a horizontal plateau in its behavior. As shown in Figure 3.5-3 the connections

appeared to follow similar and linear moment-rotation paths except for some jumps at the beginning and end of the application of dead load. Because the dead load should have been well below the elastic limit of the connection, the linear response was expected. The apparent jumps in rotation are believed to be caused by the limited ability of the combination of transducers to measure very small rotations (as most of this response was under one mrad which corresponds to potentiometer measurements of under 0.007-in.).
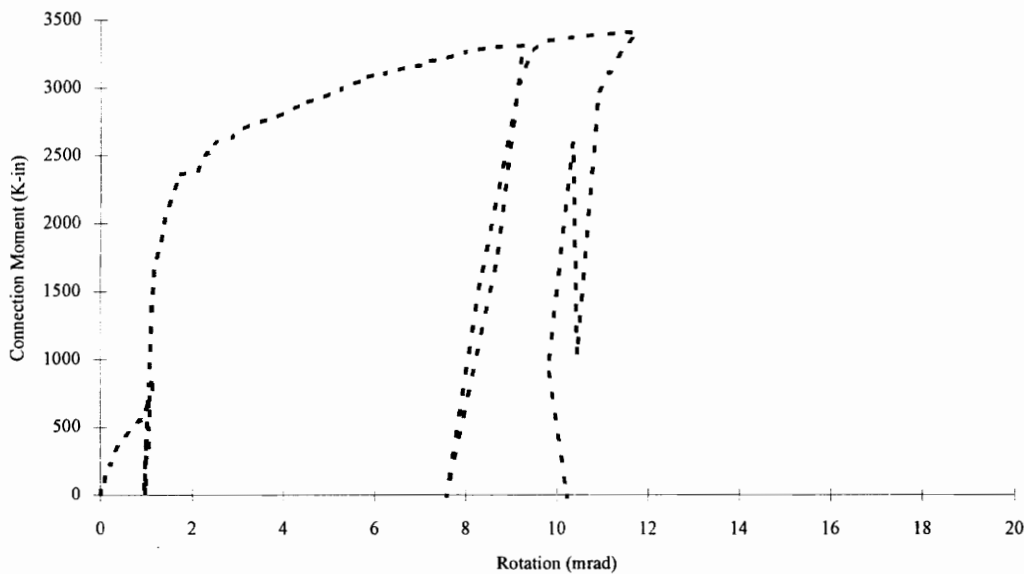
Figure 3.5-2 Moment-Rotation Behavior South Connection

After approximately 28 days the specimen was unloaded and the dead load frames were replaced with the live load frames. As can be seen in the moment-rotation diagrams presented in Figure 3.5-3, the connections followed a linear unloading path as the dead load was removed. Hairline cracks were noticed above the centerline of the girder prior to the live load frames being put in place. The origin or reason for these small cracks is unknown, but they did not appear to impair the slab structurally.

173
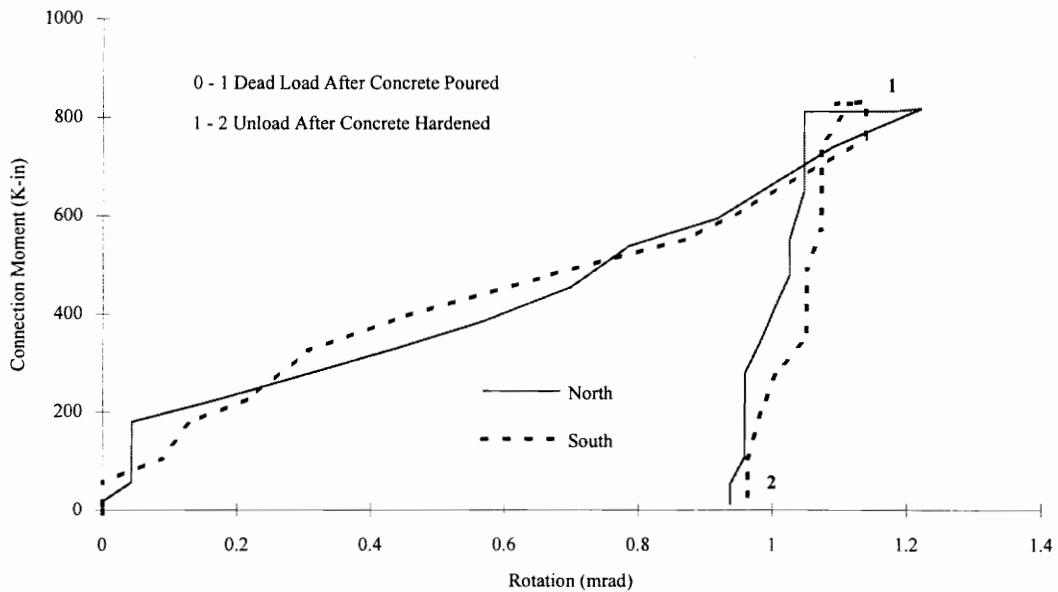
Figure 3.5-3 Moment-Rotation Behavior Steel Connections

Once the live load frames were in place the hydraulic rams were used to load the specimen back to the same point on the moment-rotation curve that it had been at prior to removal of the dead load. The connection was then unloaded. As shown in Figure 3.5-1 and Figure 3.5-2 this loading and unloading followed the same path as when the dead load was removed. This preliminary loading and unloading was conducted to ensure all instrumentation and the test frames were operating properly.

The connection was loaded back to the level of the dead load moment. After this moment was attained, load was increased in approximately two to three kip increments. The north side of the specimen exhibited an increased rate of rotation compared to the south side almost immediately after the dead load moment had been attained. This difference increased when the first crack appeared around 1300 K-in. This crack was noticed above the south side of the specimen approximately 8 to 10-in. from the centerline of and parallel to the girder.
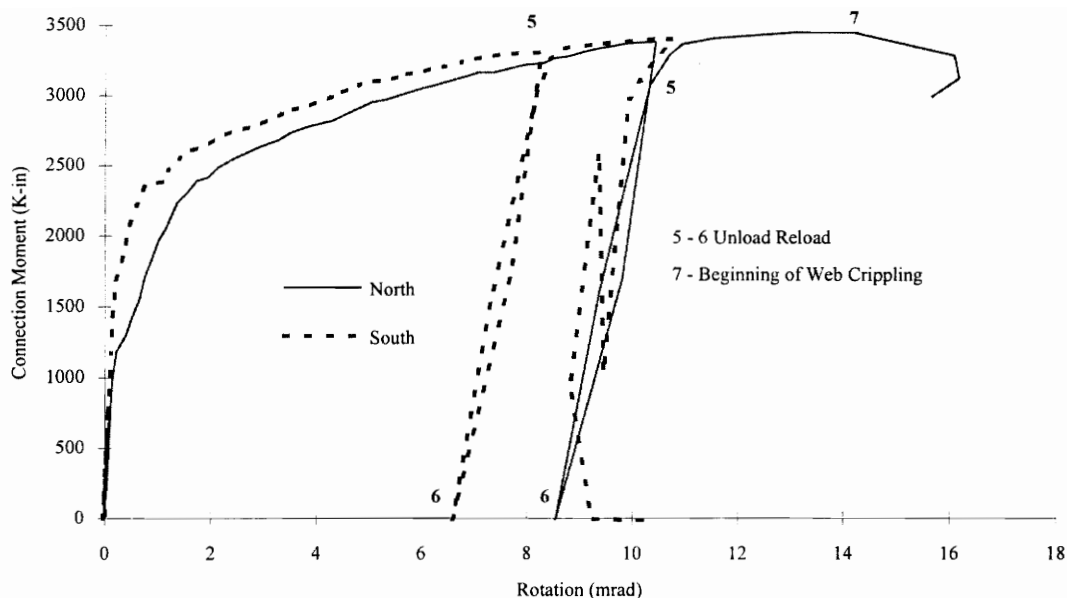
Figure 3.5-4 Moment-Rotation Behavior Composite Connections

Yielding was noticed in the toe of the beam near the connection on both sides of the specimen at about 1400 K-in. As load was increased, the yielding around the toe on the north side appeared to be more severe than on the south side. Despite the crack over the south side of the specimen the rate of rotation of the north side was still greater than the rate of rotation of the south side. The strain gages on the reinforcing steel indicated that the south side had cracked sufficiently for the concrete to shed most of the slab load to the reinforcing steel in the region of the south gage line. The reinforcing steel gages over the girder centerline indicated that load was increasing in this region, while the gages over the north indicated little or no load was being carried by the steel in this region. At approximately 2400 K-in. a crack appeared over the north gage line. At about the same time, yielding around the toe of the beam on the north side was becoming more noticeable. No severe cracking was noticed over the centerline of the girder but based on the strain gage readings in this area it was apparent that the concrete had shed most of the

175

slab load to the steel. The north side still exhibited a greater rate of rotation than the south side despite the new cracking.

Small cracks appeared around both load rams just above and parallel to the beam webs at approximately 2600 K-in. At approximately the same time the tension plates appeared to be forming hinges. These hinges formed along the top edge of the girder on both sides and along the edge of the top beam flanges adjacent to the cope. At 2800 K-in. more severe yielding of the web in the region of the beam toe on both sides was observed and the web rosettes in this region indicated that the web had reached yield. Both seat angles were showing severe yielding at about 2900 K-in. but the north side appeared to be worse than the south. One of the seat angle gages on the north side appeared to have gone off scale indicating a strain in excess of 16000 micro-strains.

At approximately 3100 K-in., yield lines were noticed around the top fillet of the girder and increased yielding of the beam webs was apparent. At the same time the north seat angle showed the first signs of vertical deflection just past the end of the beam. At approximately 3200 K-in. yielding of the tension plates was obvious. The second strain gage on north seat angle and one of the gages on the south seat angle appeared to have gone off scale, again indicating very large strains.

At approximately 3300 K-in. the vertical deformation of the north seat angle was such that two hinges formed, one located along the toe of the seat angle and the other along the line of the erection bolts. Additional slab cracking was noticed in front of both load rams. The steel deck above the south beam was noticed to have started to uplift in the region just above the connection. The slip in the south slab seemed to be increasing more rapidly than in the north slab. Multiple yield lines under the top flange of the girder were now apparent.

Because the connection appeared to be in or near its plastic region, the specimen was unloaded and then reloaded to study the unloading and reloading stiffness characteristics. Both connections appeared to come back to the previous position on the moment-rotation curve and had very linear unloading and reloading paths.

176

As the specimen was reloaded the slip in the south slab seemed to be increasing rapidly and the seat angle on the south side appeared to be hinging similar to the north but not as significant. As the north seat angle hinged the top tension plate also hinged and the north side of the specimen appeared to be dropping vertically. The crack above the north connection had a slight but noticeable vertical offset from one side to the other. Finally the beam web on the north side started to cripple and the vertical displacements on the top of the north side increased rapidly. The load was reduced and the instrumentation was removed from the north side. The load was then increased so that the final failure mode could be determined. As the web crippled the top of the beam deflected downward and the tension plate started to pull away from the top of the beam. Finally the welds holding the tension plate to the top beam ruptured and the tension plate was no longer attached to the beam. The test was ended at this point.

The center of connection rotation versus the moment at the connection is plotted in Figure 3.5-5 an Figure 3.5-6. The center of rotation started approximately two to three-in. above the centerline of the beam.
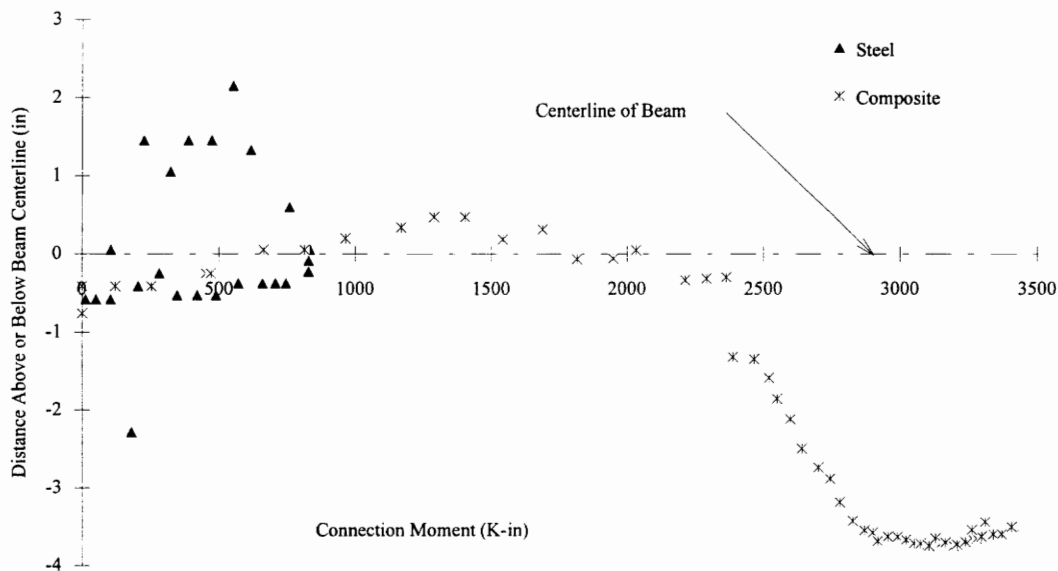
Figure 3.5-5 Center of Connection Rotation South Connection

As the dead load was applied the center of rotation on the south side dropped to about the center of the beam while the center of rotation on the north side only dropped to about 1.5-in. above the centerline of the beam. This was an indication that either the tension plate on the north side was stiffer than on the south side or that the seat angle on the north side was less stiff than the seat angle on the south side.
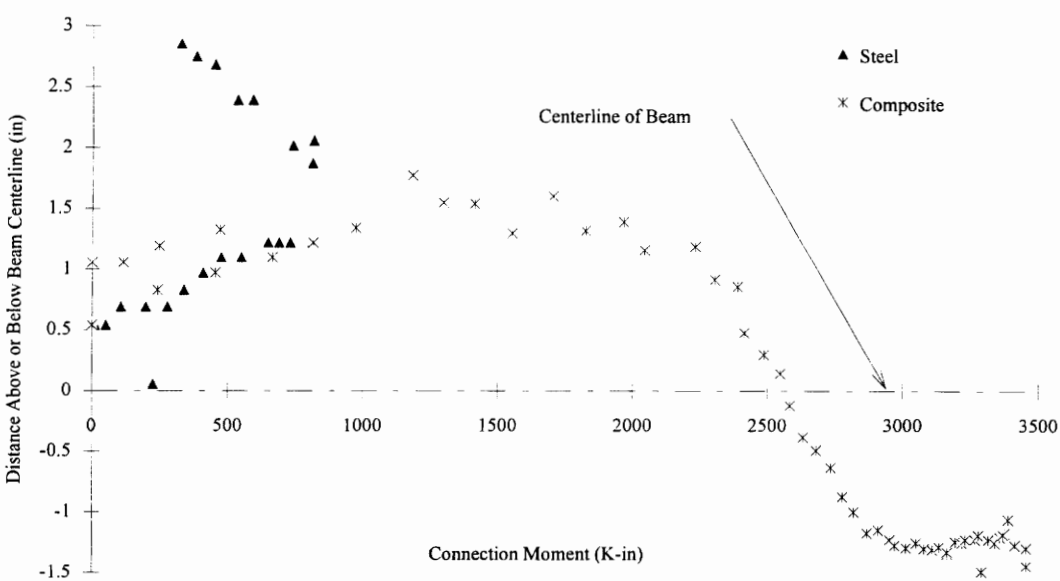
Figure 3.5-6 Center of Connection Rotation North

Once the composite slab became effective, the rotation appeared to stay at approximately the same level it had been after application of the dead load. The slab and tension plate on both sides appeared to soften around 2000 K-in. as indicated by the center of rotation starting to drop. The location of the rotation center started to level out again around 3000 K-in. but the location for the south side was four-in. below the center of the beam while the location on the north side was around 1.5-in. below the center of the beam. The rotation centers maintained these locations until the specimen began to fail. Because the center of rotation for the north side was consistently above the center of

rotation for the south side, it is evident that the seat angle on the south side was most likely stiffer than the seat angle on the north side.

3.5.2 Steel Connection Behavior

The strain gage data obtained from the locations on the top side of the tension plate (as shown in Figure 3.5-7) is presented in Figure 3.5-8. Again it should be noted that these gages were not located at critical locations for plate yielding and consequently the strain values do not give a true indication as to whether the plate was yielded or not. As seen in the Figure 3.5-8 the general pattern of the strain behavior follows the pattern of the moment-rotation behavior up to around 2500 K-in. The pattern in the region where the dead load was applied is very similar to the moment-rotation behavior. This pattern indicates that understanding the plate behavior is very important for predicting the moment-rotation behavior of the steel connection.
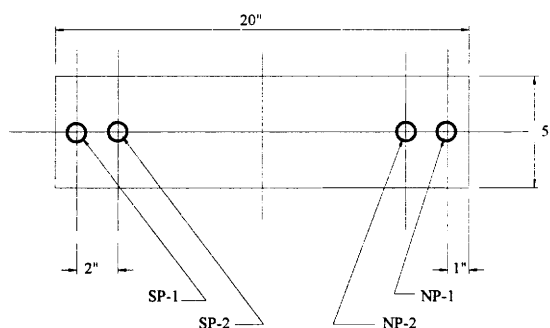
Figure 3.5-7 Strain Gage Locations on Tension Plate

Throughout the load history, until very near the failure of the specimen, the strains on the north side appear to increase in a manner very similar to the south side. There appears to be four regions of strain behavior; before the composite slab was effective, after the slab was effective, after the first crack appeared over the south side, and after the first crack appeared over the north side.

179
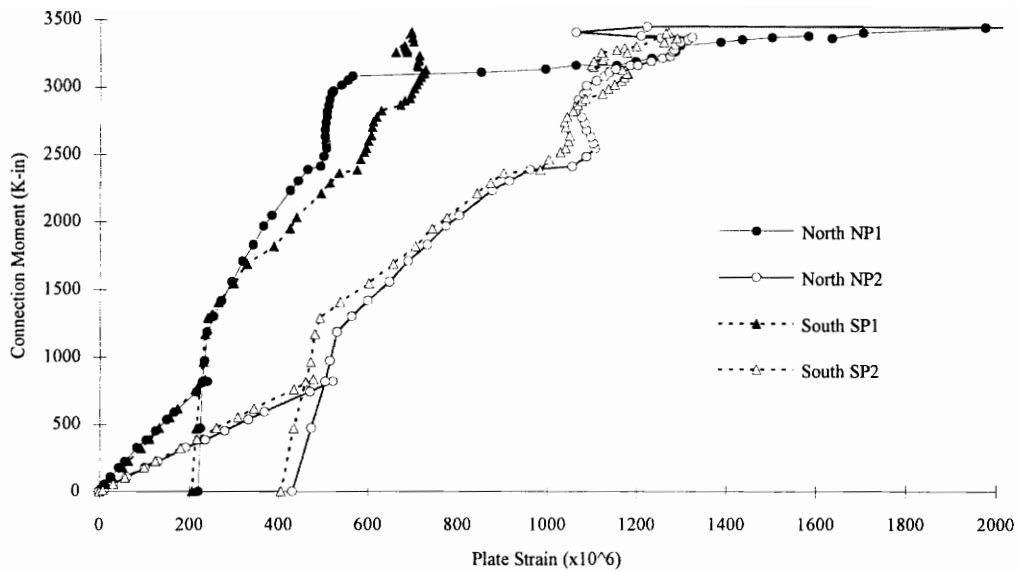
Figure 3.5-8 Axial Strains in Tension Plate Vs. Connection Moment

In general, the strain behavior was very linear within the individual regions until the slab cracked on the north side at which time the slab load seemed to be adjusting by initially taking some load off the plate and then putting it back on. The strain readings on the north side appear strange near connection failure. This is because the welds attaching the plate to the top beam flange were starting to rupture; and consequently, the stress distribution in the plate changed rapidly.

The strain readings from locations along the side of the seat angle are presented in Figure 3.5-9. The strain value indicated represents the average value from the two gages (one on each side of the seat angle). The strain behavior is very similar for both the north and the south sides. The behavior is linear up to around 1000 K-in. at which time it appears that the behavior starts to soften. This softening was probably initiated by yielding of the angle on the bottom side which is subject to compression and axial load. The behavior starts to become plastic with a slight hardening soon after the gages indicated that the yield strain was exceeded. This occurred at approximately 2000 K-in as shown in Figure 3.5-9.

180
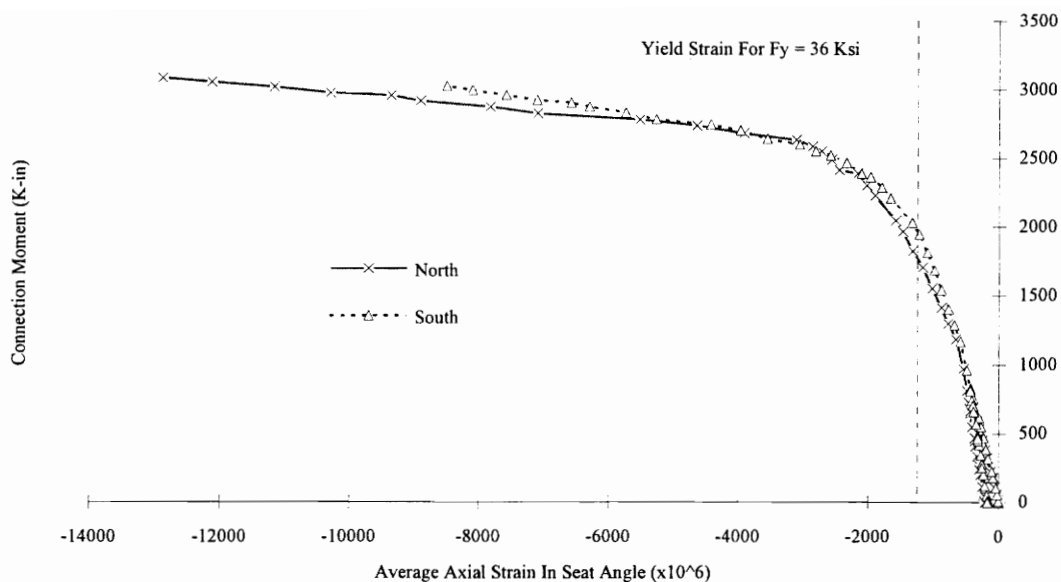
Figure 3.5-9 Axial Strain In Seat Angle Vs. Connection Moment

The information obtained from the series of rosettes that were placed along the base of the beam web near the connection is presented in Figure 3.5-10 through Figure 3.5-15. Each line represents a strain contour for a given moment similar to the stress diagrams presented for the shear plate of Connection #1. The rosettes were placed in these locations to identify a stress distribution pattern in the web of the beam and to hopefully translate that into an effective bearing length for the beam end. The gage located closest to the end of the beam was located directly above the erection bolts.

As expected for this area, the shear strains were very high, the vertical (compressive) strains were relatively high and the normal (or horizontal) strains were not as significant. What is most evident from analysis of the figures is that the shear and vertical strains drop significantly just passed the centerline of the erection bolts. The shear and vertical strains for the gage directly over the bolt line indicate severe yielding while the gage just two-in. away indicates some, but typically little, yielding. This would seem to indicate that the effective bearing length was between two to four-in. from the

beam end. It should be noted that the gage readings after the web crippled have not been included because these did not have any general discernible pattern to them.
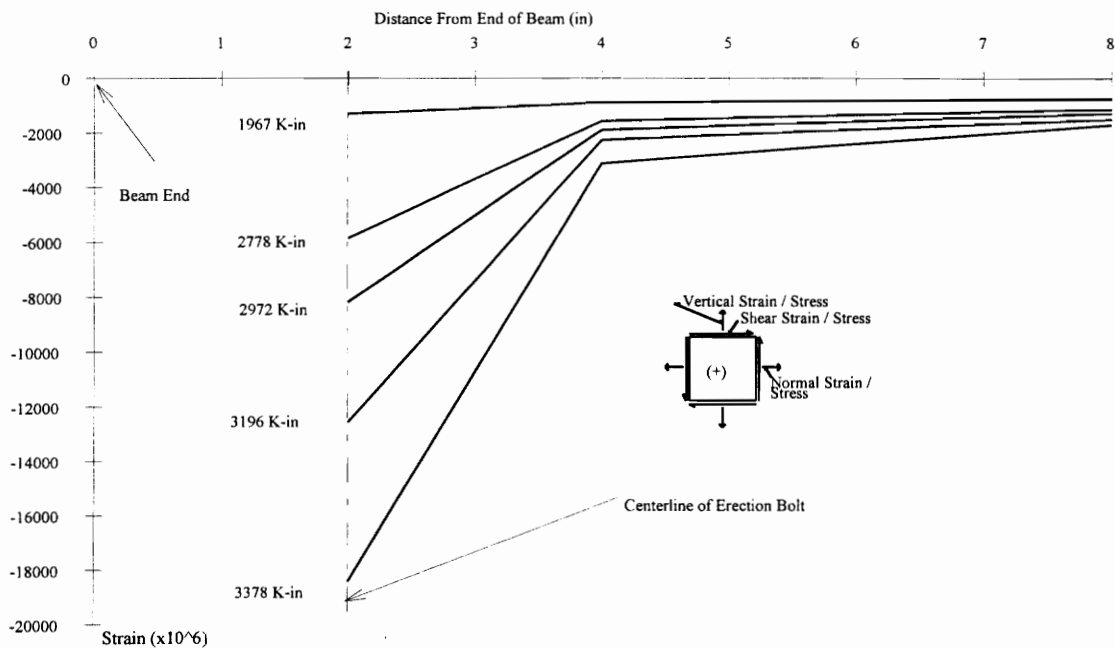
Figure 3.5-10 Shear Strain Distribution At Toe of North Beam Web
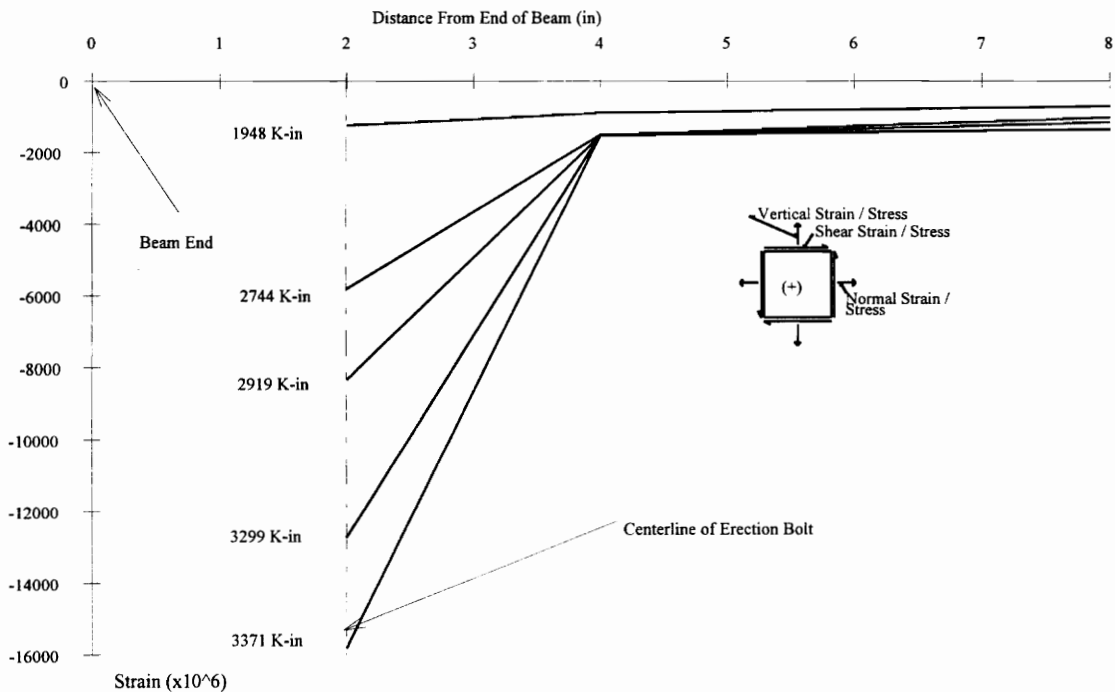
Figure 3.5-11 Shear Strain Distribution At Toe of South Beam Web
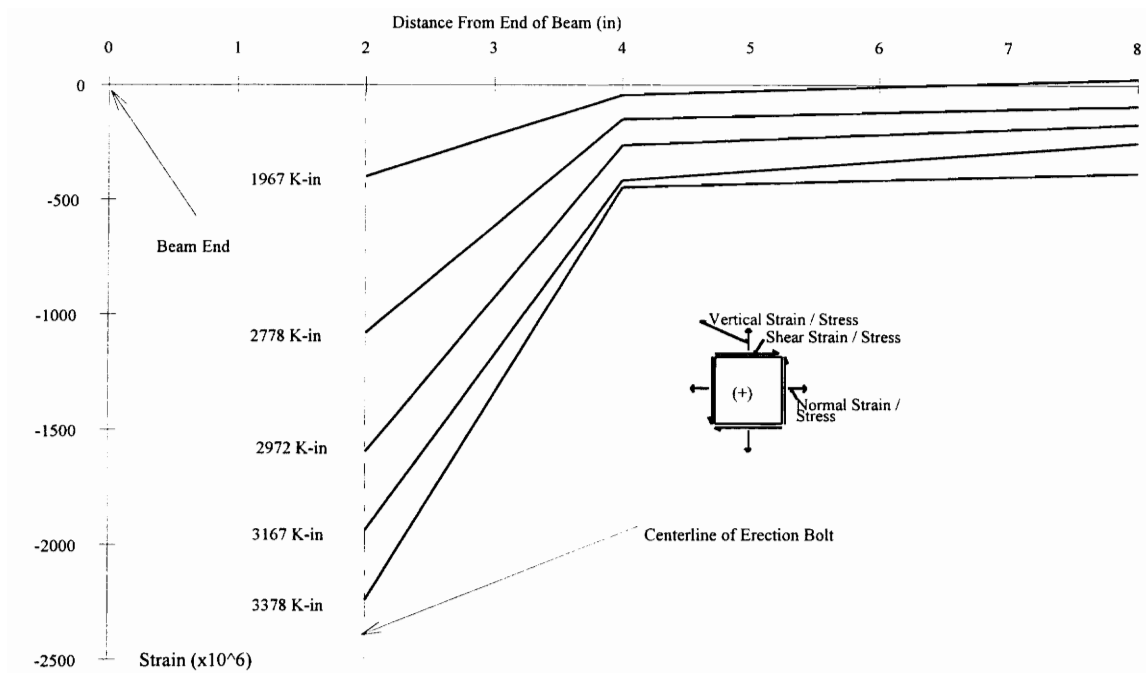
Figure 3.5-12 Vertical Strain Distribution At Toe of North Beam Web
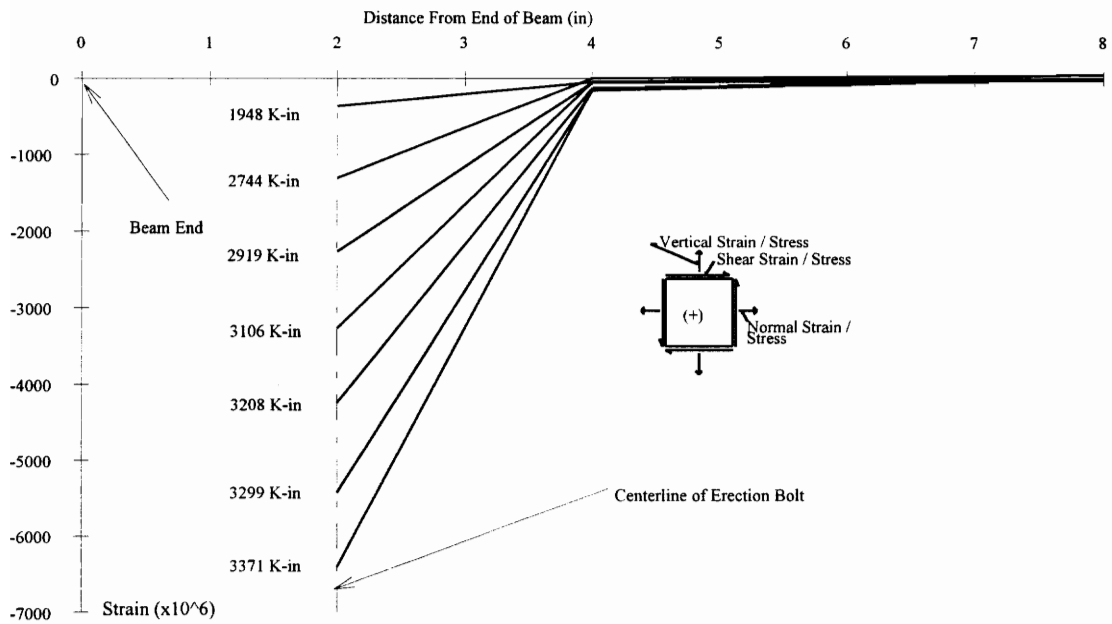
Figure 3.5-13 Vertical Strain Distribution At Toe of South Beam Web

183
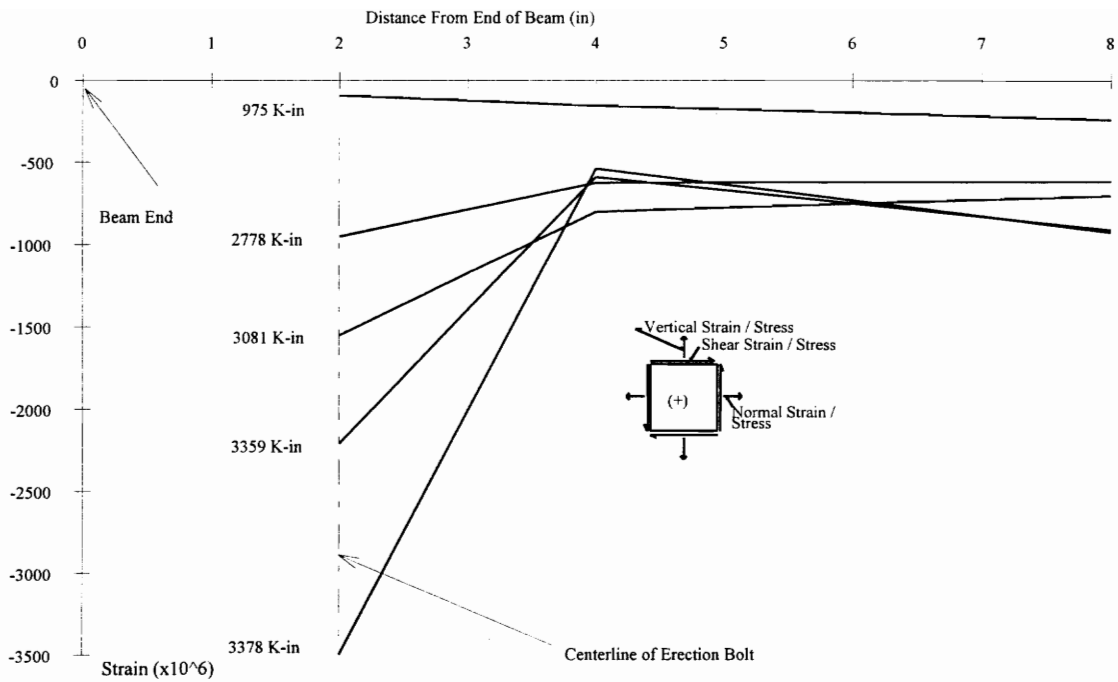
Figure 3.5-14 Normal Strain Distribution At Toe of North Beam Web
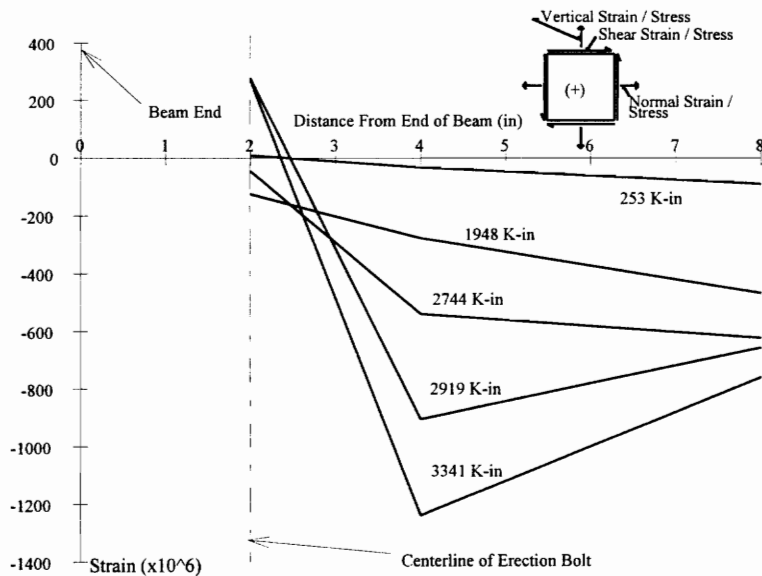
Figure 3.5-15 Normal Strain Distribution At Toe of South Beam Web

Although it would be premature to make any definitive conclusions from one test it does appear that there may be some relationship between the location of the erection bolt and the effective bearing length. This conclusion was also drawn from visual observations of

184

the hinging shape that was seen in the bottom flange and the seat angle. It is evident that this behavior led to the eventual failure mode of web crippling.

3.5.3 Composite Slab Behavior

The reinforcing bar forces along the three gage lines are presented in Figure 3.5-17 through Figure 3.5-19. The center gage line was directly over the centerline of the girder and the values represent the average value of two gages at that location. The south and north gage lines were located 12-in. on each side of the girder centerline. It should be noted that 20 out of 20 of the reinforcing bar gages functioned properly throughout the test.

Based on examination of the strain gage data, it was apparent that none of the reinforcing steel yielded (as previously discussed the yield force was 14 Kips). The specimen was designed so that the reinforcing steel would yield before the steel connection failed. Unfortunately, as a result of an error which occurred during fabrication a tension plate larger than designed was used. If the proper size tension plate had been used the connection should have behaved much differently. The ultimate moment would have been reduced but the ductility would have been increased significantly. Because the moment would have been reduced the value of the shear load being applied would have also been reduced and the web would most likely not have crippled.

The force distribution shown in Figure 3.5-17 through Figure 3.5-19 appears reasonable for low moments but at the higher moments the force contours seem to take on some strange patterns. Some of these patterns may have been caused by bending in the plane of the slab; but most likely, the patterns are a result of uneven cracking of the concrete in the region of the reinforcing bar gages.

185
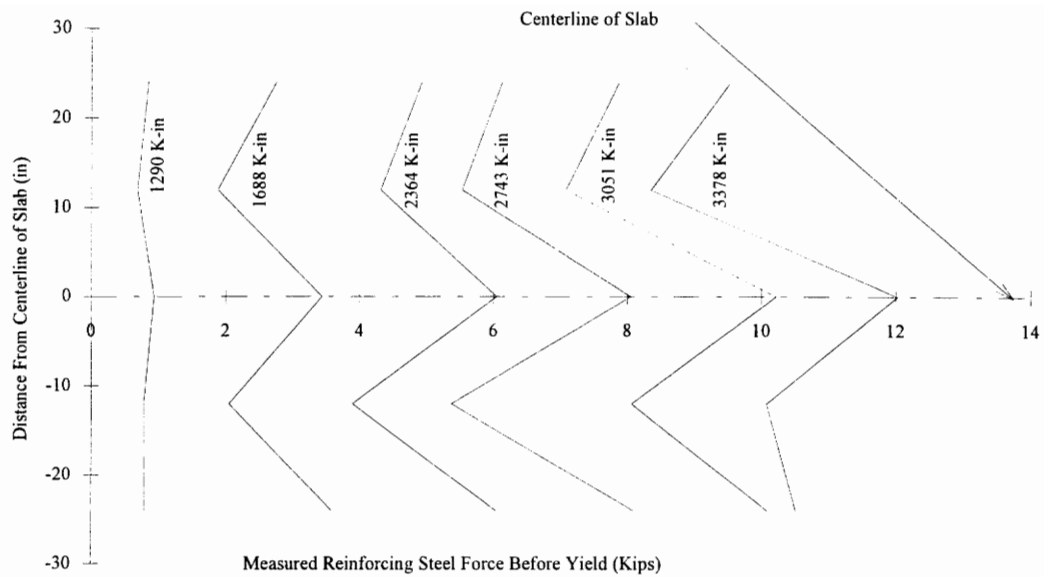
Figure 3.5-16 Reinforcing Steel Force Distribution Pattern Along South Gage Line
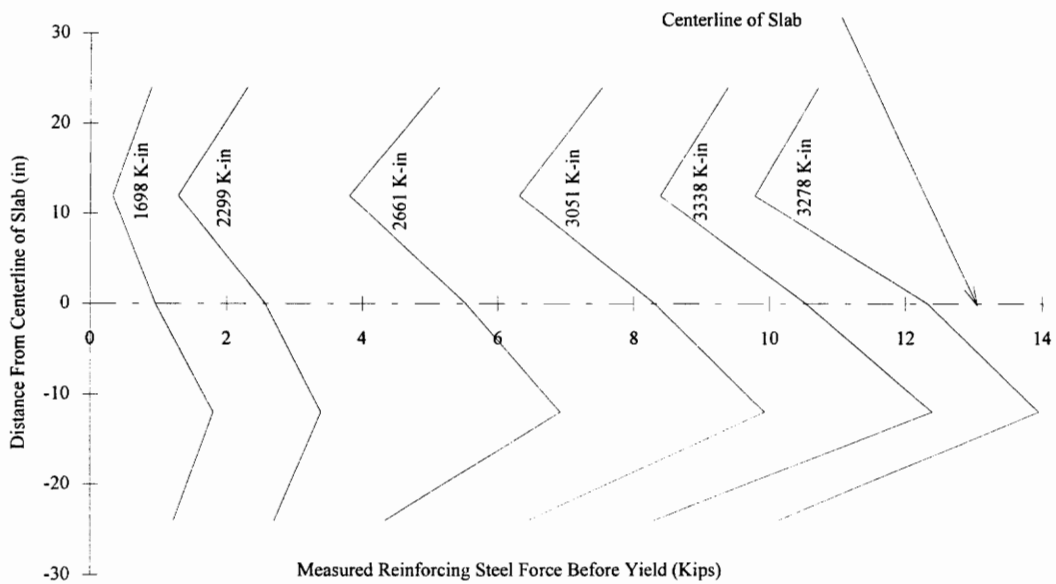
Figure 3.5-17 Reinforcing Steel Force Distribution Pattern Along Center Gage Line

186
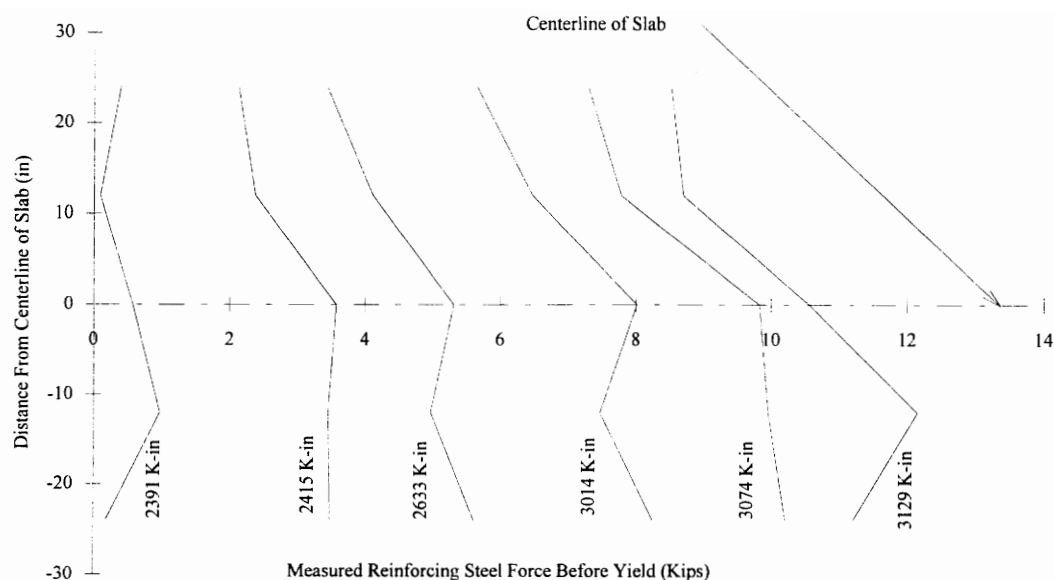
Figure 3.5-18 Reinforcing Steel Force Distribution Pattern Along North Gage Line

The force developed by the reinforcing steel versus the connection moment is plotted in Figure 3.5-19. As expected the reinforcing steel did not develop significant force until connection moments were increased beyond the dead load moment. The cracking pattern and order of crack propagation is very apparent in this figure. It appears that the south side of the specimen slab cracked sufficiently to shed most of the slab load to the reinforcing steel very early in the test while the north side did not crack sufficiently to shed load until around 2400 K-in. as indicated by the sharp jump in the reinforcing steel force. Despite the fact that no significant cracking was ever noticed over the centerline of the girder it is apparent from Figure 3.5-19 that cracking in this region was occurring slowly. This allowed the concrete to shed slab force a little at a time. This type of cracking would be ideal because it lends itself to very smooth moment-rotation behavior (i.e., no large jumps as when a sudden crack occurs).

187
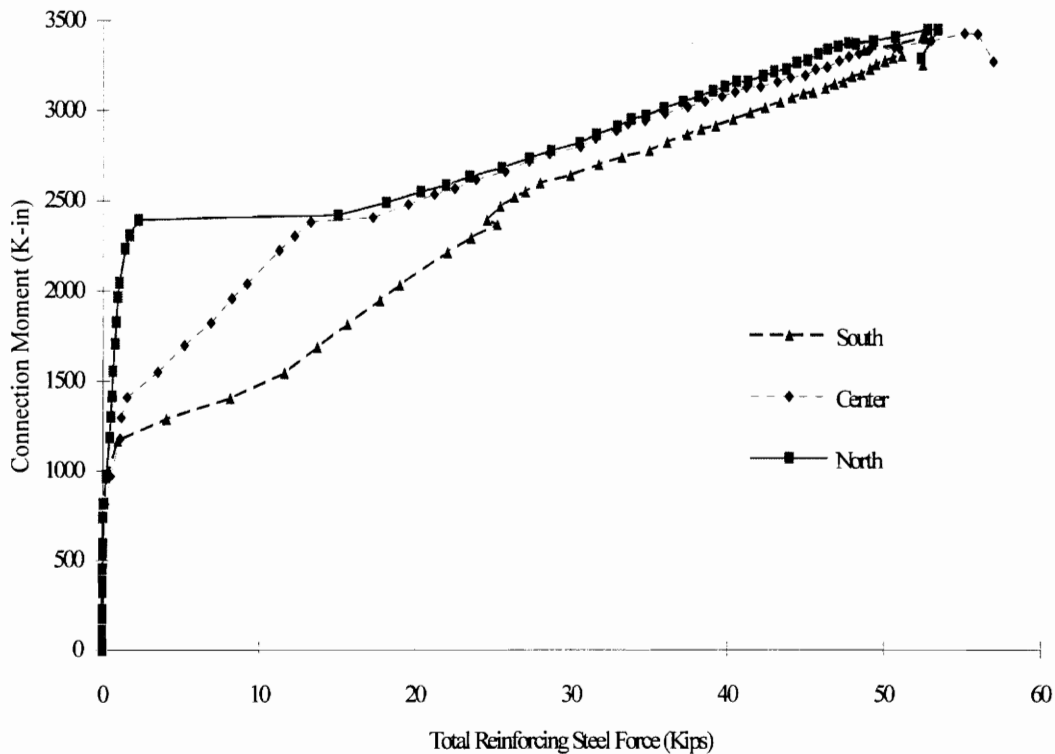
Figure 3.5-19 Reinforcing Steel Force Across Width of Slab

Before the concrete cracked the forces in the reinforcing steel appeared to be identical. After cracking began the forces in the reinforcing steel in the region of the south gage line were higher than those associated with the reinforcing steel in the region of the center and north gage lines. Even after all the concrete had cracked, the forces indicated along the south gage line were consistently higher than those along the north and center gage lines. This is most likely a result of incomplete cracking of the slab along the north and center gage lines which would also explain the strange force contours shown in Figure 3.5-18 and Figure 3.5-19.

The history of the composite slab slip is presented in Figure 3.5-20 and Figure 3.5-21. As seen in the figures, the slip measured on the south side was consistently higher than the slip measured on the north side until near failure of the specimen. This

pattern was very odd considering the north connection was rotating faster than the south connection. It is believed that the slab deformation needed for the north side to rotate must have been associated with the slip measured on the south side. Only after the slab cracked over the north side did the slip measured on the north side start to approach that on the south side.

The other strange observation, as seen in the initial region of Figure 3.5-21, is the lack of the pattern that had been typical for the first three connection tests. This makes some sense for the south side because slab cracking occurred almost immediately after the moment was increased above the dead load moment. However, this makes no sense for the north side because the slab on this side did not crack until reasonably high moment values had been attained.
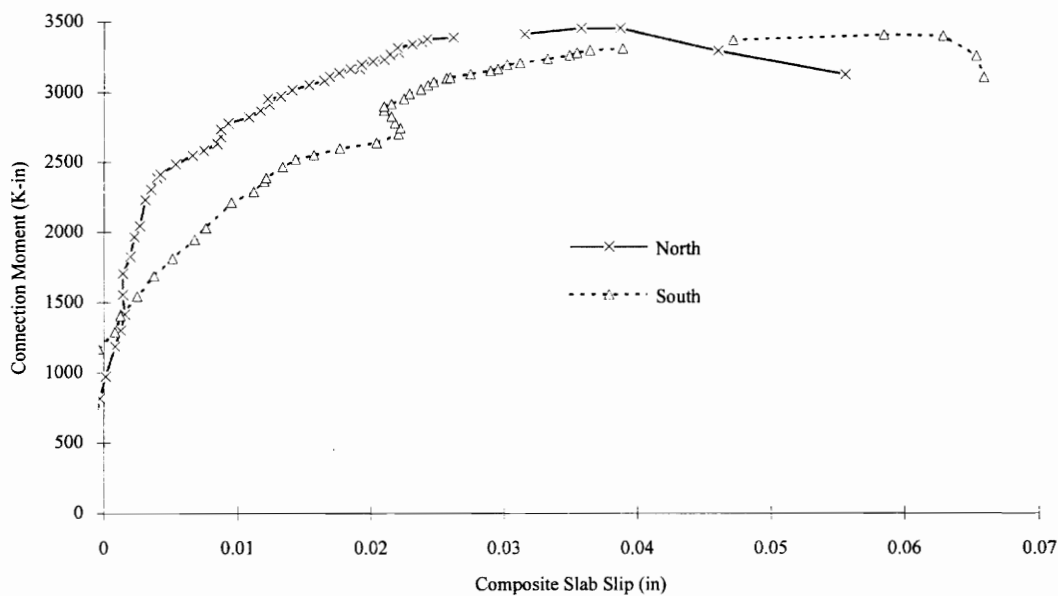
Figure 3.5-20 Composite Slab Slip Vs. Connection Moment

189
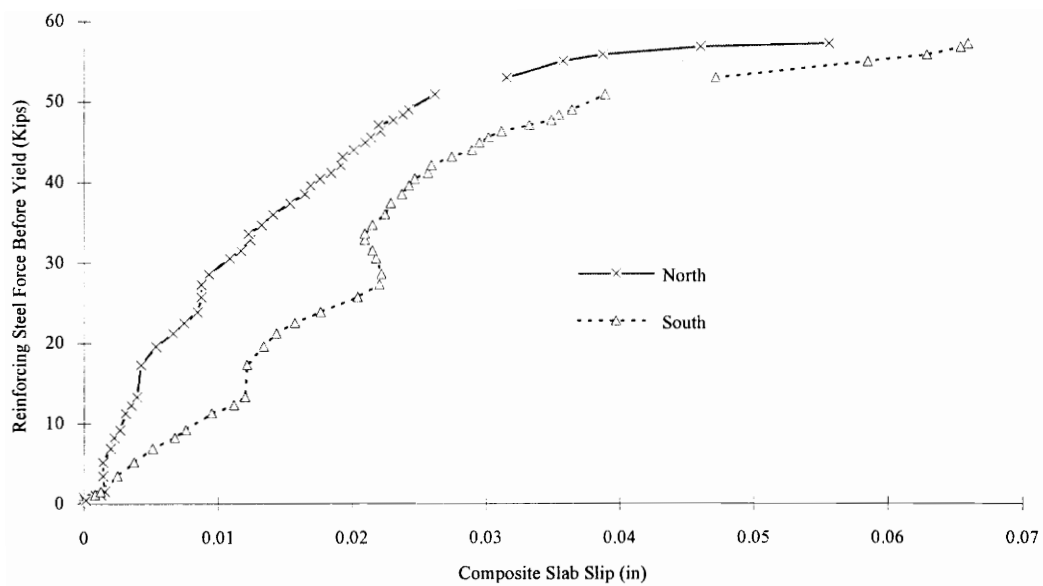
Figure 3.5-21 Composite Slab Slip Vs. Reinforcing Steel Force

CHAPTER 4.0
EVALUATION OF RESULTS

4.1 MODELING MOMENT-ROTATION BEHAVIOR

4.1.1 General

To properly account for the rotational stiffness of any connection the moment-rotation behavior for the connection must be understood. Because it would normally be prohibitively expensive to experimentally test each connection that could be designed, it is important that analytical models be constructed which accurately predict the moment-rotation behavior of connections. These models should allow the behavior to be predicted and incorporated into a design procedure based on the connection geometry and material properties. To develop such a model it is typically necessary to run parametric studies of the connection. This enables the investigator to determine the main attributes of the connection which have an effect on moment-rotation behavior. This type of study is normally too expensive to do experimentally so finite element analysis is often used. The finite element models are calibrated to available experimental data and are then used to carry out the parametric studies required. Because the eventual goal of this continuing research project is to develop a simplified analytical model it is obvious that finite element models will have to be constructed at some point in the program.

Although the finite element models and the development of simplified parametric equations are not directly within the scope of this thesis a simplified modeling scheme was developed to have some basis against which the experimental results could be compared. This modeling scheme was developed with the idea in mind that a finite element model will eventually be developed; and as such, many of the concepts used lend themselves to being incorporated into a finite element model. Models were developed to

191

predict the behavior of Connections #3 and #4 while a commercially available program was used to predict the moment-rotation behavior of Connections #1 and #2.

4.1.2 Moment-Rotation Models

The strength for Connections #1 and #2 was predicted by the methods described in Chapter 2. The full moment-rotation behavior for these connections was estimated using a preliminary version of "PRCONN" which is a commercially available program developed by Ralph M. Richard at the University of Arizona. This program was developed to generate connection curves for semi-rigid steel and composite beam-to-column connections. Because column panel zone deformations did not seem to be considered in the curve development it was believed that the estimates for the moment-rotation behavior developed by the program would be reasonable estimates for the beam-to-girder connections. At this time it is not fully understood how the program develops the behavior curves, particularly because many of the connections included in the program have never been tested. As shown Figure 4.1-1 and Figure 4.1-2 the moment-rotation behavior predictions given by "PRCONN" are reasonably close. The model does overestimate the stiffness of Connection #1 in the plastic region of the connection but this is most likely a result of the connection failing by buckling of the bottom flange instead of yielding of the reinforcing steel.

The moment-rotation behavior of Connections #3 and #4 were predicted with a modeling scheme developed by the writer. The connections were modeled by replacing the major elements of the connections with equivalent truss elements and attaching these truss elements to a vertical rigid bar as shown in Figure 4.1-3.
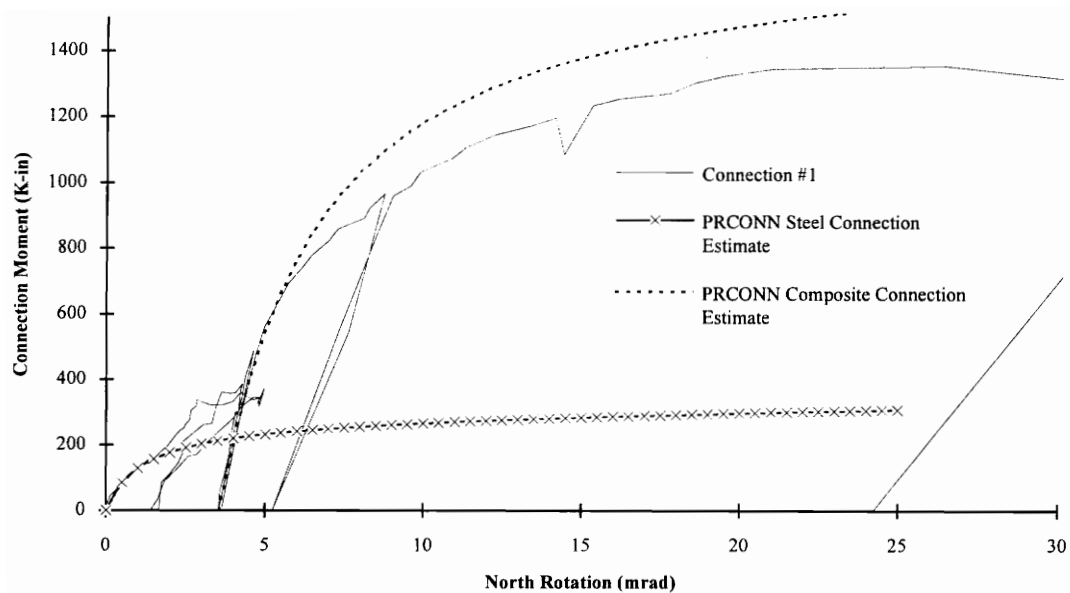
Figure 4.1-1 Behavior of Connection #1 Vs PRCONN Models
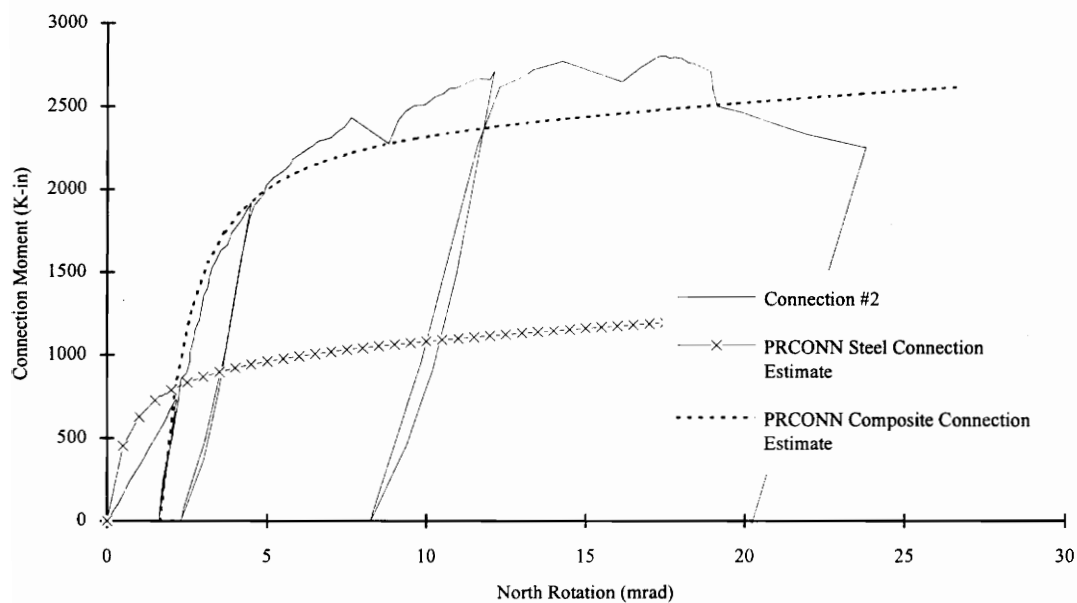
Figure 4.1-2 Behavior of Connection #2 Vs PRCONN Models

193
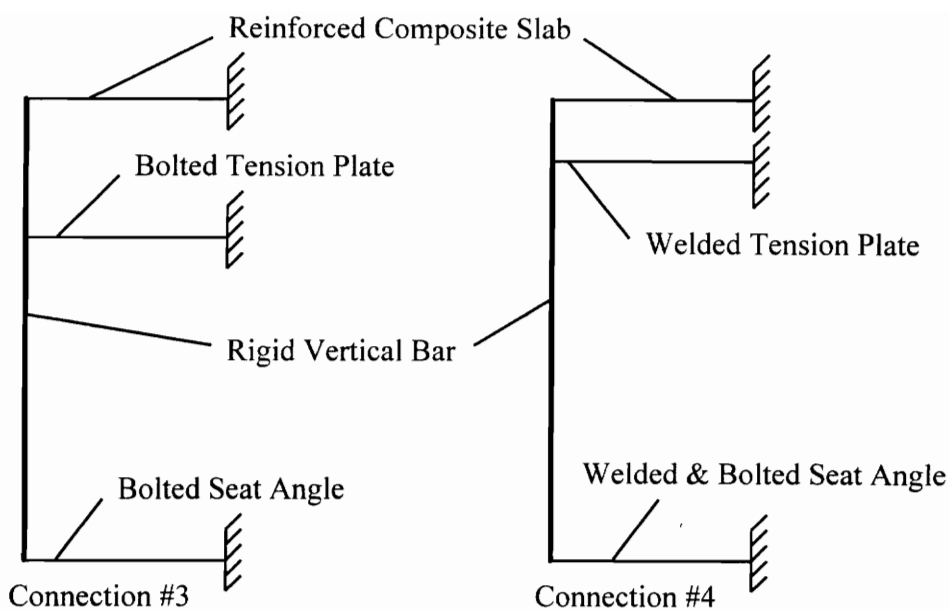
Figure 4.1-3 General Construction of Connection Stiffness Models

The constitutive response (i.e. the load-to-deformation response) for the truss elements were determined individually and then combined in the general model shown. The development of the truss elements is discussed in Section 4.1.4.

The moment-rotation behavior is developed by displacing the rigid bar through some rotation. The point on the bar about which rotation occurs is called the center of rotation and it is determined by balancing forces in the horizontal direction. As the bar rotates, it forces the connection elements to incur a horizontal deformation that depends on the element's distance from the center of rotation. The basic modeling process is summarized as follows:

1. A center of rotation is chosen.
2. The rigid bar is rotated some finite value about the center of rotation.
3. The horizontal deformation at each element is determined.
4. The force associated with the deformation of each element is determined from the previously determined constitutive responses.

5. Horizontal forces are summed.

6. A new center of rotation is chosen and steps 2 through 5 are repeated until the horizontal forces sum to zero

7. Once horizontal forces sum to zero the moment associated with the connection at the given rotation is determined by summing the individual element forces acting through the distance from the element to the center of rotation.

Because the process used to determine the various points of connection equilibrium is iterative it is ideal to be programmed into a spreadsheet that allows iterative calculations. The spreadsheet program Excel by Microsoft was used to assemble the model and determine the various points of equilibrium. The moment-rotation behavior predicted by the models is shown in Figure 4.1-4 through Figure 4.1-7 along with the moment-rotation behavior measured during the experimental testing of the connections. It should be noted that this modeling scheme assumes that the shear imposed on the connection has little or no effect on the moment-rotation behavior.
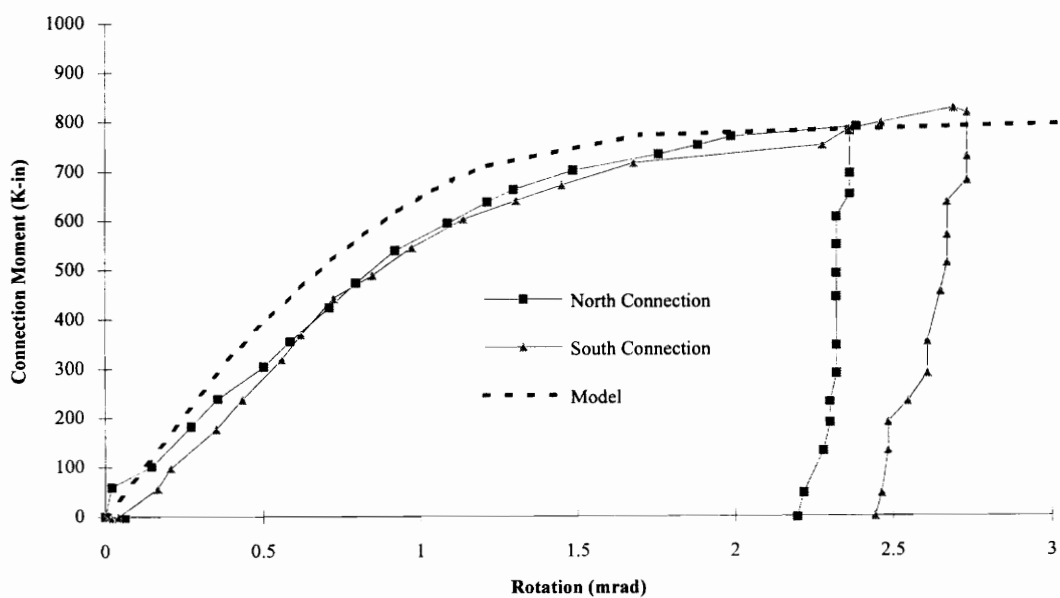
Figure 4.1-4 Model Vs Measured Behavior For Steel Connection #3

195
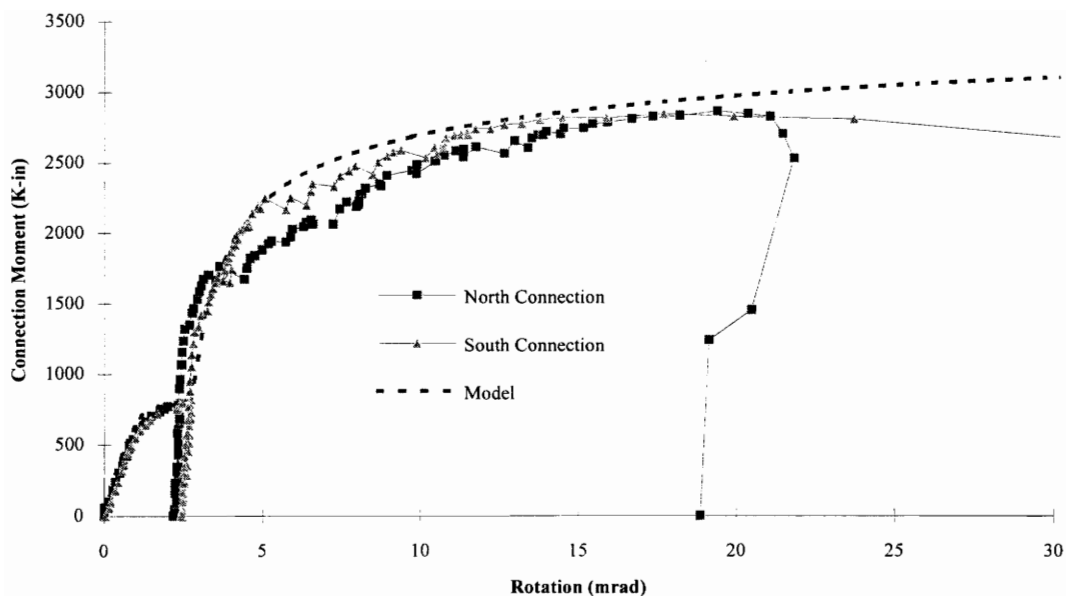
Figure 4.1-5 Model Vs Measured Behavior For Composite Connection #3
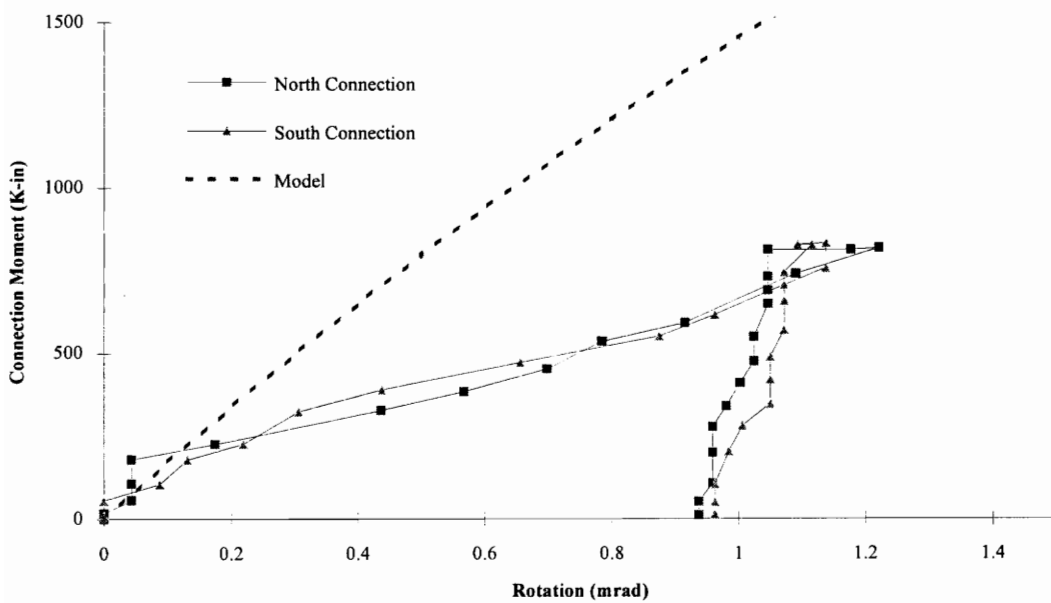
Figure 4.1-6 Model Vs Measured Behavior For Steel Connection #4
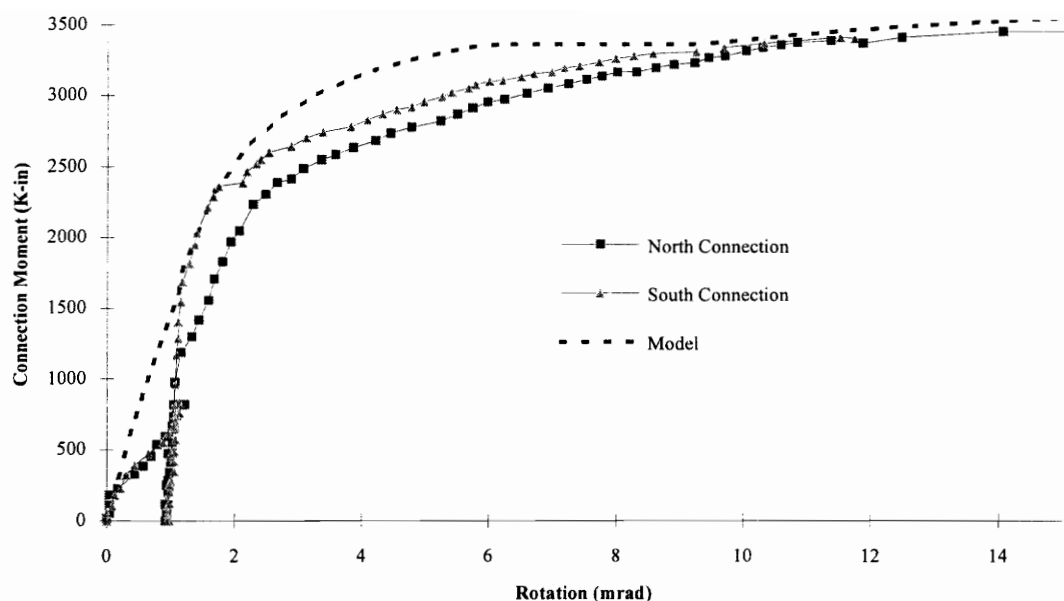
Figure 4.1-7 Model Vs Measured Behavior For Composite Connection #4

This modeling scheme predicted the behavior of Connection #3 very well; although, the model was slightly stiffer than the measured response. The increased stiffness was most likely a result of the bolted tension plate not being accurately modeled. The model of the bare steel connection of Connection #4 was much stiffer than the measured response. The model of the composite connection of Connection #4 was initially very close; but, the behavior of the model did not soften at the same moment levels when the actual connections started to soften. Once the model did soften, the response was again very similar to that measured. The models did not in either case predict the actual point of failure (which would not be expected for Connection #4 because it failed from local web crippling which is not accounted for in the model) or the failure mode. This is most evident in Figure 4.1-5 as the model and the actual connection behavior for Connection #3 diverge at the point where the tension plate failed. The reader will notice that this modeling scheme has the ability to impose initial stresses on the steel connection prior to the composite slab becoming effective as would occur in

197

typical unshored construction. This is shown by the two stages indicated in Figure 4.1-5 and Figure 4.1-7.

4.1.3 Sub Element Development

To develop the force-deformation relationships for the connection elements discussed in Section 4.1.4, the stress-strain and load-slip relationships for the components of each element had to be understood. The following sub-elements were needed to develop the force-deformation relationships for the connection elements.

1. Perforated Steel Plates
2. Fillet Welds
3. Shear Studs
4. Concrete Tension Stiffening
5. High Strength Bolts
6. Reinforcing Steel
7. Solid Steel Plates

Understanding the behavior of these elements is the key to being able to predict the overall connection behavior. If the behavior of any one of the sub elements is not accurately modeled then the overall connection behavior will certainly not be correctly predicted. Future work associated with connection modeling will include extensive literature reviews and possibly some elemental tests to better understand the behavior of these sub elements.

For purposes of the current model, a brief review of readily available information on the sub element behavior was conducted. The following is a brief summary of the relationships used to represent the behavior of the various elements.

4.1.3.1 Stress - Strain Model For Plate With Perforations

It has been shown that plates with perforations (holes) have a tensile stress-strain pattern different than plates without perforations. The basic difference is that the yield plateau normally seen in solid plate specimens is either very short or not present in plates with perforations. The yield plateau is essentially eliminated because of initial yielding at the section including the perforations. Because this yielding is limited to the region around the bolt holes the specimen does not undergo the typical large deformation seen in solid plate specimens. As the cross-sections of the plate without perforations start to yield the areas around the perforations start to strain harden. This strain hardening tends to diminish the new yield deformations. Fisher (1965) conducted a series of tests on plates with perforations and developed an analytical model to describe the stress-strain relation for these plates.

For $\varepsilon \leq \varepsilon_y$

$$\sigma = \varepsilon E \qquad P = \sigma A_g$$

For $\varepsilon_u \geq \varepsilon > \varepsilon_y$

$$\sigma = \varepsilon_y E + K\left(1 - e^{-\alpha \varepsilon^*}\right)^\beta \qquad P = \sigma A_n$$

Where:

$$\varepsilon^* = \varepsilon - \varepsilon_y$$

$$K = \sigma_u - \sigma_y$$

$$\alpha = \delta K \left(\frac{g}{g-d}\right) = K \frac{A_g}{A_n}$$

$\delta = 1$ sq. in. /Kip

σ_y = Plate Yield Stress (ksi)

σ_u = Plate Ultimate Stress (ksi)

ε_y = Strain at plate yield

ε_u = Strain at plate ultimate strai

g = Plate Width (in.)

d = Hole diameter (in.)

β = 1.5 constant to all materials and conditions

E = modulus of elasticity

P = axial force (Kips)

Values for yield stress and strain and ultimate stress, used for modeling the plate of Connection #3, were based on tensile coupon tests. Because the extensometer was not left on the specimen through the ultimate stress, the strain at ultimate stress was assumed to be a value typical for low carbon steels (approximately 0.2 as presented by Beer & Johnson (1981).

4.1.3.2 Weld Force-to-Deformation Response

Two weld force-to-deformation models were considered. One model from the 1986 LRFD Manual (*Manual of* 1986) and the other from the 1993 LRFD Specification (*Load and* 1993) Strength reduction factors were not included in these models because ideally the best model to use in this situation would be one that accurately predicts the true load-to-deformation response of welds (i.e., not a conservative or factored model).

1986 LRFD

$$R_i = R_{i,\,ult} \left[1 - \exp\left(-K_1\, \frac{\Delta_i}{\Delta_o} \right) \right]^{K2}$$

Where:

$$R_{i,\,ult} = \frac{10 + \theta}{10 + 0.582\,\theta} \left(0.791\, F_{exx}\, t_e \right)$$

200

$$K_1 = \mu \Delta_o = 8.274 \exp(0.0114\,\theta)$$

$$K_2 = \lambda = 0.4 \exp(0.0146\,\theta)$$

$$\Delta_i = \frac{r_i}{r_{max}}\, \Delta_{i,\,max}$$

$$\Delta_{i,\,max} = \Delta_o \left[\frac{\theta}{5} + 1 \right]^{-0.47}$$

$\Delta_o = 0.11$-in. $=$ maximum deformation for a weld with longitudinal axis parallel to load $(\theta = 0)$

$\theta =$ Angle of weld with respect to loading (degrees)

$t_e = 0.707\, D/16$

$D =$ Leg size of fillet weld (in 1/16-in. increments)

For: $\theta = 0$

$$\Delta_{i,\,max} = 0.11$$

$$R_i = 0.03495\, F_{exx}\, D \left[1 - \exp\left(-8.274\, \frac{\Delta_i}{0.11} \right) \right]^{0.4} \quad \text{(Kips/in.)}$$

For: $\theta = 90$

$$\Delta_{i,\,max} = 0.02757$$

$$R_i = 0.05603\, F_{exx}\, D \left[1 - \exp\left(-23.08\, \frac{\Delta_i}{0.11} \right) \right]^{1.488} \quad \text{(Kips/in.)}$$

1993 LRFD

$$R_{wi} = t_e\, F_{wi} = F_{wi}\, 0.707\, \frac{D}{16} = \frac{F_{wi}\, L_{wi}\, D}{22.63}$$

Where:

$$F_{wi} = 0.6\, F_{exx} \left(1 + 0.5\, \sin^{1.5}\theta \right) f(p)$$

$$f(p) = \left[p(1.9 - 0.9\, p) \right]^{0.3}$$

$$\rho = \Delta_i / \Delta_m$$

$$\Delta_i = \frac{r_i \, \Delta_u}{r_{crit}}$$

$$r_{crit} = r_i \text{ for element with min } \frac{\Delta_u}{r_i}$$

$$\Delta_m = 0.209 \, (\theta + 2)^{-0.32} \, D$$

$$\Delta_u = 1.087 \, (\theta + 6)^{-0.65} \, D \leq 0.17 \, D$$

θ = Angle of weld with respect to loading (degrees)

D = Leg size of fillet weld (in.)

For: $\theta = 0$

$$\Delta_u = 0.17 \, D$$

$$R_{wi} = 0.4242 \, F_{exx} \, D \left(5.97 \frac{\Delta}{D} \left(1.9 - 5.37 \frac{\Delta}{D} \right) \right)^{0.3} \text{ (Kips/in.)}$$

For: $\theta = 90$

$$\Delta_u = 0.0559 \, D$$

$$R_{wi} = 0.6363 \, F_{exx} \, D \left(20.34 \frac{\Delta}{D} \left(1.9 - 18.3 \frac{\Delta}{D} \right) \right)^{0.3} \text{ (Kips/in.)}$$

The total load developed by the weld is obtained by multiplying R_{wi} by the length of weld.

These two models result in the load-to-deformation behavior shown in Figure 4.1-8. Obviously the response modeled by these two analytical expressions is quite different. For purposes of the connection modeling done in this section the analytical expressions given by the 1986 LRFD Manual (*Manual of* 1986) were adopted. The research leading to these expressions has not been studied at this time but it is recommended that further consideration should given to this subject so that the apparently wide discrepancy between the expressions can be understood.
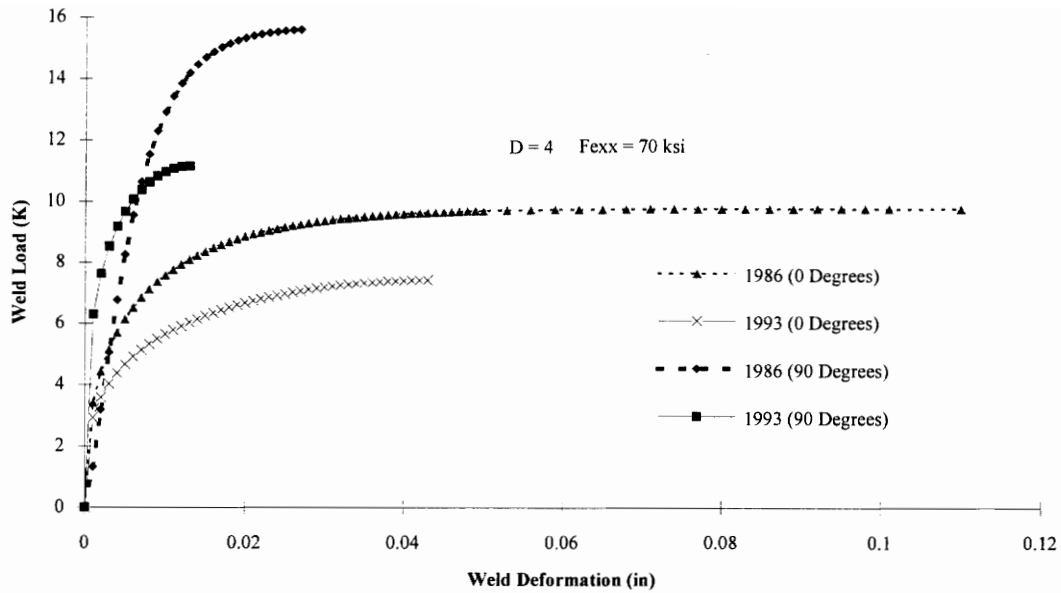
Figure 4.1-8 Weld Load-to-Deformation Response Comparison

4.1.3.3 Shear Stud Load-to-Deformation Response

To determine the amount of composite slab slip resulting from shear stud deformations a load slip relationship was needed. A number of analytical models were found but the relationship developed by Buttry (1965) was chosen based on its simplicity.

$$Q = Q_{sol}\left[\frac{80\,\delta}{1+80\,\delta}\right]$$

Where:

Q = Load on shear stud (Kips)

Q_{sol} = Ultimate load capacity of shear stud (Kips)

δ = deformation (in.)

The ultimate strength of the shear stud connectors was determined using the 1986 LRFD Specification (*Load and* 1986) with one modification. The strength reduction factor for single shear studs in steel decking was taken as a maximum of 0.75 (Easterling, et. al. 1993).

4.1.3.4 Concrete Tension Stiffening

Part of the force developed by the composite slab is attributed to tensile forces developed in the concrete. These are significant in the beginning stages of the connection moment-rotation response before the concrete cracks. In this region the force is linearly related to the strain in the slab through the concrete modulus of elasticity. After concrete cracks these forces tend to decline but they can still be significant and should not be neglected. The relationships used for these two regions of concrete behavior are given by Collins and Mitchell (1991) as follows:

For: $\varepsilon \leq \varepsilon_{cr}$

$$f_c = E_c \, \varepsilon$$

$$A_c = A_g$$

For: $\varepsilon > \varepsilon_{cr}$

$$f_c = \frac{\alpha_1 \alpha_2 f_{cr}}{1 + \sqrt{500 \, \varepsilon}}$$

$$A_c = A_e$$

Where:

E_c = Concrete modulus of elasticity

f_c = Concrete stress

ε = Concrete strain

$f_{cr} = 4\sqrt{f'_c}$

$$\varepsilon_{cr} = \frac{4\sqrt{f'_c}}{E_c}$$

α_1: Accounts for bond characteristics of reinforcement

    = 1.0 for deformed reinforcing bars

    = 0.7 for plain bars, wires, or bonded strands

    = 0.0 for unbonded reinforcement

α_2: Accounts for sustained or repeated loads

    = 1.0 for short-term monotonic loads

    = 0.7 for sustained and/or repeated loads

A_c = Area of concrete in tension (sq in.)

A_g = Gross area of concrete slab within effective width

A_e = Effective area of concrete taken as a block of concrete centered around each reinforcing bar with a height and width of 15 times the bar diameter or the portion of this value that is attainable

The strain in the concrete is assumed to be the same as the strain in the reinforcing steel on the average (i.e., no slip between the reinforcing steel and the concrete surrounding it). The concrete strength used in the model was the average strength of the concrete as determined by 28 day concrete cylinder tests.

4.1.3.5 High Strength Bolt Load-to-Deformation Response

The only general bolt load to deformation analytical model that was located was that given in the 1986 LRFD Manual (*Manual of* 1986) and 1993 LRFD Specification (*Load and* 1993). The general expression for this model was developed by Fisher (1965) while the constants were based on results of a test program conducted by Crawford and Kulak (1971) in which they tested six single bolt shear specimens placed in double shear. The bolts were all A325 3/4-in. diameter and the plates were of A36 steel. The bolts had

been tightened by the turn-of-the-nut method and the specimens were loaded in compression. The expression is given by:

$$R = R_{ult} \left(1 - e^{-\mu\Delta}\right)^{\lambda}$$

Where:

$\mu = 10$

$\lambda = 0.55$

$R_{ult} = 74 +/- 2.4$ Kips for 3/4-in. diameter A325 bolts in double shear

To better determine the load-to-deformation behavior of bolted plates in single shear, Richard et. al. (1980) conducted a series of 126 bolt tests. These tests consisted of single bolts being placed in single shear and under tension. The bolts were fully pretensioned after being brought into bearing so that there would not be any significant jumps in the load deformation response. Thirty different combinations of plate thickness, plate strengths, bolt diameters, and bolt strengths were studied. Linear regression was used to determine coefficients Kp, Ro, and n for a modified Richard equation to model the experimental results of the 30 cases. The equation is given as:

$$R = \frac{\Delta K_1}{\left[1 + \left(\frac{\Delta K_1}{R_o}\right)^n\right]^{\left(\frac{1}{n}\right)}} + \Delta K_p$$

Where:

Δ = Total bolt and plate deformation (in.)

$K_1 = K - Kp$

$K = 2E \dfrac{t_1 t_2}{t_1 + t_2}$ = initial stiffness of the response

206

t_1, t_2 = Plate thickness of the two attached plates

E = Modulus of elasticity for the attached plates

K_p = Plastic stiffness of the response

R_o = The Y-axis intercept of the plastic response

n = Curve fitting parameter

Because Richard's study seemed to better represent the type of bolting arrangements used in the connections studied by the writer, it seemed reasonable to try to use the results of Richard's work to develop a possible load-to-deformation response that could be used in the connection models developed in this section. To utilize his work, general relationships had to be determined that would allow the estimation of K_p, R_o, and n for combinations of plates and bolts not covered in Richard's study. To determine these relationships the results for the 30 different combinations were plotted along with the response prediction given by the relationship developed by Crawford and Kulak. The relationships for the latter were plotted for values of R_{ult} given by the limit states of plate bearing/tearout and bolt shear. These limit states were based on the 1993 LRFD Specification (*Load and* 1993) without strength reduction factors. A prediction curve was then plotted that used general relationships from Richard's results. These relationships were then modified until a reasonable agreement between the actual results and the prediction model was achieved. The general relationships used for the model are as follows:

n:

n = 0.6 for 3/4-in. and 7/8-in. diameter bolts

n = 0.5 for 1-in. diameter bolts

K_p:

$K_p = 0$

R_o:

For: $R_v <= 0.6 R_{bt}$

$R_o = 1/3 R_{bt} + 2/3 R_v$

For: $0.6 R_{bt} < R_v <= R_{bt}$

$R_o = 2/3 R_{bt} + 1/3 R_v$

For: $R_v > R_{bt}$

$R_o = 1/3 R_{bt} + 2/3 R_v$

Where:

R_v = Unfactored shear strength of the bolt

R_{bt} = The minimum bearing tearout strength of the two connected plates

Figure 4.1-9 presents the bolt load-to-deformation response for a 3/4-in. diameter bolt attaching two 1/2-in. thick plates. The behavior predicted by Crawford and Kulak's equation is indicated by "C&K" in the figure. As seen in the figure, the prediction curve slightly overestimates the response stiffness in the initial region and underestimates it in the latter plastic region. The reader may also notice that the prediction response given by Crawford and Kulak for the lower limit state of bolt shear appears to significantly underestimate the response as determined by Richard's test program. While, the response for the higher limit state of plate bearing/tearout severely overestimates the response. This may be an indication that the current bolt force-deformation model (Crawford and Kulak's model) used for ultimate strength analysis in the 1993 LRFD Specification (*Load and* 1993) may require some revisions in the future to more accurately model the behavior of bolted joints. It should be noted that for the 30 combinations that Richard tested, Crawford and Kulak's model did predict conservative (i.e., approximately the same or below) behavior in all cases except those that apparently failed by tearout and had a sharp reduction in load capacity in the plastic region of the response.
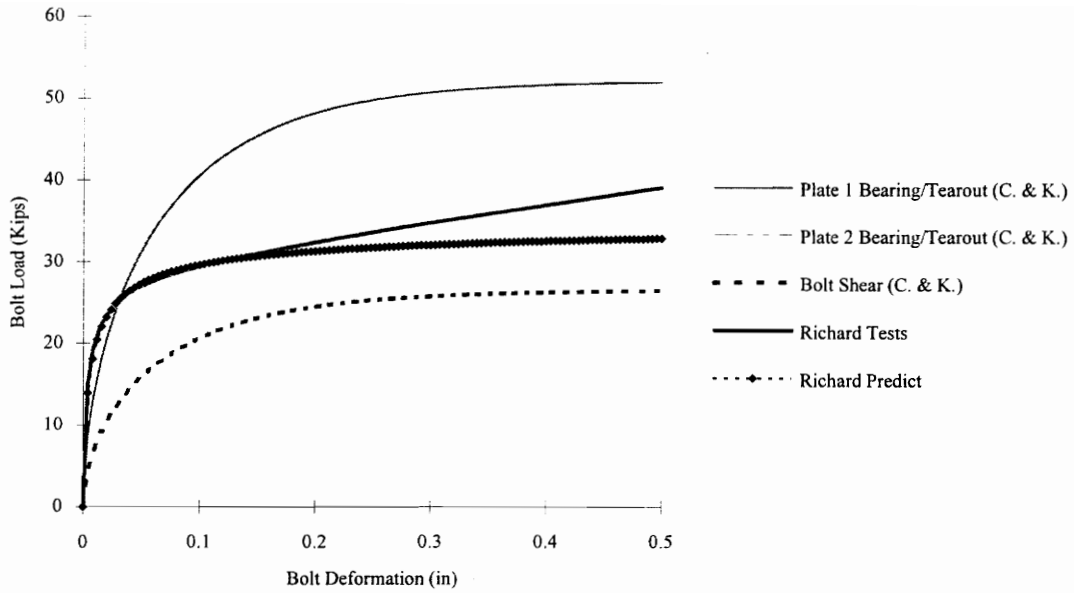
Figure 4.1-9 Bolt Load-to-Deformation Response

4.1.3.6 Stress-Strain Behavior of Reinforcing Steel

Tensile tests were conducted on four specimens of the reinforcing steel used in the connection tests. The stress-strain relationships were plotted for these tests and compared. The plots showed that the general stress-strain relationship was similar for all the reinforcing steel specimens. The stress-strain data points for one of the reinforcing steel specimens was then approximated with a mathematical model as shown in Figure 4.1-10. The mathematical model is composed of a straight line segment, a fourth order polynomial, and a failure region and is given as:

For: $\varepsilon \leq 0.002669674$

$\sigma = 26310329 \, \varepsilon$ (psi)

For: 0.002669674 < ε <= 0.0782

$$\sigma = A\varepsilon_*^4 + B\varepsilon_*^3 + C\varepsilon_*^2 + D\varepsilon_* + E \quad (psi)$$

Where:

A = 7162699877

B = -1070105066

C = 38961008

D = 715672

E = 70240

$\varepsilon_* = \varepsilon - 0.002669674$

For: ε > 0.0782

$$\sigma = 0 \quad (psi)$$
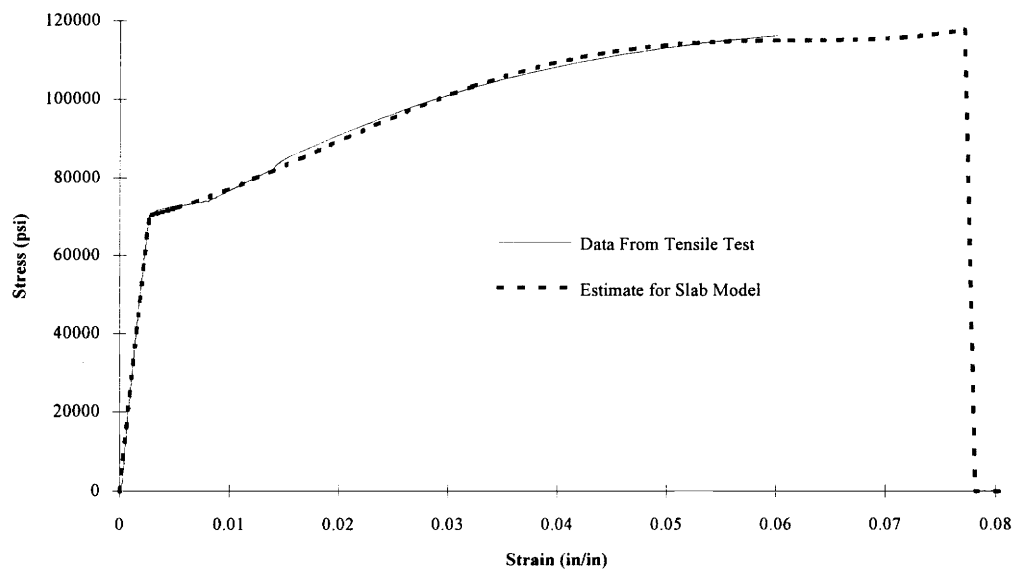
Figure 4.1-10 Reinforcing Steel Stress-Strain Behavior

The ultimate strain was not measured in the tensile tests but was assumed to be similar to the ultimate strain for grade 60 reinforcing steel which was around 0.08 as given by Wang and Salmon (1985).

4.1.3.7 Stress-Strain Behavior of Solid Steel Plates

Tensile tests were conducted on two specimens of the steel used to fabricate the tensile plates and two specimens of the steel used to fabricate the seat angles used in the connection tests. The stress-strain data points for one of each type of specimen were approximated with a mathematical model as shown in Figure 4.1-11 for the tension plate steel. The mathematical model is composed of two straight line segments, a fourth order polynomial, and a failure region. The ultimate strains are estimates as given by Beer & Johnston (1981) because the true strains at ultimate were not measured. The resulting mathematical models are given by:

TENSILE PLATE STEEL

For: $\varepsilon <= 0.0015$

$$\sigma = 32424667 \, \varepsilon \quad (\text{psi})$$

For: $0.0015 < \varepsilon <= 0.02234348$

$$\sigma = 48637 \quad (\text{psi})$$

For: $0.02234348 < \varepsilon <= 0.25$

$$\sigma = A\varepsilon_*^4 + B\varepsilon_*^3 + C\varepsilon_*^2 + D\varepsilon_* + E \quad (\text{psi})$$

Where:

$$A = -64319439$$
$$B = 31140523$$

$$C = -5757681$$
$$D = 529638$$
$$E = 48637$$
$$\varepsilon_* = \varepsilon - 0.02234348$$

For: $\varepsilon > 0.25$

$$\sigma = 0 \ (psi)$$

SEAT ANGLE STEEL

For: $\varepsilon <= 0.001061$

$$\sigma = 40110273 \ \varepsilon \ (psi)$$

For: $0.001061 < \varepsilon <= 0.019342$

$$\sigma = 42557 \ (psi)$$

For: $0.019342 < \varepsilon <= 0.25$

$$\sigma = A\varepsilon_*^4 + B\varepsilon_*^3 + C\varepsilon_*^2 + D\varepsilon_* + E \ (psi)$$

Where:

$$A = -65180668$$
$$B = 31914211$$
$$C = -5937632$$
$$D = 543275$$
$$E = 42557$$
$$\varepsilon_* = \varepsilon - 0.019342$$

For: $\varepsilon > 0.25$

$$\sigma = 0 \ (psi)$$
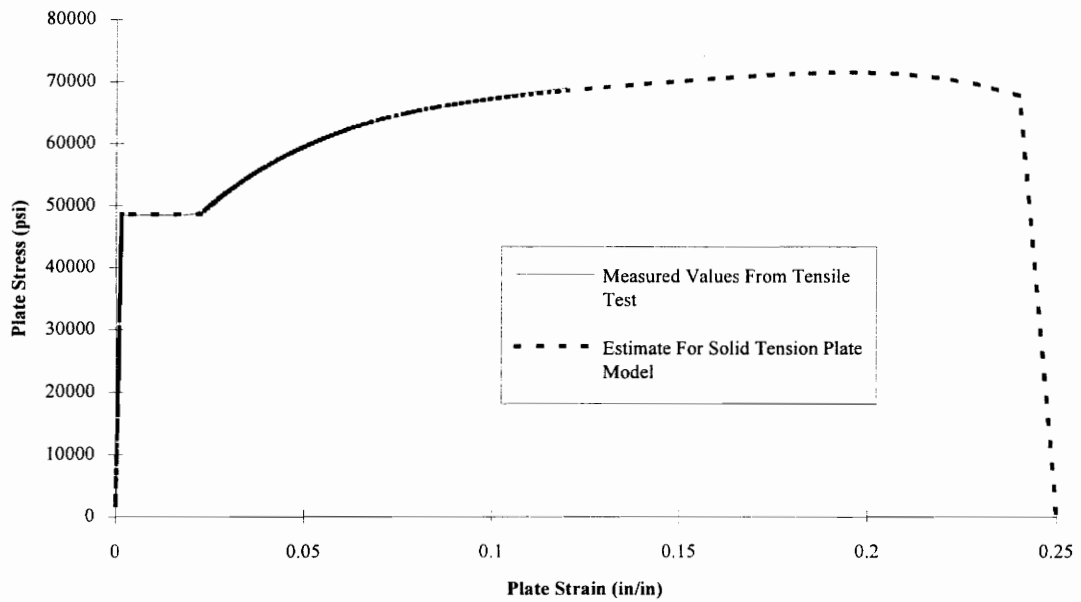
Figure 4.1-11 Solid Tension Plate Stress-Strain Behavior

4.1.4 Connection Truss Element Development

To develop models of Connections #3 and #4 a number of connection elements needed to be constructed:

1. Composite Slab
2. Bolted Seat Angle
3. Welded and Bolted Seat Angle
4. Bolted Tension Plate
5. Welded Tension Plate

The basic goal when developing each of the connection elements is to determine a force to deformation relationship that governs the response of the element.

213

4.1.4.1 Composite Slab Element

Each connection has a composite slab which consists of reinforcing steel, concrete, shear studs, and 2-in. steel deck. The force in the slab element is assumed to be developed through the reinforcing steel and concrete. It is assumed that because the steel decking is orientated perpendicular to the tensile forces that it has little or no effect.

There are two basic forms of deformation occurring in the composite slab: strain deformation and slip deformation. The total deformation is the sum of these two deformations. The strain deformation is assumed to occur over some finite length of the composite slab beginning at the girder centerline and extending to the approximate location of the first shear stud on the beam. Based on stress-strain relationships for the concrete and the reinforcing steel a force to deformation relationship can be developed for this finite length of concrete and reinforcing steel. The slip deformation is the slip associated with the shear studs. As a composite slab is loaded (i.e., as the concrete and reinforcing steel develop load) the force must be transferred to the steel beam through the shear studs. For a given force and a given number of shear studs a force to slip relationship can be developed. A complete force-deformation relationship can be developed for the composite slab by combining the force developed in the reinforcing steel and concrete and the deformations from strain and slip.

The process of combining the two deformations is iterative. A total deformation is imposed on the element. The slip deformation is assumed and then subtracted from the total deformation. The remaining deformation is the strain deformation. The strain deformation is used to determine the force developed in the steel and concrete. The force developed in the steel and concrete is used to determine the amount of slab slip. This process is repeated until values for the slab force, strain deformation, and slip deformation all converge. The iterative calculations are easily handled using any spreadsheet program.

214

A large number of points were generated for the force-deformation relationship using the iterative procedure just described. Once the points were generated a mathematical model was fit to the force-deformation curve so that it could be easily incorporated into the full connection model. The general shape of the force-deformation curve indicated that a modified Richard equation (Richard, et. al. 1980) would work nicely to model the curve. Table 4.1-1 presents the coefficients for the Richard equation and Figure 4.1-12 shows the curve developed through the iterative procedure and the associated Richard equation approximation used for the slab of Connection #4. The response for the slab of Connection #3 is very similar since the only difference between the two slabs was the concrete strength.
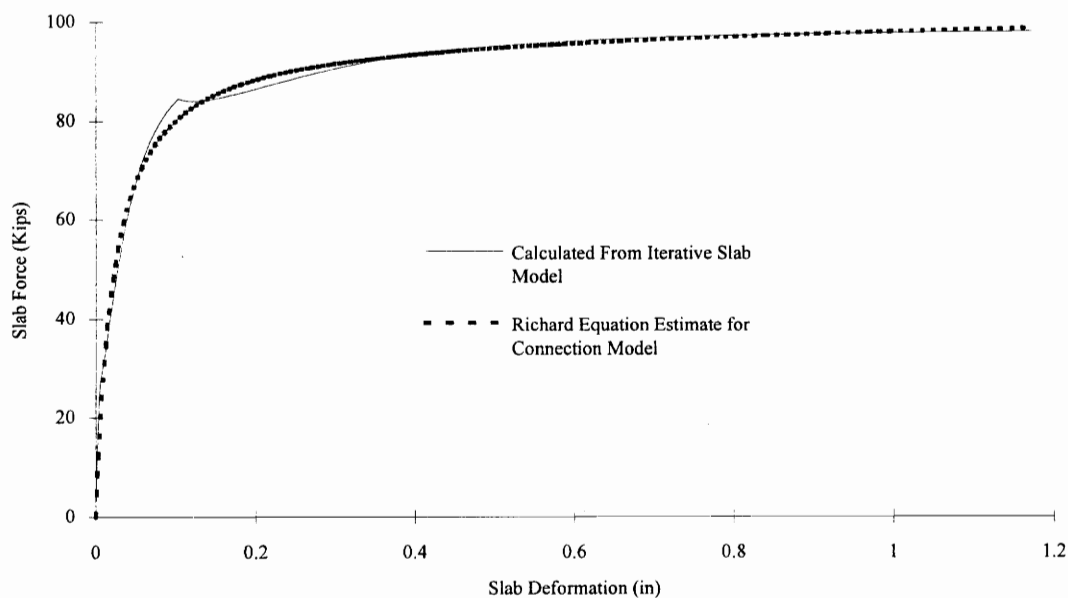
Figure 4.1-12 Composite Slab Force-Deformation Relationship For Con #4

Table 4.1-1 Richard Equation Parameters For Slab Force-Deformation

	Connection #3	Connection #4
K	4504.5	4288.9
Kp	2.11	2.54
n	1	1.01
Ro	97.87	97.5

4.1.4.2 Bolted Seat Angle

The bolted seat angle in Connection #3 consisted of a finite length of steel angle and the bolts that attached the bottom of the beam to the steel angle. The restraining force developed by the seat angle is assumed to be developed by the steel angle alone.

The total deformation for the seat angle is again composed of two parts: strain deformation and slip deformation. The strain deformation is associated with a finite length of steel angle that begins at the face of the girder and ends at the center of the bolt pattern which attaches it to the bottom beam flange. Based on stress-strain relationships for a solid steel plate a force-to-strain deformation relationship can be developed. The steel angle is treated as if it were solid even though there are holes for the bolts. This assumption is based on the idea that because the bolts fill the holes and the angle is in compression, there is not a truly reduced section at the bolt holes. The slip deformation occurs at the interface of the bottom beam flange and the steel angle. The force-to-slip deformation relationship is developed based on force-to-slip relationships for high strength bolts. An overall force-deformation relationship for the bolted seat angle was developed by combining the force in steel angle and the two components of deformation in an iterative process similar to that used to develop the composite slab behavior.

A large number of points were generated using the iterative model and a mathematical relationship was developed. The shape of the curve indicated that a combination of a modified Richard equation (Richard, et. al. 1980), a yield plateau, a

fourth order polynomial, and a failure region would sufficiently model the behavior as shown in Figure 4.1-13. The mathematical relationship is given as:

For: $\Delta <= 0.05$ in.

$$P = \frac{\Delta K_1}{\left[1+\left(\frac{\Delta K_1}{Ro}\right)^n\right]^{\left(\frac{1}{n}\right)}} + \Delta Kp \quad \text{(Kips)}$$

Where:

$$K = 22062$$
$$K_p = 192.40$$
$$n = 1.09$$
$$R_o = 179.61$$
$$K_1 = K - K_p$$

For: $0.05 < \Delta <= 0.144$ in.

$$P = 170.23 \quad \text{(Kips)}$$

For: $0.144 < \Delta <= 2.5$ in.

$$P = A\Delta_*^4 + B\Delta_*^3 + C\Delta_*^2 + D\Delta_* + E \quad \text{(Kips)}$$

Where:

$$A = -38.93$$
$$B = 166.30$$
$$C = -250.80$$
$$D = 163.56$$
$$E = 170.23$$
$$\Delta_* = \Delta - 0.144$$

For: $\Delta > 2.5$ in.

P = 0 (Kips)
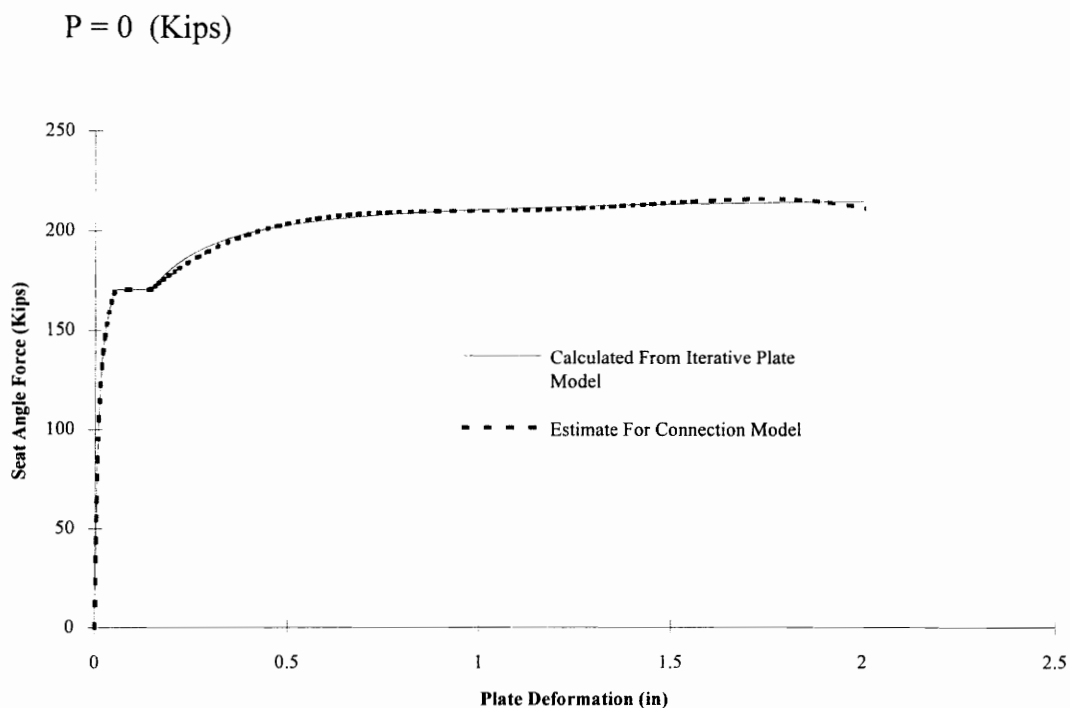
Figure 4.1-13 Bolted Seat Angle Force-Deformation Relationship For Con #3

4.1.4.3 Welded and Bolted Seat Angle

The seat angle in Connection #4 was welded and bolted to the bottom beam flange. This element consists of a finite length of steel angle and fillet welds with their longitudinal axis at zero degrees to the direction of loading. Since the bolts were not fully pre-tensioned, they were not considered to contribute to the load carrying capacity. Consequently, th bolts were not included in the model of this element.

The total deformation of this seat angle consists of strain deformation associated with the steel angle and welds. The strain deformation of the seat angle is over a finite length of steel angle that begins at the face of the girder and ends at the center of the weld

218

pattern which attaches it to the bottom beam flange. Based on stress-strain relationships for solid steel plates a force to strain deformation relationship can be developed. The weld strain deformation occurs at the interface of the bottom beam flange and the steel angle. Based on force-deformation relationships for fillet welds, a force deformation relationship was developed. To determine an overall force-deformation relationship for the welded and bolted seat angle, the force developed by the steel angle and the stain deformations were combined in an iterative process similar to that used to develop the composite slab behavior.

A large number of points were generated using the iterative model and a mathematical relationship was developed to model the resulting response. The shape of the behavior curve indicated that a combination of a Richard equation (Richard, et. al. 1980), a yield plateau, a fourth order polynomial, and a failure region would sufficiently model the element behavior as shown in Figure 4.1-14. The total deformation before failure is much shorter for this seat angle than for the bolted seat angle because of the increased stiffness provided by the weld and finally failure of the weld. The mathematical model is given by:

For: $\Delta <= 0.014$ in.

$$P = \frac{\Delta K_1}{\left[1+\left(\dfrac{\Delta K_1}{Ro}\right)^{n}\right]^{\left(\frac{1}{n}\right)}} + \Delta Kp \quad (Kips)$$

Where:

$K = 41131$

$K_p = -905.62$

$n = 0.76$

$R_o = 366.88$

$K_1 = K - K_p$

219

For: $0.014 < \Delta <= 0.096$ in.

    $P = 170.23$ (Kips)

For: $0.096 < \Delta <= 0.375$ in.

    $P = A\Delta_*^4 + B\Delta_*^3 + C\Delta_*^2 + D\Delta_* + E$ (Kips)

    Where:

        $A = -1110.78$

        $B = 575.25$

        $C = -930.10$

        $D = 432.85$

        $E = 170.23$

        $\Delta_* = \Delta - 0.096$
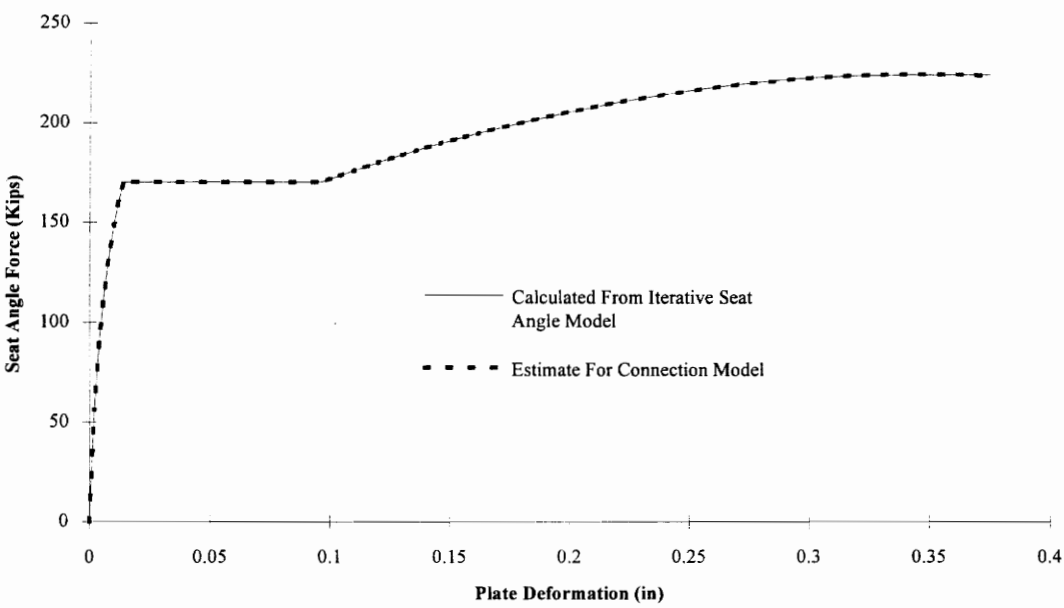
Figure 4.1-14 Welded & Bolted Seat Angle Force-Deformation Con #4

For: $\Delta > 0.375$ in.

$P = 0$ (Kips)

4.1.4.4 Bolted Tension Plate

A four-in. wide by 3/8-in. thick plate was used as the top portion of the steel connection in Connection #3. This plate was bolted to the web of the beam and welded to the web of the girder. The element model consisted of a steel plate and high strength bolts. The force was assumed to be developed in the steel plate alone and the deformations associated with the weld to the girder were ignored.

The total deformation of the tension plate consists of two parts: strain deformation associated with the steel plate and slip deformation associated with the high strength bolts. The strain deformation is over a finite length of steel plate that begins at the face of the girder and ends at the center of the bolt pattern which attaches it to the web of the beam. Based on stress-strain relationships for perforated plates in tension, a force to strain deformation relationship was developed. The slip deformation occurs at the interface of the plate and the beam web. Based on a force-deformation relationship for high strength bolts a force-to-slip relationship was developed. To determine an overall force-deformation relationship for the bolted tension plate the force developed by the steel plate and the two components of deformation are combined in an iterative process similar to that used to develop the composite slab behavior.

A large number of points were generated on the force-deformation curve using the iterative model and a mathematical relationship was developed to model the behavior. The shape of the behavior curve indicated that a combination of two polynomials and a failure region would sufficiently model the element behavior as shown in Figure 4.1-15. The mathematical model is given by:

For: $\Delta <= 0.02$ in.

221

$$P = A\Delta^2 + B\Delta \quad (\text{Kips})$$

Where:

$$A = -142182$$

$$B = 5415.65$$
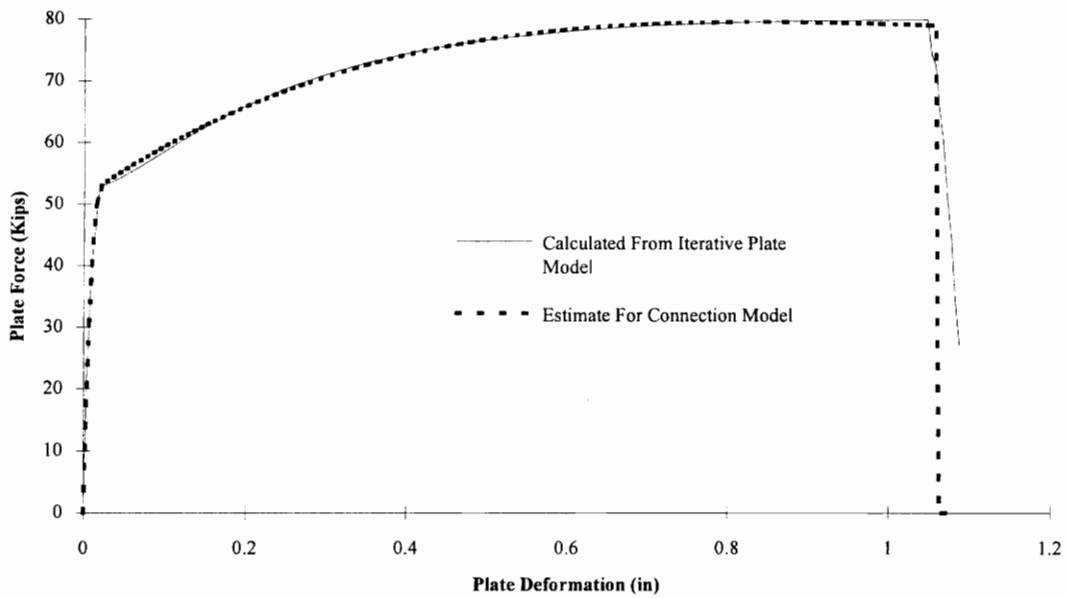
Figure 4.1-15 Bolted Tension Plate Force-Deformation Relationship

For: $0.02 < \Delta <= 1.06$ in.

$$P = A\Delta_*^4 + B\Delta_*^3 + C\Delta_*^2 + D\Delta_* + E \quad (\text{Kips})$$

Where:

$$A = -5.34$$

$$B = 41.91$$

$$C = -97.21$$

$$D = 86.70$$

$$E = 53.05$$

$\Delta_* = \Delta - 0.02$

For: $\Delta > 1.06$ in.

$P = 0$ (Kips)

4.1.4.5 Welded Tension Plate

A five-in. wide by 3/8-in. thick plate was used as the top portion of the steel connection in Connection #4. This plate was welded to the top flange of the both beams and passed across the top of the girder. Consequently, the model element consists of a solid steel plate and fillet welds. The force was assumed to be developed in the steel plate alone.

The total deformation of the tension plate consists of two parts: strain deformation associated with the steel plate and strain deformation associated with the welds. The first strain deformation is over a finite length of steel plate that begins at the centerline of the girder and ends at the end of the plate which is attached to the top beam flange with fillet welds all around the plate. Based on a stress-strain relationship for a solid steel plate a force to strain deformation relationship was developed. The weld strain deformation occurs at the interface of the plate and the beam flange. Based on a force-deformation relationship for fillet welds a force-to-deformation relationship was developed for the welds used. To determine an overall force-deformation relationship for the welded tension plate the force developed by the steel plate and the two components of deformation are combined in an iterative process similar to that used to develop the composite slab behavior.

A large number of points were generated using the iterative model and a mathematical relationship was developed to model the behavior. The shape of the behavior curve indicated that a combination of a polynomials, a constant force region,

and a failure region would sufficiently model the element behavior as shown in Figure 4.1-16. The mathematical model is given by:

For: $\Delta <= 0.018$ in.

$P = A\Delta^2 + B\Delta$ (Kips)

Where:

$A = -50467$

$B = 6016$

For: $0.018 < \Delta <= 0.224$ in.

$P = 91.19$ (Kips)

For: $0.224 < \Delta <= 2.5$ in.

$P = A\Delta_*^4 + B\Delta_*^3 + C\Delta_*^2 + D\Delta_* + E$ (Kips)

Where:

$A = -11.71$

$B = 56.80$

$C = -105.80$

$D = 98.17$

$E = 91.19$

$\Delta_* = \Delta - 0.224$

For: $\Delta > 2.5$ in.

$P = 0$ (Kips)
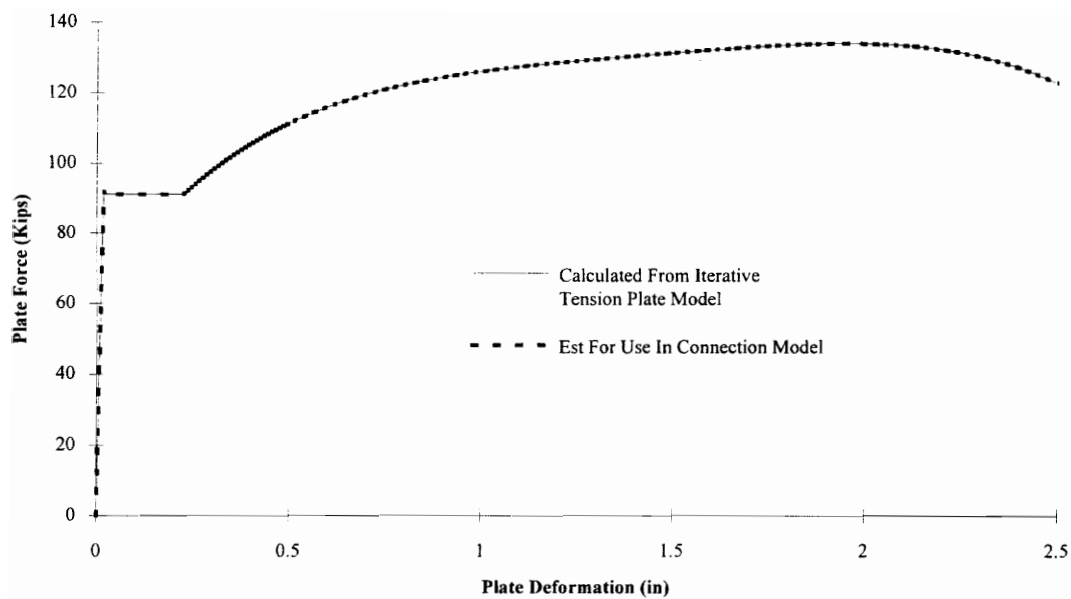
Figure 4.1-16 Welded Tension Plate Force-Deformation Relationship

4.2 EVALUATION OF CONNECTION BEHAVIOR RESULTS

To evaluate the possible influence semi-rigid steel and composite beam-to-girder connections might have on composite filler beam behavior, a brief analytical study was conducted. The study compares the response of a composite beam which is attached with connections of varying degrees of rigidity. The hypothetical beam design used to initially proportion the test connections was used as the basis for design in order to be consistent with what had been done so far and to allow the use of the experimentally determined moment-rotation curves. The following connection behaviors were included in the study:

1. Perfectly pinned
2. Connection #1
3. Connection #2
4. Connection #3
5. Connection #4
6. Perfectly rigid (with reinforcing of Connection #1)
7. Perfectly rigid (with reinforcing of Connection #2)

The pin and rigid cases are included as a basis for comparison of the beam response. Two rigid cases are included so that the two reinforcing ratios used in the connection specimens could be evaluated.

4.2.1 Details of The Specimens

The composite beam used in the study was a W18 x 40 A572 Gr 50 steel beam with a five-in. concrete slab on two-in. deep steel deck. Full shear connection was assumed. The beam was 40-ft. long and spaced at 15-ft. center to center. The reinforcing steel was Gr 60 and the concrete was assumed to have a 28-day strength of 4 ksi. The

cover to the center of the reinforcing steel was 3/4-in. The dead load was 54 psf based on the beam, concrete, and steel decking weight. The construction live load was taken as 20 psf and the service live load was 100 psf unreduced.

The moment capacity and flexural properties for the composite beams in both negative and positive flexure were determined using the 1986 LRFD Specification (*Load and* 1986) and are given in Table 4.2-1. The amount of reinforcing steel used was the same as that used in the test connections. No reinforcing was used in the simply supported case because this would provide no benefit for a beam without negative bending regions. The effective width in the positive region was assumed to be that predicted by the 1986 LRFD Specification (*Load and* 1986) and the effective width in the negative region is not important since the concrete is assumed cracked.

Table 4.2-1 Strength & Flexural Properties of Composite Beams

Connection	Area of Reinforcing Steel (sq in)	Itr (+) (in^4)	Itr (-) (in^4)	Mpc (+) (Kip-in)	Mpc (-) (Kip-in)
Simple	0	1935	612	6633	3347
Connection #1	2.4	1935	960	6633	4683
Connection #2	1	1935	773	6633	3972
Connection #3	1	1935	773	6633	3972
Connection #4	1	1935	773	6633	3972
Fixed #1	2.4	1935	960	6633	4683
Fixed #2	1	1935	773	6633	3972

The behavior of the test connections had to be mathematically represented so they could be incorporated into an analysis procedure. One possible method of accomplishing this is to represent the connection behavior as a series of straight line segments: two lines (bi-linear), three lines (tri-linear) or multiple lines (multi-linear). Another is to represent the connection with a more complex function that more closely follows the constantly changing behavior associated with semi-rigid connections. One mathematical curve used

to represent connection behavior is a modified Richard equation (Richard, et. al. 1980), given by:

$$R = \frac{\Phi K_1}{\left[1 + \left(\frac{\Phi K_1}{R_o}\right)^n\right]^{\left(\frac{1}{n}\right)}} + \Phi K_p$$

Where:

Φ = Connection rotation

$K_1 = K - K_p$

K = Initial stiffness of the response

K_p = Plastic stiffness of the response

R_o = The Y-axis intercept of the plastic response

n = Curve fitting parameter

Because of the physical meaning associated with each of the constants (except for the curve fitting constant) the Richard equation was used to represent connection behavior of the four test specimens. The actual and approximated connection curves are presented Figure 4.2-1 and Figure 4.2-2. The values of the constants for the modified Richard equation are given Table 4.2-2. Since only the initial response of the steel connections was determined it was assumed that their connection curves (except for Connection #4) became plastic soon after the last tested point. The steel curve for Connection #4 was chosen based on the stiffness model developed in Section 4.1. This was done because assuming that this connection would have a horizontal response just after the last test point would have probably been overly conservative.

The beams were loaded in the typical unshored composite construction sequence. Dead load was applied to the steel section up to the service values to determine construction load deflections. Factored construction loads were then applied to the plain

steel section to determine the factored construction moments induced into the beam. In these load cases the connection model used was that of the steel connection only.

Table 4.2-2 Richard Equation Parameters For Tested Connections

Connection		Connection #	Connection #	Connection #	Connection #4
Steel	K	110	340	600	900
	Kp	10	10	10	10
	n	20	20	4	4
	Ro	310	720	780	1500
	K1	100	330	590	890
Composite	K	1598.15	2663.64	4000	186000
	Kp	-22.8	-104.36	-35	-90
	n	0.42	0.51	0.55	0.22
	Ro	4090.42	8756.59	5000	17000
	K1	1620.95	2768	4035	186090
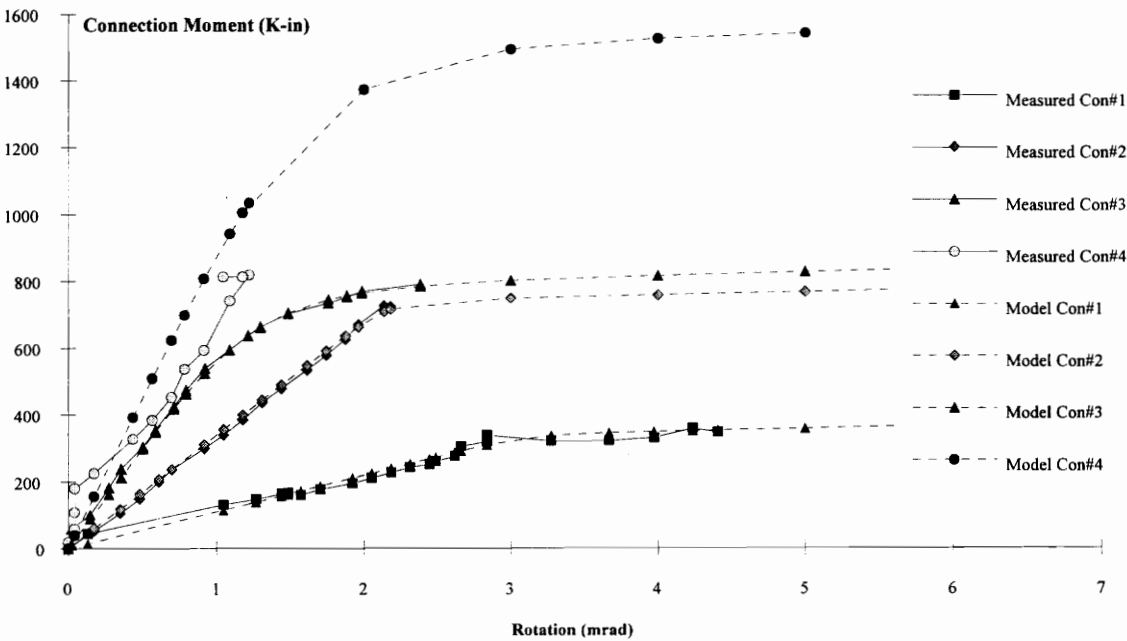
Figure 4.2-1 Steel Semi-Rigid Connection Curves

229
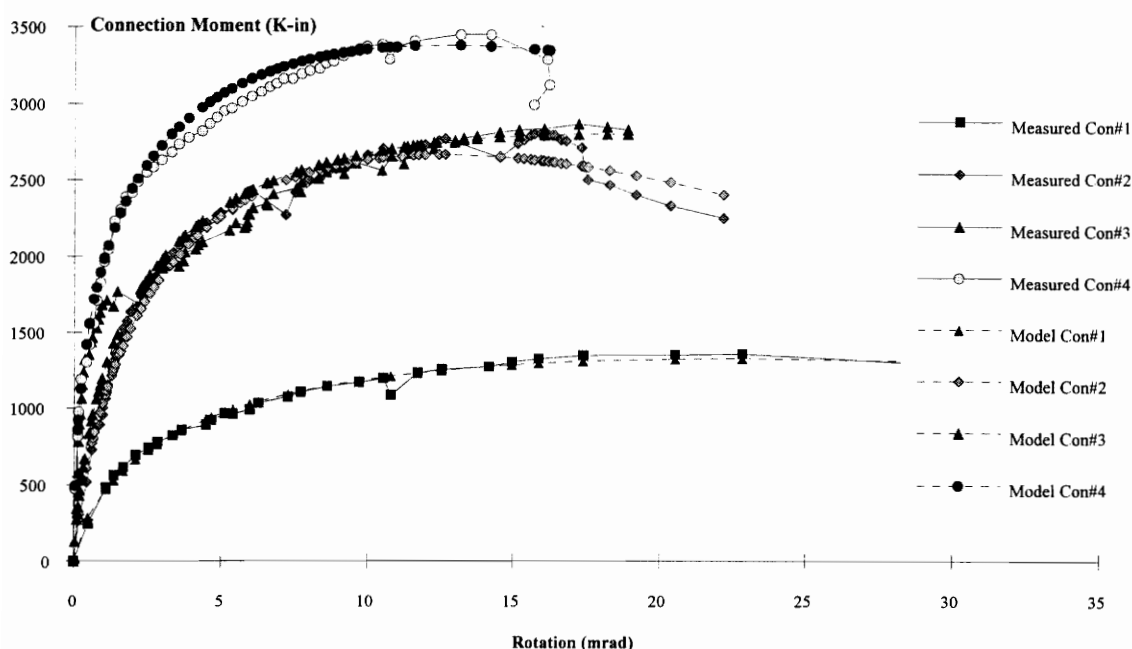
Figure 4.2-2 Composite Semi-Rigid Connection Curves

The bare steel connection model was replaced with the composite connection behavior and the composite beam was subjected to the service live and dead loads to determine live load deflections. The value of the live load was then increased until the beam moment at mid-span reached the moment capacity of the composite beam in positive flexure ($M_{pc}^{(+)}$). In the case of the rigid connections, the live load was increased until the moment at the support reached the moment capacity of the composite beam in negative flexure ($M_{pc}^{(-)}$).

4.2.2 Analysis of Beams With Semi-Rigid Connections

A simple matrix analysis technique was used to analyze the beams. The general details of the beam model are shown in Figure 4.2-3. The beam model was constructed of six elements; four, four-degree of freedom beam elements and two, two-degree of freedom rotational spring elements. Four beam elements were used to allow the non-

prismatic properties of a composite beam in both positive and negative bending to be accounted for.
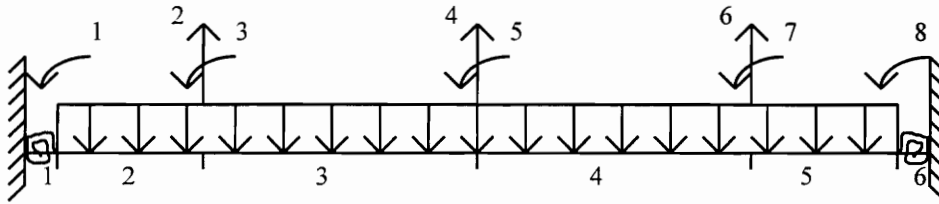
Figure 4.2-3 Basic Details of Beam Model

The two exterior beam elements (elements 2 and 5) were assigned the properties of the composite beam in negative flexure while the two interior beam elements (elements 3 and 4) were assigned the properties of the composite beam in positive flexure. The length of the beam elements are adjusted such that the moments at the joints which connect element 2 to element 3 and which connect element 4 to element 5 are zero (i.e., an inflection point). The exterior beam elements are attached to rigid supports by means of rotational spring elements. By varying the stiffness of the spring element the beam can be modeled anywhere between a pin supported beam to a rigid supported beam. It should be noted that analyzing a single composite beam isolated from the influence of adjacent beams would not be correct in general. If adjacent beams are subject to unequal loading or the adjacent beams have unequal span lengths their could be an initial rotation imposed on the support which would influence the behavior of the beam. The possible influence of adjacent beams has been ignored for purposes of this analytical study.

Because most commercial matrix analysis programs do not include a rotational spring element, it was necessary to create a crude matrix analysis program that included a spring element. This program was constructed using the spreadsheet program Excel which has matrix manipulating utilities incorporated. The six elements were assembled

231

as would be done in a conventional program by combining their individual stiffness matrices and solving for the unknown degrees of freedom.

The four-degree of freedom beam element is nothing new and the derivation is found in many text books. The two degree of freedom rotational spring element is not new either but is certainly less understood. A full derivation of the elemental stiffness matrix is presented in Holzer (1985) and a brief summary of the development is presented below.

Consider the element depicted in Figure 4.2-4. The element itself has negligible length thus no change in moment or shear occurs in the element. Let d_1 equal the rotation from horizontal on the left side of the spring (θ_l) and d_2 equal the rotation from horizontal on the right side of the spring (θ_r). The total rotation of the spring (θ_t) is then the combination of $\theta_r - \theta_l$. From equilibrium f_1 and f_2 must add to zero. Thus:

$$-f_1 = f_2 = \text{Element moment M}$$
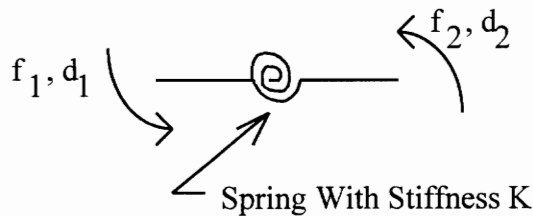
Figure 4.2-4 General Details of Rotational Spring Element

From Compatibility:

$$M = K\ \theta_t = K(\theta_r - \theta_l)$$

Combining:

$$-f_1 = K(\theta_r - \theta_l)$$
$$f_2 = K(\theta_r - \theta_l)$$

Finally:

$$\begin{bmatrix} f_1 \\ f_2 \end{bmatrix} = K \begin{bmatrix} 1 & -1 \\ -1 & 1 \end{bmatrix} \begin{bmatrix} \theta_l \\ \theta_r \end{bmatrix}$$

This stiffness matrix is combined with beam matrices in the same fashion as another beam matrix.

The rotational spring element only uses a linear connection stiffness (K) and because the actual response is non-linear an iterative method of determining the connection stiffness for a given rotation and moment was adopted. The basic idea is that a stiffness is assumed for the stiffness matrix. The matrix is solved and the connection rotation is determined. The connection rotation is then used to determine where the response lies on the actual connection curve (actually the mathematically approximated curve). A new stiffness is chosen which represents the slope of a line from the origin of the moment-rotation region to the point on the connection curve determined from the previous rotation. The process is repeated until the stiffness used is the same as the slope from the origin to the moment-rotation position on the connection curve. This procedure is handled very rapidly with the iterative calculation capabilities of any spreadsheet program.

4.2.3 Study Results

The results are presented in Table 4.2-3. The value of the dead load deflection of the plain steel beam is presented in Column (1) and the value of the flexural moment at the beam midspan when the steel beam was subjected to the factored construction loads are presented in Column (3). The behavior of the bare steel semi-rigid connections was used to determine the beam response for these deflections and moments.

The value of the service load deflection for the composite beam is presented in Column (5). For the beams with composite semi-rigid connections, this value was

obtained by determining the deflection caused by the combination of live and dead load and then subtracting the deflection caused by the dead load only. The uniform live load that caused failure in the composite beam is presented in Column (7). The beam was considered to fail when the moment at midspan or at the beam end (in the case of the rigid connections) exceeded the moment capacity of the composite beam at that section. The uniform live load was superimposed on the uniform dead load.

Table 4.2-3 Results of Analytical Study

	(1) Dead Load Deflection	(2) Ratio to Simple Connection	(3) Factored Construction Load Moment	(4) Ratio to Simple Connection	(5) Service Live Load Deflection	(6) Ratio to Simple Connection	(7) Live Load @ Failure	(8) Ratio to Simple Connection
Connection	(in)		(K-in)		(in)		(psf)	
Simple	2.629	1.00	3841	1.00	1.54	1.00	119	1.00
Connection #1	1.94	0.74	3255	0.85	1.18	0.77	154	1.29
Connection #2	1.35	0.51	2894	0.75	0.83	0.54	192	1.61
Connection #3	1.26	0.48	2841	0.74	0.83	0.54	195	1.64
Connection #4	0.7	0.27	2207	0.57	0.74	0.48	211	1.77
Fixed #1	0.523	0.20	1280	0.33	0.367	0.24	186	1.56
Fixed #2	0.523	0.20	1280	0.33	0.384	0.25	166	1.39

Two basic items of design being considered here are mid-span deflections and beam flexural moments. The results seem to indicate that deflections are reduced much more than mid-span moments for the plain steel beams with semi-rigid connections. In general this is true but this is particularly exaggerated here because the loads applied for deflection calculations are smaller than the factored loads used to check factored construction load moments. As the load increased the moment resisted by the connection increased. However, the ratio of the increase in load over the increase in connection moment is larger than when the unfactored loads were applied to check deflection. This is simply because the connection stiffness starts to reduce at higher moments.

The dead load deflections are shown to reduce very rapidly even for the behavior of Connection #1 which was fairly flexible. This would be a particularly beneficial effect for design firms that set limits on the amount of camber that is specified to remove dead

load deflections. This would also be beneficial for reducing the amount of concrete that ponds when beams are not cambered to remove dead load deflections. The live load deflections are also significantly reduced but not as much as the dead load deflections since the connections have typically started to soften at the increased load levels.

The uniform live load at beam failure was shown to increase significantly for all four connections with the minimum increase being nearly 30% for Connection #1 and the maximum increase nearly 77% for Connection #4. The loads at failure for the beams with rigid connections did not increase as much as the semi-rigid connections since the rigid connections forced beam failure at the supports long before failure of the mid-span section could be achieved. If the beams with rigid connections were designed using plastic design methods the results would most likely indicate much higher failure loads.

This brief analytical study was simplified and more detailed studies will be included as part of the continuing research program. The main point of this study was to provide some evidence that accounting and designing for the actual connection stiffness of beam-to-girder joints may significantly improve load carrying capacity and reduce deflections of composite beams.

CHAPTER 5.0
SUMMARY, CONCLUSIONS, AND RECOMMENDATIONS

5.1 SUMMARY

Advancements in design methods and construction materials are resulting in shallower and lighter composite floor systems. As a result, serviceability issues, rather than strength considerations, are starting to control designs. Partial continuity in composite floor systems may be one method by which serviceability characteristics of floor systems can be improved. Composite semi-rigid beam-to-girder connections are being investigated as a means by which this partial continuity could be developed in composite floors. The development of these is an extension of the composite semi-rigid beam-to-column connection research that has been conducted in recent years. The beam-to-column connection research has shown that connections with very simple details can possess tremendous rotational stiffness if a reinforced composite slab is present.

Four composite semi-rigid beam-to-girder connections (Connection #1 through Connection #4) were designed and tested experimentally. Connection #1 was a simple single shear plate connection. The experimental results indicated that the bare steel connection had little rotational stiffness but that this connection became very stiff when it was combined with a reinforced composite slab. In fact, the composite connection developed nearly 37% of the plastic moment capacity of the steel beam. This connection failed as a result of local buckling of the bottom beam flange.

Attaching a steel framing angle to the bottom beam flange (a seat angle) had been shown in the research on composite semi-rigid beam-to-column connections to increase rotational stiffness and provide stability for the bottom flange. With this in mind, Connection #2 was detailed similar to the first but with the addition of a seat angle. This connection showed significant stiffness with and without a composite slab. Although the bare steel connection was not loaded to failure, it was shown to develop a moment

236

capacity of at least 20% of the plastic moment capacity of the steel beam. The composite connection developed a moment of resistance of approximately 80% of the plastic moment capacity of the steel beam and had a rotational capacity far in excess of what would be needed in typical composite beam designs.

Connections #3 and #4 were two innovative connections developed in an attempt to increase the rotational stiffness of the beam-to-girder connections before a composite slab could contribute to the rotational stiffness. Both connections were combinations of a seat angle and a tension plate which was used to attach the top portion of the beam to the girder. Both of the bare steel connections exhibited very stiff moment-rotation behavior. The composite connections were also very efficient, attaining nearly 80% and 100% of the plastic moment capacity of the steel beam.

Simple stiffness models were developed in an attempt to simulate the moment-rotation behavior of Connections #3 and #4. The models make use of simple stiffness relationship for the key elements of these connections in order to simulate the connection behavior. The results of the model were remarkably good considering their simplicity.

A brief experiment was conducted to determine the affect of bolt tensioning on the moment-rotation behavior of a semi-rigid steel connection. In addition, a brief analytical study was conducted to consider what affect including the semi-rigid steel and semi-rigid composite connections might have on the behavior of a composite beam.

5.2 CONCLUSIONS

The behavior exhibited by the composite beam-to-girder semi-rigid connections tested indicated that simple steel beam-to-girder connections, which may not have any significant rotational stiffness on their own, can be turned into very stiff connections with the addition of a reinforced composite slab. Additional conclusions include:

1. When combining a simple steel connection such as a shear tab, with a reinforced composite slab the bottom beam flange is very susceptible to becoming unstable. To

237

ensure that instability does not occur, and at the same time increase the rotational stiffness of the connection, a seat angle or a plate needs to be attached to the bottom flange. If the angle or plate is not provided then detailing of the reinforcing steel should be given careful consideration (i.e., the amount of reinforcing steel should be detailed so that the reinforcing steel yields prior to any local instabilities in the connection).

2. Connections using fully tensioned bolts will typically be characterized by behavior which is stiffer and more predictable than connections which use only snug tight bolts.

3. To ensure that the connection has sufficient ductility, the details of the steel connection need to be given careful consideration. If the steel connection is too stiff and does not allow the reinforcing steel to properly yield, then the connection will likely fail as a result of local instabilities at relatively low rotations compared to a connection in which the reinforcing steel fully yields.

4. An effective slab width of at least 60-in. could be assumed in the design of these connections based on the force distribution seen in the composite slabs of the test specimens which indicated little or no shear lag.

5. The ability to develop analytical models to predict the behavior of these connections is directly related to the ability to predict the behavior of the components of the connection. The better the behavior of the connection components is understood, the better the ability to predict the behavior of the connection as a whole.

6. Accounting for the rotational restraint provided by these connections should lead to decreased deflections and moments. This, in turn, should allow more efficient designs and possibly an eventual reduction in construction costs.

5.3 RECOMMENDATIONS

Based on the experimental and analytical investigation to date the following recommendations are made for future work in this subject:

1. One or two connection details need to be determined which will provide rotational stiffness before and after the composite slab is effective. The details should be simple and easy to incorporate into current design, fabrication, and erection procedures. Once the details are determined, every aspect of the connection needs to be fully explored so that their behavior can be fully understood and comprehensive design criteria can be developed.

2. Because the seat angle appears to be a crucial element of most composite connections, the behavior of the seat angle should be better understood. This may include finite element modeling of the angle in combination with experimental tests.

3. These tests were carried out with fixed values of moment-to-shear at the connection. Future tests should try to allow for a changing moment-to-shear ratio so the effect of shear on the moment capacity of the connection can be determined.

4. The effects of cyclic loading on composite beam-to-girder connections needs to be explored.

5. Feasibility studies need to be conducted to determine where composite beam-to-girder connections can be most effectively used and how they may improve the efficiency of composite floor design.

239

6. To better understand the elemental behavior of the connection components an extensive review of prior research needs to be undertaken. This work may need to be complimented with additional elemental tests to better understand the behavior.

7. Because reasonable connection behavior estimates were developed with "PRCONN" (Richard 1991), it is recommended that a copy of the newly released version be acquired and that discussions with Dr. Richard be instigated so that the method used to develop the connection response can be understood. Understanding how this program works may be very important in the latter parts of the continuing research program as this may allow development of a similar program which would estimate the behavior of beam-to-girder connections. This would be important to allow easy development of connection curves such that they could readily be implemented into design procedures.

REFERENCES

Acroyd, M.H. and Gerstle, K.H. (1990). "Behavior and Design of Flexibly Connected Building Frames," *AISC Engineering Journal*, **27**(1), 22-29.

Altmann, R., Maquoi, R., and Jaspart, J.P. (1991). "Experimental Study of the Non-Linear Behavior of Beam-to-Column Composite Joints," *Journal of Constructional Steel Research*, **18**(1), 45-54.

Amadio, C., Puhali, R., and Zandonini, R. (1989). "Joint behavior and response of braced composite frames," Proceedings of International Colloquium Bolted and Special Structural Connections, No.3, Moscow, 127-134.

Ammerman, D. J. and Leon, R. T. (1990). "Unbraced frames with semi-rigid composite connections," *AISC Engineering Journal*, **27**(1), 12-21.

Ammerman, D.J. and Leon, R.T. (1987). "Behavior of Semi-Rigid Composite Connections," *AISC Engineering Journal*, **24**(2), 53-61.

Anderson, D. and Benterkia, Z. (1990). "Analysis of Semi-Rigid Steel Frames and Criteria for Design," *Stability of Steel Structures,* International Conference, Budapest, Hungary, Vol. 1, ed. M. Ivanyi and K. Akademiai, 705-712.

Ballerini, M. (1992). "Limit State Analysis of Composite Beams in Semi-Continuous Non Sway Frames," Internal Report n. 1, Department of Structural Mechanics & Design Automation, University of Trento (*In Italian*).

Banard, P.R. (1970). "Innovations in Composite Floor Systems," *Canadian Structural Engineering Conference Proceedings*, Canadian Steel Industries Construction Council, 1-13.

Beer, F.P. and Johnston, Jr. E.R. (1981). *Mechanics of Materials*, McGraw-Hill

Benussi, F., Puhali, R., and Zandonini, R. (1989). "Semi-rigid joints in steel concrete composite frames," *Costruzioni Metalliche*, (5), 237-265.

Benussi, R., Puhali, R. and Zandonini, R. (1987), "Composite Braced Frames with Semi-Rigid Joints," *International Symposium on Composite Steel Concrete Structures*, Bratislava, 104-111.

Bernuzzi, C., Noe', S., and Zandonini, R. (1991). "Semi-Rigid Composite Joints: Experimental Studies," *Connections in Steel Structures II: Behavior, Strength, and Design*, ed. R. Bjorhovde, G. Haaijer and A. Colson, ASCE, 189-200.

Bijlaard, F.S.K. and Zoetemeijer, P. (1986). "Influence of Joint Characteristics on the Structural Response of Frames," *Steel Structures: Recent Research Advances and Their Application to Design*, ed. M.N. Pavlovic, Elsevier Applied Science, London.

Brett, P. R., Nethercot, D. A., and Owens, G. (1987). "Continuous construction in steel for roofs and composite floors," *The Structural Engineer*, **65A**(10), 355-368.

Brett, P.R., Nethercot, D.A., and Owens, G.W. (1988). "Discussion: Continuous Construction in Steel for Roofs & Composite Floors," *The Structural Engineer*, **66**(14/19), 216-227.

Buttry, K.E. (1965). "Behavior of Stud Shear Connectors in Lightweight and Normal-Weight Concrete," *M.S. Thesis, University of Missouri*

Collins, M.P. and Mitchell, D. (1991). *Prestressed Concrete Structures*, Prentice Hall, 142-154.

Crawford, S.F. and Kulak, G.L. (1971). "Eccentrically Loaded Bolted Connections," *Journal of the Structural Division*, **97**(ST3), 765-783.

Daniels, J.H., Kroll, G.D., and Fisher, J.W. (1970). "Behavior of composite beam to column joints," *Journal of Structural Division*, **96**(3), 671-685.

Davison, J.B., Lam, D., and Nethercot, D.A. (1990). "Semi-Rigid Action of Composite Joints," *The Structural Engineer*, **68**(24/18), 489-499.

Easterling, W.S., Gibbings, D.R., and Murray, T.M. (1993). "Strength of Shear Studs in Steel Deck on Composite Beams and Joists," *AISC Engineering Journal*, **30**(2), 44-55.

Eurocode 3: Design of Steel Structures, Part 1.1: General Rules For Buildings, (1993), Commission of The European Communities

Eurocode 4: Common Unified Rules for Composite Steel and Concrete Structures (DRAFT), (1992). Commission of the European Communities, Rep. EUR 9886.

Fisher, J.W. (1965). "Behavior of Fasteners and Plates With Holes," *Journal of Structural Division*, **91**(ST6), 265-286.

Garrett, J.H. Jr. and Brockenbrough, R.L. (1986). "Design Loads for Seated-Beam in LRFD," *AISC Engineering Journal*, **23**(2), 84-88.

Holzer, S.M. (1985). *Computer Analysis of Structures Matrix Structural Analysis Structured Programming*, Elsevier

Jaspart, J.P. and Maquoi, R. (1990). "Guidelines for the Design of Braced Frames with Semi-Rigid Connections," *Stability of Steel Structures,* International Conference, Budapest, Hungary, Vol. 1, ed. M. Ivanyi and K. Akademiai, 713-720.

Johnson, R.P. and Hope-Gill, M.C. (1972). "Semi-rigid Joints in composite frames," Preliminary Report of the Ninth congress of IABSE, 133-144.

Johnson, R.P. and Law, C.L.C. (1981), "Semi-Rigid Joints For Composite Frames," *Joints in Structural Steelwork,* Teeside, ed. J.H. Howlett, John Wiley & Sons, New York, 3.3-3.19.

Kato, B., Ohtake, F., Okuto, K., Sakamoto, S., Takada, K., and Nose, H. (1985). "Composite Beams Using Newly Developed H-Shaped Steel With Protrusions," *Symposium on Steel in Buildings,* Luxembourg, IABSE-ECCS, 309-316.

Kulkarni, P. (1990). "Analytical Determination of the Moment Rotation Response of Semi-Rigid Composite Connections," M.S.C.E. University of Minnesota.

Leon, R. (1990). "Semi-Rigid Composite Construction," *Journal of Constructional Steel Research,* **15**(1), 99-120.

Leon, R. T. and Ammerman, D.J. (1990), "Semi-Rigid Composite Connections for Gravity Loads," *AISC Engineering Journal,* **27**(1), 1-11.

Leon, R. T., Ammerman, D. A., Lin, J.A. and McCauley, R.D. (1987). "Semi-Rigid Composite Steel Frames," *AISC Engineering Journal,* **24**(4), 147-155.

Leon, R.T. (1987). "Behavior of semi-rigid composite frames," *Composite steel structures: Advances, Design and Construction,* ed. Narayanan, R., Elsevier Applied Science, London, England, 145-153.

Leon, R.T. (1988). "Behavior and design of semi-rigid composite frames," Proceedings of 13th Congress, IABSE, Helsinki, 669-704.

Leon, R.T. (1993). "Design of Frames with Semi-Rigid Composite connection," *Proc. of The National Steel Construction Conference,* Orlando, Florida, AISC, 24.1-24.21.

Leon, R.T. and Forcier, G.P. (1991). "Parametric Study of Composite Frames," *Connections in Steel Structures II: Behavior, Strength, and Design,* ed. R. Bjorhovde, G. Haaijer and A. Colson, ASCE, 152-159.

Leon, R.T. and Forcier, G.P. (1991). "Performance of Semi-Rigid Composite Frames," *Annual Technical Session, SSRC,* Chicago, 259-269.

Leon, R.T. and Zandonini, R. (1992). "Composite Connections," *Constructional Steel Design: An International Guide,* ed. P.J. Dowling, J.E. Harding and R. Bjorhovde, Elsevier Applied Science, London, 501-522.

Load and Resistance Factor Design Specification for Structural Steel Buildings (1986). American Institute of Steel Construction, Chicago, Illinois.

Load and Resistance Factor Design Specification for Structural Steel Buildings, "Final Draft" (1993). American Institute of Steel Construction, Chicago, Illinois.

Manual of Steel Construction Allowable Stress Designl (1989). American Institute of Steel Construction, Chicago, Illinois.

Manual of Steel Construction Load and Resistance Factor Design (1986). American Institute of Steel Construction, Chicago, Illinois.

Manual of Steel Construction Volume II Connections (1992). American Institute of Steel Construction, Chicago, Illinois.

Nethercot, D.A. (1991). "Tests on Composite Connections," *Connections in Steel Structures II: Behavior, Strength, and Design*, ed. R. Bjorhovde, G. Haaijer and A. Colson, ASCE, 177-188.

Nethercot, D.A. and Zandonini, R. (1989). "Methods of Prediction of Joint Behavior: Beam-Column Connections," *Structural Connections - Stability and Strength*, ed. Narayanan, R., Elsevier Applied Science, London, 23-62.

Owens, G.W. and Echeta, C.B. (1981). "A semi-rigid connection for composite frames-Initial test results," *Joints in Structural Steelwork*, ed. J.H. Howlett, W.M. Jenkins, and R. Stainsby, John Wiley & Sons, NY, New York, 6.93-6.121.

Puhali, R. Smotlak, I. and Zandonini, R. (1990). "Semi-rigid composite action: experimental analysis and a suitable model," *Journal of Constructional Steel Research*, **15**(1), 121-151.

Richard, R.M., Gillett, P.E., Kriegh, J.D., and Lewis, B.A. (1980). "The Analysis & Design of Single-plate Framing Connections," *AISC Engineering Journal*, 2nd Qtr., 38-52.

Salmon, C. G. and Johnson, J. E. (1990). *Steel Structures: Design and Behavior*, Third Edition, Harper and Row, New York.

Specification for Structural Steel Buildings Allowable Stress Design and Plastic Design (1989). American Institute of Steel Construction, Chicago, Illinois.

Van Dalen, K. and Godoy, H. (1982). "Strength and Rotational Behavior of Composite Beam-Column Connections," *Canadian Journal of Civil Engineering*, **9**(2), 313-322.

Wald, F. (1991). "Energy-Based Prediction for Composite Joints Modeling," *Connections in Steel Structures II: Behavior, Strength, and Design*, ed. R. Bjorhovde, G. Haaijer and A. Colson, ASCE, 168-176.

Wang, C.K. and Salmon, C.G. (1985). *Reinforced Concrete Design*, Fourth Edition, Harper & Row, New York.

Zandonini, R. (1989). "Semi-Rigid Composite Joints," Strength and Stability Series, Vol. 8, *Connections*, ed. R. Narayanan, Elsevier, London, 63-120.

Zandonini, R. and Zanon, P. (1992). "Semi-Rigid Joint Action in Composite Frames: Numerical Analysis and Design Criteria," *Composite Construction in Steel and Concrete II*, Potosi, Missouri, ed. W.S. Easterling, W.M. Kim Roddes, ASCE, 397-412.

Zandonini, R. and Zanon, P.(1991). "Beam Design in PR Braced Steel Frames," *AISC Engineering Journal*, **?**(3), 85-97.

APPENDIX A

ONE PAGE SUMMARIES OF RESEARCH ON SEMI-RIGID CONNECTIONS

**EXCLUDING WORK ASSOCIATED WITH
LEON AND ZANDONINI**

Fisher, Kroll, Daniels (1970) Specimens J1 & J2

Concrete Deck		Steel Deck			
Thickness	4"	None			
Width	72"				
Weight	Normal				
Reinforcing	Area	Steel/Slab			
J1	2.42	0.84%	Longitudinal		
J2	2.2	0.76%	Longitudinal		
Shear Studs	Dia	Height	Spacing	Number	
Mid Section	0.5	2	2/5"	10Spa	
End	0.5	2	2/2.5"	6Spa	
Material Properties		Fy (Ksi)	Fu (Ksi)		
Joist Flange		36.40			
Joist Web		40.00			
Slab Reinforcing (A615)		40			
Concrete			4.10		

bf/2tf =6.9
d/tw = 52.5

16x6x1" Spreader Plate
16WF40
14WF68
Top 4#3 @ 12" 3#5
3#3
Top 11#3 @ 6" Bottom & Top
6#3 @ 12" Bottom   TEST SPECIMEN J1
Top 4#3 @ 12" 3#5 1#3
3#3
Top 11#3 @ 6" Bottom 3#3
3#3
7#3 @ 12" Bottom   TEST SPECIMEN J2
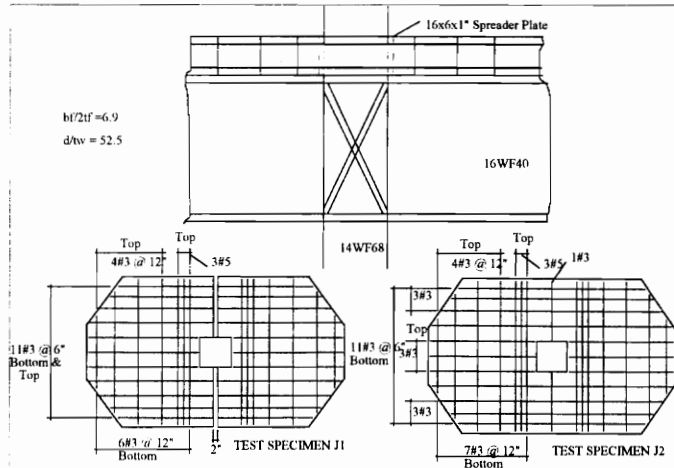
Results   Mp approx 2700 K-in

	Muc	Muc/	Øu	
Designation	(K-in)	Mp	mRad	Comments
J1L	4500	1.67	3.1	Rocker support collapsed
J2L	4600	1.70	7	Crushing of the concrete slab as well as plastification and fracture of the beam
J1R	3450	1.28	4	Excessive deformations
J2R	3500	1.30	3.6	Buckling of lower beam flange & Web & excessive deformation

Test Notes

Concrete Cracking
In J1L the slab was extensively cracked along the diagonal lines which extended to the edges of the slab

In J2L the cracking was mainly limited to two parallel lines symmetrically placed on each side of the steel beam flange

Local Effects
J2L at fracture was after substantial deformation and strain hardening had occured, curvature was 40-50 times the elastic limit

Local buckling of the top flange occured in the left side of J2

If local buckling had not controlled, it is felt that J2R would have reached the theoretical Mpc (-)

The strength of the steel beam plus the continuous longitudianl slab reinforcemtn appeared to be effective for the full slab width

Additional General Notes
The right side was braced after failure for both J1 & J2 in order to allow development of failure of the left side

Sufficient rotation capcity of the composite beam exists in the vicinity of the joint to enable plastic design theory to be used

58 days between pour and test of specimens

Ultimate moment should be reached within curvatures not exceeding 10-15 times the yield curvature for use of plastic design theory

Test Setup

Hydraulic Tension Jack
48"
Gap only for J-1
Rocker J1 / Roller J2
48"   65"   65"
Calibrated Tension Dynometer

M-Theta
Fisher, Kroll, Daniels
M (K-in)
Rotation (mrad)
J1L
J2L
J1R
J2R
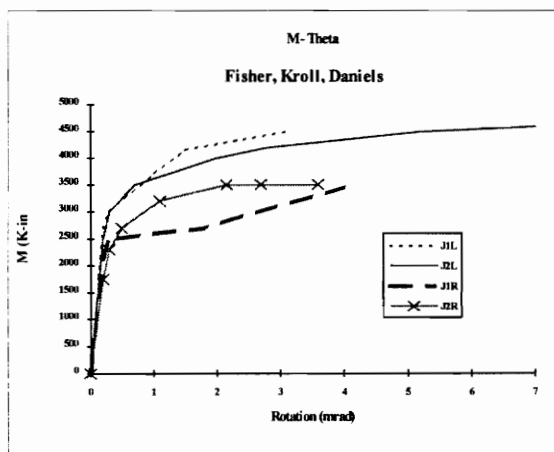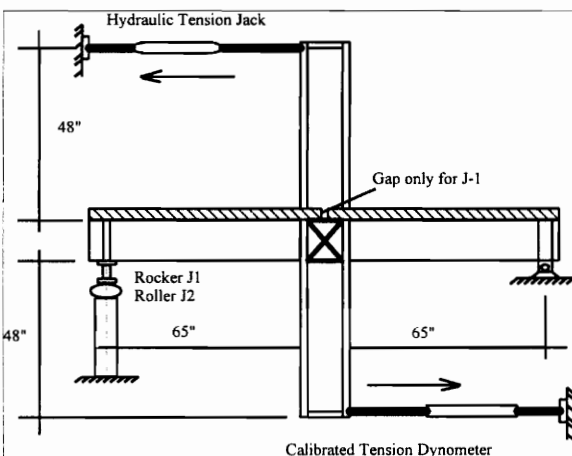
Johnson, Hope-Gill (1972) Specimens HB50 - HB54

Concrete Deck		Steel Deck		
Thick(50)	3.25		None	
HB51-54	3.5			
Width	30		Ar*fyr/	
Reinforcing	Area	Steel/Slab	Af*fyf	
HB50	1.39	1.42%	1.011	
HB51	0.876	0.84%	0.479	
HB52	1.871	1.78%	1.06	
HB53	2.063	1.97%	1.148	
HB54	2.102	2.01%	1.38	
Shear Studs	Dia	Height	Spacing	Number

HB50: 203x133 UB25
HB51-53: 305x165 UB40
HB54: 406x140 UB39

	dw/tw	bf/tf	D
HB50	32.4	16.6	8.11
HB51	46.4	16.5	12.14
HB52	46.0	16.4	12.14
HB53	43.4	17.1	12.14
HB54	56.4	17.0	16.00

Material Properties	Fy (Ksi)	Fy (Ksi)	Mp (K")
	Rebar	Struc. Steel	
HB50	52.6	45	716
HB51	56.6	40.2	1655
HB52	58.6	40.2	1627
HB53	58.3	42.5	1547
HB54	56.7	45.7	1993

Results	Mdc	Mpc(-)	Muc	Muc/	Muc/	Muc/	Øuc	
Designation	(K-in)	(K-in)	(K-in)	Mdc	Mp	Mpc(-)		Comments
HB50	761	1062	894	1.17	1.24	0.84	68	Failure of shear connectors
HB51	690	2000	929	1.35	0.56	0.47	75	Large rotations & failure of shear connectors
HB52	1510	2204	1964	1.3	1.21	0.89	70	Large rotations (limited by test rig)
HB53	2004	2522	2248	1.11	1.45	0.89	30	Longitudinal shear failure of slab
HB54	2523	3000	2681	1.06	1.35	0.89	33	Buckling along free edge of web

Mdc = the calculated joint capacity = Ar*fry*kd (kd = moment arm)

Test Notes

Concrete Cracking

The transverse reinforcement in the slab of HB53 was designed by ultimate-strength to be just sufficient at M'uc

Bottom Angle

Slip first detected @ 1.04 M'uc HB51, @0.72 M'uc HB52-54 (lower loads than intended when designed)

Jointsdesigned with a slip factor of .45 and nuts tightened by part-turn method (slip appeared to occur @ factors of .32-.36)

It may be necessary to design for first slip at a higher proportion of M'uc than .7

Local Effects

Suggests using 64% shear connector strength design in hogging moment regions to prevent failure as in HB50

Suggests use of a bolted web cleat to prevent failure as in HB54

Felt little flange buckling occured as a result of the restraint provided by the seat angles

semi-rigid joints felt to have greater resistance to buckling and much greater rotation capacity than rigid connections

Joint gap felt important to allow for sufficient rotation of the joint @ full composite loads of the beam

Additional General Notes

Each test extended over 2-3 days

Suggests using M'uc/Mp ratios of 1 to increase the beam capacity between 67 and 40%

Suggests designing shear connectors & longitudinal reinforcing for M'uc and not above

Test Setup

Possible Test Setup (Actual is unknown @ this time)

Hydraulic ram

M - Theta

JOHNSON & HOPE-GILL

M (K-in)

Rotation (mrad)

**Rotations are of free end relative to column center line
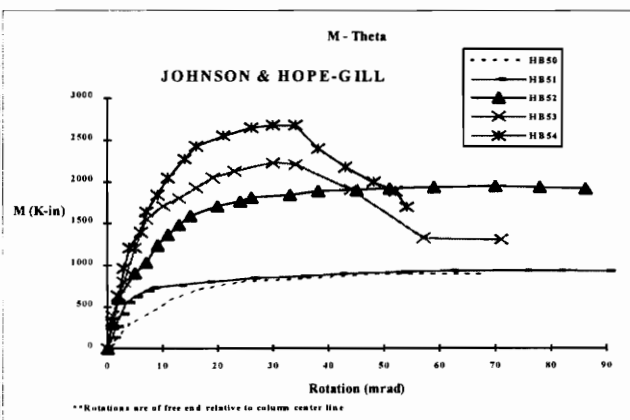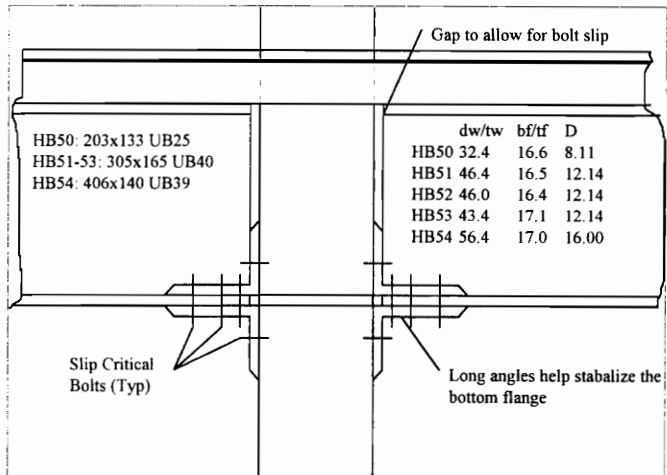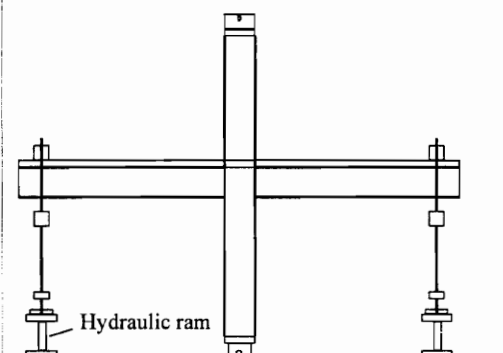
Echeta, Owens (1981) Specimen 1B

Concrete Deck		Steel Deck			
Thickness	3	Height	None		
Width	41.3				
Weight	?		Ar*fyr/		
Reinforcing	Area	Steel/Slab	Af*fyf		
1BS		0.51	0.716		
1BN		0.51	0.413		
Shear Studs	Dia	Height	Spacing	Number	
1B	0.5		Uniform	8/ea	
Material Properties		Fy (Ksi)	Fu (Ksi)		
Joist Flange		43.10	68.02		
Joist Web		47.70	67.73		
Column		54.10	77.16		
Slab Reinforcing		78.32	111.40		
Concrete		6.24			
Stud Capacity					

Diagram annotations:
- 8-8mm bars @ 4.92"
- Transverse reinforcement to prevent longitudinal shear
- 10" c/c
- 8mm concrete cover
- 5mm fillet welds 3 sides
- Used to stabilize beam during construction 40x40x5mm web cleat
- dw/tw = 37.6
- bf/tf = 10.2
- D = 10.18
- 150x100x5mm RHS Filled
- 254x102 UB28
- M12 Grade 8.8 bolts (typ)
- 2mm gap
- 150x90x10mm flange cle Designed for no slip up to 1.1 service load
- 6mm fillet welds 3 sides
- 1BS
- 1BN

Results	Mp= 929								
	Mdc	Mpc(-)	Muc	Muc/	Muc/	Muc/	Øuc		
Designation	(K-in)	(K-in)	(K-in)	Mdc	Mp	Mpc(-)	(radx10^3)	Comments	
1BS	601	1230	982	1.63	1.06	0.8	>32	Excessive deformation	
1BN	601	1230	982	1.63	1.06	0.8	>32	Excessive deformation	

Mdc = design connection capacity   (1"gap btwn column & top flange of beam)

Test Notes

Concrete Cracking

maximum crack width =.0157" (1BN linear portion), increased to .03937" @ Mp

Bottom Angle

slip only in the 1BN specimen

Local Effects

Suggests required inelastic rotation of 0.013 rad w/o web/flange instability

Web cleats pulled away from columns @ approximately 1.45 Mp

No seperation between the concrete slab & steel beam interface

No local buckling noticed

Additional General Notes

P1, P2 controlled so that V/M ratio in joint zone varied while M stayed constant in order to simulate moment redistribution

Shear connectors combined capacity > maximum tension developable in the tension reinforcement

Rotation measured by means of a standard arrangement of lightboxes, mirrors & telescopes

The moment capacity can be estimated from Ar, fyr, and d

The rotation capacity is high enough to allow a high degree of moment redistribution

No adverse interaction between high shear force & high moment on the connection

Test Setup
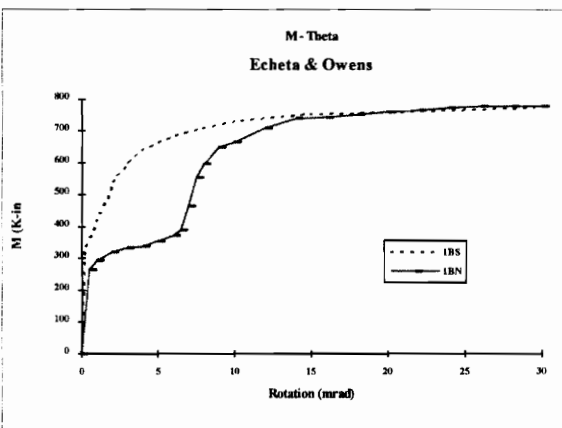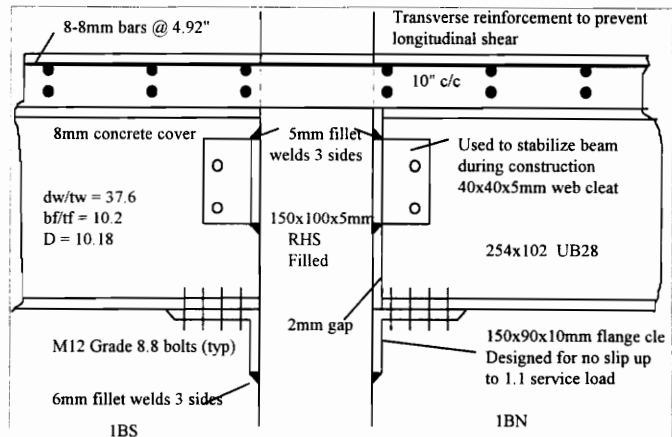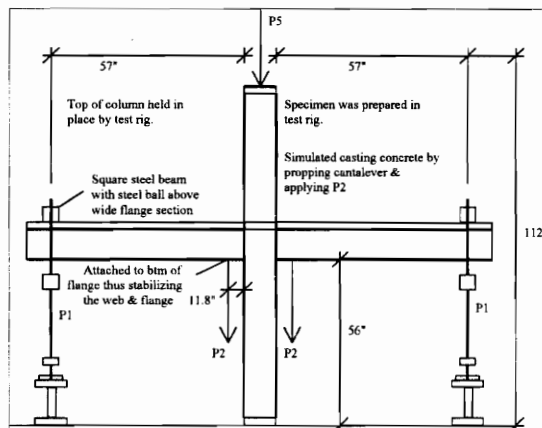
Dalen, Godoy (1982) Specimens CB1 and CB2

Concrete Deck		Steel Deck			
Thickness	4"	Height	None		
Width	48"				
Weight	?		Ar*fyr/		
Reinforcing	Area	Steel/Slab	Af*fyf		
CB1	0.88	0.46	0.709		
CB2	1.54	0.8	1.233		
Shear Studs	Dia	Height	Spacing	Number	
CB1	0.4"	2.5"	2/Even	18/Ea	
CB2	0.4"	2.5"	2/Even	18/Ea	
Material Properties		Fy (Ksi)	Fu (Ksi)		
Joist Flange		43.95	70.05		
Joist Web		46.99	70.63		
Seat Angle		57.73	80.35		
Top Plate		34.37	59.90		
Slab Reinforcing		70.05	108.78		
Concrete	CB1		6.27		
	CB2		6.57		
Stud Capacity	7 K/Stud				

Results — Mp = 841

Designation	Mpc(-) (K-in)	Mdc (K-in)	Muc (K-in)	Muc/ Mdc	Muc/ Mp	Muc/ Mpc(-)	Øuc (radx10^3)	Reason for Termination of Test
SB1(Stl Only)	-	-	239	-	0.28	-	95	Failure of top angle
CB1	1089	620	1062	1.71	1.26	0.98	47	Load defficult to maintain excessive crack widths
CB2	1257	1124	1443	1.28	1.72	1.15	36	Capacity of load cell reached slab fully cracked

*Mdc = design connection capacity

Test Notes

SB1 Buckling of bottom flange and slip between angles and bottom flange did not occur

CB1 & CB2 Concrete Cracking

First Cracks at 239 K-in (Pattern affected by transverse reinforcing)

Cracks extending from column flange tip to edge of slab @ 300 K-in

Cracks Extended to bottom face of deck

CB1 had small number of large cracks

CB2 had large number of small cracks

No longitudinal cracks but some cracks @ 45

Bottom Angle Slip

Slip between bottom flange and seat angles @ 221 K-in

CB1 Developed much larger slip @ low loads

Local Effects

Loud Reports @ 300 K-in (Thought to be breakdown of concrete steel interface)

No seperation between slab & steel section

No fracture of top angle

Buckling of bottom flange noticed at tips of seat angles

No column deformation reported
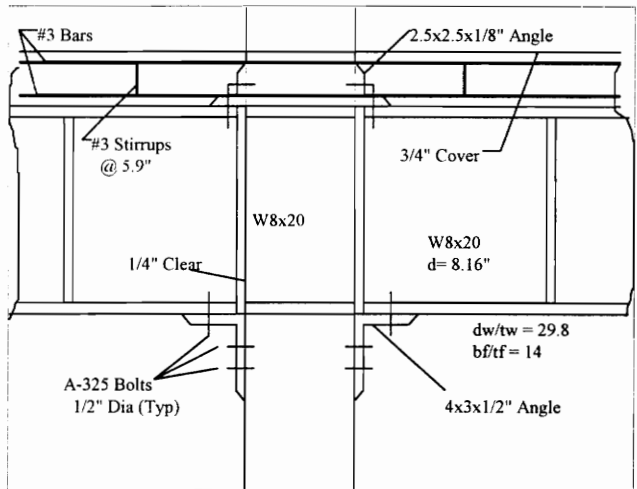
Test Setup
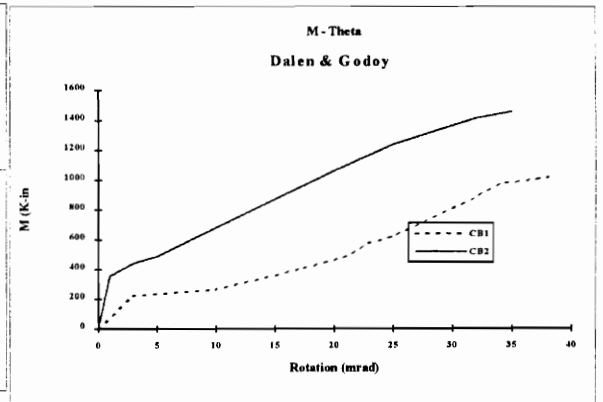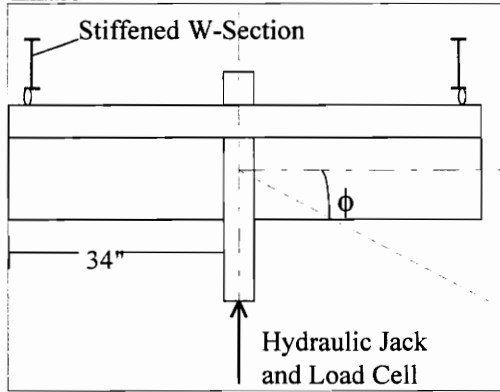
Dalen, Godoy (1982) Specimens CB3

Concrete Deck		**Steel Deck**		
Thickness	4"	Height	None	
Width	48"			
Weight	?			
Reinforcing	Area	Steel/Slab		
CB3	1.54	0.8		

Shear Studs	Dia	Height	Spacing	Number
CB3	0.4"	2.5"	2/Even	18/Ea

Material Properties		Fy (Ksi)	Fu (Ksi)
Joist Flange		43.95	70.05
Joist Web		46.99	70.63
Seat Angle		57.73	80.35
Top Plate		34.37	59.90
Slab Reinforcing		70.05	108.78
Concrete	CB3		6.41
Stud Capacity	7 K/Stud		

Labels in diagram: #3 Bars; #3 Stirrups @ 5.9"; Full Grove Welds; 1/4" Clear; W8x20; 3/4" Cover; Cope Holes; W8x20; dw/tw = 29.8; bf/tf = 14; A-325 Bolts 1/2" Dia (Typ); 4x3x1/2" Angle
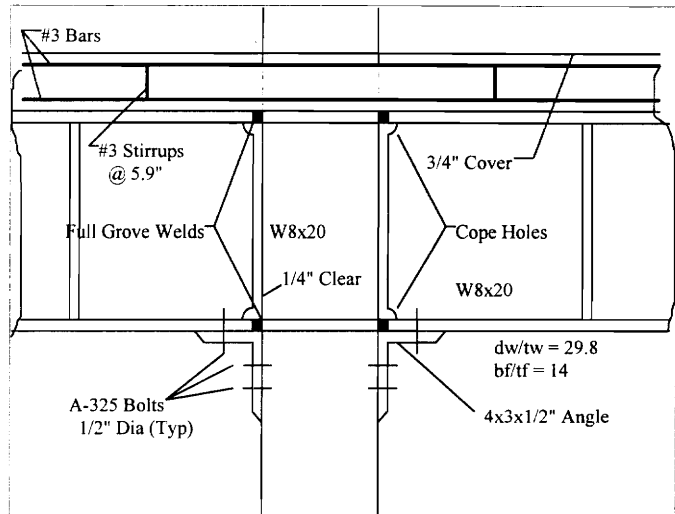
Results

Designation	Description	Steel/Slab Ratio (%)	Myc (K-in)	Muc (K-in)	Myc/ Myb	Muc/ Mub	Øuc (radx10^3)	Reason for Termination of Test
SB2	Steel Only	-	690	902	0.92	1.07	9	Failure of top weld
CB3	Composite	0.8	1044	1389	1.04	1.11	10	Capacity of load cell reached

Test Notes

SB2   Minor deformation of bottom flange near the column face and of the column at the btm flange level

CB3   Concrete Cracking

First Cracks at 239 K-in (Pattern affected by transverse reinforcing)

Cracks extending from column flange tip to edge of slab @ 300 K-in

Large number of small cracks

No longitudinal cracks but some cracks @ 45

Bottom Angle Slip

None, Bottom flange welded

Local Effects

Loud Reports @ 300 K-in (Thought to be breakdown of concrete steel interface)

No seperation between slab & steel section

Buckling of bottom flange noticed at tips of seat angles (less than in CB2)

Deformation of column at the level of btm flange was evident

Test Setup

Stiffened W-Section

34"

Hydraulic Jack and Load Cell

M - Theta
Dalen & Godoy

M (K-in) vs Rotation (mrad), legend: CB3

Dalen, Godoy (1982) Specimens CB4 and CB5

Concrete Deck		**Steel Deck**			
Thickness	4"	Height	None		
Width	48"				
Weight	?		Ar*fyr/		
Reinforcing	Area	Steel/Slab	Af*fyf		
CB4	0.88	0.46	0.709		
CB5	1.54	0.8	1.233		
Shear Studs	Dia	Height	Spacing	Number	
CB4	0.4"	2.5"	2/Even	18/Ea	
CB5	0.4"	2.5"	2/Even	18/Ea	
Material Properties		Fy (Ksi)	Fu (Ksi)		
Joist Flange		43.95	70.05		
Joist Web		46.99	70.63		
Seat Angle		57.73	80.35		
Top Plate		34.37	59.90		
Slab Reinforcing		70.05	108.78		
Concrete	CB4		6.68		
Concrete	CB5		6.18		
Stud Capacity	7 K/Stud				

Diagram labels: #3 Bars; #3 Stirrup @ 5.9"; 3/4" Cover; Fillet Weld; Top Plate; Full Grove Welds; W8x20; Cope Holes; 1/4" Clear; W8x20; A-325 Bolts 1/2" Dia (Typ); dw/tw = 29.8; bf/tf = 14; 4x3x1/2" Angle

Results

Mp = 841

Designation	Mpc(-) (K-in)	Mdc (K-in)	Muc (K-in)	Muc/ Mdc	Muc/ Mp	Muc/ Mpc(-)	Øuc (radx10^3)	Reason for Termination of Test
SB3	-	-	531	-	0.63	-	66	Load difficult to maintain, excessive elongation of top plate
CB4	1089	620	1221	1.97	1.45	1.12	22	Load difficult to maintain, excessive crack widths
CB5	1257	1124	1434	1.28	1.71	1.14	14	Capacity of load cell reached

*Mdc = design connection capacity

Test Notes

SB2   Rotation capacity agreed well with the theoretical 20% elongation of the top plate

CB4 & CB5   Concrete Cracking

    First Cracks at 239 K-in (Pattern affected by transverse reinforcing)

    Cracks extending from column flange tip to edge of slab @ 300 K-in

    CB4, Cracks extended to the bottom of the slab

    CB4, Small number of wide cracks

    CB5, Large number of small cracks

   No longitudinal cracks but some cracks @ 45

    Bottom Angle Slip

    None, Bottom flange welded

    Local Effects

    Loud Reports @ 300 K-in (Thought to be breakdown of concrete steel interface)

    No seperation between slab & steel section

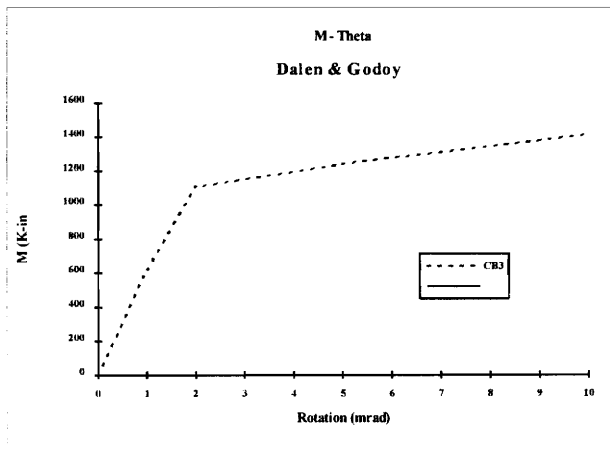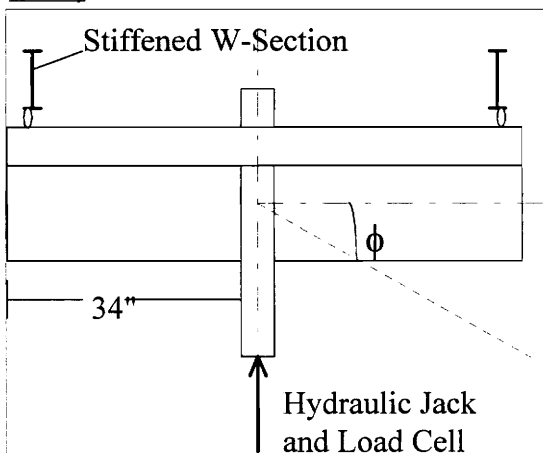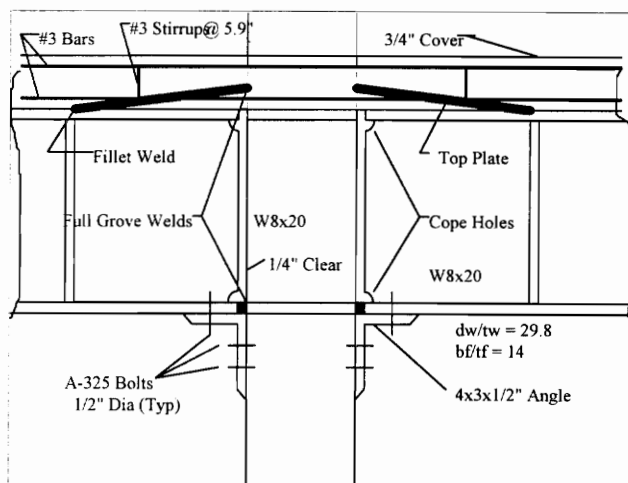   Buckling of bottom flange noticed at tips of seat angles (less than in CB2)

    Deformation of column at the level of btm flange was evident

Test Setup

Stiffened W-Section; 34"; φ; Hydraulic Jack and Load Cell

M - Theta
Dalen & Godoy
M (K-in) vs Rotation (mrad)
CB4, CB5
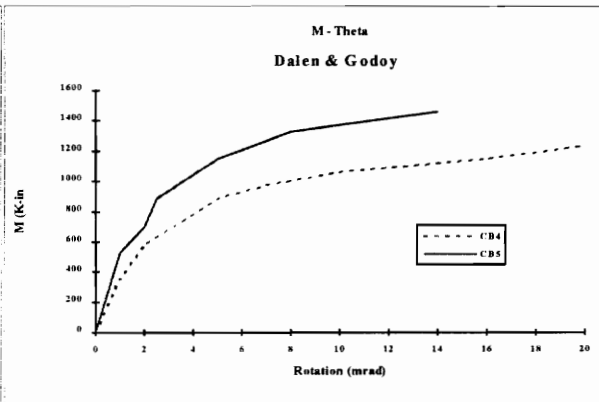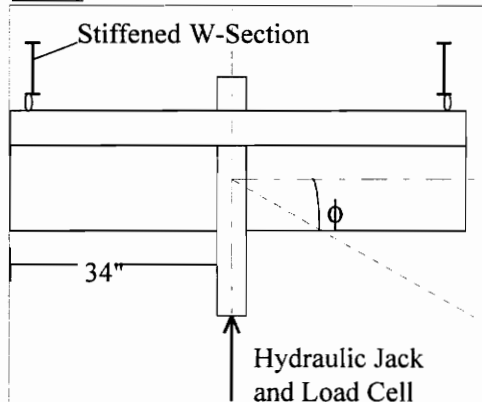
Nethercot, Lam, Davison (1990) Specimens C1 - C3

Concrete Deck		Steel Deck			
Thickness	4.75"	PMF CF46 (.05")			
Width(C3)	47.25	H=1.81"			
Width(C1&2)	70.87"				
Weight	Lightweight (Grade 25)				
Reinforcing	Dia	Area	Steel/Slab		
C1	Mesh only				
C2	0.39	0.714	0.34%		
C3	Mesh only				
Shear Studs	Dia	Height	Spacing	Number	
Welded Shear Studs			1/rib		
Material Properties		Fy (Ksi)	Fu (Ksi)		
Beam	Mp= 1752 ksi				
Girder	Mp= 2947 ksi				
Slab Reinforcing					
Concrete(C1)			6.73		
Concrete(C2)			6.87		
Concrete(C3)			6.67		

Single Layer of A-142 Mesh
For All Specimens

Deck Direction
C1 Perpendicular
C2 Perpendicular 203x203x46 UC
C3 Parallel

M20 Gr. 8.8
Bolts (Typ)
(.87" Dia all holes)

Additional Reinforcing

L2.75x2.75x0.3x6.3" single angle

305x165x46 UB (C1&2

356x171x67 UB (C3 & S

L4.9x3x.4 Seat Angle

Additional Reinforcing
C2 6-T 10mm, 47.25" lon

Results

Designation	Øu (radx10^3)	Ømax	Mc/ Mp	Mc/ Mpc	Comments
C1	22.5	27	0.149	0.097	Unable to take additional load or violent failure appeared likely
C2	21.5	26.5	0.253	0.164	Failure due to cracks in concrete behind column
C3	20.5	21.5	0.18	0.128	Unable to take additional load or violent failure appeared likely
S1		65	0.058	-	Steel only connection
S2		66	0.044	-	Steel only connection

Test Notes

Slab Cracking

Suddend reductions in stiffness at low rotations attributable to first cracking of slab

Bottom Angle

Slip of cleat connections was observed and was erratic, felt to have precipitated the formation of cracks in the slab

Local Effects

Additional General Notes

High yield bars and welded fabric mesh have limited ductility and can lead to sudden failure

Steel components of settup were fabricated by local fabricator and delivered and placed in apparatus

Specimens were tested 12-30 days after casting (shorter periods due to high early strength in concrete cube specimens)

Test Setup

Servo Controled
Hydraulic Jack

51.18"

M- Theta

Davison, Lam, Nethercot

M(K-in)

Rotation (mrad)

- - - - C1
——— C2
- - · - C3

Nethercot, Lam, Davison (1990) Specimens C4 - C5

<table>
<tr><td colspan="3">Concrete Deck</td><td colspan="2">Steel Deck</td></tr>
<tr><td>Thickness</td><td>4.75"</td><td></td><td>PMF CF46 (.05")</td><td></td></tr>
<tr><td>Width(C4)</td><td>35.4"</td><td></td><td>H=1.81"</td><td></td></tr>
<tr><td>Width(C5)</td><td>23.62"</td><td></td><td></td><td></td></tr>
<tr><td>Weight</td><td colspan="4">Lightweight (Grade 25)</td></tr>
<tr><td>Reinforcing</td><td>Dia</td><td>Area</td><td>Steel/Slab</td><td></td></tr>
<tr><td>C4</td><td>Wire Mesh Only</td><td></td><td></td><td></td></tr>
<tr><td>C5</td><td>0.39</td><td>0.714</td><td>0.79%</td><td></td></tr>
</table>

<table>
<tr><td>Shear Studs</td><td>Dia</td><td>Height</td><td>Spacing</td><td>Number</td></tr>
<tr><td>Welded Shear Studs</td><td></td><td></td><td>1/rib</td><td></td></tr>
<tr><td>Material Properties</td><td></td><td>Fy (Ksi)</td><td>Fu (Ksi)</td><td></td></tr>
<tr><td>Beam</td><td>Mp= 1752 ksi</td><td></td><td></td><td></td></tr>
<tr><td>Girder</td><td>Mp= 2947 ksi</td><td></td><td></td><td></td></tr>
<tr><td>Slab Reinforcing</td><td></td><td></td><td></td><td></td></tr>
<tr><td>Concrete(C4)</td><td></td><td></td><td>6.34</td><td></td></tr>
<tr><td>Concrete(C5)</td><td></td><td></td><td>5.48</td><td></td></tr>
</table>

Single Layer of A-142 Mesh
All Specimens

Additional Reinforcing

Deck Direction
C4 Perpendicular M20 Gr. 8.8
C5 Parallel   Bolts (Typ)
                   (.87" Dia all holes)

L2.75x2.75x0.3x6.3"
single angle

356x171x67 UB

Additional Reinforcing
C5 6-T 10mm, 63" long & 2-T 10 trim

203x203x46 UC

L4.9x3x.4 Seat Angl

EXTERNAL

Results

Designation	Øu (radx10^3)	Ømax	Mc/ Mp	Mc/ Mpc	Comments
C4	28	28	0.042	0.03	Unable to take additional load or violent failure appeared likely
C5	18	27	0.28	0.2	Unable to take additional load or violent failure appeared likely
S3		72	0.036		Steel only connection

Test Notes

<u>Slab Cracking</u>

Suddend reductions in stiffness at low rotations attributable to first cracking of slab
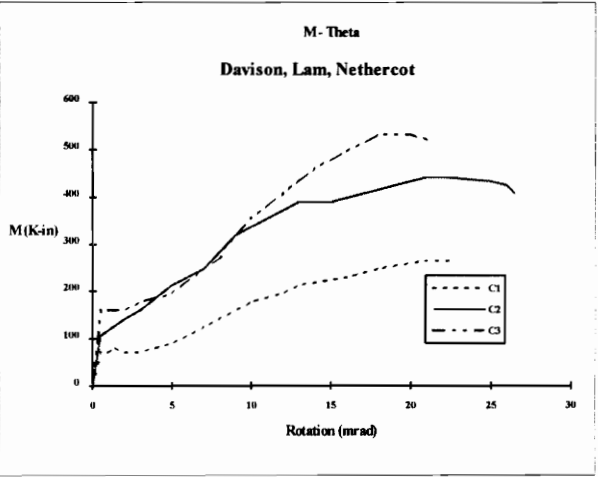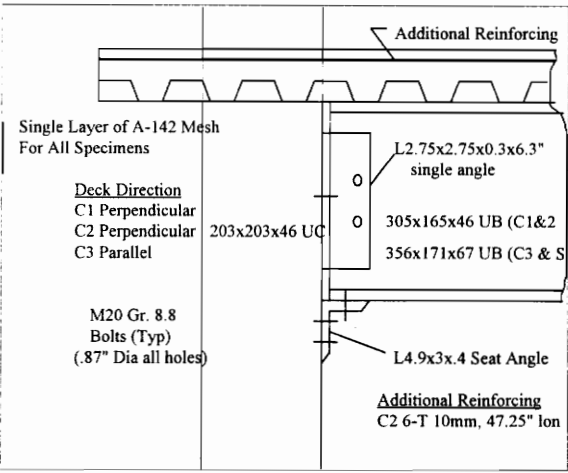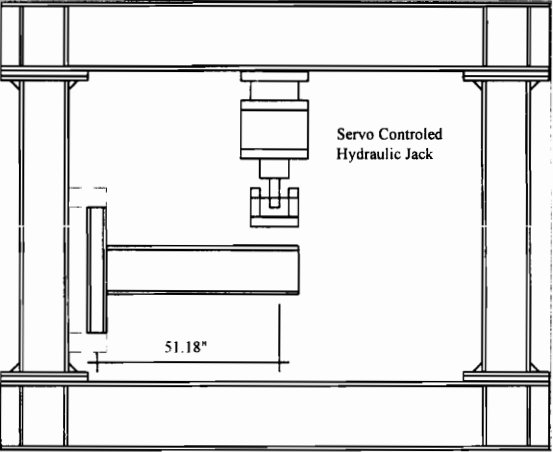
<u>Bottom Angle</u>

Slip of cleat connections was observed and was erratic, felt to have precipitated the formation of cracks in the slab

<u>Local Effects</u>

Additional General Notes

High yield bars and welded fabric mesh have limited ductility and can lead to sudden failure

Steel components of settup were fabricated by local fabricator and delivered and placed in apparatus

Specimens were tested 12-30 days after casting (shorter periods due to high early strength in concrete cube specimens)

Test Setup

Servo Controlled
Hydraulic Jack

59.1"   63"

M - Theta
Davison, Lam, Nethercot

M (K-in)

Rotation (mrad)

C4
C5

Nethercot, Lam, Davison (1990) Specimens C6 - C9

Concrete Deck		Steel Deck			
Thickness	4.75"	PMF CF46 (.05")			
Width	70.86"	H=1.81"			
Weight	Lightweight (Grade 25)				

Reinforcing	Dia	Area	Steel/Slab		
C6	Wire Mesh Only				
C7	0.39	0.714	0.34%		
C8	0.47	1.4024	0.67%		
C9	0.47	1.0518	0.50%		

Shear Studs	Dia	Height	Spacing	Number
Welded Shear Studs			1/rib	

Material Properties		Fy (Ksi)	Fu (Ksi)
Beam	Mp= 1752 ksi		
Girder	Mp= 2947 ksi		
Concrete(C6)			4.41
Concrete(C7)			4.79
Concrete(C8)			5.63
Concrete(C9)			5.61

Single Layer of A-142 Mesh Specimens — Additional Reinforcing

M20 Gr. 8.8 Bolts (Typ) (.87" Dia all holes)

L2.75x2.75x0.3x6.3" single angle

305x165x46 UB

Deck Direction C6,7,8,9 Perpendicular

203x203x46 UC

L4.9x3x.4 Seat Angle

Additional Reinforcing
C7 6-T 10mm, 63" long
C8 8-T 12mm, 74.8" long
C9 6-T 12mm, 133.86" long

Results

Designation	Øu (radx10^3)	Ømax	Mc/ Mp	Mc/ Mpc	Comments
C6	10	26	0.159	0.104	Mesh reinforcement fractured
C7	31	38	0.707	0.461	Failure sudden & premature because of the formation of cracks @ sections
C8	32.5	38	0.914	0.385	located @ ends of reinforcing bars
C9	15	28	0.808	0.526	Sudden failure when two of 6 bars fractured
S4		68	0.066		Steel only connection

Test Notes

Slab Cracking
Suddend reductions in stiffness at low rotations attributable to first cracking of slab

Bottom Angle
Slip of cleat connections was observed and was erratic, felt to have precipitated the formation of cracks in the slab

C9 was modified to prevent slip (metal packs inserted to take up end clearance, thought to be linked to premature failure)

Local Effects
Premature failure of C9 felt to be related to the increased stiffness of the bottom, thus the ductility had to come from rebar yielding
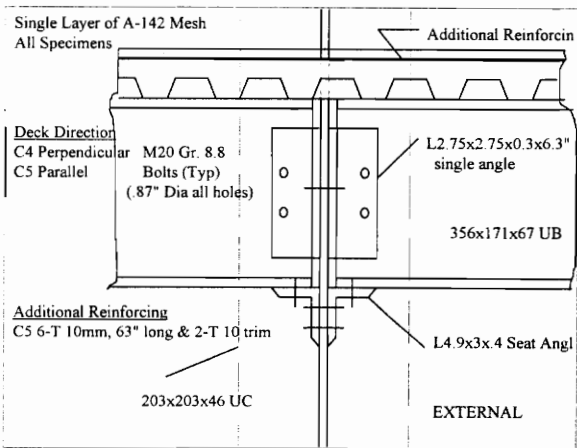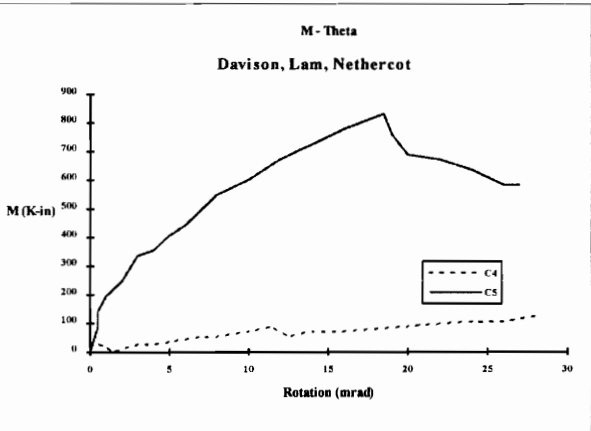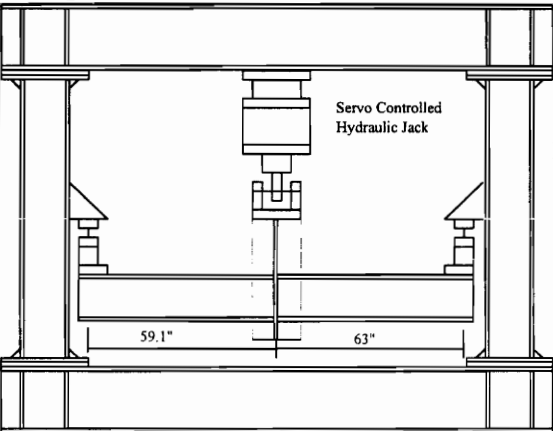
Additional General Notes
High yield bars and welded fabric mesh have limited ductility and can lead to sudden failure

Steel components of setup were fabricated by local fabricator and delivered and placed in apparatus

Specimens were tested 12-30 days after casting (shorter periods due to high early strength in concrete cube specimens)

Test Setup

Servo Controlled Hydraulic Jack

59.06"   63"

M - Theta

Davison, Lam, Nethercot

M (K-in)

Rotation (mrad)

C6
C7
C8
C9

255
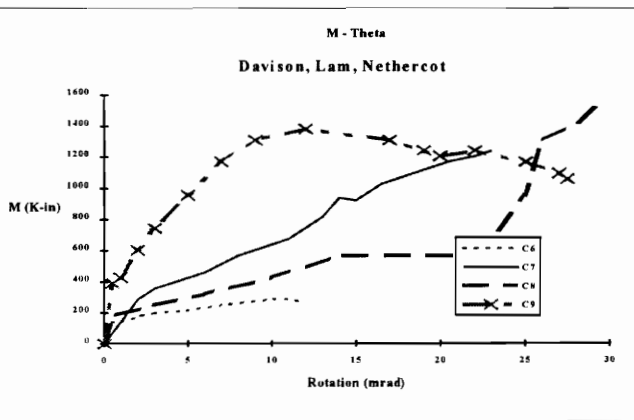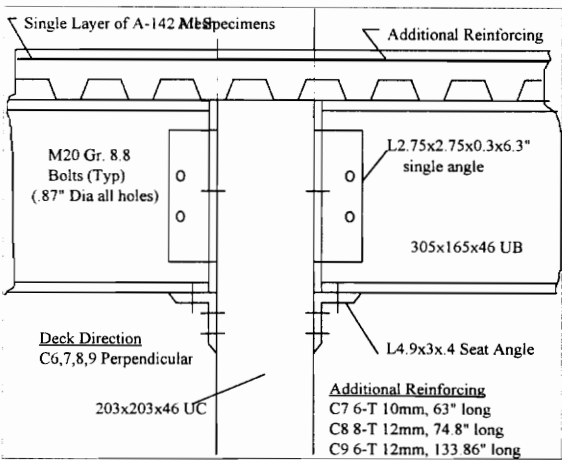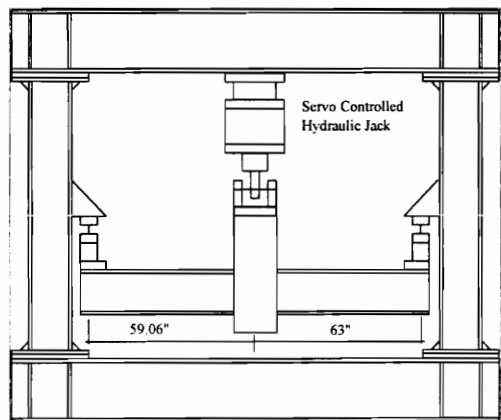
Nethercot, Lam, Davison (1990) Specimens C10 - C11

Concrete Deck		Steel Deck	
Thickness	4.75"	PMF CF46 (.05")	
Width(C10)	47.25	H=1.81"	
Width(C11)	70.87"		
Weight	Lightweight (Grade 25)		
Reinforcing	Dia	Area	Steel/Slab
C10	Wire Mesh Only		
C11	0.47	1.05	0.50%
Shear Studs	Dia	Height	Spacing	Number
Welded Shear Studs			1/rib	
Material Properties		Fy (Ksi)	Fu (Ksi)
Beam	Mp= 1752 ksi		
Girder	Mp= 2947 ksi		
Slab Reinforcing			
Concrete(C10)			5.85
Concrete(C11)			5.15

Single Layer of A-142 Mesh
All Specimens
Additional Reinforcin

Deck Direction
C10 Parallel   M20 Gr. 8.8
C11 Perpendicular Bolts (Typ)
(.87" Dia all holes)

L2.75x2.75x0.3x6.3"
single angle

356x171x67 UB

Additional Reinforcing
C11 6-T 12mm, 133.86" long

L4.9x3x.4 Seat Angl

203x203x46 UC

INTERNAL

Results

Designation	Øu (radx10^3)	Ømax	Mc/ Mp	Mc/ Mpc	Comments
C10	23	23	0.526	0.372	Unable to take additional load or violent failure appeared likely
C11	12	12	0.601	0.426	Max @ 1770 K-in, failure never reached due to inadaquate jack capacity
S5		36	0.043		Steel only connection
S6		75	0.044		Steel only connection

Test Notes

Slab Cracking

  Suddend reductions in stiffness at low rotations attributable to first cracking of slab

  First cracking in C11 occured @ 283 K-in

Bottom Angle

  Slip of cleat connections was observed and was erratic, felt to have precipitated the formation of cracks in the slab

Local Effects

  Initial stiffness of C11 5620 K/rad
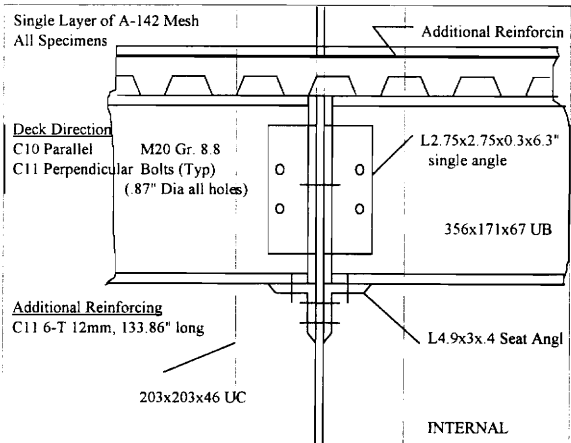
Additional General Notes

  High yield bars and welded fabric mesh have limited ductility and can lead to sudden failure

  Steel components of settup were fabricated by local fabricator and delivered and placed in apparatus

  Specimens were tested 12-30 days after casting (shorter periods due to high early strength in concrete cube specimens)

Test Setup

Servo Controlled
Hydraulic Jack

59.1"   63"

M - Theta

Davison, Lam, Nethercot

M (K-in)

Rotation (mrad)

..... C10
—— C11

Nethercot, Lam, Davison (1990) Specimen C12

Concrete Deck		Steel Deck			
Thickness	4.75"	PMF CF46 (.05")			
Width	70.87	H=1.81"			
Weight	Lightweight (Grade 25)				
Reinforcing	Dia	Area	Steel/Slab		
C12	Wire Mesh Only				
Shear Studs	Dia	Height	Spacing	Number	
Welded Shear Studs			1/rib		
Material Properties		Fy (Ksi)	Fu (Ksi)		
Beam	Mp= 1752 ksi				
Girder	Mp= 2947 ksi				
Slab Reinforcing					
Concrete			5.93		
Stud Capacity					

Single Layer of A-142 Mesh

M20 Gr. 8.8
Bolts (Typ)
(.87" Dia all holes)

L2.75x2.75x0.3x6.3"
single angle

305x165x46 UB

Deck Direction
C12 Perpendicular

L4.9x3x.4 Seat Angle

****UNSURE OF ACTUAL CONNECTION
INTERNAL

Results

Designation	Øu (radx10^3)	Ømax	Mc/ Mp	Mc/ Mpc	Comments
C12	15	15	0.091	0.059	Unable to take additional load or violent failure appeared likely
S7		68	0.031		Steel only connection

Test Notes

Slab Cracking

Suddend reductions in stiffness at low rotations attributable to first cracking of slab

Bottom Angle

Slip of cleat connections was observed and was erratic, felt to have precipitated the formation of cracks in the slab
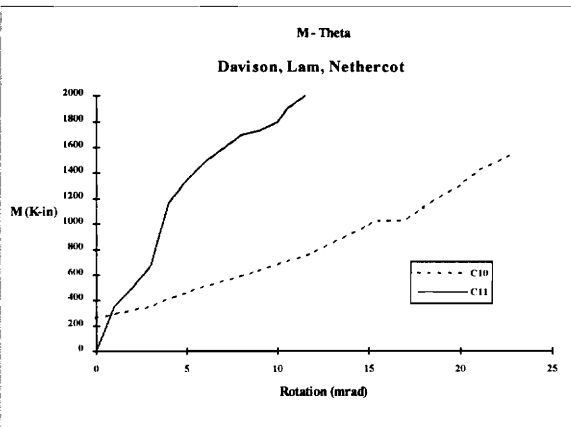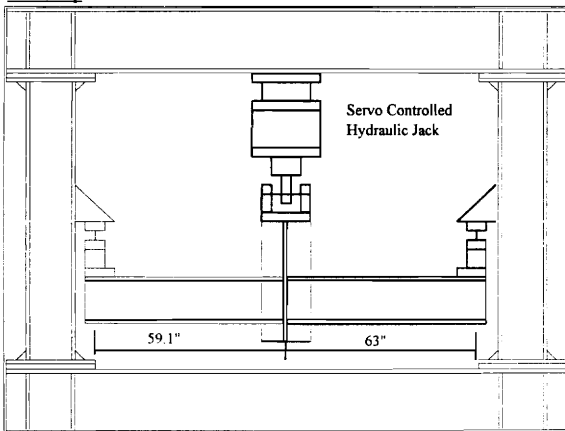
Local Effects

Additional General Notes

High yield bars and welded fabric mesh have limited ductility and can lead to sudden failure

Steel components of setup were fabricated by local fabricator and delivered and placed in apparatus

Specimens were tested 12-30 days after casting (shorter periods due to high early strength in concrete cube specimens)

Test Setup

Servo Controlled
Hydraulic Jack

59.1"   63"

**UNSURE OF ACTUAL TEST SETUP **

M - Theta

Davison, Lam, Nethercot

M (K-in)

Rotation (mrad)

- - - - - C12

257

Altman, Maquoi, Jaspart (1991) Specimens 30 x 3c. 1,2,3,6,7,8

Concrete Deck		Steel Deck		
Thickness	4.7"	None		
Width	47.24"			
Weight	Normal			
Reinforcing	Dia	Area	Steel/Slab	
30x3c.2,6	0.394	1.4630636	0.67%	
30x3c.3,8	0.551	2.8613696	1.30%	
30x3c.1,7	0.709	4.73765281	2.10%	
Shear Studs	Dia	Height	Spacing	Number
Full interaction				

Material Properties	Fy (Ksi)	Fu (Ksi)
Beam		
Column		
Plate		
Slab Reinforcing		
Concrete		
Stud Capacity		

6 - 10, 14, 18 mm Dia. Bar Ea. Layer

4.7" slab

8.8 H. S. Bolts (Typ) (1mm clearance typ)

IPE 300

HEB 200

L5.9x3.5x(0.39 or 0.51) single angles

0.59" clearance

30x3c.1,2,3 = .39 angles

30x3c.6,7,8 = .51 angles

Results

Designation	Ø (radx10^3)	Mc/ Mp	Comments on failure
30x3c.2		0.99	Buckling of the column web at the level of the lower cleats; attained max vert. disp.
30x3c.3		0.98	Buckling of the column web at the level of the lower cleats
30x3c.1		0.94	Buckling of the column web at the level of the lower cleats
30x3c.6		1.14	Buckling of the column web at the level of the lower cleats; attained max vert. disp.
30x3c.8		0.95	Buckling of the column web at the level of the lower cleats
30x3c.7		0.95	Buckling of the column web at the level of the lower cleats

Test Notes

Bottom Angle

 Slip between lower cleat and beam flange significant source of deformation

Local Effects

 Most tests failed by buckling of column web or by excessive yielding of rebar

 Single web cleat felt to produce small bending moments in the web

Additional General Notes

 Rotational rigidity and ultimate capacity of the connection was not believed to be strongly affected by the thickness of the cleats

 Top cleat does not have a significant affect until all rebars have yielded

 % of slab steel had significant influence on moment capacity and rigidity

 Buckling of lower beam flange controlled all tests that had IPE 240 beams

Test Setup

95.25"   95.25"

90.5"

Jack (50 ton w/ 7.87" disp.)

258

Altman, Maquoi, Jaspart (1991) Specimens 30 x 2c. 1,2,3,5,6,7

Concrete Deck		Steel Deck		
Thickness	4.7"	None		
Width	47.24"			
Weight	Normal			
Reinforcing	Dia	Area	Steel/Slab	
30x2c.2,5	0.394	1.4630636	0.67%	
30x2c.1,6	0.551	2.8613696	1.30%	
30x2c.3,7	0.709	4.73765281	2.10%	
Shear Studs	Dia	Height	Spacing	Number
Full interaction				

Material Properties		Fy (Ksi)	Fu (Ksi)
Beam			
Column			
Plate			
Slab Reinforcing			
Concrete			
Stud Capacity			

6 - 10, 14, 18 mm Dia. Bar Ea. Layer

4.7" slab

8.8 H. S. Bolts (Typ) (1mm clearance typ)

IPE 300

HEB 200

L5.9x3.5x(0.39 or 0.51) single angles

0.59" clearance

30x2c.1,2,3 = .39 angles
30x2c.5,.6,7 = .51 angles

Results

Designation	Ø (radx10^3)	Mc/ Mp	Comments on failure
30x2c.2		0.81	Reached max possible verticle deflection; due to excessive yielding of rebar
30x2c.1		0.89	Brittle Failure; bolts connecting lower cleats & beam flange failed in shear
30x2c.3		0.94	Buckling of the column web at the level of the lower cleats
30x2c.5		0.79	Reached max possible verticle deflection; due to excessive yielding of rebar
30x2c.6		0.99	Buckling of the column web at the level of the lower cleats
30x2c.7		0.94	Buckling of the column web at the level of the lower cleats

Test Notes

Bottom Angle

Slip between lower cleat and beam flange significant source of deformation

Local Effects

Most tests failed by buckling of column web or by excessive yielding of rebar

Single web cleat felt to produce small bending moments in the web
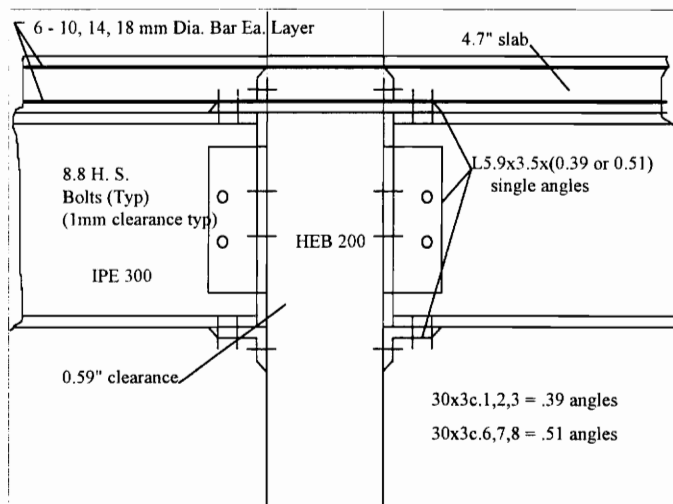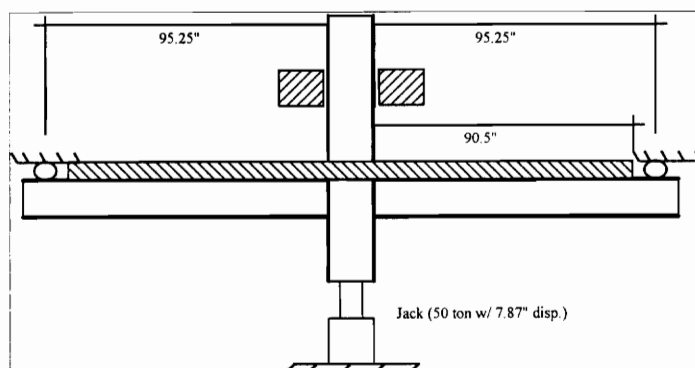
Additional General Notes

Rotational rigidity and ultimate capacity of the connection was not believed to be strongly affected by the thickness of the cleats

% of slab steel had significant influence on moment capacity and rigidity

Buckling of lower beam flange controlled all tests that had IPE 240 beams

Test Setup

95.25"   95.25"

90.5"

Jack (50 ton w/ 7.87" disp.)

259

Altman, Maquoi, Jaspart (1991) Specimens 36 x 3c. 1,2,3,5,6,7

Concrete Deck		**Steel Deck**		
Thickness	4.7"	None		
Width	47.24"			
Weight	Normal			
Reinforcing	Dia	Area	Steel/Slab	
36x3c.1,5	0.394	1.4630636	0.67%	
36x3c.2,6	0.551	2.8613696	1.30%	
36x3c.3,7	0.709	4.73765281	2.10%	
Shear Studs	Dia	Height	Spacing	Number
Full interaction				

Material Properties		Fy (Ksi)	Fu (Ksi)
Beam			
Column			
Plate			
Slab Reinforcing			
Concrete			
Stud Capacity			

Diagram labels:
6 - 10, 14, 18 mm Dia. Bar Ea. Layer
4.7" slab
8.8 H. S. Bolts (Typ) (1mm clearance typ)
L5.9x3.5x(0.39 or 0.51) single angles
HEB 200
IPE 360
0.59" clearance
36x3c.1,2,3 = .39 angles
36x3c.5,6,7 = .51 angles
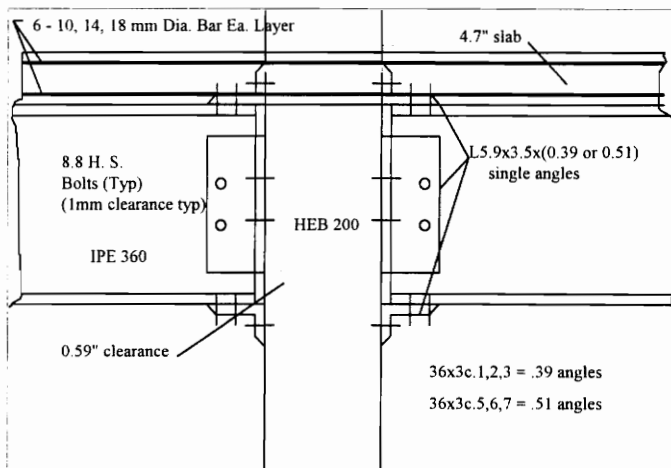
Results

Designation	Ø (radx10^3)	Mc/ Mp	Comments on failure
36x3c.1		0.77	Buckling of the column web at the level of the lower cleats
36x3c.2		0.79	Buckling of the column web at the level of the lower cleats
36x3c.3		0.8	Buckling of the column web at the level of the lower cleats
36x3c.5		0.79	Buckling of the column web at the level of the lower cleats
36x3c.6		0.84	Buckling of the column web at the level of the lower cleats
36x3c.7		0.85	Buckling of the column web at the level of the lower cleats

Test Notes

Bottom Angle
 Slip between lower cleat and beam flange significant source of deformation

Local Effects
 Most tests failed by buckling of column web or by excessive yielding of rebar
 Single web cleat felt to produce small bending moments in the web
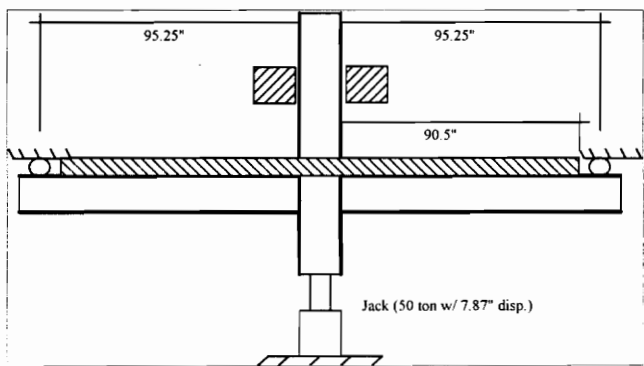
Additional General Notes
 Rotational rigidity and ultimate capacity of the connection was not believed to be strongly affected by the thickness of the cleats
 Top cleat does not have a significant affect until all rebars have yielded
 % of slab steel had significant influence on moment capacity and rigidity
 Buckling of lower beam flange controlled all tests that had IPE 240 beams

Test Setup

Diagram labels:
95.25"
95.25"
90.5"
Jack (50 ton w/ 7.87" disp.)

260

Altman, Maquoi, Jaspart (1991) Specimens 36 x 2c. 1,2,3,5,6,7

Concrete Deck		Steel Deck			
Thickness	4.7"	None			
Width	47.24"				
Weight	Normal				
Reinforcing	Dia	Area	Steel/Slab		
36x2c.2,7	0.394	1.4630636	0.67%		
36x2c.1,6	0.551	2.8613696	1.30%		
36x2c.3,5	0.709	4.73765281	2.10%		
Shear Studs	Dia	Height	Spacing	Number	
Full interaction					

Material Properties		Fy (Ksi)	Fu (Ksi)
Beam			
Column			
Plate			
Slab Reinforcing			
Concrete			
Stud Capacity			

Results

Designation	Ø (radx10^3)	Mc/ Mp	Comments on failure
36x2c.2		0.67	Collapse (in tension) of the reinforcements in the concrete slab
36x2c.1		0.78	Buckling of the column web at the level of the lower cleats
36x2c.3		0.82	Buckling of the column web at the level of the lower cleats
36x2c.7		0.67	Reached max possible verticle deflection; due to excessive yielding of rebar
36x2c.6		0.77	Buckling of the column web at the level of the lower cleats
36x2c.5		0.83	Buckling of the column web at the level of the lower cleats

Diagram labels: 6 - 10, 14, 18 mm Dia. Bar Ea. Layer; 4.7" slab; 8.8 H. S. Bolts (Typ) (1mm clearance typ); HEB 200; IPE 360; L5.9x3.5x(0.39 or 0.51) single angles; 0.59" clearance; 36x2c.1,2,3 = .39 angles; 36x2c.5,.6,7 = .51 angles

Test Notes

Bottom Angle

Slip between lower cleat and beam flange significant source of deformation

Local Effects

Most tests failed by buckling of column web or by excessive yielding of rebar

Single web cleat felt to produce small bending moments in the web
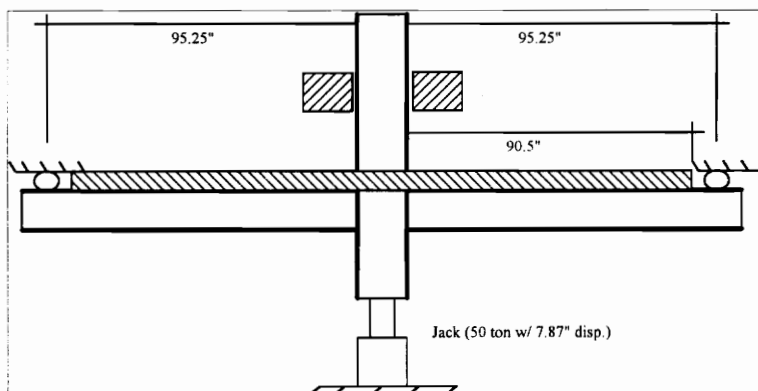
Additional General Notes

Rotational rigidity and ultimate capacity of the connection was not believed to be strongly affected by the thickness of the cleats

% of slab steel had significant influence on moment capacity and rigidity

Buckling of lower beam flange controlled all tests that had IPE 240 beams

Test Setup

Diagram labels: 95.25"; 95.25"; 90.5"; Jack (50 ton w/ 7.87" disp.)

261

APPENDIX B

ONE PAGE SUMMARIES OF RESEARCH ON SEMI-RIGID CONNECTIONS ASSOCIATED WITH LEON

LEON (1987) SPECIMENS SRCC1MR & SRCC1ML

Concrete Deck		Steel Deck		
Thickness	4	Height	None	
Width	60			
Weight	110		Ar*fyr/	
Reinforcing	Area	Steel/Slab	Af*fyf	
SRCC1Mx	1.6	0.66	0.684	

Shear Studs	Dia	Height	Spacing	Number
SRCC1Mx	5/8"	2-1/2"	1/6"	19/ea

Material Properties		Fy (Ksi)	Fu (Ksi)
Joist Flange		42.50	?
Joist Web		42.50	?
Seat Angle		36.00	58.00
Slab Reinforcing		63.10	90.00
Concrete	SRCC1Mx		?
Stud Capacity	?		

dw/tw = 42.2
bf/tf = 13.1

W14x99

1/2" Clear

SRCC1ML

A-325 3/4"Dia Bolts (Typ)
(All holes 1/16" oversize)
(friction grip)

8-#4 Bars

2L4x3.5x1/4x8.5" double web angles

W14x38

SRCC1MR

L6x4x3/8x8" seat angle
(top & bottom right side only)

Results Mp= 2610

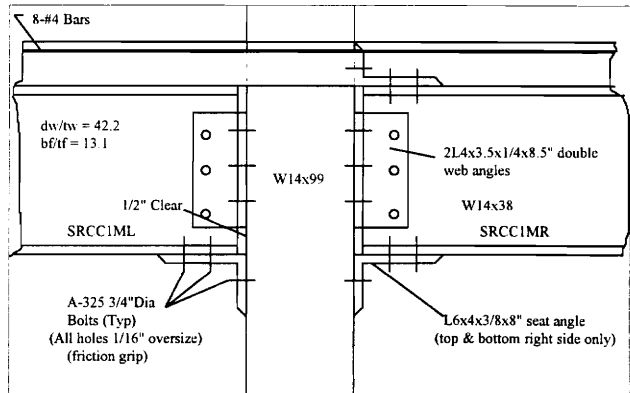| Designation	Mdc (K-in)	Mpc(-) (K-in)	Muc (K-in)	Muc/ Mdc	Muc/ Mp	Muc/ Mpc(-)	Øuc (radx10^3)	Comments
SRCC1ML	1682	3469	2080	1.24	0.8	0.6	39	Beam end deflection = 2.5"
SRCC1MR	1682	3469	2700	1.61	1.03	0.78	47	Beam end deflection = 7.5"
								two bolts in btm angle fractured in shear

Test Notes

Concrete Cracking
* First cracking observed in left beam at 500 K-in begging @ column flange tips and extending to slab edge and through slab
* @ 560 K-in same cracking occured in the right beam

Bottom Angle
* @ 700 K-in loud noised heard signifying the slippage of the left bottom angle
* No visible yielding of the bottom angles noted

Local Effects
* @970 K-in, nut on one bolt in left bottom flange showed large crack (specimen was unloaded and nut was replaced)
* Unloading resulted in residual deformations of .57" and .19" for the left and right beam respectively
* Rebar began to yield @ 1,800 K-in
* Yielding of column web began @ 1250 K-in (even though the web and flange met AISC criteria for a load up to 94 K (80 K applied))
* @ 1300 K-in, Yielding of btm left beam flange was noticed near the connection and yielding of web angles

Additional General Notes
* The horizontal shear in the bolts at failure was 45K (3x allowed)
* Three distinct phases: Linear behavior lasting until the friction capacity of the bolts was exceeded in the bottom angles
  (M<600 K-in); Slippage of bolts until they began to work in bearing (600 - 1500 K-in); Long almost
  plastic curve with no strength deterioration and excellent ductility
* Much more initial linear behavior associated with the top angle connection
* Strain gage readings indicated outer bars carrying about half as much load as inner bars up to yield
* Web crippling might not be as severe a problem in semi-rigid connections as in rigid connections

Test Setup

120"   120"

WF 14x99

145-7/8"

WF 14x38

Reference Frame

1'

Load Cell

Hydraulic ram

M - Theta
LEON

Initial Stiffness
M R = 2.26 M K"/rad
M L = 2.00 M K"/rad

M (K-in)

- - - - SRCC1MR
——— SRCC1ML

Rotation (mrad)
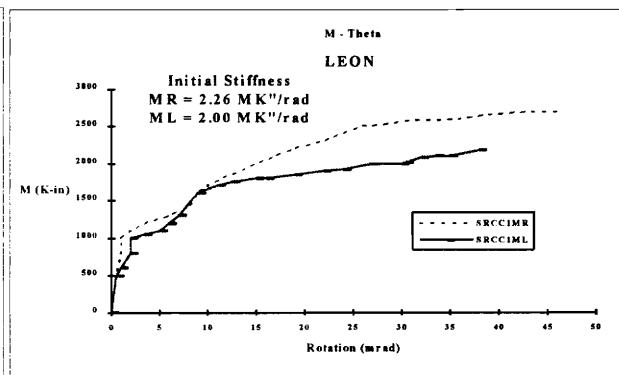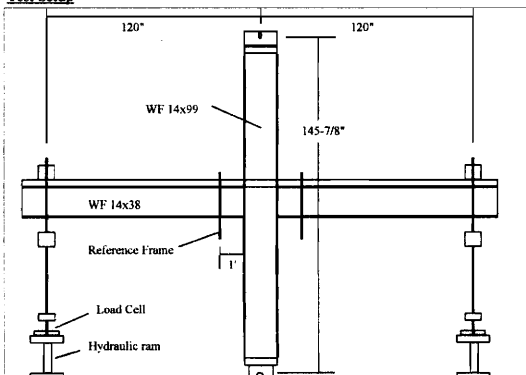
LEON (1987) SPECIMEN SRCC1C

Concrete Deck		Steel Deck	
Thickness	4	Height	None
Width	60		
Weight	110		Ar*fyr/
Reinforcing	Area	Steel/Slab	Af*fyf
SRCC1Cx	1.6	0.66	0.684

Shear Studs	Dia	Height	Spacing	Number
SRCC1Cx	5/8"	2-1/2"	1/6"	19/ea

Material Properties		Fy (Ksi)	Fu (Ksi)
Joist Flange		?	?
Joist Web		?	?
Seat Angle		36.00	58.00
Slab Reinforcing		60.00	90.00
Concrete	SRCC1Cx		?
Stud Capacity	?		

Results Mp=2610 K"

8-#4 Bars

dw/tw = 42.2
bf/tf = 13.1

W14x99

1/2" Clear

SRCC1CL

2L4x3.5x1/4x8.5" double web angles

W14x38

SRCC1CR

A-325 3/4"Dia Bolts (Typ) (All holes 1/16" oversize) (friction grip)

L6x4x3/8x8" seat angle (top & bottom right side only)

Designation	Pos Mom Load Stage	Ml (K-in)	Mr (K-in)	Ø mRad	Ø mRad	Ml/My	Mr/My	Comments
SRCC1Cx	1	240	162	0	0.60			Linear behavior
SRCC1Cx	2	625	536	2	1.40			
SRCC1Cx	3	923	926	4	3.80			
SRCC1Cx	4	1052	1048	6	6.10			
SRCC1Cx	5	1145	1188	10	8.50			
SRCC1Cx	6	1313	1283	17.7	12			Residual deformation of 1" & 2"

Test Notes

Concrete Cracking
* Cracking of slab @ column face giving early loss of stiffness
* Opening of cracks and angles pulling away from the column gave rise to pinching of the hysteresis loop in later cycles

Bottom Angle
* Angle began to seperate from column face @ 1.02% drift, as well as slip along beam flange
* Cracking of the angle was observed

Local Effects
* Yielding of rebar starting @ 1.02% drift leading to large non-linearities
* @ the high levels of drift significant shear strains and a small amount of yielding were present in the panel zone
          (no loss of web stability)

Additional General Notes
* The moment rotation curve follows the moment rotation for the monotonic testing
* Strains in the column web not nearly as severe compared to rigid connections (felt concrete btwn column flanges acts as stiffner)
* The top angle felt not to have much affect, and removal decreases cost and simplifies erection
* Possible failure modes for type 1 connections; Buckling or yielding of compression members; slip and shearing of bolts; shear
          failure of the web connection
* As bars farther away start to yield, bars adjacent to column start strain hardening
* Rotations in excess of 60 mrad recorded for type 1 connections

Test Setup   (Unsure of actual test setup)

120"   120"

WF 14x99

145-7/8"

WF 14x38

Reference Frame

1'

4x4x1/4" Tube

M - Theta

LEON

M (K-in)

SRCC1CL
SRCC1CR

Rotation (mrad)
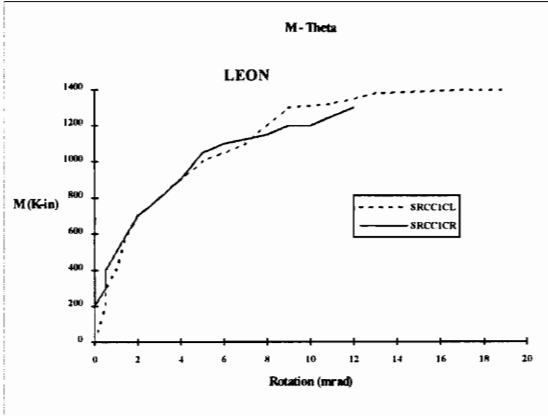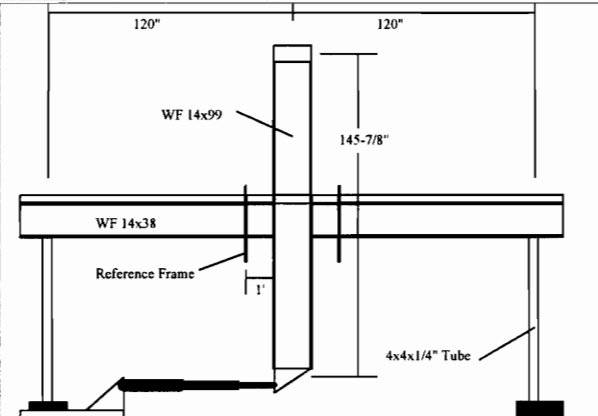
LEON (1987) SPECIMEN SRCF2C

Concrete Deck		Steel Deck			
Thickness	4 or 3 ?"	Height	2"		
Width	60				
Weight	110				
Reinforcing	Area	Steel/Slab			
SRCF2C	1.6	0.66			

Shear Studs	Dia	Height	Spacing	Number	
SRCF2C	?	?	2/12"	Full Comp	

| Material Properties		Fy (Ksi)	Fu (Ksi)		
Joist Flange		?	?		
Joist Web		?	?		
Seat Angle		36.00	58.00		
Slab Reinforcing		60.00	90.00		
Concrete	SRCF2C		?		
Stud Capacity	?				

8-#4 Bars

2L4x4x1/4x11" double web angles

W14x120

W14x38

1/2" Clear

A-325 1"Dia Bolts (Typ) (Turn of nut method) (friction grip)

L7x4x3/8x8" seat angle

Results

Designation	Description	Steel Area (in^2)	Mc (K-in)	Muc (K-in)	Myc/ Myb	Muc/ Mub	Ø (radx10^3)	Comments
SRCF2C	Gravity load	1.6	621	NA	-	NA	0.3	End of gravity loading
SRCF2C	Interior	1.6	1440	NA	-	NA	8	Reaced drift of 3.5%
SRCF2C	Exterior	1.6	1760	NA	-	NA	17	
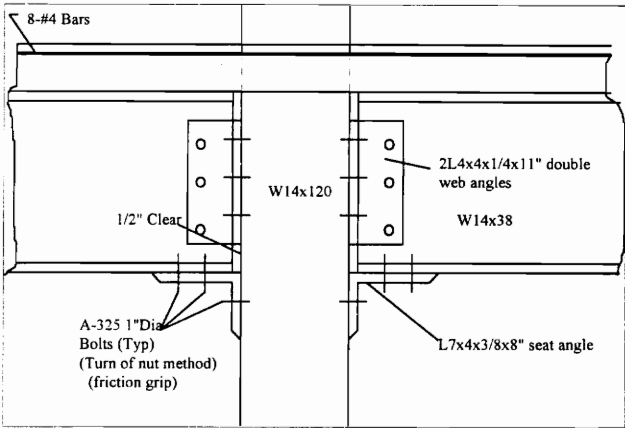
Test Notes

Concrete Cracking

Small cracks appeared at the end of the gravity loading

Exterior connection with one transverse bar failed at a drift of 1.5% due to large longitudinal cracks but was able

to readjust and surpass the previous maximum load

Exterior connection with 3 transverse bars exibited very well distributed cracking and continued to increase load until end of tests

Very large cracks in slab at drifts of 3% and & 3.5%

Bottom Angle

Angles in tension seperated about 1/32" from the column face

Angles yielded at drifts of 3% & 3.5%

No slippage of angles was noted throughout the test

Angles failed in low-cycle fatigue, angles were replaced and frame behave similar to frame before failure

Local Effects

Connection behaved linear with gravity and lateral loads up to 0.1% and 0.25% drift

Yeilding in the colum panel zone starting @ 1% drift (primarily @ interior connection) even though web and flanges

met all recommendations for fully rigid connections (cause thought to be difference in force transmission to

column)

Additional General Notes

Effective width of 8*t was arbitrary

Deeper beams should yield a linear increase in strength

Stiffness should be proportional to the square of the increase in depth

Initial stiffness is higher in the hogging than in the sagging moment region due to bottom angle pullout

Rotation measured with pair of LVDTs attached to beam @ 12" from column face

Gravity load (P) applied first, then lateral loads applied, lateral loads were deflection controlled

Test Setup

1-#4 Transverse Bar

P (up to 16 K)

3-#4 Transverse Bars

13'

2'

W14x38

W14x120

25'-8"   25'-8"

M - Theta

LEON

SRCF2C

M (K-in)

Ki = 2.07 x 10^6 K/in @ Rotation = 0.3 mrad

Rotation (mrad)
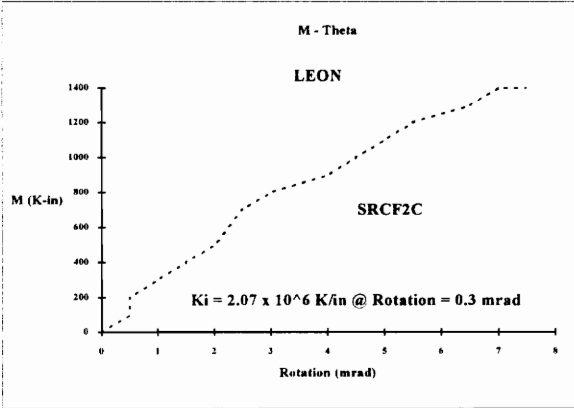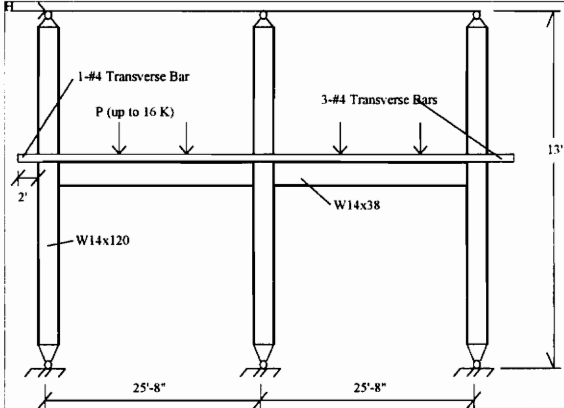
LEON (1987) SPECIMEN SRCC3C

Concrete Deck		Steel Deck		
Thickness	4 or 4-3/4"	Height	2" ??	
Width	60			
Weight	110			
Reinforcing	Area	Steel/Slab		
SRCC3C	1.6	0.66		

Shear Studs	Dia	Height	Spacing	Number
SRCC3C	5/8"	2-1/2"	1/6"	19/ea

Material Properties		Fy (Ksi)	Fu (Ksi)
Joist Flange		?	?
Joist Web		?	?
Seat Angle		36.00	58.00
Slab Reinforcing		60.00	90.00
Concrete	SRCC3C		?
Stud Capacity	?		
Results	Mp= 2610 K"		

8-#4 Bars
W14x120
1/2" Clear
2L4x4x1/4x11" double web angles
W14x38
A-325 3/4"Dia Bolts (Typ) (Turn of nut method) (friction grip)
L7x4x1/2x9-1/2" seat angle

Designation	Description	Steel Area (in^2)	Mc (K-in)	Muc (K-in)	Myc/ Myb	Muc/ Mub	Ø (radx10^3)	Comments
SRCC3C	West	1.6	960	NA	-	NA	4	
SRCC3C	East	1.6	1488	NA	-	NA	4	
SRCC3C	Neg Mom	1.6	1277	NA	-	NA	3.72	
SRCC3C	Pos Mom	1.6	1034	NA	-	NA	3.63	
SRCC3C	Neg Mom	1.6	NA	1878	NA	-		
SRCC3C	Pos Mom	1.6	NA	1718	NA	-		

Test Notes

Concrete Cracking

Cracking of slab begging at column face @ 0.25% drift loading

@ 1% story drift cracks in slab began to open signalling the first yield of the slab steel

Bottom Angle

No observable slip of the tension angles up to drift of 1%

Significant slip at drifts of 2%

Maximum slip of 0.09" at drift of 3.5%

Local Effects

Behavior elastic up to a 0.75% drift

Extensive shear yielding of the web of the column was observed beginning at drifts of 1.0% and increased steadily

Additional shear yielding possibly due to larger angles

Additional General Notes

Effective width of 8*t was arbitrary

Deeper beams should yield a linear increase in strength

Stiffness should be proportional to the square of the increase in depth

Possibly replace the 4EI/L stiffness coefficient with 3.8EI/L for a connection with 90% of full rigidity

Paper provides a list of requirements for a semi-rigid model

Test Setup

112-3/4"   112-3/4"
WF 14x120
155-1/3"
WF 14x38
Reference Frame
1'
4x4x1/4" Tube

M - Theta
LEON
SRCC3C
M (K-in)
Rotation (mrad)
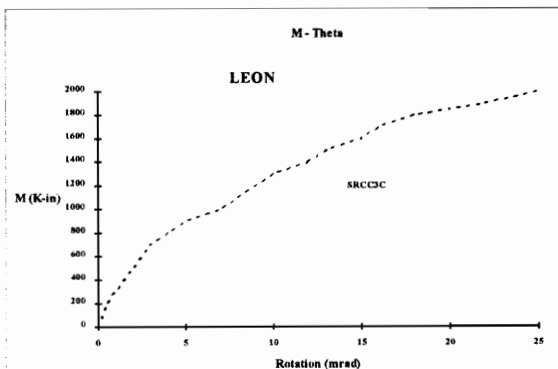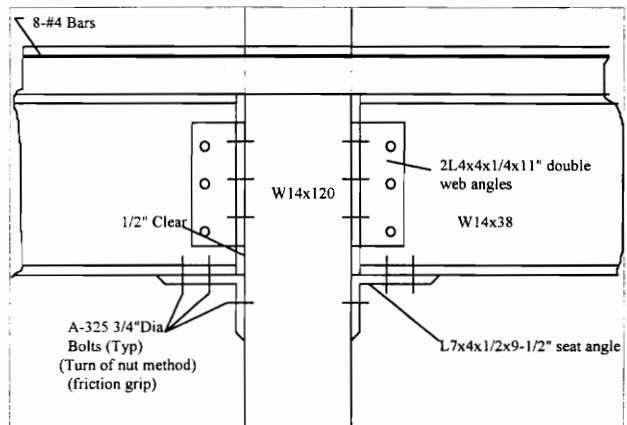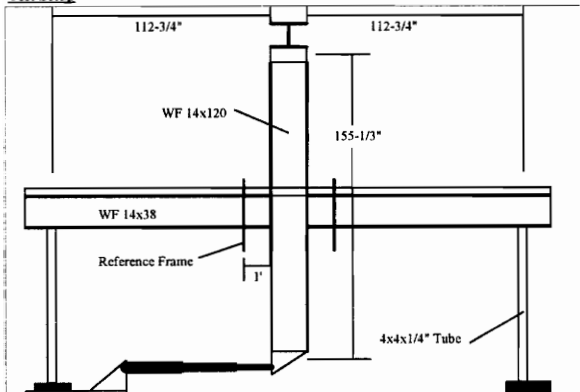
LEON (1990) SPECIMEN SRCC4M

Concrete Deck		Steel Deck	
Thickness	5	Height	2
Width	?		
Weight	?		

Reinforcing	Area	Steel/Slab
SRCC4M	1.6	0.66

Shear Studs	Dia	Height	Spacing	Number
SRCC4M	3/4"	?	2/flute	?

Material Properties		Fy (Ksi)	Fu (Ksi)
Beam		36.00	
Column			
Plate			
Slab Reinforcing			
Concrete	SRCC4M		
Stud Capacity			
Results		Mp=4644	Z = 129

8-#4 Bars

5" slab on 2" deck

A-325 7/8"Dia Bolts (Typ) (twist off)

W14x145

2L5x5x5/16x14.5" double web angles

W21x57

0.5"x8" fillet (ea/side) full pen grove weld

PL 8" wide x 0.5" thick x 10" long
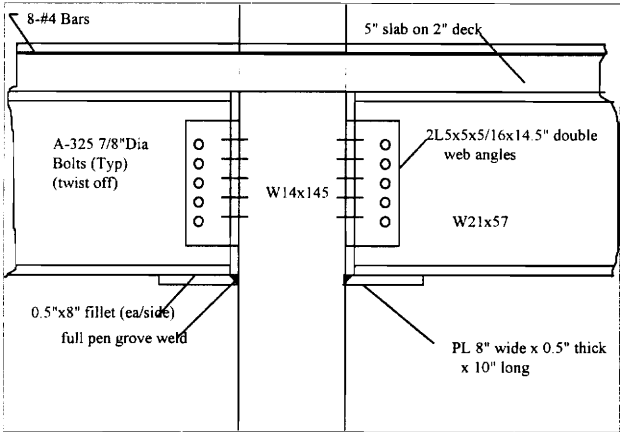
Designation	Description	Mc (K-in)	Muc (K-in)	Mc/ My	Mc/ Mp	Ø (radx10^3)	Comments
SRCC4M		830			0.16	0.1	Initial slab cracking
SRCC4M		2972			0.64	3.2	First yield of reinforcing bars
SRCC4M			4505		0.97	12.3	Maximum Moment
SRCC4M		4000			0.86	17	Test stopped

Test Notes

Concrete Cracking

Slab cracked @ 830 K-in Stiffness decreased to about 1/10 of initial value

Bottom Plate

Local Effects

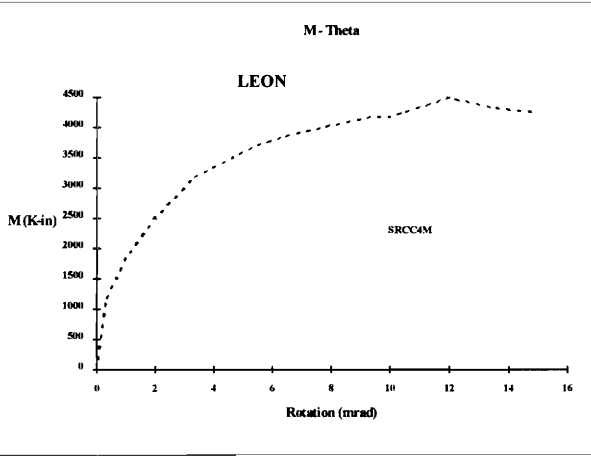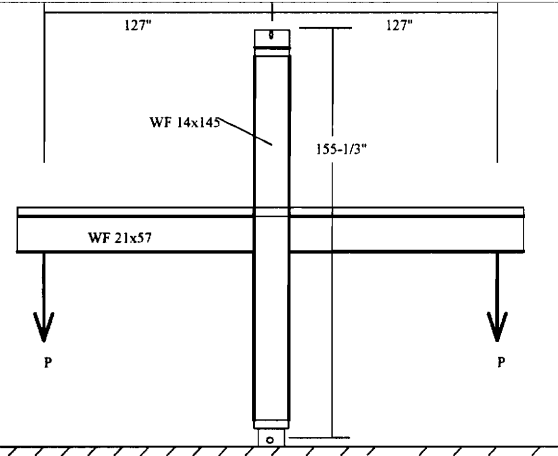Reinforcing began yield @ 2972, stiffness dropped to 1/6 of prior yield

Additional General Notes

Flange plate could possibly be replaced with T-stub or very thick end plate

Test Setup

127"   127"

WF 14x145

155-1/3"

WF 21x57

P   P

M - Theta

LEON

4500
4000
3500
3000
M (K-in) 2500
2000
1500
1000
500
0

SRCC4M

0   2   4   6   8   10   12   14   16

Rotation (mrad)

LEON (1990) SPECIMEN SRCC5M

Concrete Deck		Steel Deck			
Thickness	5	Height	2		
Width	?				
Weight	?				
Reinforcing	Area	Steel/Slab			
SRCC5M	1.6	0.66			

Shear Studs	Dia	Height	Spacing	Number
SRCC5M	3/4"	?	2/flute	?

Material Properties		Fy (Ksi)	Fu (Ksi)
Beam		36.00	
Column			
Seat Angle			
Slab Reinforcing			
Concrete	SRCC5M		
Stud Capacity			
Results	Mp=4644	Z = 129	

8-#4 Bars

5" slab on 2" deck

A-325 7/8"Dia Bolts (Typ) (twist off)

W14x145

W21x57

L8x8x3/4x10.25" seat angle
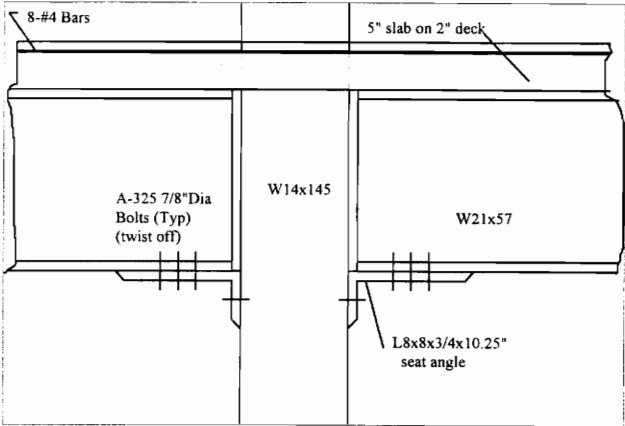
Designation	Description	Mc (K-in)	Muc (K-in)	Mc/ My	Mc/ Mp	Ø (radx10^3)	Comments
SRCC5M		1667			0.36	3	
SRCC5M		2842			0.61	10	
SRCC5M			3343		0.72	39	Ultimate
SRCC5M		3019			0.65	43.3	Sudden slippage of btm angle connection

Test Notes

Concrete Cracking

Slab cracked @ 830 K-in Stiffness decreased to about 1/10 of initial value

Bottom Angle

Sudden slippage .15" occured at 134K (2.19 *allowable force for this detail)

Local Effects

Reinforcing began yield @ 2972, stiffness dropped to 1/6 of prior yield

Small amount of yielding in the fillet of the column where the btm angle bore

Additional General Notes

Small clip angle near top probly required during construction

Care must be taken to avoid local web failure

Test Setup

127"   127"

WF 14x145

155-1/3"

WF 21x57

P   P

M- Theta

LEON

SRCC5M

M(K-in)

3000

2500

2000

1500

1000

500

0

Rotation (mrad)

0 1 2 3 4 5 6 7 8 9 10
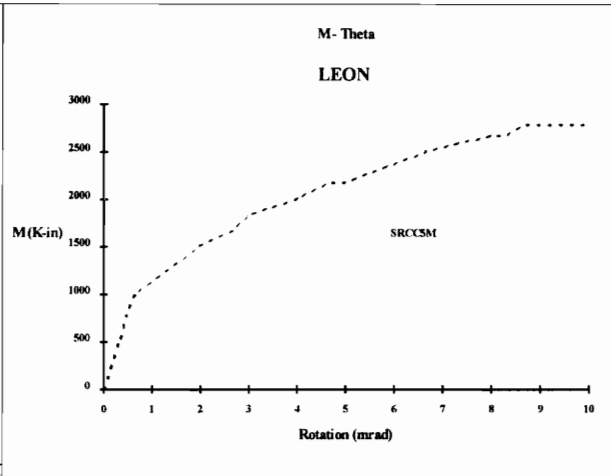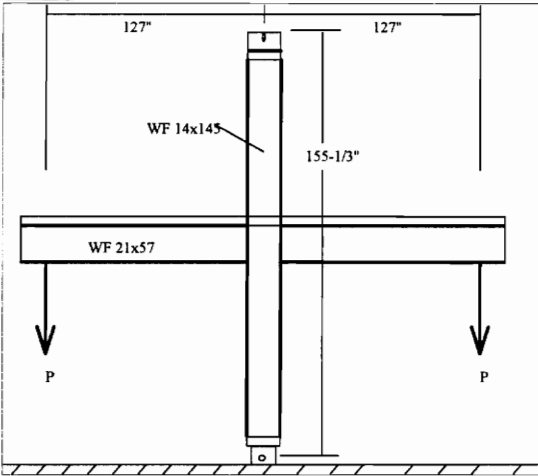
LEON (1990) SPECIMEN SRCC6C

Concrete Deck		Steel Deck			
Thickness	5	Height	2		
Width	?				
Weight	?				
Reinforcing	Area	Steel/Slab			
SRCC6C	1.6	0.66			

Shear Studs	Dia	Height	Spacing	Number
SRCC6C	3/4"	?	1/flute	

Material Properties		Fy (Ksi)	Fu (Ksi)
Beam		36.00	
Column			
Web Angles			
Slab Reinforcing			
Concrete	SRCC6C		
Stud Capacity			

Diagram labels:
8-#4 Bars
5" slab on 2" deck
A-325 7/8"Dia Bolts (Typ) (twist off)
SRCC6CL
W14x145
2L5x5x1/2x17.5" double web angles
SRCC6CR
W21x57
PL 8" wide x 0.5" thick x 10" long

Results   Mp=4644   Z = 129

Designation	Description	Mc (K-in)	Muc (K-in)	Mc/ My	Mc/ Mp	Ø (radx10^3)	Comments
SRCC6CL		1533			0.33	10	
SRCC6CL			2500 ??		0.54	8	
SRCC6CR		1500			0.32	23.9	

Test Notes

Concrete Cracki Concrete Cracking

 Slab was cracked but the number and size of cracks were less than SSRC4M & SSRC5M

Web Angle

 SRCC6CL slipped early @ 0.1 Mp (most likely due to improper tightening prior to torquing)

 SRCC6CR slipped @ 8.5 mrad rotation

 Slippage was continuous after 0.75% drift
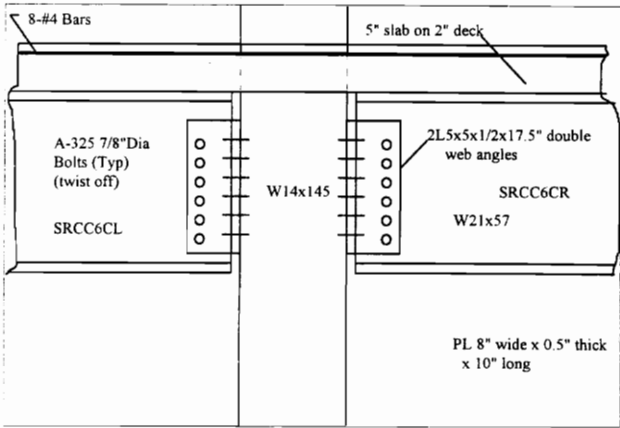
Local Effects

 Large local elongation of the two bottom bolts and local beam yielding (drifts >2%)

 Heels of web angles yielded near top and bottom

 No evidence of the slab steel yielding

Additional General Notes

 Block shear failure needs to be checked carefully

 Suggests as many fasteners as possible

 Keep Web clips as low as possible

 A semi-rigid composite system can be very economical

 Use in unbraced frames should be limited to 10 stories in braced frame construction if the design LL >2*DL

Test Setup

Test setup labels:
120"   120"
WF 14x145
155-1/3"
WF 21x57
H

M - Theta chart:
M - Theta
LEON
M (K-in)
SRCC6CL —— SRCC6CR
Rotation (mrad)

269
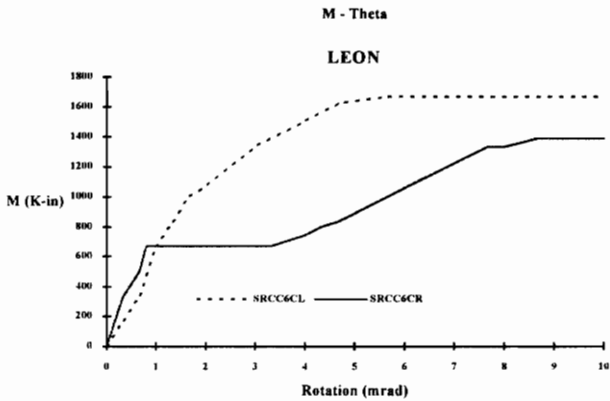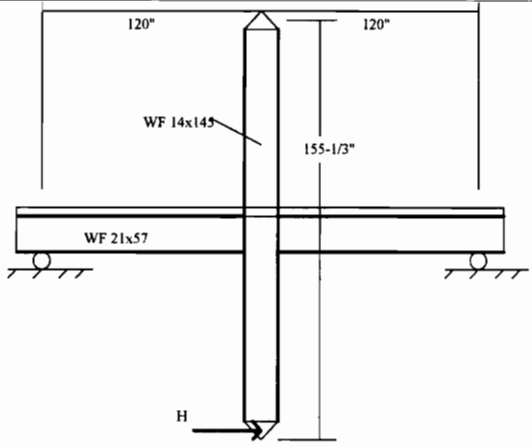
APPENDIX C

**ONE PAGE SUMMARIES OF RESEARCH ON
SEMI-RIGID CONNECTIONS ASSOCIATED WITH
ZANDONINI**

ZANDONINI (1989) SPECIMENS SJA10 & SJA14

Concrete Deck		Steel Deck			
Thickness	4.72	Height	None		
Width	39.37				
Weight	?		Ar*fyr/		
Reinforcing	Area	Steel/Slab	Af*fys		
SJA10	1.31	0.71%	0.91		
SJA14	2.25	1.21%	1.3		
Shear Studs	Dia	Height	Spacing	Number	
	0.79	3.94	2/5.91		

Material Properties		Fy (Ksi)	Fu (Ksi)
Joist Flange		41.77	62.80
Joist Web		41.77	62.80
Slab Reinforcing		72.00	SJA10
		60.00	SJA14
Strain Hardening @ 1.6 Fy Strain (10mm)			
Strain Hardening @ 1.8 Fy Strain (14mm)			
Concrete			6.10

Diagram labels:
- 8-10 or 14 mm Bars
- 8-6mm Bars
- End Plate t = .47"
- IPE300
- M20 Grade 8.8 4 ea/side Typ (Pretensioned)
- HEB260
- 6mm Stirrups @ 4"/3" Adj Column/End of slab
- IPE300
- Only welded to web
- D = 11.86"
- dw/tw = 39.2
- bf/tf = 14

Results

Mp = 1602

Designation	Mdc (K-in)	Mpc(-) (K-in)	Muc (K-in)	Muc/ Mdc	Muc/ Mp	Muc/ Mpc(-)	Øu mRad	mments on Failure
SJA10	1381	2195	1460	1.06	0.91	0.67	21	Excessive joint deformation
SJA14	2009	2416	1956	0.97	1.22	0.81	24	Excessive joint deformation

Test Notes

Concrete Cracking

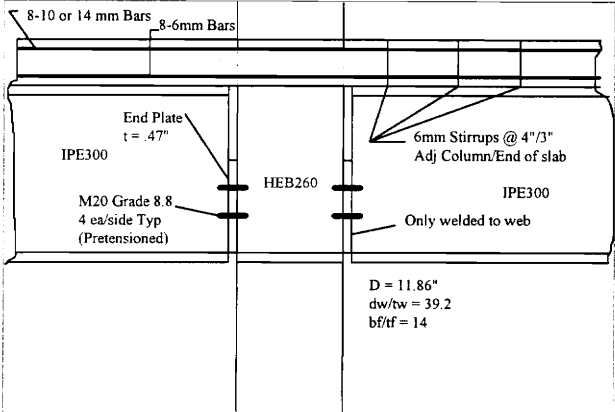First cracks appeared @ moments of 266 K-in & 354 K-in & reached edge of slab at 442 K-in (Mcr calculated @ 425 K")

Away from the column the cracks were straight lines equally spaced @ right angles to the beam (i.e., absence of shear lag)

Local Effects

SJB-14 L only subject to experience local buckling of the bottom flange

Yielding of outermost reinforcing was always attained

After yielding further load increments possible due to stress hardening

	Ke	Ke,cr
SJA10	601848	165509
SJA14	991278	229233
	Mcr (K")	
SJA10	433	
SJA14	451	

Additional General Notes

Full Composite Action Developed by shear studs

Loaded to 1/3 predicted collapse then unloaded, then step loaded

Improving joint capacity easier through proper selection of slab steel than through more complex detailing of joint

Test setup diagram with labels: 76.8", 72.8", Hydraulic Jack, 55.51", L IPE300, 11.81", IPE300 R, 5.9", 9.8", 44.1"

Multi-Linear Response Approximation — SJA14, SJA10, Bottom End Plates, Zandonini

M - Theta, Zandonini; legend: SJA14-R, SJA14-L, SJA10-R, SJA10-L; axes M (K-in) vs Rotation (mrad)

271

Concrete Deck | | **Steel Deck**
Thickness	4.72	Height	None
Width	39.37		
Weight	?		Ar*fyr/
Reinforcing	Area	Steel/Slab	Af*fys
SJB10	1.31	0.71%	0.91
SJB14	2.25	1.21%	1.3
Shear Studs	Dia	Height	Spacing	Number
	0.79	3.94	2/5.91	

Material Properties		Fy (Ksi)	Fu (Ksi)
Joist Flange		41.77	62.80
Joist Web		41.77	62.80
Slab Reinforcing		72.00	SJA10
		60.00	SJA14
Strain Hardening @ 1.6 Fy Strain (10mm)			
Strain Hardening @ 1.8 Fy Strain (14mm)			
Concrete			6.10

8-10 or 14mm Bars 8-6mm Bars

End Plate
t = .47"

IPE300

M20 Grade 8.8
4 ea/side Typ
(Pretensioned)

HEB260

6mm Stirrups @ 4"/3"
Adj Column/End of slab

IPE300

Welded to beam web
and flanges

D = 11.86
dw/tw = 39.2
bf/tf = 14

Results | Mp = 1602

Designation	Mdc (K-in)	Mpc(-) (K-in)	Muc (K-in)	Muc/ Mdc	Muc/ Mp	Muc/ Mpc(-)	Øu mRad	mments on Failure
SJB10	1381	2195	1841	1.33	1.15	0.84	22	Excessive joint deformation
SJB14	2009	2416	2310	1.15	1.44	0.96	24	Local buckling of steel beam

Test Notes
Concrete Cracking

First cracks appeared @ moments of 266 K-in & 354 K-in & reached edge of slab at 442 K-in (Mcr calculated @ 425 K")

Away from the column the cracks were straight lines equally spaced @ right angles to the beam (i.e., absence of shear lag)
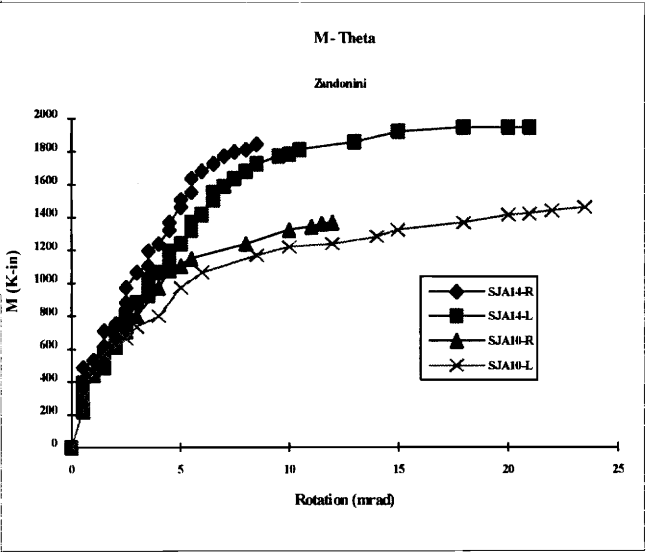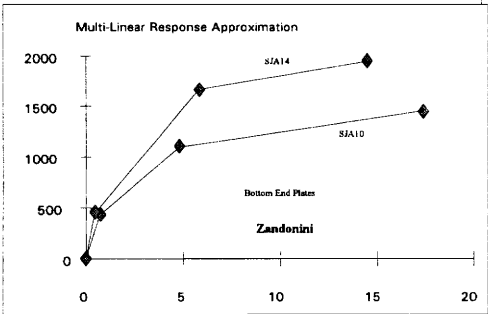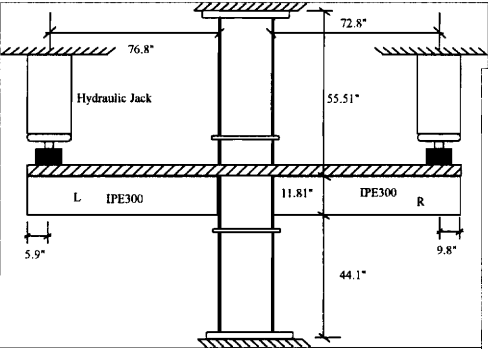
Local Effects

SJB-14 L only subject to experience local buckling of the bottom flange

Yielding of outermost reinforcing was always attained

After yielding further load increments possible due to stress hardening

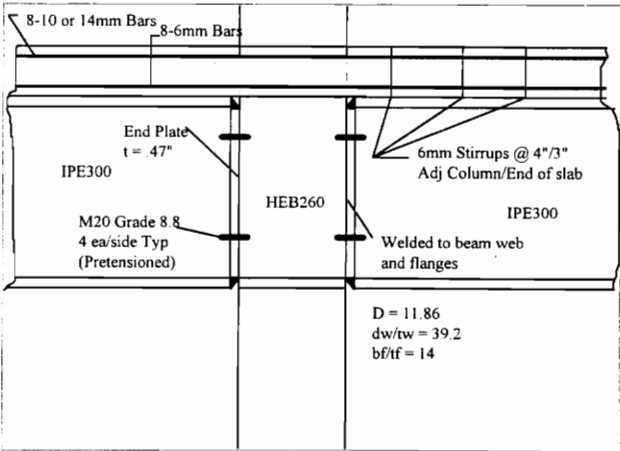|	Ke	Ke,cr
SJB10	1239098	263751
SJB14	2679107	549628

Additional General Notes

Full Composite Action Developed by shear studs

Loaded to 1/3 predicted collapse then unloaded, then step loaded

Improving joint capacity easier through proper selection of slab steel than through more complex detailing of joint

	Mcr (K")
SJB10	451
SJB14	451

72.8"

76.8"

Hydraulic Jack

55.51"

L   IPE300

11.81"   IPE300   R

5.9"   9.8"

44.1"

Multi-Linear Response Approximation

SJB14

SJB10

Flush End Plates

Zandonini

M- Theta

Zandonini

M (K-in

Rotation (mrad)

- SJB14-R
- SJB14-L
- SJB10-R
- SJB10-L

ZANDONINI (1990) SPECIMEN SJA14/1

Concrete Deck		Steel Deck		
Thickness	4.72	Height	None	
Width	39.37			
Weight	?			Ar*fyr/
Reinforcing	Area	Steel/Slab		Af*fys
SJA14/1	2.25	1.21%		1.23
Shear Studs	Dia	Height	Spacing	Number
SJA14/1	0.47	2.95		
	(Welded Shear Studs)			
Material Properties		Fy (Ksi)	Fu (Ksi)	
Joist Flange		46.00	65.00	
Joist Web		46.00	65.00	
Slab Reinforcing		62.00	97.00	
Concrete			4.35	

8-14 mm Bars — 8-6mm Bars

End Plate t = .47"

IPE300

HEB260

M20 Grade 8.8 4 ea/side Typ (Pretensioned)

6mm Stirrups @ 4"/3" Adj Column/End of slab

IPE300

Only welded to web

D = 11.86"
dw/tw = 39.2
bf/tf = 14
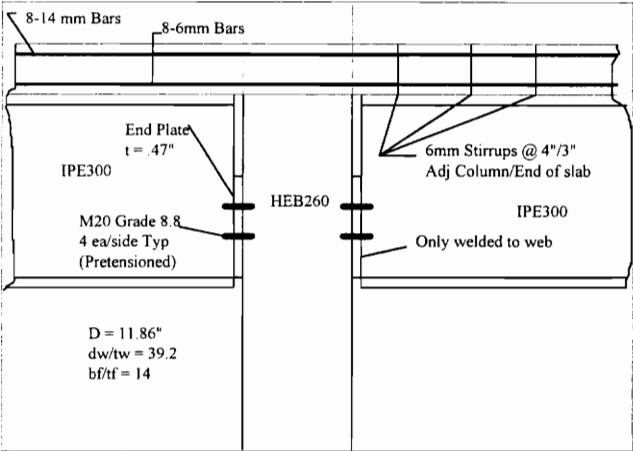
Results

Designation	Mcr (K-in)	Muj (K-in)	Mpj (K-in)	Øu mRad	Mu/Mpc (+Cap)	Mu/Mpc (-Cap)	Mu/Mps	Comments
SJA14/1	539	2177	1756	27	0.61	0.86	1.24	Excessive joint deformation

Test Notes
(Mpj = M @ entering plastic region, i.e., all rebars yielded)

Concrete Cracking
First cracking @ 478 K" (Mcr,th = 389 K") starting @ column flange tips and rapidly expanded to the slab edges

Little inclination of cracks except very near the column suggesting limited shear lag

Factors investigated (slab-column interaction, shear connector flexibility & imbalanced moments) had little effect
on the cracking pattern

Local Effects
Yielding of column web @ 1300 K", but buckling was never detected

Yielding of slab longitudinal reinforcement started @ avg of 1770 K"

Yielding of lower beam flange @ avg of 2020 K", but strain hardening of rebar allowed further moment development

Nodal stiffness approached 0 when bottom flange & adjacent web of the beam buckled

Additional General Notes
Specimens designed for full composite action

Test specimen supposed to be almost identical to SJA14

	Ke	Ke,cr
SJA14/1	1029336	280567

Test Setup
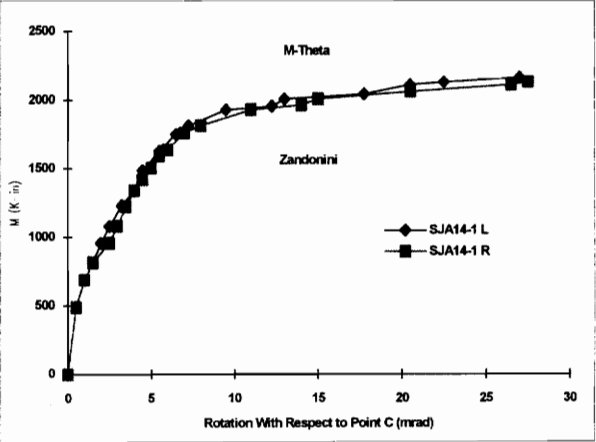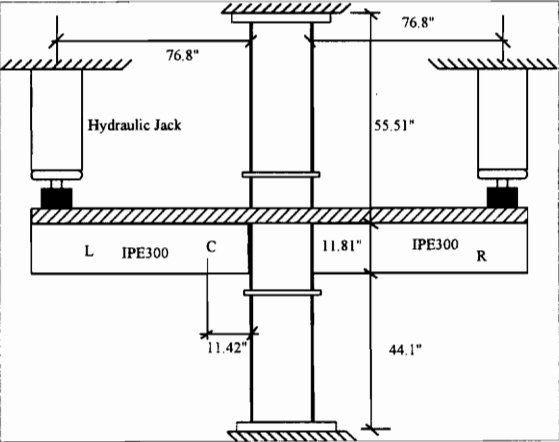
ZANDONINI (1990) SPECIMEN SJA14/2 & SJA14/4

Concrete Deck		Steel Deck			
Thickness	4.72	Height	None		
Width	39.37				
Weight	?		Ar*fyr/		
Reinforcing	Area	Steel/Slab	Af*fys		
SJA14/2	2.25	1.21%	1.23		
SJA14/4	2.25	1.21%	1.23		
Shear Studs	Dia	Height	Spacing	Number	
SJA14/2	0.47	2.95	(Studs)		
SJA14/4	(Mech Fasteners)				
Material Properties		Fy (Ksi)	Fu (Ksi)		
Joist Flange		46.00	65.00		
Joist Web		46.00	65.00		
Slab Reinforcing		62.00	97.00		
Concrete	SJA14/2	4.50			
	SJA14/4	3.00			

8-14 mm Bars
8-6mm Bars
1" Gap along flange
End Plate t = .47"
IPE300
6mm Stirrups @ 4"/3" Adj Column/End of slab
IPE300
HEB260
M20 Grade 8.8 4 ea/side Typ (Pretensioned)
Only welded to web
D = 11.86"
dw/tw = 39.2
bf/tf = 14
Mech Fastener
Hilti

Results

Designation	Mcr (K-in)	Muj (K-in)	Mpj (K-in)	Øu mRad	Mu/Mpc (+Cap)	Mu/Mpc (-Cap)	Mu/Mps	Comments
SJA14/2	415	2142	1756	21/41	0.60	0.85	1.22	Excessive joint deformation
SJA14/4	415	2124	1756	28/48*	0.59	0.84	1.21	Excessive joint deformation

Test Notes (Mpj = M @ entering plastic region, i.e., all rebars yielded) * L/R

Concrete Cracking

First cracking @ 478 K" (Mcr,th = 389 K") starting @ column flange tips and rapidly expanded to the slab edges

Little inclination of cracks except very near the column suggesting limited shear lag

Factors investigated (slab-column interaction, shear connector flexibility & imbalanced moments) had little effect
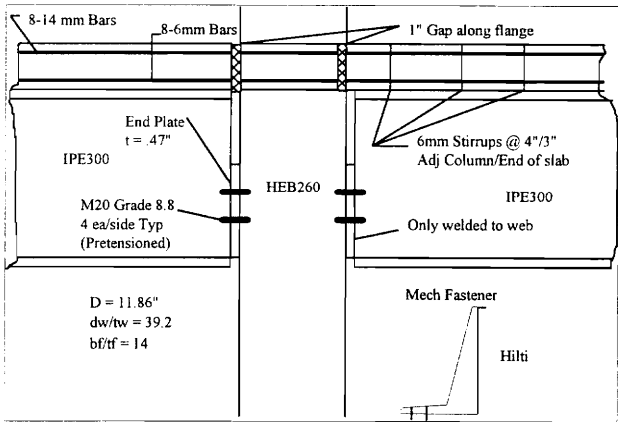on the cracking pattern

Local Effects

Yielding of column web @ 1300 K", but buckling was never detected

Yielding of slab longitudinal reinforcement started @ avg of 1770 K"

Yielding of lower beam flange @ avg of 2020 K", but strain hardening of rebar allowed further moment development

Nodal stiffness approached 0 when bottom flange & adjacent web of the beam buckled

	Ke	Ke,cr
SJA14/2	1002784	282337
SJA14/4	923128	225696

Additional General Notes

Specimens designed for full composite action

The type of shear connector was felt to have a modest influence

Gradient of slip increase was greater for specimens with pin fastened shear connectors

Non-welded connectors experienced a significant uplift of the slab with respect to the steel section @ approx. 2020 K"

Test Setup

76.8"
76.8"
Hydraulic Jack
55.51"
L IPE300 C
11.81" IPE300 R
11.42"
44.1"

M - Theta
Zandonini

Legend: SJA14/2 L, SJA14/2 R, SJA14/4 L, SJA14/4 R

Y-axis: M (K in)
X-axis: Rotation With Respect to Point C (mrad)

ZANDONINI (1990) SPECIMEN SJA14/3 & SJA14/5

Concrete Deck		Steel Deck			
Thickness	4.72	Height	None		
Width	39.37				
Weight	?				
Reinforcing	Area	Steel/Slab			
SJA14/3	2.25	1.21%			
SJA14/5	2.25	1.21%			
Shear Studs	Dia	Height	Spacing	Number	
SJA14/3	0.47	2.95	(Studs)		
SJA14/5	(Mech Fasteners)				
Material Properties		Fy (Ksi)	Fu (Ksi)		
Joist Flange		46.00	65.00		
Joist Web		46.00	65.00		
Slab Reinforcing		58.00	97.00		
Concrete			3.91		

8-14 mm Bars   8-6mm Bars   1" Gap along flange

End Plate t = .47"

IPE300

M20 Grade 8.8 4 ea/side Typ (Pretensioned)

HEB260

6mm Stirrups @ 4"/3" Adj Column/End of slab

IPE300

Only welded to web

D = 11.86 "
dw/tw = 39.2
bf/tf = 14

Mech Fastener

Hilti

Results

Designation	Muj (K-in)	Øu mRad	Mu/Mpc (+Cap)	Mu/Mpc (-Cap)	Mu/Mps	Comments
SJA14/3	2018	24/36*	0.56	0.80	1.26	
SJA14/5	1991	23/40*	0.56	0.79	1.24	* L/R

Test Notes

Concrete Cracking

First cracking @ 478 K" (Mcr,th = 389 K") starting @ column flange tips and rapidly expanded to the slab edges

Little inclination of cracks except very near the column suggesting limited shear lag

Factors investigated (slab-column interaction, shear connector flexibility & imbalanced moments) had little effect
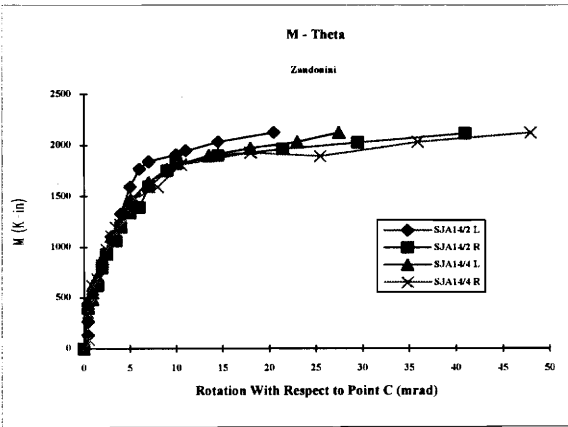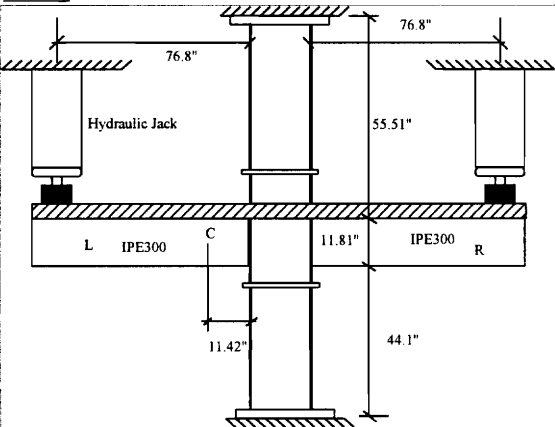   on the cracking pattern

Local Effects

Yielding of column web @ 1300 K", but buckling was never detected

Yielding of slab longitudinal reinforcement started @ avg of 1770 K"

Yielding of lower beam flange @ avg of 2020 K", but strain hardening of rebar allowed further moment development

Nodal stiffness approached 0 when bottom flange & adjacent web of the beam buckled
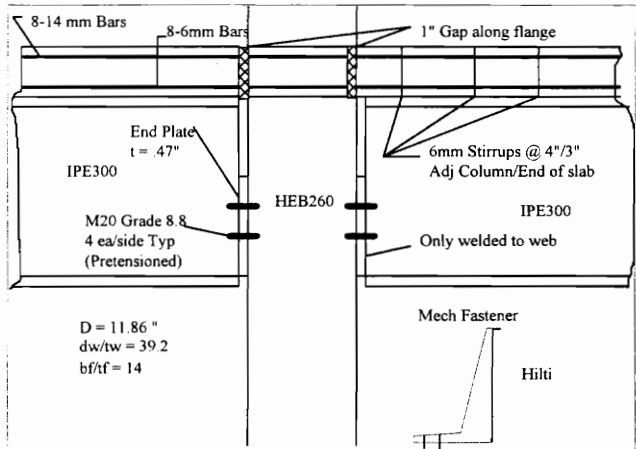
Additional General Notes

Specimens designed for full composite action

The type of shear connector was felt to have a modest influence

Gradient of slip increase was greater for specimens with pin fastened shear connectors

Non-welded connectors experienced a significant uplift of the slab with respect to the steel section @ approx. 2020 K"

The response of the node showed a higher flexibility with respect to the symetric tests

Test Setup
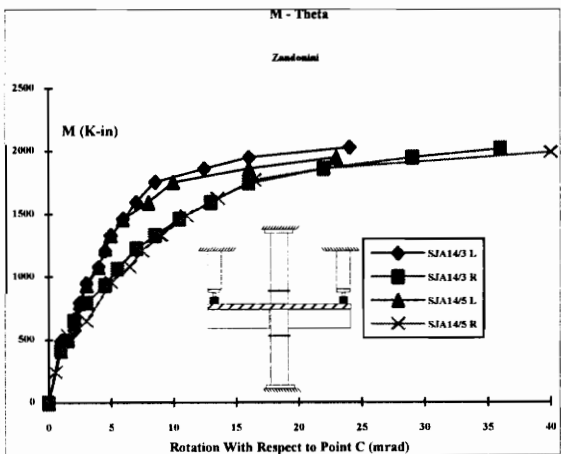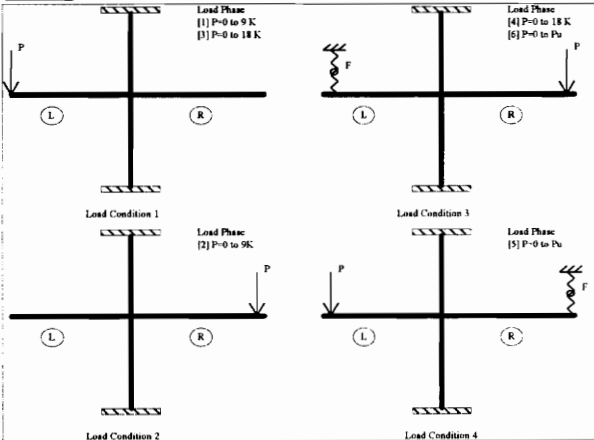
ZANDONINI (1990) SPECIMEN RJ14

Concrete Deck		Steel Deck		
Thickness	4.72	Height	None	
Width	39.37			
Weight	?		Ar*fyr/	
Reinforcing	Area	Steel/Slab	Af*fys	
SJA14/5	2.25	1.21%	1.23	

Shear Studs	Dia	Height	Spacing	Number
SJA14/5	0.47	2.95	(Studs)	

Material Properties	Fy (Ksi)	Fu (Ksi)
Joist Flange	46.00	65.00
Joist Web	46.00	65.00
Slab Reinforcing	62.00	97.00
Concrete		3.50

8-14 mm Bars   8-6mm Bars   1" Gap along flange

IPE300

Stiffner   HEB260

6mm Stirrups @ 4"/3"
Adj Column/End of slab

IPE300

D = 11.86
dw/tw = 39.2
bf/tf = 14

Results

Designation	Mcr (K-in)	Muj (K-in)	Mpj (K-in)	Øu mRad	Mu/Mpc (+Cap)	Mu/Mpc (-Cap)	Mu/Mps	Comments
RJ14	415	2540	1756	31	0.71	1.01	1.45	Local buckling of beam

13 as printed in REX103

Test Notes

(Mpj = M @ entering plastic region, i.e., all rebars yielding)

Concrete Cracking

First cracking @ 451 K" (Mcr,th = 389 K") starting @ column flange tips and rapidly expanded to the slab edges

Little inclination of cracks except very near the column suggesting limited shear lag

Factors investigated (slab-column interaction, shear connector flexibility & imbalanced moments) had little effect
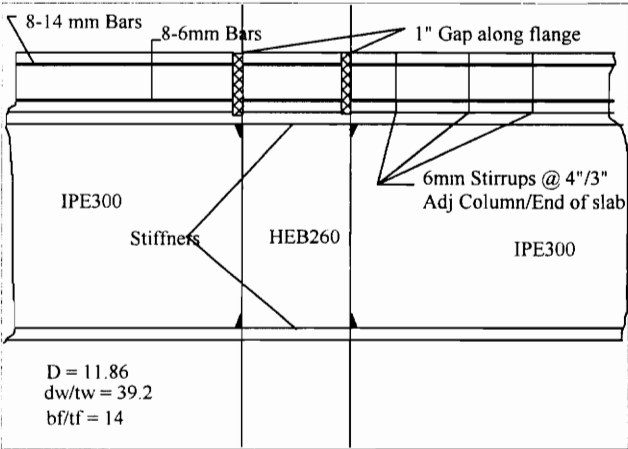   on the cracking pattern

Local Effects

NA near top flange causing increased portion of beam web to be in compression

Yielding of slab longitudinal reinforcement started @ avg of 2124 K"

Web flange instability reduced the rotation capacity of the node (slight buckling at 13 mrad but not failure)

Additional General Notes

Specimens designed for full composite action

	Ke	Ke,cr
RJ14	1789611	913392

Test Setup

76.8"

76.8"

Hydraulic Jack

55.51"

L   IPE300   C   11.81"   IPE300   R

5.9"   9.8"

11.42"   44.1"

M - Theta

Zandonini

M (K-in)

RJ14R

Rotation With Respect to Point C (mrad)

276
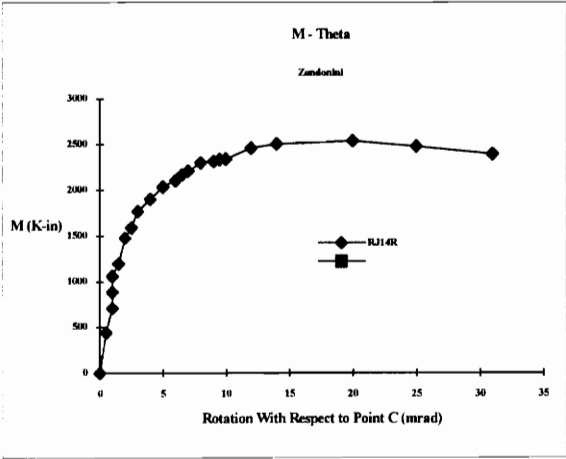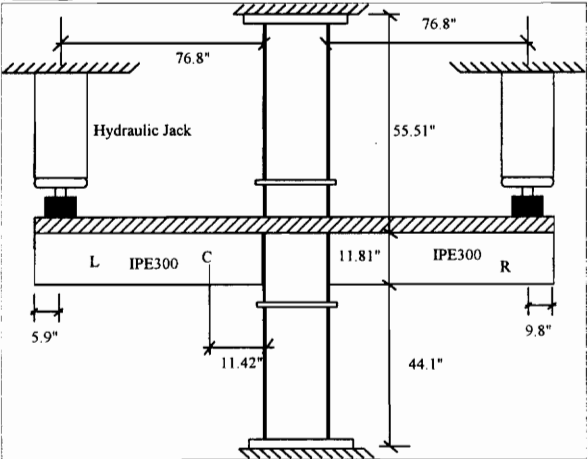
ZANDONINI (1991) SPECIMEN CT1

Concrete Deck		Steel Deck			
Thickness		YES			
Width					
Weight			Ar*fyr/		
Reinforcing	Area	Steel/Slab	Af*fys		
CT1	1.91	1.10%	0.98		

Shear Studs	Dia	Height	Spacing	Number
CT1	Welded studs			

Material Properties		Fy (Ksi)	Fu (Ksi)
Joist Flange		47.70	
Joist Web		47.70	
Slab Reinforcing		70.00	
Concrete		CT1	5.22

	Ke	Ke, cr
CT1	1161211	168163

8-14 mm Bars
M20 Grade 8.8 (Pretensioned)
HE 260
IPE330
Longitudinal Reinforcement
Transverse Reinforcement
6mm @250mm

Results

Designation	Mcr (K-in)	Mu (K-in)	Mp (K-in)	Øu mRad	Mu/Mpc (+Cap)	Mu/Mpc (-Cap)	Mu/Mp	Comments
CT1	469	2638	2236	31	0.56	0.80	1.18	Failure of slab in shear

Test Notes

Concrete Cracking

Fracture of the slab was believed to be due to inadequate transverse reinforcing

Cyclic tests on similar joints with increased transverse reinforcing indicated that the rotation capacity may have been improved
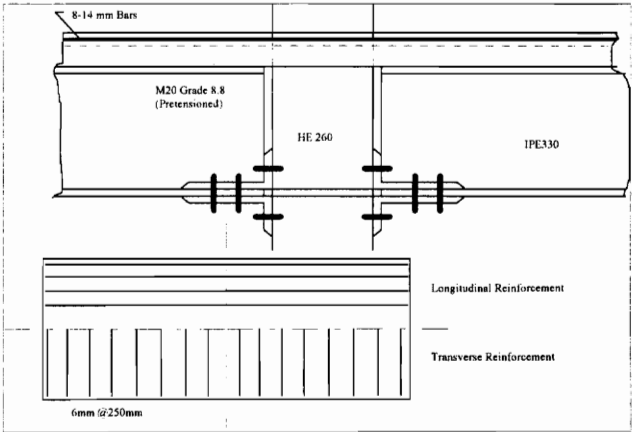
Local Effects

stiffness of joint reduced as a result of slip between the angles & beam flange (lower than its counter part SJA14)

Subsequent analysis utilizing this joint showed showed joint rotation at collapse of beam @ 14-23 mrad

Additional General Notes

4-phases: 1) elastic w/uncracked slab, 2) elastic w/cracked slab, 3) inelastic w/progressive deterioration of stiffness

4) plastic w/moderate hardening mainly due to the steel connection and strain hardening of rebar

The ultimate resistance was only slightly less than its counter part SJA14

Analysis using this type of joint shows that the first hinge forms at midspan and that the joint has enough rotation capacity to achieve the

plastic collapse mechanism, thus these joints would be adequate for use in plastic design

Rotation may be limited by local buckling or longitudinal shear failure of the slab

Test Setup

M - Theta
Zandonini
CT1
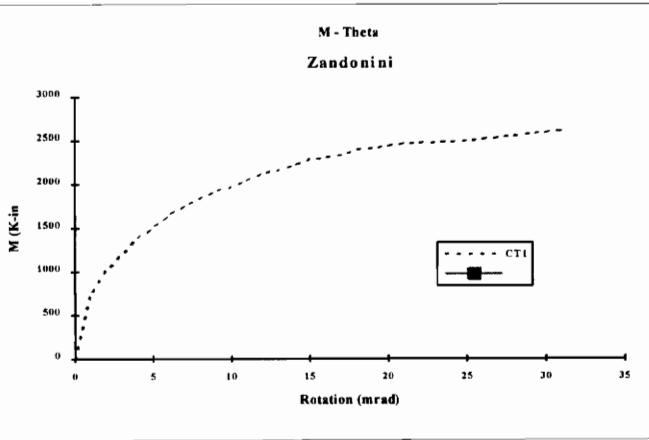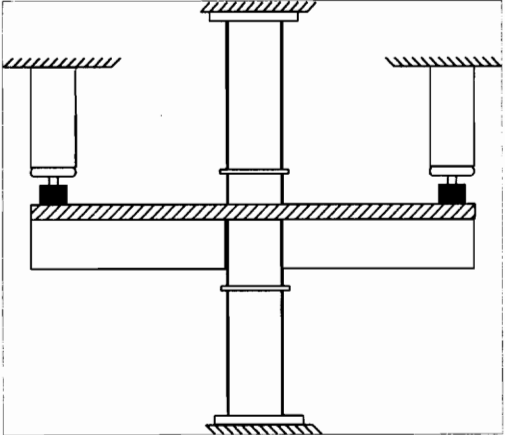
ZANDONINI (1991) SPECIMEN CT2 & CT3

Concrete Deck		Steel Deck			
Thickness		YES			
Width					
Weight			Ar*fyr/		
Reinforcing	Area	Steel/Slab	Af*fys		
CT2	1.91	1.10%	0.99		
CT3	1.91	1.10%	1.02		
Shear Studs	Dia	Height	Spacing	Number	
	Welded Studs				
Material Properties		Fy (Ksi)	Fu (Ksi)		
Joist Flange		69.00			
Joist Web		69.00			
Reinforcing	CT2	46.00			
	CT3	45			
Concrete	CT2		5.70		
	CT3		5.90		
	Ke	Ke, cr			
CT2	1539136	665573			
CT3	1560378	541663			

8-14 mm Bars

M20 Grade 8.8 (Pretensioned)

CT3 Concrete filled structural tube (8mm steel)
CT2 HE section
IPE330

Longitudinal Reinforcement

Transverse Reinforcement

6mm @ 250mm

Results

Designation	Mcr (K-in)	Mu (K-in)	Mp (K-in)	Øu mRad	Mu/Mpc (+Cap)	Mu/Mpc (-Cap)	Mu/Mp	Comments
CT2	48.7	3151	2250	13	0.69	0.98	1.4	Fracture of slab in shear
CT3	48.7	2655	2231	11	0.59	0.83	1.19	Fracture of slab in shear

Test Notes

Concrete Cracking

Fracture of the slab was believed to be due to inadequate transverse reinforcing

Cyclic tests on similar joints with increased transverse reinforcing indicated that the rotation capacity may have been improved

Local Effects

forces transmitted by upper tension bolts caused early nonlinearity dut to inelastic deformations of the column wall

the inelastic deformations induced a higher stress state in the slab, leading to earlier failure

Additional General Notes

4-phases: 1) elastic w/uncracked slab, 2) elastic w/cracked slab, 3) inelastic w/progressive deterioration of stiffness
4) plastic w/moderate hardening mainly due to the steel connection and strain hardening of rebar

As a result of the low rotation capacities, analysis of beams using these joints would not allow the formation of a mechanism at midspan
thus these joints would be inadequate for use in plastic design

Rotation may be limited by local buckling or longitudinal shear failure of the slab

Test Setup

M - Theta
Zandonini

..... CT2
— — CT3

M (K-in)

Rotation (mrad)

278
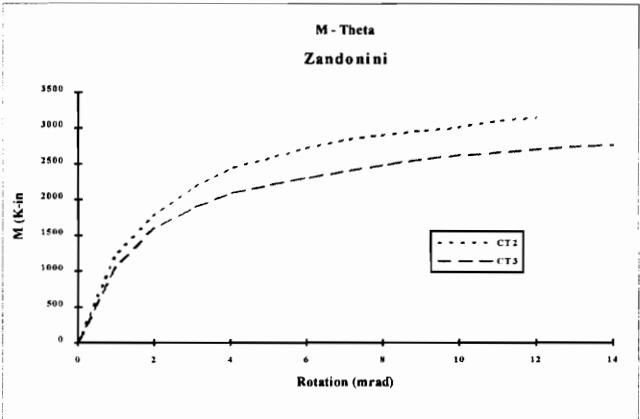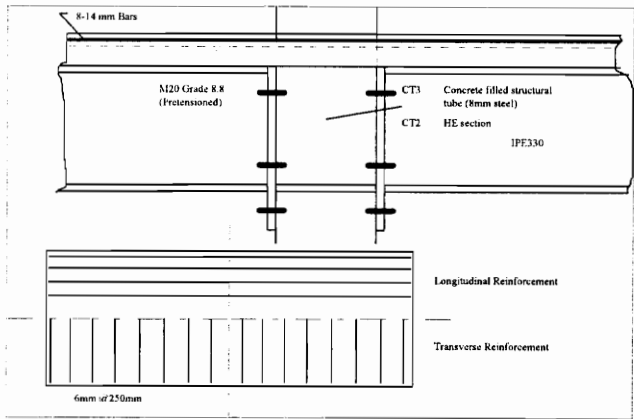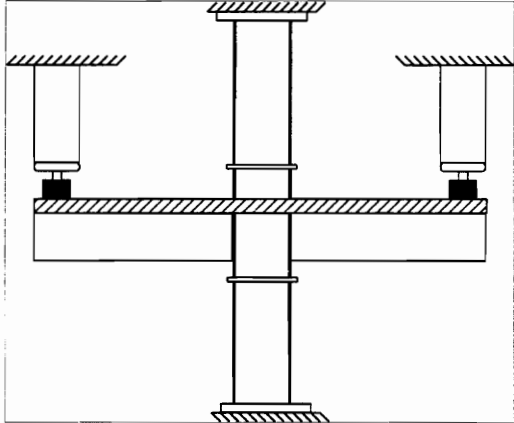
APPENDIX D

MEASURED MATERIAL PROPERTIES

Table D 1 Description of Material Specimens

<u>Steel Specimens</u>

Beam Web

2WV	Vertical sample from beam used in Connection #2
2WH	Horizontal sample from beam used in Connection #2
3WH	Horizontal sample from beam used in Connection #3

Beam Flange

2BF-1	Sample taken from bottom flange of beam used in Connection #2
2BF-2	Sample taken from bottom flange of beam used in Connection #2
3BF-1	Sample taken from bottom flange of beam used in Connection #3
3BF-2	Sample taken from bottom flange of beam used in Connection #3

Girder Web

GWV	Vertical sample from girder web
GWH	Horizontal sample from girder web

Girder Flange

GTF-1	Sample from top flange of girder
GTF-2	Sample from top flange of girder

Seat Angle

SA-1	Sample taken from seat angle stock
SA-2	Sample taken from seat angle stock

4" x 3/8" Plate

PL-1	Sample taken from plate stock
PL-2	Sample taken from plate stock

Reinforcing Steel

R-01	Sample taken from reinforcing steel stock
R-02	Sample taken from reinforcing steel stock
R-03	Sample taken from reinforcing steel stock
R-04	Sample taken from reinforcing steel stock

<u>Concrete Specimens</u>

Connection #1	Twelve 4-inch dia. cylinders cast on day slab was cast
Connection #2	Twelve 4-inch dia. cylinders cast on day slab was cast
Connection #3	Twelve 4-inch dia. cylinders cast on day slab was cast
Connection #4	Twelve 4-inch dia. cylinders cast on day slab was cast

Table D 2 Steel Specimen Measured Properties

Tensile Test Specimen	Thickness (in)	Width/Dia. (in)	Yield Stres (ksi)	Ult. Stress (ksi)	Percent Elongation
2WV	0.319	0.319	49300	62900	26
2WH	0.316	0.316	47000	62900	26
3WH	0.325	0.325	45000	61900	29
2BF-1	0.492	0.492	44600	61600	28
2BF-2	0.516	0.516	44700	61400	25
3BF-1	0.490	0.490	41600	61200	28
3BF-2	0.497	0.497	43500	60600	27
GWV	0.391	0.391	48700	64100	24
GWH	0.385	0.385	47600	64700	42
GTF-1	0.494	0.494	-	64400	32
GTF-2	0.485	0.485	46200	64400	26
SA-1	0.487	0.487	42700	65400	30
SA-2	0.488	0.488	42400	65400	30
PL-1	0.367	0.367	48500	71300	29
PL-2	0.370	0.370	49300	71500	29
R-01	-	0.390	70200	116700	6
R-02	-	0.419	72600	118800	6
R-03	-	0.375	70100	119400	8
R-04	-	0.406	70600	119700	7

Table D 3 Concrete Specimen Measured Properties

Concrete Specimen	Average Crushing Load (lbs)	Cylinder Area (sq in)	Concrete Stress f'c (psi)
Connection #1	33,167	12.57	2,639
Connection #2	66,000	12.57	5,251
Connection #3	53,400	12.57	4,248
Connection #4	43,563	12.57	3,466

APPENDIX E

MOMENT-ROTATION DATA

Table E 1 Moment-Rotation Data For Connection #1

North		South		North		South	
Rotation (mili-rad)	Moment (K-in.)	Rotation (mili-rad)	Moment (K-in.)	Rotation (mili-rad)	Moment (K-in.)	Rotation (mili-rad)	Moment (K-in.)
0	0	0	0	4	383	11	365
0	43	0	34	4	382	11	365
1	132	1	156	4	373	11	338
1	148	1	170	4	299	11	300
1	167	2	126	4	300	11	253
1	166	2	125	4	232	11	229
2	160	2	141	4	163	11	163
2	177	2	125	4	108	10	101
2	195	2	130	4	62	10	59
2	211	2	156	4	25	10	27
2	228	2	210	4	0	10	0
2	243	3	217	4	0	10	5
2	252	3	223	4	207	11	216
2	261	3	230	4	265	11	269
3	276	3	234	4	350	11	359
3	305	3	240	4	408	11	417
3	319	3	320	5	487	11	491
3	338	3	322	4	0	10	5
3	322	3	337	4	244	11	253
4	323	4	416	5	482	11	496
4	331	5	433	5	561	12	575
4	360	5	445	5	614	12	612
4	348	5	451	6	694	14	702
5	338	6	455	6	741	14	755
5	342	6	463	6	779	14	786
5	316	8	429	7	821	15	834
5	356	8	447	7	858	15	865
5	364	9	463	8	890	15	902
5	372	9	478	8	922	17	934
5	326	11	429	9	964	18	976
5	344	11	426	8	546	17	559
5	344	11	382	5	0	14	11
4	320	11	330	7	551	16	565
4	279	10	312	9	837	18	849
3	228	10	144	9	959	18	971
3	170	9	95	10	990	19	1008
3	165	9	75	10	1033	19	1045
2	135	9	56	11	1075	22	1092
2	87	8	0	11	1107	23	1124
2	31	8	0	12	1144	23	1156
1	0	8	0	13	1170	24	1187
1	0	8	0	14	1197	24	1214
1	0	8	0	14	1086	30	1103
2	0	8	0	15	1234	31	1251
2	84	8	59	16	1255	32	1272
2	110	8	96	18	1271	32	1287
2	146	9	113	19	1303	33	1319
2	183	9	181	19	1324	33	1340
2	208	9	168	21	1345	34	1361
3	261	10	217	24	1351	35	1367
3	264	10	243	26	1356	35	1377
3	317	10	255	32	1298	34	1319
4	361	10	280	35	1266	34	1287
4	357	11	303	35	1261	34	1282
4	359	11	315	24	0	28	11
4	386	11	367				

Table E 2 Moment-Rotation Data For Connection #2

North		South		North		South	
Rotation (mili-rad)	Moment (K-in.)	Rotation (mili-rad)	Moment (K-in.)	Rotation (mili-rad)	Moment (K-in.)	Rotation (mili-rad)	Moment (K-in.)
0	-1	0	-1	2	6	3	2
0	-1	0	1	2	85	3	87
0	0	0	0	3	478	4	485
0	51	0	57	4	1042	4	1041
0	105	0	110	4	1547	5	1544
0	149	0	153	4	1829	5	1831
1	200	1	199	5	1901	5	1903
1	236	1	235	5	1973	6	1975
1	299	1	297	5	2026	6	2027
1	340	1	337	5	2071	6	2079
1	385	1	382	5	2111	6	2119
1	437	1	433	6	2150	7	2158
1	479	2	474	6	2183	7	2197
2	534	2	530	6	2222	7	2236
2	578	2	581	6	2268	8	2282
2	626	2	635	7	2288	8	2308
2	670	2	674	7	2307	8	2334
2	727	2	733	7	2353	8	2373
2	725	2	730	7	2373	9	2399
2	725	2	728	8	2432	9	2458
2	725	2	728	9	2275	10	2302
2	668	2	668	9	2419	10	2452
2	629	2	631	9	2471	10	2504
2	572	2	576	10	2504	10	2537
2	533	2	536	10	2511	11	2543
2	482	2	487	10	2557	11	2595
2	436	2	440	11	2576	11	2615
2	390	2	394	11	2609	12	2654
2	338	2	340	11	2609	12	2654
2	295	2	294	11	2635	12	2680
2	247	2	248	12	2668	12	2713
2	197	2	195	12	2662	13	2713
2	150	2	150	12	2707	13	2759
2	104	2	104	11	1488	12	1505
2	55	2	52	10	911	11	917
2	1	2	-8	9	452	11	453
2	-1	2	15	8	-7	9	2
2	242	2	244	8	26	9	35
2	399	2	401	10	963	11	982
2	511	2	512	11	1842	12	1877
2	655	2	655	12	2262	13	2321
2	-1	2	9	12	2616	14	2693
2	268	2	270	13	2655	14	2739
2	517	2	518	13	2694	15	2778
2	727	2	727	13	2721	15	2811
2	799	2	799	14	2734	15	2831
2	858	2	858	14	2760	15	2857
2	891	3	890	14	2773	16	2876
3	957	3	956	16	2648	15	2759
3	1003	3	995	17	2740	16	2857
3	1062	3	1054	17	2766	16	2889
3	1101	3	1093	17	2793	16	2922
3	1153	3	1152	17	2806	16	2935
3	1212	3	1204	18	2806	17	2942
3	1258	3	1256	18	2793	17	2935
3	1311	3	1302	18	2793	18	2942
3	1357	3	1348	18	2799	19	2955
3	1409	4	1400	18	2793	19	2955
3	1468	4	1459	18	2793	20	2961
3	1527	4	1518	18	2766	21	2948
3	1573	4	1563	18	2760	23	2955
4	1632	4	1622	19	2714	25	2935
4	1665	4	1655	19	2596	29	2857
4	1737	5	1720	19	2504	32	2752
4	1770	5	1759	20	2471	39	2772
4	1816	5	1805	21	2406	46	2733
4	1862	5	1857	22	2334	54	2687
4	1921	5	1916	24	2255	69	2674
3	780	4	779	20	-20	63	-5
3	360	4	355				

Table E 3 Moment-Rotation Data For Connection #3

North		South		North		South	
Rotation (mili-rad)	Moment (K-in.)	Rotation (mili-rad)	Moment (K-in.)	Rotation (mili-rad)	Moment (K-in.)	Rotation (mili-rad)	Moment (K-in.)
0	0	0	0	4	1677	4	1664
0	-4	0	-4	4	1755	4	1743
0	0	0	0	5	1822	4	1803
0	59	0	57	5	1840	4	1827
0	101	0	98	5	1882	4	1869
0	182	0	177	5	1925	4	1906
0	239	0	238	5	1943	4	1930
1	304	1	319	6	1937	4	1918
1	355	1	369	6	1973	4	1954
1	424	1	444	6	2028	4	2014
1	474	1	490	6	2046	4	2026
1	539	1	545	6	2076	4	2056
1	595	1	604	7	2094	5	2074
1	638	1	641	7	2064	5	2050
1	664	1	673	6	956	4	959
1	702	2	718	5	6	3	6
2	735	2	753	5	6	3	12
2	753	2	785	5	103	3	103
2	771	2	800	5	630	4	633
2	791	3	829	6	944	4	941
2	782	3	819	6	1380	4	1369
2	782	3	820	6	1870	4	1851
2	696	3	731	7	2040	5	2020
2	654	3	683	7	2064	4	2044
2	608	3	639	7	2173	5	2141
2	551	3	572	8	2221	5	2195
2	493	3	515	8	2203	5	2177
2	445	3	457	8	2276	5	2249
2	347	3	356	8	2191	6	2171
2	289	3	291	8	2276	6	2255
2	232	3	233	8	2227	6	2201
2	189	2	191	8	2318	6	2297
2	132	2	134	9	2349	7	2352
2	46	2	46	9	2336	7	2334
2	-2	2	1	9	2409	7	2406
2	6	2	0	10	2445	8	2442
2	24	2	24	10	2488	8	2478
2	163	2	163	10	2421	8	2418
2	230	2	229	10	2512	9	2509
2	315	3	308	11	2554	9	2551
2	430	3	422	11	2585	9	2581
2	508	3	507	11	2597	9	2593
2	684	3	675	11	2542	10	2539
2	793	3	784	12	2615	10	2611
2	109	2	103	13	2566	10	2563
2	0	2	-6	13	2657	11	2653
2	0	2	0	13	2609	11	2611
2	18	2	18	14	2675	11	2677
2	345	3	344	14	2700	11	2695
2	581	3	573	14	2700	11	2702
2	781	3	772	14	2724	11	2720
2	896	3	880	14	2706	11	2702
2	962	3	953	15	2748	12	2744
2	1065	3	1055	15	2748	12	2744
2	1156	3	1140	15	2778	13	2774
2	1235	3	1218	16	2790	13	2780
3	1320	3	1303	17	2815	14	2810
3	1350	3	1339	17	2833	14	2822
3	1435	3	1417	18	2839	16	2822
3	1465	3	1447	19	2869	18	2852
3	1531	3	1514	20	2851	20	2834
3	1586	3	1568	21	2833	24	2816
3	1628	3	1610	21	2712	30	2677
3	1677	4	1652	22	2536	41	2478
3	1707	4	1688	20	1453	60	1465
4	1671	4	1652	19	1241	83	1248
4	1767	4	1749	19	0	73	6

Table E 4 Moment-Rotation Data For Connection #4

North		South		North		South	
Rotation	Moment	Rotation	Moment	Rotation	Moment	Rotation	Moment
(mili-rad)	(K-in.)	(mili-rad)	(K-in.)	(mili-rad)	(K-in.)	(mili-rad)	(K-in.)
0	0	0	0	2	2306	2	2291
0	-21	0	-17	3	2391	2	2364
0	0	0	0	3	2415	2	2388
0	17	0	11	3	2488	2	2466
0	57	0	57	3	2548	2	2521
0	108	0	105	4	2585	2	2551
0	180	0	179	4	2633	3	2599
0	225	0	227	4	2681	3	2641
0	328	0	324	4	2736	3	2702
1	384	0	390	5	2778	3	2744
1	453	1	474	5	2821	4	2780
1	537	1	553	6	2869	4	2828
1	594	1	618	6	2911	4	2870
1	742	1	760	6	2954	5	2901
1	819	1	834	6	2972	5	2919
1	814	1	829	7	3014	5	2955
1	813	1	829	7	3051	5	2991
1	813	1	829	7	3081	5	3021
1	733	1	746	8	3111	6	3051
1	690	1	708	8	3135	6	3075
1	650	1	660	8	3166	6	3099
1	551	1	572	8	3166	6	3106
1	477	1	490	9	3196	7	3130
1	410	1	421	9	3220	7	3154
1	340	1	348	9	3232	7	3166
1	278	1	282	9	3269	7	3196
1	199	1	205	10	3281	7	3208
1	108	1	104	10	3317	8	3238
1	52	1	51	10	3341	8	3262
1	11	1	14	11	3359	8	3280
1	0	1	0	11	3378	9	3298
1	115	1	121	11	3390	9	3311
1	248	1	253	11	1701	9	1701
1	454	1	452	9	-12	8	-6
1	666	1	663	10	1598	8	1580
1	817	1	814	11	3075	9	3045
1	242	1	253	12	3293	9	3262
1	0	1	0	12	3372	10	3341
1	472	1	470	12	3414	10	3371
1	817	1	814	14	3456	12	3413
1	975	1	965	15	3456	12	3407
1	1186	1	1170	17	3293	11	3262
1	1301	1	1290	17	3129	11	3112
1	1416	1	1405	17	2996	11	2979
2	1556	1	1544				
2	1707	1	1688				
2	1828	1	1815				
2	1967	1	1948				
2	2046	1	2032				
2	2234	2	2213				

APPENDIX F

NOMENCLATURE

a	= distance from beam end to point of inflection
a_x	= the horizontal distance from the center of the connection to the location of the I.C.
a_y	= vertical distance from the center of the connection to the location of the I.C.
A	= polynomial constant
A_b	= effective cross-sectional area of bolt
A_c	= area of concrete
A_e	= effective area of concrete
A_g	= gross area of concrete
A_g	= gross plate area
A_{gb}	= gross area of the steel beam
A_n	= net plate area
A_r	= area of reinforcing steel
A_{sl}	= cross-sectional area of seat angle
A_{wl}	= cross-sectional area of web angles
α	= regression coefficient for plates with perforations (Fisher 1965)
α_1	= concrete tension stiffening constant accounting for bond characteristics of reinforcing steel (Collins and Mitchel 1991)
α_2	= concrete tension stiffening constant accounting for loading (Collins and Mitchel 1991)
B	= polynomial constant
β	= regression constant for plates with perforations (Fisher 1965)
C	= compression force
C	= polynomial constant
C1	= moment-rotation equation constant (Kulkarni 1990)
C2	= moment-rotation equation constant (Kulkarni 1990)
C3	= moment-rotation equation constant (Kulkarni 1990)
C4	= moment-rotation equation constant (Kulkarni 1990)
χ	= beam-column interaction coefficient (Puhali, et. al. 1990)
d	= hole diameter
d	= the nominal depth of the steel beam section
d_i	= vector sum of d_x and d_y

$d_{i,max}$ = the maximum distance from any bolt in a connection to the I.C. of the connection

d_r = distance from center of connection to c.g. of reinforcing steel

d_w = depth of the beam web

d_x = horizontal distance from the I.C. to the bolt

d_y = vertical distance from the I.C. to the bolt

D = Leg size of fillet weld (in 1/16 in. increments)

D = polynomial constant

D = distance from the bottom flange of the beam to the c.g. of the reinforcing steel

DL = dead load

δ = beam deflection at midspan

δ = deformation of shear stud

δ_o = midspan deflection of a simply supported beam subject to w_o

δ_s = service load deflection limit

$\delta_{Simple\ Support}$ = beam midspan deflection for a simply supported beam under service loads

δ_{SL} = beam midspan deflection from service load

δ_u = maximum deflection limit

$\bar{\delta}_u$ = normalized maximum deflection limit

$\bar{\delta}$ = normalized midspan beam deflection

$\bar{\delta}_s$ = normalized service load deflection limit

Δ = total deformation of bolt and bearing deformation of the connected material (can also be strain, rotation, or linear displacement)

Δ = vertical deflection of a beam

Δ_* = difference between actual deformation and some constant deformation value

Δ_i = deformation of weld elements

$\Delta_{i,max}$ = maximum deformation of a given weld segment

Δ_m = deformation of weld element at maximum stress

Δ_o = maximum weld deformation for a weld with $\theta = 0$

Δ_u = deformation of weld element at ultimate stress (fracture), usually in element furthest from the I.C.

e = base of natural logarithm

E = modulus of elasticity

E = polynomial constant

Ec	= modulus of elasticity for concrete
ε	= strain
ε_*	= difference between actual strain and some constant strain value
ε^*	= difference between actual strain and yield strain
ε_{cr}	= cracking strain of concrete
ε_u	= strain at ultimate stress
ε_y	= strain at yield stress
f'_c	= ultimate stress of concrete
f_c	= concrete stress
f_{cr}	= concrete cracking stress
F	= applied force
F_{exx}	= classification strength of weld metal
F_u	= ultimate tensile stress
F_v	= bolt shear stress
F_{wi}	= nominal stress in weld element
F_x	= force in direction of x-axis
F_y	= force in direction of y-axis
F_{yb}	= the yield stress of the steel beam
F_{yr}	= reinforcing steel yield stress
F_{ysl}	= seat angle yield stress
F_{ywl}	= web angle yield stress
ϕ	= strength reduction factor
Φ_o	= maximum end rotation for a simply supported beam subject to w_o
$\bar{\Phi}$	= normalized connection rotation
Φ	= connection rotation
g	= plate width
γ	= non-dimensional parameter related to the ratio between uncracked and cracked composite beam stiffness
H	= horizontal force
H_a	= horizontal force
H_{all}	= allowable horizontal force
H_r	= required horizontal force
I	= moment of inertia

$I(+)$	= moment of inertia for a composite beam in positive flexure
$I(-)$	= moment of inertia for a composite beam in negative flexure
I.C.	= instantaneous center of rotation for a connection
I_b	= the moment of inertia of the steel beam
I_c^+	= composite beam moment of inertia in positive flexure
I_c^-	= composite beam moment of inertia in negative flexure
I_{cb}	= weighted average moment of inertia for composite beam
I_{cbn}	= composite beam moment of inertia in negative flexure
I_{cbp}	= composite beam moment of inertia in positive flexure
I_r	= the moment of inertia of the reinforcing steel
$I_{tr}^{(+)}$	= composite beam moment of inertia in positive flexure
$I_{tr}^{(-)}$	= composite beam moment of inertia in negative flexure
k	= modulus of shear stud connectors
K	= connection stiffness
K	= difference between ultimate and yield stress
K_1	= difference between initial and plastic stiffness
K_1	= regression coefficient for weld load-deformation equation (*Manual of* 1986)
K_1	= stiffness in first region of trilinear moment-rotation approximation (Leon, et.al. 1990)
K_2	= stiffness in second region of trilinear moment-rotation approximation (Leon, et.al. 1990)
K_2	= regression coefficient for weld load-deformation equation (*Manual of* 1986)
K_3	= stiffness in third region of trilinear moment-rotation approximation (Leon, et.al. 1990)
K_4	= stiffness in fourth region of trilinear moment-rotation approximation (Leon, et.al. 1990)
K_o	= initial stiffness used by Johnson and Law (1981) in equation development
K_p	= slope of response in the extreme yielding stage for Richard equation (Richard, et. al. 1980)
l_a	= seat angle width
L	= beam length
L	= distance from the connection to the point where load F is applied (simulating distance to the inflection point of the beam)
L_{in}	= length of an interior beam

L_{out} = length of an exterior beam

LL = live load

L.F. = load factor applied to all loads after concrete has hardened

LVDT = linear voltage displacement transducer

λ = regression constant for bolt force-slip equation (Crawford and Kulak 1971)

$\bar{m}^-$ = normalized composite beam moment capacity in negative flexure

$\bar{m}$ = normalized connection moment

$\bar{m}_{cr}$ = normalized cracking moment capacity of the composite beam

M = moment (typically referring to connection moment)

M_1 = moment at intersection of region 1 and region 2 of trilinear moment-rotation approximation (Leon, et.al. 1990)

M_2 = moment at intersection of region 2 and region 3 of trilinear moment-rotation approximation (Leon, et.al. 1990)

M_3 = maximum connection moment for trilinear moment-rotation approximation (Leon, et.al. 1990)

M_c = moment at center of beam

M_c^* = connection moment resulting from steel connection components

M_{cr} = cracking moment of a composite beam

M_e = moment at end of beam

M_{fe} = fixed end moment

M_i = moment in a connection resulting from a single bolt force

M_p = plastic moment capacity of a beam

M_{pc} = plastic moment capacity of a composite beam

$M_{pc}^{(+)}$ = composite beam plastic moment capacity in positive flexure

$M_{pc}^{(-)}$ = composite beam plastic moment capacity in negative flexure

M_{pc}^{+} = composite beam plastic moment capacity in positive flexure

M_{pc}^{-} = composite beam plastic moment capacity in negative flexure

$M_{\theta s}$ = connection moment at service load

$M_{\theta u}$ = connection moment at factored loads

M_r = connection moment resulting from reinforcing steel force

M_{ue} = connection Moment Capacity

292

M_v	= connection moment resulting from vertical shear force
μ	= regression constant for bolt force-slip equation (Crawford and Kulak 1971)
μ	= regression constant for weld load-deformation equation (*Manual of* 1986)
n	= shape parameter for Richard equation (Richard, et. al. 1980)
P	= concentrated force
Q	= load on shear stud
Q	= stiffness factor used by Johnson and Law (1981) in equation development
Q_{sol}	= ultimate load capacity of shear stud
ΣQ_n	= shear stud connector force required for a composite beam in positive flexure
θ	= angle of longitudinal axis of weld with respect to the direction of force
θ	= connection rotation
θ_1	= rotation at intersection of region 1 and region 2 of trilinear moment-rotation approximation (Leon, et.al. 1990)
θ_2	= rotation at intersection of region 2 and region 3 of trilinear moment-rotation approximation (Leon, et.al. 1990)
θ_3	= maximum expected rotation for trilinear moment-rotation approximation (Leon, et.al. 1990)
θ_l	= rotation on the left side of a rotational spring element
θ_r	= rotation on the right side of a rotational spring element
θ_{SR}	= rotation of connection at service load
θ_t	= total rotation of a rotational spring element
r_{crit}	= distance from I.C. to weld element with minimum Δ_u/r_i ratio
$r_{i,max}$	= maximum r_i for a given connection
r_i	= distance from elemental weld to the I.C. of a welded connection
R	= bolt force, stress, reaction
$R_{i,ult}$	= ultimate force that a single bolt can develop
R_i	= force developed by a single bolt
R_n	= nominal bolt strength
R_o	= reference constant for Richard equation (Richard, et. al. 1980)
R_{ult}	= ultimate bolt force
R_x	= x-axis component of single bolt force
R_y	= y-axis component of single bolt force
ρ	= ratio of element weld deformation to the maximum element weld deformation
s	= shear stud connector spacing

S_s	= steel beam section modulus
S_{tr}	= transformed composite beam section modulus
σ	= stress
σ_t	= total stress in steel beam
σ_D	= stress in steel beam from dead load
σ_L	= stress in steel beam from live load
σ_u	= ultimate stress
σ_y	= yield stress
T	= tension force
t_1	= plate thickness for number one of two plates
t_2	= plate thickness for number two of two plates
t_a	= seat angle thickness
t_e	= effective throat of a fillet weld
t_f	= flange thickness
t_w	= thickness of the beam web
V	= shear force
V_b	= shear force per bolt
V_u	= factored shear load
w	= uniform load
w_o	= maximum uniform load for a simply supported composite beam
$\bar{w}$	= normalized uniform load
W_s	= uniform serviceability load
$W_{u,e}$	= uniform elastic factored load
$W_{u,p}$	= uniform plastic factored load
W_u	= factored uniform load
Y2	= the distance from the top of the beam to the c.g. of the reinforcing steel
z	= distance from connection to point of ram load
z	= distance from the c.g. of the steel beam to the c.g. of the reinforcing steel
Z_x	= plastic section modulus of steel beam

VITA

Clinton Owen Rex was born in Lima, Ohio on the 5th of August 1968. He graduated valedictorian of Ada High School in 1987. He graduated Summa Cum Laude with his Bachelor of Science in Civil and Environmental Engineering from The University of Cincinnati in 1992. As an undergraduate he worked for a variety of engineering firms including Peterman and Associates (Engineering and Surveying Consultants), Turner Construction Company (General Contractors), and Dames & Moore (Environmental Consultants). In the fall of 1992 he entered the Charles Edward Via, Jr. Department of Civil Engineering in pursuit of a Master of Science in Civil Engineering in the Spring of 1994.